

Transcriptomic and cellular responses in the intestine of Atlantic salmon

Youngjin Park

FACULTY OF BIOSCIENCES AND AQUACULTURE

Transcriptomic and cellular studies on the
intestine of Atlantic salmon

Discovering intestinal macrophages using omic tools

Youngjin Park

A thesis for the degree of
Philosophiae Doctor (PhD)

PhD in Aquatic Biosciences no. 37 (2021)
Faculty of Biosciences and Aquaculture

PhD in Aquatic Biosciences no. 37 (2021)

Youngjin Park

Transcriptomic and cellular studies on the intestine of Atlantic salmon

Discovering intestinal macrophages using omic tools

© Youngjin Park

ISBN: 978-82-93165-34-7

Print: Trykkeriet NORD

Nord University

N-8049 Bodø

Tel: +47 75 51 72 00

www.nord.no

All rights reserved.

No part of this book may be reproduced, stored in a retrieval system, or transmitted by any means, electronic, mechanical, photocopying or otherwise, without the prior written permission from Nord University.

Transcriptomic and cellular studies on the intestine of Atlantic salmon

Discovering intestinal macrophages using omic tools

Youngjin Park

Preface

This thesis is submitted in fulfilment of the requirements for the degree of Philosophiae Doctor (PhD) at the Faculty of Biosciences and Aquaculture (FBA), Nord University, Bodø, Norway. The studies included in this dissertation represent original research that was carried out over a period of 3 years from 01.08.2017 to 31.07.2020. This PhD research was supported by funds from multiple sources: i) INFISH project (Regional Forskningsfond Nord-Norge), ii) INMOLS project (DSM Nutritional Products, Switzerland) and iii) Nord University internal research grants. Youngjin Park was financially supported by Korean Government Scholarship—National Institute for International Education, South Korea.

The project team consists of:

Youngjin Park, MSc, FBA, Nord University: PhD candidate

Kiron Viswanath, Professor, FBA, Nord University: Main supervisor

Jorge M.O. Fernandes, Professor, FBA, Nord University: Co-supervisor

Geert F. Wiegertjes, Professor, Aquaculture and Fisheries Group, Wageningen University & Research: Co-supervisor



Youngjin Park

Bodø, 14. 09. 2020

Acknowledgements

I express my profound gratitude to my main supervisor, Professor Kiron Viswanath for his scholastic guidance, valuable suggestions, helpful advice and constant encouragement during my research period and while writing my thesis. This thesis could not have been completed without your endless support. A big thank you from the bottom of my heart.

My heartfelt thanks is also extended to my co-supervisor, Professor Jorge Fernandes for his countless help, thoughtful guidance and valuable comments. Your experienced guidance has been really invaluable for my personal growth. I am really lucky to have had the opportunity to work with you.

I would like to express my sincere gratitude to my co-supervisor, Professor Geert Wiegertjes from Wageningen University and Research, the Netherlands, for his valuable comments and support. Your insightful feedbacks on my studies have been very helpful.

I am obliged to Bisa Saraswathy for the support I received – you taught me how to analyze data, interpret results and write scientific papers throughout my PhD. I remember all the precious time shared with you.

I am thankful to Professor Daniel Barreda (University of Alberta, Canada), Professor Sylvia Brugman (Wageningen University and Research, the Netherlands) and Dr. Sebastian Thalmann (Luminex Corporation, the Netherlands) for their helpful advice and support on the flow cytometry work.

I gratefully appreciate the scientific involvement of Dr. Viviane Verlhac Trichet in certain studies included in this dissertation and acknowledge the funding support received from DSM Nutritional Products, Switzerland.

I sincerely thank Professor Mette Sørensen and Professor Pål Olsvik for all the help, advice and support. I am indebted to you both for having involved me in your projects. Many thanks are extended to Professor Dagmar Mudronova at University of Veterinary Medicine and Pharmacy in Košice, Slovakia for sharing her knowledge and encouraging me. I also thank Dr. Qirui Zhang (Lund University, Sweden), Dr. Prabhugouda Siriyappagounder and Isabel Sofia Abihssira Garcia for their considerable help during my experiments.

I am grateful to the members of Nord University Research Station, especially Bjørnar Eggen, Roald Jakobsen, Jens Kristensen, Steinar Johnsen and Kaspar Klaudiussen for supporting the live animal experiments. I express my gratitude to Ghana Vasanth, Dalia Dahle, Heidi Ludviksen, Ingvild Berg and Martina Kopp for their great help in conducting my studies. I must also acknowledge the support received from the faculty administrative staff who helped me during the course of my studies, especially, Jeanett Kreutzmann and Kristine Vevik.

I extend my gratitude to the members of the Cell Biology and Immunology Group, Wageningen University, the Netherlands for teaching me the principles of flow cytometry.

I am also thankful to the National Institute for International Education (NIIED, South Korea) for providing me the Korean Government Scholarship to pursue my Doctoral study in Norway.

I am glad to have been able to perform my doctoral studies at Nord University, and I thank the Faculty of Biosciences and Aquaculture for giving me the opportunity to build my skills employing state-of-the-art research infrastructure.

I am deeply grateful to all my good friends and colleagues. Thank you really so much for your support all the time. Without you I never know what true happiness is.

Finally I would like to thank the members of my former laboratory at Pukyong National University—Korean professors, lab mates, friends and family who have supported me in many different ways. The following part is written in Korean for them.

먼저, 부족한 저를 배움의 길로 인도해주신 배승철 교수님의 깊은 은혜에 감사의 인사를 드립니다. 교수님, 항상 건강하시고 행복하시길 바랍니다. 또한, 저의 학부와 대학원 과정 동안 뜻 깊은 강의와 학업의 흥미를 이끌어주신 부경대학교 해양바이오신소재학과 김창훈 교수님, 김동수 교수님, 김종명 교수님, 남윤권 교수님, 공승표 교수님 그리고 하늘에 계신 장영진 교수님께 깊은 감사를 드립니다.

국비유학 준비 기간 동안 많은 조언과 가르침을 주신 해양생산시스템관리학부 홍철훈 교수님께 진심어린 감사를 드립니다. 또한, 제게 논문작성법에 대한 깊은 가르침을 주신 홍성윤 명예교수님께 감사의 말씀을 드립니다. 면역학의 흥미를 일깨워주신 수산생명의학과 정현도 교수님께도 깊은 감사를 드립니다.

대학교 생활의 대부분을 보낸 영양대사학 실험실과 사료영양연구소에 모든 선,후배님들께 감사의 말을 전합니다. 특히, 실험실 생활에 많은 도움을 주신 고수홍 박사님, 이준호 박사님, 박건현 박사님, 윤현호 박사님, 이진혁 박사님, 이승형 박사님, 이승한 박사님, 이영광, 최세라, 홍정휘, 원성훈, 성민지, 김도영, 조하윤, 배민정, 배진호, 송유진, 제형우, 박민혜, 김하함, 최원석님께 감사를 드립니다. Dr. Erfan, Dr. Kumar, Dr. Mizan, Dr. Monir, Dr. Ali, Fernando, Ozgun and Jim – A big thanks to all of you.

연구에 대한 흥미와 재미를 느끼게 해주신 군산대학교 정주영 박사님, 김교찬 박사님 그리고 김수환 후배님께 깊은 감사를 드립니다.

멀리 떨어져있지만 항상 마음으로 응원해주는 한국에 있는 소중한 형님, 동생, 친구님들에게 깊은 감사를 드립니다.

박사과정동안 저를 믿고 이해해주고 항상 옆에 있어 준 여자친구 김지안님에게 진심어린 감사를 드립니다.

끝으로, 지금의 제가 있기까지 끝없는 사랑과 헌신으로 저를 키워주신 존경하는 어머니, 아버지 진심으로 감사합니다. 늘 든든한 버팀목이 되어 준 하나뿐인 누나에게도 두손모아 감사를 드립니다.

함께 해주신 모든 분들께 이 논문을 바칩니다. 사랑합니다.

Table of contents

Preface	i
Acknowledgements.....	ii
Table of contents	v
List of abbreviations.....	vi
List of figures and tables	vii
List of papers	viii
Abstract	1
1. Introduction	2
1.1. Fish immune system.....	2
1.2. Mucosal immune system in mammals and fish	4
1.3. Key contributors of the intestinal immune defence in fish	6
1.3.1. T cells	7
1.3.2. B cells and immunoglobulins.....	8
1.3.3. Monocytes/macrophages	9
1.4. Intestinal homeostasis and inflammation	11
1.5. Imaging flow cytometry	17
1.6. Transcriptomic approaches	17
2. Objectives.....	20
3. General discussion	22
3.1. Imaging flow cytometry protocols for studying immune cells	22
3.2. Characterization of salmon intestinal cells.....	26
3.3. Link between inflammation and the intestinal adherent cells.....	36
4. Conclusions	47
5. Contribution to the field	49
6. Future perspectives	51
7. References.....	53

List of abbreviations

APC	Antigen presenting cell
CD	Cluster of differentiation
CSF	Colony stimulating factor
DC	Dendritic cell
DE	Differentially expressed
FC	Flow cytometry
GALT	Gut-associated lymphoid tissue
IBD	Inflammatory bowel disease
IEC	Intestinal epithelial cell
IEL	Intraepithelial lymphocyte
IFC	Imaging flow cytometry
IFN	Interferon
Ig	Immunoglobulin
IL	Interleukin
LP	Lamina propria
LPL	Lamina propria leucocyte
MALT	Mucosa-associated lymphoid tissue
MHC	Major histocompatibility complex
miRNA	microRNA
mRNA	messenger RNA
NF- κ B	Nuclear factor kappa-light-chain-enhancer of activated B cells
pIgR	Polymeric Ig receptor
RNA-Seq	RNA sequencing
TCR	T cell receptor
TGF	Transforming growth factor
TLR	Toll-like receptor
TNF	Tumor necrosis factor

List of figures and tables

Figure 1. Schematic description of the components of the mucosal immune system in the gastrointestinal tract.

Figure 2. Workflow of RNA-Seq-based transcriptome analysis.

Figure 3. Overview of the different studies undertaken in this dissertation.

Figure 4. Intestinal doublets and epithelial cells in mammals and teleost fish.

Figure 5. The expression of genes linked to macrophages in the distal intestine of salmon fed soybean products or control diets.

Figure 6. Diet-induced changes in intestinal cell population and phagocytic activity in salmon.

Figure 7. Graphical summary of the results presented in this dissertation.

Table 1. List of studies that investigated the changes in gene expression in the intestine of fish fed soybean- or soy saponin-containing diets.

List of papers

Paper I Park, Y., Abihssira-García, I.S., Thalmann, S., Wiegertjes, G.F., Barreda, D.R., Olsvik, P.A. and Kiron, V. (2020) Imaging flow cytometry protocols for examining phagocytosis of microplastics and bioparticles by immune cells of aquatic animals. *Front. Immunol.* 11:203.

Paper II Park, Y., Zhang, Q., Wiegertjes, G.F., Fernandes, J.M.O., and Kiron, V. (2020) Adherent intestinal cells from Atlantic salmon show phagocytic ability and express macrophage-specific genes. *Front. Cell Dev. Biol.* 8:580848.

Paper III Park, Y., Zhang, Q., Fernandes, J.M.O., Wiegertjes, G.F., and Kiron, V. (2020) miRNA and mRNA profiles unveil macrophage heterogeneity among intestinal cells of Atlantic salmon. Manuscript.

Paper IV Kiron, V., Park, Y., Siriyappagouder, P., Dahle, D., Vasanth, G., Dias, J., Fernandes, J.M.O., Sørensen, M., and Verlhac Trichet, V. (2020) Intestinal transcriptome analysis reveals soy derivative-linked changes in Atlantic salmon. *Front. Immunol.* 11:596514.

Abstract

Fish intestine is the primary site where the interaction among dietary components, microbiota and immune system takes place. Teleost gut-associated lymphoid tissue differs from those of mammals morphologically and functionally; it has a diffuse and complex structure. However, there is not much knowledge regarding the intestinal cells of teleost, including Atlantic salmon. Therefore, I have characterized certain intestinal cells and studied the inflammatory responses resulting from a common problem associated with the salmon industry.

Imaging flow cytometry protocols were first optimized to examine the intestinal immune cells and study phagocytosis. This approach helped to understand that salmon intestinal cells have diverse cell populations. Focusing on the isolated adherent intestine cells, I performed an integrative analysis of mRNA and small RNA to identify the cell types. Based on their specific markers the adherent intestinal cells seem to have polarized macrophages. The transcriptomic and cellular study on salmon fed soy products revealed inflammation-induced disturbances in ion transport and metabolic pathways as well as predominance of M2-macrophages during inflammation.

This thesis gives insights into the intestinal cell types, and the tissue responses to an allergen. Future studies on the adherent cell population would cast light on how these cells participate in intestinal defence.

1. Introduction

1.1. Fish immune system

Fishes are a diverse group of vertebrates, and their abundance, richness and phylogenetic diversity make them excellent models for studying the immune system (Gorman and Karr, 1978). From an evolutionary perspective, fishes seem to have undergone a transition in reliance on their immune system. While the more primitive and fundamental defence mechanism, the innate immune system, was mainly found in most early fish, the mammalian-like adaptive immune system appeared first in jawed fish 450 million years ago (Flajnik and Kasahara, 2010). Teleost fish, the largest group of living vertebrates, possess both innate and adaptive immune systems, as in mammals. Although there are similarities between the piscine and mammalian immune systems, their structure and form are quite different (Scapigliati et al., 2018). Generally, teleost fish lymphoid tissues have a diffuse and complex system. Fishes lack bone marrow and lymph nodes which are the main lymphoid organs in mammals and instead their key immunological organs are thymus, kidney and spleen. Among them, anterior kidney (or head kidney), the key hematopoietic organ in fish has a role similar to that of bone marrow in mammals. Hence, fishes have been proposed as a model to understand human immune system. For example, zebrafish (*Danio rerio*) is an exciting and popular animal model that has been employed for human disease research due to several advantages such as a high genetic similarity to humans, rapid development, and ease of genetic manipulation (Xu and Zon, 2010). Furthermore, carnivorous fishes like Atlantic salmon (*Salmo salar*) have been spotlighted as an in vitro model to study cardiac disease mechanism, host-pathogen interaction (Noguera et al., 2017) and intestinal inflammation (Krogdahl et al., 2015).

The innate immune system is the first-line of defence that deploys components that are effective against invading foreign substances such as bacteria, virus and parasites. Smith et al. (2019) reviewed the fish immune system and categorized the innate

immune component into: (1) physical barriers, (2) cellular components, and (3) humoral components. The major physical barriers include mucosal areas where the host-pathogen encounter takes place. To prevent the entry of pathogens into the epithelial layer, the system stimulates the goblet cells to secrete mucus, which washes out the invaders and act as both physical and chemical barrier (Esteban, 2012). However, once pathogens evade the defence line, cellular components start to work and respond to the pathogens by recognizing their typical pathogen-associated molecular patterns and stimulating the signaling pathway to activate the adaptive immune system (Smith et al., 2019). The innate immune cells also produce macromolecules such as lysozyme, antimicrobial peptides and acute-phase proteins, which are considered as humoral components (Smith and Fernandes, 2009, Ruangsri et al., 2012).

The adaptive immune system in fish consists of humoral and cellular components (Smith et al., 2019). B and T cells are essential components of the adaptive immune system. Humoral components (antibody-mediated) are mainly activated by the secretion of antibodies that are produced by plasma B cells (Chiaruttini et al., 2017). T lymphocytes are important for both humoral and cellular responses. After the antigens are presented by antigen presenting cell (APC), T cells are activated; after CD4⁺ T cells receive the exogenous antigens from MHC-II and under the effect of inductive cytokines, T cells differentiate and produce characteristic cytokines such as the proinflammatory cytokines. Treg lymphocytes of the T cell subset have immunosuppressive properties and produce regulatory cytokines. On the other hand, cytotoxic CD8⁺ T cells (antigen-specific cytotoxicity) are activated when endogenous antigens are presented via MHC-I (Smith et al., 2019).

Like mammals, fish immune cells consist of T and B lymphocytes, granulocytes, monocytes, macrophages and dendritic cells (DCs) (Neumann et al., 2001, Scapigliati et al., 2018). Tissue-specific phenotypes of these immune cells are reported in fish, and their numbers increase or decrease in response to various stimuli e.g. infection or

vaccination (Salinas, 2015). While B cells are present dominantly in most systemic compartments such blood, spleen, and head kidney (Parra et al., 2015), T cells are mainly linked to mucosa-associated lymphoid tissues (MALTs) such as the skin, gills and intestine (Koppang et al., 2010). A thorough understanding of the different immune cell populations and their responses to antigens is necessary to advance our knowledge of the fish immune system.

1.2. Mucosal immune system in mammals and fish

The mucosal immune system stands in the forefront of the defence system that is responsible for protecting the mucosal surface against mainly potential viral, bacterial and fungal pathogens. Three main roles ascribed to the mucosal immune system are: 1) serving as the first-line of defence against antigens and infection by activating signaling pathways in epithelial barriers, 2) evoking local and systemic immune responses to commensal bacteria and food antigens (oral tolerance) and 3) initiating an immune response and stimulating other secondary lymphoid tissues (such as spleen, lymph nodes) where lymphocytes are activated (Baumgart and Dignass, 2002, Montilla et al., 2004). In humans, the mucosal immune system is localized in the oral-pharyngeal cavity, gastrointestinal tract, respiratory tract and urogenital tract, as well as the exocrine glands (Murphy and Weaver, 2016). Among them, intestine has the largest population of microbes in human body, and hence this site has to effectively manage antigen encounters than any other part (Whitman et al., 1998). The GI mucosal immune system consists of three compartments: epithelial layer, lamina propria (LP) and gut-associated lymphoid tissues (GALTs) (Wu et al., 2014). The lymphoid elements of GALT can be morphologically and functionally subdivided into two: 1) the organized mucosa-associated lymphoid tissue including mucosal follicles and 2) the diffuse mucosa-associated lymphoid tissue, consisting of leukocytes scattered throughout the epithelium and lamina propria of the mucosa (Neutra et al., 1996). In higher vertebrates, two main cell populations are present: intraepithelial lymphocytes (IELs)

and lamina propria leukocytes (LPLs). IELs reside between intestinal epithelial cells (IECs) and are capable of a wide range of effector functions during infection, while LPLs include T and B cells, plasma cells, mast cells and macrophages (Schley and Field, 2002). DCs, one of APCs that are present both near the epithelial cells and in the LP capture antigens by extending their dendrite through the epithelium. In addition, DCs near microfold cells in Peyer’s patches receive antigen information and migrate to mesenteric lymph nodes. Subsequently, antigen-specific T cells, after receiving antigen information from APCs, become activated and get differentiated into effector cells including helper, killer and regulatory T cells (Figure 1).

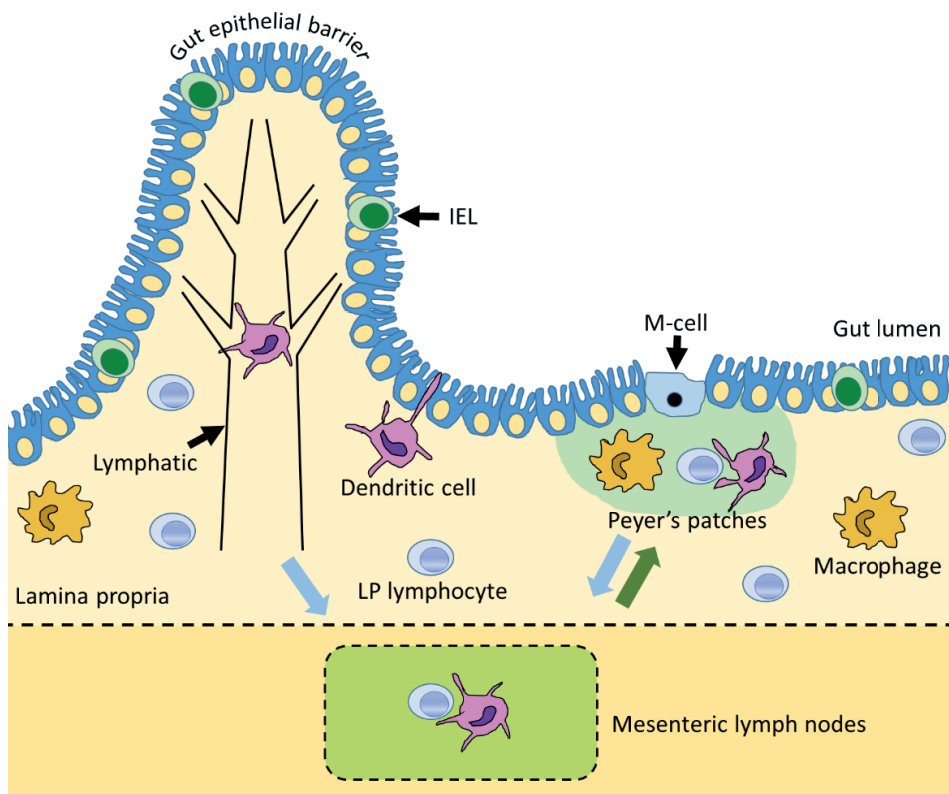


Figure 1. Schematic diagram of the components of the mucosal immune system in the gastrointestinal tract of mammals. LP, lamina propria; IEL, intraepithelial lymphocyte; M-cell, microfold cell. Based on Wu et al. (2014).

Fish mucosal surfaces play critical roles in nutrition uptake, ion exchange, and immune defence. Like mammals, teleost fish possess MALTs that take part in the immune defence at the mucosal areas (Parra et al., 2015). The MALTs include the GALT, skin-associated lymphoid tissue, the gill-associated lymphoid tissue and the nasopharynx-associated lymphoid tissue. However, the knowledge about the fish mucosal immune system is rather limited because of the following reasons: (1) the essential mammalian immune components, such as Peyer's patches, IgA- and IgM-joining J chain are not yet reported in teleost fishes (Parra et al., 2016), (2) lack of appropriate cell markers and intestinal cell isolation techniques and (3) incomplete knowledge about other immune cells such as DCs and M-cells. For instance, the existence of important immune cells like DCs in fish that respond to pathogens has not been well understood although few studies have reported that fish dendritic-like cells have similar morphological features as those of mammalian DCs and they express DC marker genes (Lugo-Villarino et al., 2010, Haugland et al., 2012).

1.3. Key contributors of the intestinal immune defence in fish

Teleost fish have three intestinal segments that can be distinguished based on morphological and functional traits. Each segment has different immune cell populations and roles (Parra et al., 2015). Macronutrient uptake occurs through the absorptive cells in the anterior intestine and uptake and transport of antigens take place in the mid intestine. The distal intestine is the immunologically-relevant segment where the antigens are sampled from lumen by the APCs (Rombout et al., 2011). In one of the early studies on rainbow trout (*Oncorhynchus mykiss*), immune cells such as lymphocytes, macrophages, and some plasma cells were found in the mid and distal segments of the intestine (Georgopoulou and Vernier, 1986). In Atlantic salmon, expression of several marker genes of T-lymphocytes (*cd4-1*, *cd8a*, *tcra* and *tcrg*) and B-lymphocytes (*slgm*, *mlgm*, *slgt* and *mlgt*) were relatively low in esophagus and stomach, but higher in the pyloric caeca, mid- and distal intestine. Also, the messenger

RNA (mRNA) levels of *igm* and *igt* were found to increase from the pyloric caeca to the distal intestine (Løkka et al., 2014). In addition, in rainbow trout (Perdiguero et al., 2019), percentage of IgD⁺IgM⁻ cells was higher in the intestine compared to that in the spleen. Therefore, special attention should be paid to the immunological roles of mid- and distal intestine.

The first study on intestine cell isolation was performed on rainbow trout (McMillan and Secombes, 1997). Later, many researchers put in effort to isolate and characterize intestinal immune cells in other fish such as gilthead seabream (*Sparus aurata*) (Salinas et al., 2007) and Atlantic salmon (Attaya et al., 2018). However, lack of monoclonal antibodies and complexity of intestinal cell isolation procedures are still limiting our understanding of immune cells in fish.

1.3.1. T cells

Teleost fish have mucosal T cells, and they express genes related to T cell receptors (TCR) such as *tcrab* and *tcr gb*, *cd3*, *cd4* and *cd8*, as well as *mhc1* and *mhc2* genes (Toda et al., 2011, Fischer et al., 2003). The presence of T cells in the intestinal epithelium and LP of carp (*Cyprinus carpio* L.) was demonstrated nearly two decades ago (Rombout et al., 1998). A later study on salmonids revealed the presence of more CD3ε⁺ cells in the thymus, gills, and intestine (Koppang et al., 2010). Dietary components may also influence the intestinal T cell populations - a significant increase in expression of the genes *cd3pp*, *cd4* and *cd8b* was reported in the distal intestine of Atlantic salmon fed soybean meal (Bakke-McKellep et al., 2007). An induction of T cells as an intestinal inflammatory response to dietary allergens has been reported in humans (Sollid, 2002). It is worthwhile to monitor the changes in different T cell populations in fish intestine to extend our understanding on intestinal immune system of fish .

1.3.2. B cells and immunoglobulins

Antibody or immunoglobulin (Ig) is produced by differentiated B cells called plasma cells. In teleost fish, three major Ig isotypes are expressed on the surface of B cells: IgM, IgT or IgZ and IgD. In mammals, the J chain and polymeric Ig receptor (pIgR) are essential for the transportation of IgA and IgM across IECs (Johansen et al., 2000). However, it has been suggested that the presence of J chain may not be a requirement for the pIgR-immunoglobulin interaction in fish (Zhang et al., 2010). Rainbow trout has a pIgR and its secretory component is similar to those of mammalian IgA and IgM (Zhang et al., 2010) while fugu (*Takifugu rubripes*) pIgR is associated only with IgM (Hamuro et al., 2007). IgM is the main antibody in teleost fish, and probably its isotypes could have similar functions as those of mammalian IgA, which is abundant in mucous secretions (Cerutti et al., 2011). The latter neutralizes toxin and pathogenic microbes and prevents the attachment of commensal microbiota on the epithelial cells (Macpherson et al., 2008). Intestinal bacteria in rainbow trout was found to be coated with IgT, which responded to intestinal parasites in the gut, indicating their special role in mucosal immunity (Zhang et al., 2010).

The proportion of B cells within the GALT is different in teleost fishes. In carp (Rombout et al., 1998) and rainbow trout (Zhang et al., 2010), about 2-12% B cells among leukocytes isolated from LP of both anterior and posterior intestine were IgM⁺ cells. In Atlantic halibut (*Hippoglossus hippoglossus*), IgM⁺ cells were present within the epithelium and LP (Grove et al., 2006). In addition to their role in adaptive immunity, B-lymphocytes have been reported to perform phagocytosis. In the peritoneal cavity of mice (Parra et al., 2012) around 10-15% B cells have phagocytic ability. In teleosts, around 60% of B cells found in all systemic compartments perform phagocytosis (Li et al., 2006).

1.3.3. Monocytes/macrophages

In mammals, there are two macrophage subsets; classically and alternatively activated (Zhou et al., 2014). The classically activated macrophages that take part in inflammatory or microbicidal responses belong to the M1 types that are primed by interferon-gamma (IFN γ) and tumor necrosis factor-alpha (TNF α). On the other hand, the alternatively activated forms are called M2 macrophages and are involved in tissue repair and wound healing. There are three M2-macrophage subtypes; M2a subset is activated by interleukin-4 and/or interleukin-13; M2b is stimulated by immune complexes or apoptotic cells and M2c is primed by interleukin-10 (IL-10), transforming growth factor-beta (TGF- β) and/or glucocorticoid (Zhou et al., 2014). Although the polarization and functionality of mammalian macrophage subsets are clearly described, such details about fish macrophages are not yet reported. Nevertheless, Wiegertjes et al. (2016), Grayfer et al. (2018) and Hodgkinson et al. (2015) have reviewed the different types of fish macrophages.

Fish M1 macrophages that can phagocytize are classically polarized by colony stimulating factor-1 (CSF-1), IFN γ , IFN γ -related (IFN γ -rel) and TNF α 1/2. The M2 types in fishes are believed to be primed by IL-4/IL-13, IL-10 and glucocorticoids (Grayfer et al., 2018, Forlenza et al., 2011). Furthermore, Wiegertjes et al. (2016) reported reliable markers for M1-macrophages (NOS-2) and M2-macrophages (arginase-2). A recent study on transcriptome of carp macrophages revealed the potential markers for M1 (*il1b*, *nos2b* and *saa*) and M2 (*timp2b*, *tgm2b* and *arg2*), which indicate that fish macrophages could have conserved functions and common transcripts to mammals (Wentzel et al., 2020b). Macrophages in fishes are stimulated by CSF-1 (Rieger et al., 2014, Rieger et al., 2013). However, the production of soluble CSF-1 receptor through CSF-1 stimulation causes the polarization to M2 form (Rieger et al., 2013). This soluble receptor evokes the expression of the anti-inflammatory cytokine IL-10 (Rieger et al., 2015). However, it should be noted that some teleosts including the Japanese pufferfish have more than one CSF1R (Williams et al., 2002), and it is not yet clear how

these act together to promote the differentiation of macrophages. Hence, the polarization in mammals and fish cannot be presumed to be identical. Previous studies have indicated possible IFN γ -induced polarization to M1-like macrophages in goldfish (Grayfer and Belosevic, 2009) and carps (Arts et al., 2010). Although fishes are known to have two forms of this type II interferon (IFN γ and IFN γ -rel), both of them can cause M1-polarization and they have distinct and redundant functions in the differentiation (Grayfer et al., 2010, Grayfer and Belosevic, 2009). It has also been reported that IFN γ -rel strongly influences macrophage phagocytosis and nitric oxide production (Grayfer et al., 2010, Grayfer and Belosevic, 2009). In addition, carp M1-macrophages increased nitric oxide production while the M2-macrophages increased oxidative phosphorylation and glycolysis, suggesting that IFN γ may influence macrophage metabolic reprogramming (Wentzel et al., 2020a). Tumor necrosis factor alpha 1 and 2 (*tnfa1* and *tnfa2*) in fishes are thought to have roles similar to TNF α of mammals (Nguyen-Chi et al., 2015).

As for the phagocytosis in macrophage subsets, in mammals both M1- and M2-macrophages are known to have higher phagocytic ability compared with that of naive macrophages (M0) (Lam et al., 2016). However, M2-macrophages showed higher phagocytic affinities and capacities than M1-macrophages (Schulz et al., 2019). Furthermore, a study in mice showed that phagocytosis of *Porphyromonas gingivalis* by M1-macrophages produced higher expression levels of TNF- α , IL-12 and iNOS compared to those of M0- and M2-macrophages, indicating that the activation of M1-macrophages could contribute to the initiation of inflammatory responses (Lam et al., 2016). Like mammals, fish inflammatory/M1-macrophages are well known to have ability to phagocytose pathogens and produce pro-inflammatory cytokines, reactive oxygen and nitrogen intermediates as reviewed by Grayfer et al. (2018). These studies are mainly focused on head kidney-derived macrophages. As for the intestinal macrophages in teleost fishes, some studies have suggested the presence of intestinal macrophage-like cells in Atlantic cod (*Gadus morhua*) (Inami et al., 2009) and rainbow

trout (Georgopoulou and Vernier, 1986). In Atlantic salmon that were anally intubated with fluorescent yeast, the microbial cells were found near the large nuclei of macrophage-like cells that were located near the epithelium, indicating that intestinal macrophage-like cells could sample antigens like mammalian macrophages (Løkka et al., 2014b). Thorough functional and morphological characterization using cell markers are warranted in fish.

1.4. Intestinal homeostasis and inflammation

The intestine is one of the organs where interactions between the host and their cohabiting organisms take place. It is known that the resident microorganisms and host establish a mutually beneficial relationship to sustain the host's health status. However, failure to maintain an optimal microbial balance can lead to intestine dysfunction, negatively impacting the local and systemic organ health in mammals (Garrett et al., 2010). Under normal conditions, mucosal barrier avoids unnecessary immune responses and keep the microbial balance in check without getting adversely affected by environmental changes in the intestinal lumen (Okumura and Takeda, 2018). In other words, impaired barrier functions allow bacteria to translocate across epithelium, triggering massive cellular responses and causing the development of immune disorders like inflammatory bowel diseases (IBD) (Okumura and Takeda, 2018).

Intestinal inflammation is a protective response against harmful stimuli that break epithelial barriers, triggers localized tissue damages and then causes systemic response (Maloy and Powrie, 2011, Okumura and Takeda, 2018). A study on IBD (Zhang et al., 2017a) demonstrated that a breach in the mucus barrier and the increased intestinal permeability allowed more bacteria to adhere to the intestinal epithelial cells in IBD patients, which led to changes in both composition of microbiota and the expression levels of pro-inflammatory cytokines. This indicates that the composition of intestinal microbiota is influenced by environmental factors as in the case of IBD, and the interaction between microbiota and intestinal immune cells is crucial to maintain

intestinal homeostasis. However, it is largely unknown how dysbiosis occurs and leads to intestinal inflammation.

To maintain the intestinal homeostasis and safeguard the organ from inflammation-caused complications, the resident microorganisms must communicate with immune effectors in the epithelium, which are known to initiate metabolic/immunological reactions (Forchielli and Walker, 2005). IECs in most vertebrates including teleost fish express various pattern recognition receptors (Li et al., 2017). Of the receptors, toll-like receptors (TLRs) play a pivotal role in initiating immune response by sensing conserved molecular structures in bacteria, viruses, fungi and parasites known as pathogen-associated molecular patterns (Nie et al., 2018). Teleost fishes have TLR1-5, TLR7-9, TLR13-14, TLR18-23 and TLR25-28 (Sundaram et al., 2012, Nie et al., 2018). Although fish TLRs have high structural similarities with those of mammalian TLRs, the former types have very distinct functional features. For example, *tlr4*, *tlr6* and *tlr10* that are associated with the recognition of bacterial lipids or proteins are absent in most fish genomes (Palti, 2011). In zebrafish, unique TLR genes have been identified, namely the *tlr4*-like paralogues *tlr4a* and *tlr4b*, which are not orthologous to their mammalian counterparts (Sepulcre et al., 2009, Sullivan et al., 2009, Loes et al., 2019). They cannot recognize LPS and these genes inversely regulate MyD88-dependent signaling pathway, suggesting their unique roles in TLR4 signaling against pathogen-associated molecular patterns (Sepulcre et al., 2009). These authors inferred that mammalian-like TLR4s in zebrafish are specific to alternative ligands for the TLR-mediated immune defenses. In mammals, bacteria-initiated signaling via TLR4/MyD88 stimulates the IECs to produce antimicrobial molecules (Vaishnava et al., 2011, Kobayashi et al., 2005). Furthermore, compared to wild-type mice, mice with IELs lacking MyD88 exhibited more tissue damage, barrier disruption, impaired goblet cell responses, and in infected mice more pathogenic bacteria penetrated into the intestinal epithelium (Bhinder et al., 2014).

Studies in teleosts have revealed that environmental factors-induced immune responses can influence intestinal homeostasis; the responses are dependent on the type of foreign antigen. In rainbow trout the expression of *il1b*, *il8*, *tnfa* and *ifnr* increased in the intestine after a challenge with *Aeromonas salmonicida* (Mulder et al., 2007). Conversely, seabass (*Lateolabrax japonicus*) larva fed a probiotic diet (*Lactobacillus delbrueckii* ssp.) had significantly higher number of intestinal T cells, higher mRNA levels of *tcr* and lower levels of *il1b* and *il10*, *cox2* and *tgfb* than those of control, suggesting that probiotics may cause an expansion of immature T cells (Picchietti et al., 2009). Furthermore, a study on salmon (Vasanth et al., 2015) reported that dietary probiotics helped alleviate intestinal inflammation. It should be noted that IECs in mammals play important roles in regulating not only nutrient absorption but also barrier functions by sensing microbial stimuli and coordinating the subsequent immune responses (Peterson and Artis, 2014). An intestinal epithelial cell line from the gastrointestinal tract of rainbow trout, called RTgutGC, has been developed and the authors found that their viability decreased in an LPS dose-dependent manner (Kawano et al., 2011). A recent study employing this cell line showed that RTgutGC cells expressed pro-inflammatory cytokines such as *il1b* and *il8* in response to various stimuli including LPS, nucleotides, mannan-oligosaccharides, and beta-glucans (Wang et al., 2019a). Taken together, it is clear that pro-inflammatory cytokine responses are triggered in the teleost intestine as a consequence of danger signals. However, cell-specific immune responses and the signaling pathways that drive inflammation in the intestine remain unclear.

Intestinal health in farmed fish is an active research area, propelled by the increasing use of plant- and other novel ingredients in aquafeeds. For instance, the soy bean-linked intestinal inflammation in fish is attributed to saponin. Such diet-induced inflammation can reduce growth and nutrient utilization (Gu et al., 2018, Zhang et al., 2018). Soybean-induced inflammation can alter the structure of lamina propria, increase inflammatory cells and reduce the absorptive vacuoles in the enterocytes in the distal intestine of fish (Bakke, 2011). Soy saponin is an antinutritional compound

that is commonly present in soybean derived feed ingredient, which is a current fishmeal replacer. It is well known that saponin could trigger inflammation process in intestine (Johnson et al., 1986) and disturb digestion of proteins and lipids in mammals (Francis et al., 2002). It has been shown in Atlantic salmon that the severity of inflammation can increase with the dose of the compound (Krogdahl et al., 2015). Several studies have delineated the gene expression in the intestine of fish fed soybean or soy saponin containing diets, as presented in Table 1. In most studies, the expression of inflammatory cytokines such as *il1b*, *il17* and *tnfa* increased in the intestine. Furthermore, higher mRNA level of *il8*, a major mediator during inflammatory responses was noted in the soy-fed groups. Studies have also reported that the expression of anti-inflammatory cytokine *il10* are down-regulated in the intestine of soybean fed fish. Considering the adverse effects of saponin, it is essential to study the responses in the fish intestine at greater depth employing advanced sequencing and cell-based approaches.

Table 1. List of studies that investigated the changes in gene expression in the intestine of fish fed soybean- or soy saponin-containing diets.

Species	Diets	Sampling time	Tissue	Up-regulated genes	Down-regulated genes	References
Atlantic salmon (<i>Salmo salar</i>)	Soybean meal (20%)	Early- day 3, 4, 5 & 7 Late- day 10, 14, 17 & 21	DI	<i>il17a</i> , <i>il17g</i> , <i>il1b</i> , <i>ifna</i> , <i>ifng</i> , <i>tcrg</i> , <i>cd4a</i> , <i>cd8</i> , <i>tgfb</i> , <i>par2</i> and <i>myd88</i>	<i>gilt</i>	Marjara et al. (2012)
	Soybean meal (46%)	Day 1, 3 & 7	DI	<i>cd3g</i> and <i>cd8b</i> <i>il1b</i> was not induced with high variation	<i>gilt</i> and <i>tgfb</i>	Lilleeng et al. (2009)
	Soybean meal (20%)	Day 1, 2, 3, 5 & 7	DI	NFκb-related genes, regulator genes of T cell and B cell function	Anti-oxidant activity-related genes	Sahlmann et al. (2013)
	Soybean meal (20%)	Day 54	DI	<i>anxa1</i> , <i>anxa3</i> , <i>anxa4</i> , <i>anxa5</i> and <i>tnfr</i>	<i>mhc1</i> and <i>mhc2a</i>	Skugor et al. (2011)
	Soy concentrate (30%) or Soybean molasses (30%)	Week 3	MI, DI	<i>igm</i> in distal intestine (only soybean molasses diet)	-	Krogdahl et al. (2000)
	Soy saponin supplementation to pea protein	Day 80	DI	<i>nfkβ</i> , <i>tnfa</i> , and <i>anxa1</i>	<i>ifn</i>	Kortner et al. (2012)
	Soy saponin (0, 2, 4, 6, 10 g/kg)	Week 10	DI	<i>myd88</i> and <i>mmp13</i> <i>il17a</i> (highest in 10g/kg diet)	<i>tcrg</i>	Krogdahl et al. (2015)
	Soybean meal (26, 40 or 54%)	Week 8	DI	<i>il1b</i> , <i>il8</i> , <i>tnfa</i> , <i>il17a</i> , <i>il22</i> and <i>tgfb</i>	-	Gu et al. (2016)

Turbot (<i>Scophthalmus maximus</i> L.)	Soybean meal (40%)	Week 4	DI		<i>il1b, tnfa</i> and <i>nfkfb</i>	<i>tgfb, pparg</i> and <i>ampk</i>	Liu et al. (2018)
		Week 12	DI		<i>tnfa</i> and <i>nfkfb</i>	<i>tgfb, pparg</i> and <i>ampk</i>	
Japanese seabass (<i>Lateolabrax japonicus</i>)	Soy saponin (2.5, 7.5 or 15%)	Week 8	DI		<i>il1b, il8</i> and <i>tnfa</i>	-	Gu et al. (2018)
	Soybean meal (50 or 75%)	Week 8	Fore and mid gut		<i>tnfa, il1b, il2</i> and <i>il8</i>	<i>il4</i>	Zhang et al. (2018)
Zebrafish (<i>Danio rerio</i>)	Soybean meal (50%) or Soy protein isolate (43%) or Soy saponin (50%)	9 dpf	Larvae		<i>il1b</i> and <i>il8</i>	<i>il10</i> (only for Soy saponin 50% diet)	Hedraera et al. (2013)
Orange-spotted grouper (<i>Epinephelus coioides</i>)	Soybean meal (50 or 100%)	Day 30	Intestine		<i>il1b</i> and <i>il16</i>	<i>il10</i>	Wang et al. (2017)
Common carp (<i>Cyprinus carpio</i> L.)	Soybean meal (20%)	Week 1 & 3	DI		<i>il1b</i> and <i>tnfa1</i> (week 1)	<i>il10</i> (week 1)	Urán et al. (2008)
		Day 63	DI		<i>tgfb</i> (week 3) <i>il1b, il10</i> and <i>il17f</i>	-	Miao et al. (2018)
Juvenile Totoaba (<i>Totoaba macdonaldi</i>)	Soybean meal (0, 22, 44 or 64%)	Week 4 & 8	DI		<i>il8</i> (22% in week 4)	<i>il8</i> (for 44% and 64% in week 4)	Fuentes-Quesada et al. (2018)

1.5. Imaging flow cytometry

Flow cytometry (FC) is a technique to quantify information about cell phenotypes, their characteristics and functions. However, conventional FC is not suitable to identify small-sized particles (<300 nm) (Görgens et al., 2019) and does not provide information about the marker localization within the cells. Furthermore, another obstacle in conventional FC is auto-fluorescence. Thus, the system is unable to distinguish between false-positive and false-negative events (Barteneva et al., 2012).

Imaging flow cytometry (IFC), also called multispectral imaging flow cytometry, is a powerful tool to collect the information from single cells, employing fluorescent imaging. Unlike conventional FC, IFC offers various gating strategies to accurately analyze the cells; based on real cell images and morphological information including an aspect ratio of cells, diameter and cell volume, and other morphological features (Barteneva et al., 2012). Another advantage of IFC is that it provides information about not only single cell but also cell aggregates including doublets to study cell-cell interaction (Terjung et al., 2010). For example, Ahmed et al. (2009) analyzed T cell—macrophage conjugates to evaluate movements of molecules between immune cells and/or between an immune cell and pathogen.

So far, few researchers have employed IFC to understand cells in fish species such as zebrafish (Rességuier et al., 2017) and gold fish (Rieger et al., 2010). These studies have used IFC for cell identification using nucleus staining dye and for measuring phagocytic activity using fluorescent particles.

1.6. Transcriptomic approaches

Transcriptomic studies are important to reveal transcriptome profiles and identify differentially expressed (DE) genes and the interaction between the genes. Traditionally, to study fish immune responses, the abundance of target gene

transcripts are measured using RT-qPCR. After the introduction of Next Generation Sequencing techniques, RNA sequencing (RNA-Seq) has been widely employed to explore the transcriptome profile in fish tissues or cells i.e. Generally, RNA-Seq has four steps, according to the work-flow described in Figure 2.

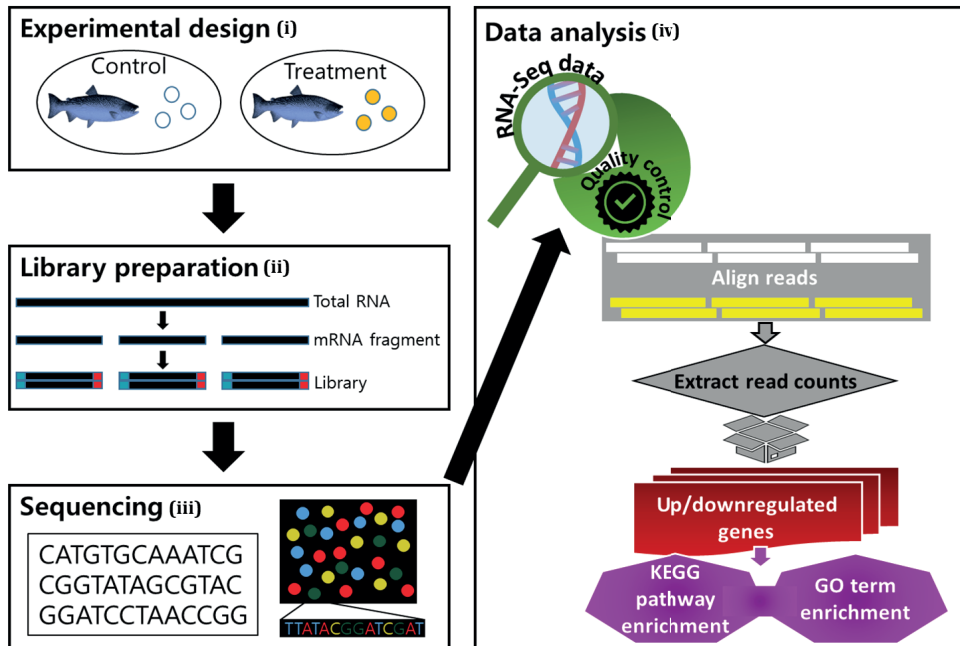


Figure 2. Workflow of RNA-Seq-based transcriptome analysis. The four major steps are: (i) Experimental design, (ii) Sample preparation and library generation, (iii) Next-generation sequencing of the library, (iv) *de novo* assembly, annotation and read count determination and (v) Bioinformatic analysis. In the fifth step, quality of RNA-Seq data is evaluated and then the reads (quality score > 30) are aligned to a reference genome. Next, the read counts are extracted, and then DE genes between the two experimental groups are obtained for further interpretation. Functional analysis including KEGG pathway and GO term enrichment analysis can then be performed employing the DE genes.

Earlier studies in fish focused on the immunological tissues such as liver, spleen and head kidney to study transcriptome responses to infections and stresses (Martin et al., 2016). However, with the growing interest on the interaction between nutrients/feed ingredients, GALT and microbiota, investigations on gut transcriptome have gained

importance in fish nutrition studies. Global gene profiles revealed by RNA-Seq allowed researchers to understand soybean meal-induced inflammation in the distal intestine of Atlantic salmon (De Santis et al., 2015, Król et al., 2016). In the study of De Santis et al. (2015), a set of immune-related genes, namely T cell-related genes, *tnf* and *nfkb* signalling pathways were up-regulated in the distal intestine of fish fed soybean meal for 12 weeks. Król et al. (2016) used a transcriptome profiling technique to study the effects of dietary plant proteins (single or different plant ingredients as fishmeal replacers) on the distal intestine of salmon, and found 78 potential biomarkers for diet-induced enteritis.

Non-coding RNAs including microRNAs (miRNAs) regulate the expression of genes in organisms. MicroRNAs bind to the 3' UTR of mRNAs and negatively regulate their target transcripts (Ambros, 2004). In teleost fish, studies have indicated that miRNAs are involved in regulating growth (Yi et al., 2013, Campos et al., 2014), gonad development (Presslauer et al., 2017), organ development (Yan et al., 2013) and cell differentiation (Ramachandran et al., 2010). A recent study on salmon (Woldemariam et al., 2019) has profiled the miRNAs from different tissues (including intestine) and across developmental stages. The study showed that certain subsets of miRNAs are abundant depending on tissues and embryonic development, suggesting important biological functions of miRNAs. Furthermore, another study on salmon (Smith et al., 2020) that examined the changes in miRNA expression in adherent head kidney cells reported that miRNAs could influence macrophage differentiation; based on the morphological changes of the cells on day 1 and day 5 of culture. However, there are no studies that report the miRNA profile and their target gene regulation in the intestinal cells of fish.

2. Objectives

The intestine of fish is an important site where immunological responses to environmental changes such as diet, stress and microbes take place. Our knowledge of the fish intestinal immune system is rather limited. Hence, in this PhD project, I focused on the intestine of Atlantic salmon to study different aspects at the tissue or cellular level. For this, I employed two high-throughput technologies: (1) imaging flow cytometry (IFC), to study intestinal cell counts and their phagocytic activity and (2) transcriptomics, to characterize intestinal cells and tissue responses. The overall aim of this thesis was to develop a protocol to isolate the different cell populations from the intestine of Atlantic salmon and to study adherent cells and their phagocytic activity, and characterize their transcriptomes. Then both these approaches were employed to examine how intestinal inflammation influences transcriptomic and cellular responses in the intestine of Atlantic salmon.

Specific objectives are as follows (Figure 3):

1. To optimize IFC protocols for examining cell counts of head kidney (HK) leukocytes and phagocytic properties of HK macrophage-like cells in Atlantic salmon (**Paper I**).
2. To isolate and characterize distal intestinal (DI) cells of Atlantic salmon at the cellular and molecular levels (**Paper II**).
3. To study the mRNA and miRNA transcriptomes in DI cells of Atlantic salmon (**Paper III**).
4. To understand whether intestinal inflammation influences cellular and transcriptomic responses in DI tissues or cells of Atlantic salmon (**Paper IV**).

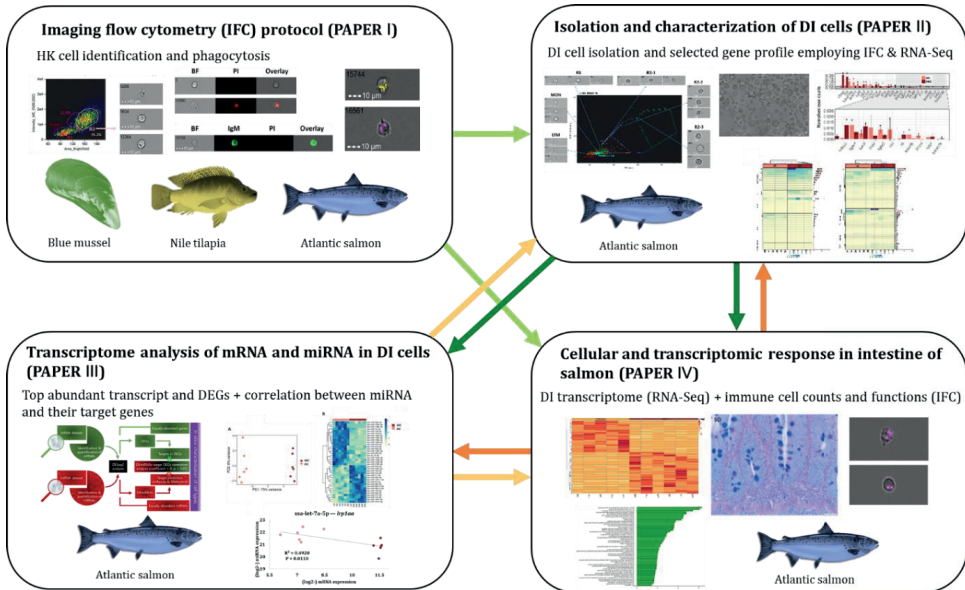


Figure 3. Overview of the different studies undertaken in this dissertation.

3. General discussion

Mucosal barriers in the fish intestine play critical roles in maintaining intestinal homeostasis. Many intestinal cells are involved in the immune response, and they are presumed to act in harmony to regulate the local (Okumura and Takeda, 2016) as well as systemic responses (Biteau et al., 2011, Ramakrishnan et al., 2019). Thus, in-depth knowledge of fish intestine is necessary to understand the crosstalk between antigen and epithelium as well as the immunological functions of GALTs. I employed a combination of IFC and transcriptomics to gather knowledge about the intestinal cells in Atlantic salmon as there is lack of appropriate cell markers. Therefore, firstly IFC protocols were optimized to differentiate the immune cells and study phagocytosis (**Paper I**). Then, to understand the characteristics of the intestinal cells, they were isolated and studied employing two high-throughput techniques, IFC and transcriptomics (**Paper II**). In addition, I performed an integrative analysis of mRNAs and miRNAs in the adherent cells from the intestine and head kidney of salmon to further understand their characteristics (**Paper III**). Finally, I investigated how intestinal inflammation influences transcriptomic and cellular responses in the intestine of salmon (**Paper IV**).

3.1. Imaging flow cytometry protocols for studying immune cells

Imaging flow cytometry (IFC) that is frequently employed in cell analysis has many advantages compared to conventional FC. The IFC method can accurately generate cell information by distinguishing false positive and negative events employing image-based analysis tools. IFC has been used in mammalian studies to understand cell/nucleus morphology, cell-cell interaction, phagocytosis, and rare cell detection (Barteneva and Vorobjev, 2016). For instance, a murine study (McGrath et al., 2017) employed IFC to delineate morphological characteristics of red blood cells and their nuclear size, and reported seven erythroid populations in bone marrow. The IFC

protocol has now been employed for studying fish intestinal cells (**Papers I, II and IV**). The molecular and cellular components of these cells are conserved across vertebrate species (Scapigliati et al., 2018). Therefore, the cell types in mammals and teleost fish are comparable to some extent (Figure 4). Zhao et al. (2014) detected doublets in mice intestinal cells with the help of IFC and suggested the interaction between DCs and T cells. In **Paper II**, I observed several doublets as well as oval shaped phagocytes among salmon intestinal cell populations. Another IFC study (Trapecar et al., 2014) quantified STAT1 and NF-kB expression in human intestinal epithelial cells, which are oval-shaped cells as observed in our study. It should be noted that mammalian endothelial cells are also oval shaped as discussed in **Paper II**. However, further investigation on their identity should be undertaken by employing specific cell markers.

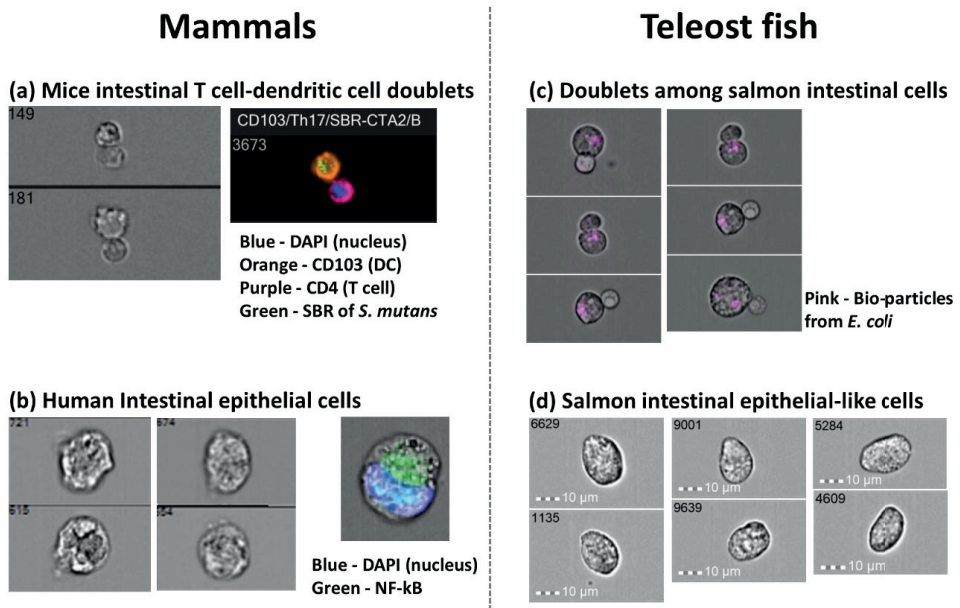


Figure 4. Intestinal doublets and epithelial cells in mammals and teleost fish. IFC images showing intestinal doublet cells in mice (a) and salmon (c), and epithelial cells in human (b) and salmon (d). Mammalian cell images are reproduced from Zhao et al. (2014) and Trapecar et al. (2014) with the permission from the American Society for Microbiology (ASM) and PLOS One, respectively.

For comparative purposes I also examined the head kidney macrophage-like cells (**Papers II and IV**) using the procedure described in **Paper I**. Similar to my approach, previous studies on salmon that employed conventional FC (Pettersen et al., 2008, Ulvestad, 2017) used the FSC vs SSC plot to study the cell population. For further understanding the head kidney cell populations, I used an IgM-specific antibody to determine the lymphocyte-like cell area within the BF area vs SSC intensity plot. These IgM⁺ cells that were separated by MACS were placed in low BF area vs low SSC intensity in the plot as shown by Jenberie et al. (2018) who used conventional FC. It should be noted that the low BF area vs low SSC intensity area includes not only IgM⁺ cells but also other cell types such as T lymphocytes and natural killer cells. Hence, we named the cells in the gate “lymphocyte-like cells”. Although around 90% of IgM⁺ cells were separated by MACS, they are not 100% pure IgM⁺ cells since the Fc-part of immunoglobulin M can bind to the Fc-receptors on macrophages. Jenberie et al. (2018) have reported that salmon HK IgM⁺ cells expressed macrophage markers, but their expression levels were very low (Cq > 36). Future studies must therefore consider blocking the immunoglobulins to Fc-receptors on other cells such as macrophages.

Another aspect that I investigated employing the IFC protocol was phagocytosis, which is a fundamental process in immunity and important for tissue homeostasis (Rosales and Uribe-Querol, 2017). In **Paper I**, IFC protocols for phagocytosis were established using the head kidney adherent cells or macrophage-like cells because they are better known compared to the intestinal cells. Several authors (Jenberie et al., 2018, Iliev et al., 2010) have already revealed that the adherent cells separated from head kidney leukocytes express specific markers of macrophages including *marco*, *csf1* and *mhc2b*, which agrees with the results reported in **Paper II**. IFC allowed us not only to quantify the number of particles engulfed by the phagocytes but also to detect the localization of the particles. Smirnov et al. (2015) also reported an IFC protocol to discriminate the binding and internalization of bacteria labeled with fluorescent particles by primary human neutrophils. In **Paper I**, two different types of particles, non-degradable (microplastic) and degradable particles (bio-particles from *Escherichia*

coli) were tested. Compared to microplastic particles, the bio-particles emit fluorescence when engulfed by cells. However, this occurs only upon acidification following ingestion by the cell. Thus, the brightness of the bio-particles within the cells will not be the same. Hence, the present study recommends the use of the fluorescent intensity feature rather than the spot count feature (commonly employed for detecting non-degradable particles) for accurately assessing the counts of degradable particles in phagocytes. The method of Smirnov et al. (2015) employed another algorithm, namely bright detail similarity score, which works similar to the fluorescent intensity feature to quantify the particles engulfed by human neutrophils. After standardizing the protocols for quantification of phagocytosis by monocytes/macrophages, the usefulness of this method for measuring phagocytosis by cells from three different aquatic animals, Atlantic salmon, Nile tilapia and blue mussel was demonstrated. From the study, it is clear that the phagocytic activity of cells from salmon and tilapia are influenced by incubation temperature. Similarly, the uptake of *E. ictaluri* by catfish peritoneal macrophages was significantly decreased at 4°C compared to 32°C (Kordon et al., 2018). Furthermore, uptake of *E. ictaluri* by zebrafish kidney macrophages was higher at 30°C and 37°C compared to 4°C (Hohn et al., 2009). The abovementioned studies indicate that the phagocytic activity of fish macrophages will be higher at their optimum temperature compared to lower or higher temperatures. The phagocytic activity of human leukocytes is also known to be affected by incubation temperature (Peterson et al., 1977). Interestingly, the phagocytic activity of hemocytes from mussel, a eurythermal species that can live in a wide range of temperatures, -1 to 20°C (Thyrring et al., 2015, Hiscock and Tyler-Walters, 2006), was not affected by incubation temperature. Culture condition could affect cellular functions including phagocytosis (Santos et al., 1995) and activity of bacteria (Hohn et al., 2009, Oben and Foreman, 1988) that were used for phagocytosis assay in **Paper I**. Furthermore, studies have indicated that the magnitude of phagocytic ability of human retinal epithelial cells depends on the culture media. This finding suggests that environmental factors including culture media could influence cell

functions as well as their phenotypes (Karl et al., 2006, Tian et al., 2005). In addition, nutrient composition in culture media could influence the metabolic activity of cells. In a salmonid study, the viability of RTgutGC cells reduced with increasing concentration of zinc in the medium, indicating that intestinal cell viability is determined by the nutrients in the medium (Antony Jesu Prabhu et al., 2018). Thus, future studies are needed to determine the effect of different culture media on phagocytosis of fish immune cells to optimize the culture condition and IFC phagocytosis assay. Cell isolation methods and in vitro culture may alter cell phenotypes and their transcriptional profiles. A mammalian study (Zhang et al., 2012) showed that adherent cells enzymatically detached by trypsin-EDTA solution did not have significant expression of receptors of tumor necrosis factor-related apoptosis-inducing ligand compared to the expression in cells isolated with citric saline buffer. This result made us aware that trypsinization could break off some receptors from cell surface and hence, non-enzymatic solution was used in **Papers I, II and IV**. Thus it is clear that the optimum culture conditions should be clarified before conducting experiments with adherent cells. I have already validated the phagocytosis assay (**Paper I**), which can be employed to unravel the effects of factors including temperature on phagocytic activity of different fish immune cells.

In the four studies (**Papers I, II, III and IV**) generated through this PhD project, the information from the images of single cells were gathered; to understand their features and functions. The methods have hardly been used before to study fish cells. Hence, IFC methods should be used to shed new light on the different immune cells of fish and their functions.

3.2. Characterization of salmon intestinal cells

Intestinal epithelium, immune cells and microbiota interact with each other to maintain the homeostasis at the microenvironment. In **Papers II, III and IV**, I succeeded in isolating cells from the distal intestine of healthy salmon (>90% of viable cells). Using

the established IFC protocols (**Paper I**), I found that the intestinal leukocytes have a diverse cell population compared to head kidney leukocytes (**Paper II**). Many studies have also reported that the intestinal cells are diverse in carp (Rombout et al., 1998), gilthead seabream (Salinas et al., 2007), rainbow trout (Attaya et al., 2020) and Atlantic salmon (Attaya et al., 2018). The cells with larger nucleus (lymphocytes and monocyte/macrophages) and polymorphonuclear leukocytes (granulocytes) among the intestinal leukocytes that were observed in **Paper II** are similar to those reported by Attaya et al. (2018). Other researchers were also able to isolate cell populations from the intestine of Atlantic salmon (Attaya et al., 2018) and gilthead seabream (Salinas et al., 2007), but they did not specifically examine adherent cells and their phagocytic activity. In **Paper II**, different types of phagocytes were observed in the adherent intestinal cell population. In addition to many round-shaped phagocytic cells, there were few oval-shaped phagocytes, which can be either epithelial or endothelial cells. Lindell et al. (2012) reported that oval shaped skin epithelial cells in trout can phagocytose *Vibrio anguillarum*. Furthermore, human endothelial cells were shown to have the ability to internalize pathogenic bacteria (Rengarajan et al., 2016). Our findings show that the intestinal adherent cell population includes mainly phagocytes, and these various shaped cells have a different morphology compared to the head kidney adherent cells. Jutras and Desjardins (2005) described that phagocytosis and killing of pathogens by phagocytes is the basic form of host innate immune response, and subsequently the antigenic peptides are presented by the phagocytes to specific lymphocytes, which could activate adaptive immune system. This means that phagocytes could act as a bridge between the innate and adaptive arms of the immune system. Therefore, their characteristics need to be elucidated because early immune response by phagocytes is crucial in regulating the intestinal immune system.

First to get an overview of the immune cell types among the phagocytes, I employed RNA-Seq to profile the expression of selected immunologically-relevant genes from the isolated adherent intestinal cells of Atlantic salmon (AIC). Here, I compared their gene

expression with those of the adherent cells in head kidney (AKC), which are considered as monocyte-derived macrophage-like cells (**Paper I**). In **Paper II**, I found that AIC express genes associated with macrophages, T cells, and endothelial cells. Similarly, the known adherent cells in mammals are macrophages (Selvarajan et al., 2011), T cells (Bierer and Burakoff, 1988, Shimizu et al., 1991), endothelial cells (Braniste et al., 2016), epithelial cells (Kihara et al., 2018) and DCs (only upon antigen exposure) (Yi and Lu, 2012). The morphological differences also suggest the heterogeneous population among adherent distal intestinal cells (**Paper II**). They include different cell types that communicate with one another (**Paper III**) to maintain intestinal homeostasis. For example, I observed doublets (of which one was a phagocytic cell) in the adherent cells from salmon intestine (**Paper II**). Furthermore, both IFC and transcriptome results indicated the presence of oval-shaped cells among the intestinal phagocytes (**Paper II**). The transcriptome analysis revealed expression of genes that are associated with structural cells, such as endothelial (*segn* and *scg3*) and epithelial cells (*epcam1*, *tm4sf4* and *t4s1*) (Pipp et al., 2007, Li et al., 2018, Litvinov et al., 1994, Allioli et al., 2011, Subramanian et al., 2014). These findings in **Paper III** are consistent with the results of **Paper II**; supporting the evidence of the presence of endothelial cells and epithelial cells among the adherent cell population.

In addition to epithelial and endothelial cells, AIC and AKC had different shaped phagocytes. Both had apparently higher expression of macrophage-related markers (*h2-eb1*, *cd74*, *cd68*, *marco*, *capg*, *mpeg1*, *cd200r1* and *csf1r*) than markers of other cell types including T and B cells (**Paper II**). This shows that macrophages could be a major cell type in the adherent cells and their increased number could contribute to a higher phagocytic activity. Many of DEGs and DE miRNAs that were upregulated in AIC were linked to both mammalian M1 and M2 macrophages (**Paper III**). For instance, the upregulated genes such as *stc1*, *rln1*, *ssa-miR-210-5p*, *ssa-miR-125a-5p*, *ssa-miR-429-3p* and *ssa-miR-194a-5p* point to the existence of M1 macrophages in AIC (Melton et al., 2016, Xiao et al., 2015, Kong et al., 2018). LPS/IFN γ -induced M1 human macrophages was found to have higher expression levels of STC1 (Leung and Wong,

2021) and RLNL significantly increased pro-inflammatory cytokine IL-6 in human macrophages (Horton et al., 2011). These evidences indicate the presence of M1 macrophages in the AIC populations. However, the downregulation of *ssa-miR-181a-5p*, *ssa-miR-155-5p* and *cd147* that are associated with M1 macrophages does not have a clear explanation. For instance, *p2rx* is a target gene of *ssa-miR-181c-5p* that acts as a danger signal (Burnstock, 2016) and this points to the presence of M1 macrophages. Mammalian M1 macrophages are known to act as inflammatory mediators and play a critical role in host defense against infection (Liu et al., 2014a). Thus, from these results I assume that there are distinct roles for teleost M1 macrophages under certain immune conditions, especially during inflammation in different mucosal and systemic tissues.

The upregulated genes, *adcyap1*, *ssa-miR-100a-5p*, *ssa-let-7a-5p*, *ssa-miR-125a-5p* and *ssa-miR-192a-5p* are linked to M2 polarization (Wang et al., 2018, Hashemi et al., 2018, Zhang et al., 2013, Zhang et al., 2020). A gene, namely glucagon family neuropeptides precursor (*adcyap1*) increases M2 polarization during chronic inflammation (Wan and Sun, 2019). In mammals, the tissue-resident macrophages are predominately M2 phenotypes (Davies et al., 2013, Murray and Wynn, 2011), which have fundamental roles in maintaining tissue homeostasis and resolution of inflammation (Mantovani et al., 2013, Mantovani et al., 2005). Replenishment of tissue-resident macrophages takes place locally and is maintained independently of circulating monocytes (Hashimoto et al., 2013, Yona et al., 2013, Ginhoux and Jung, 2014), which contradicts the notion that tissue macrophages are recruited from circulating monocyte precursors (van Furth et al., 1972). Tissue-resident macrophage-like cells with typical migratory behaviour were observed in zebrafish that lacks *c-mab* (Soza-Ried et al., 2010). The self-renewal of the tissue resident macrophages could be a conserved process in vertebrates including teleost fishes. Our results indicate that the morphology and functions of intestinal macrophages (resident macrophages) may be different from those of head kidney-derived macrophages (newly produced macrophages), as shown in human and murine studies (Bain and Schridde, 2018).

Moreover, Gordon et al. (2014) demonstrated that unlike mice bone marrow-derived macrophages, intestinal macrophages express distinct markers such as receptors for collagens and several connective tissue-related genes including elastin and proteoglycans, indicating the presence of M2 macrophages that perform specialized functions in different tissues. Thus, I believe that intestinal-resident macrophages of salmon have more M2-macrophage characteristics than monocyte-derived macrophages, and the above mentioned miRNAs could be involved in switching of macrophage phenotypes. On the other hand, the downregulation of certain genes (e.g., *mrc2l*, *ltb4rl*, *EIF5* and *lrp1aa*) that are also associated with mammalian M2 macrophages are puzzling findings (Madsen et al., 2013, Zhang et al., 2017b, Puleston et al., 2019).

M1- and M2-like subsets were revealed in the gut of zebrafish (Nguyen-Chi et al., 2015), and only M1-like macrophages were characterized by the expression of cytokines such as *tnfa*, *tnfb*, *il1b* and *il6*. However, specific macrophage subsets could not be identified due to lack of available cell surface antibodies. Furthermore, I found differences and similarities between the macrophages in the adherent intestinal and head kidney cells. Four major macrophage-related markers—*mst1ra*, *romo1*, *prdx4* and *calm1* (Stella et al., 2001, Brunelleschi et al., 2001, Lee et al., 2017, Tan et al., 2016, Hanaka et al., 2019, Zhang et al., 2011), were expressed in both the populations (**Paper III**). In addition, there were five macrophage-related miRNAs that were equally abundant in AIC and AKC; *let-7b-5p*, *ssa-miR-125b-5p*, *ssa-miR-462a-5p*, *ssa-miR-150-5p* and *ssa-let-7c-5p*. These miRNAs are known to be involved in macrophage polarization and monocyte-to-macrophage differentiation (Wang et al., 2016, Banerjee et al., 2013, Chaudhuri et al., 2011, Smith et al., 2020). Similarly, a salmon study (Smith et al., 2020) has reported the presence of many mammalian (miR-155) and teleost-specific miRNAs (miR-2188, miR-462 and miR-731) in cultured head kidney adherent leukocytes wherein they observed differentiation of monocytes to macrophages. These miRNAs were also detected in **Paper III**, suggesting a link between the adherent intestinal cells and macrophage differentiation. Nevertheless, there are differences in

expression of these macrophage-related genes or miRNAs in AIC and AKC, which could be attributed to the organ-linked diversity of macrophages (Gautier et al., 2012). The miRNAs, *ssa-miR-192a-5p* and *ssa-miR-194a-5p*, that had higher expression in AIC, were reported to be abundant in salmon intestine (Woldemariam et al., 2019). In humans and mice, miR-192 and miR-194 are dominantly expressed in the gastrointestinal tract (Beuvink et al., 2007, Takada et al., 2006). The teleost-specific miRNA, *ssa-miR-2188-3p*, is the dominant type in salmon HK macrophage-like cells (Smith et al., 2020). In our study, the expression of *saa-miR-2188-5p* was higher in AIC. Moreover, some miRNAs that were upregulated in AIC were linked to mammalian macrophage activation: miR-196b-5p, miR-196, miR-194a-5p, and miR-10b-5p (Yuan et al., 2018, Velu et al., 2009, Zhang et al., 2017c). Among the miRNAs that were downregulated in AIC, *ssa-miR-155-5p* and *ssa-miR-21b-5p* were detected in salmon head kidney macrophage-like cells (Smith et al., 2020) while *ssa-miR-731-5p*, which is a teleost specific miRNA, was found in cod head kidney macrophages (Eslamloo et al., 2018). *ssa-miR-128-1-5p* was also downregulated in AIC, and this miRNA was found to downregulate colony stimulating factor-1 (CSF1) in human ovarian cancer cells (Woo et al., 2012). Colony stimulating factor-1 induces monocyte differentiation into macrophages, which produces soluble CSF-1 receptors (Rieger et al., 2014, Rieger et al., 2013). Mature macrophages express these receptors through M2-polarizing responses (Rieger et al., 2013). In **Paper II**, I found that the expression of *csf1r* is higher in AKC compared to AIC. Considering the expression levels of miR-128-1-5p and *csf1r* in **Papers II** and **III**, I speculate macrophage differentiation in AKC.

The differences between AIC and AKC populations were inferred by considering the genes that they express. For example, *mip2a* (macrophage inflammatory protein 2), was downregulated in AIC. During acute inflammation, human macrophages that expressed MIP2A bind to CXCR1 and CXCR2 to stimulate neutrophil recruitment and activation (Qin et al., 2017). The expression level of *cxcr1* was significantly lower in AIC compared to those of AKC (**Paper II**). Thus, I suggest that these genes should be studied together to find their potential roles during inflammation. Both AKC and AIC have M1

macrophage characteristics; AKC had high levels of *il1* and *il6*, as observed in mammalian M1-macrophages (Luckett-Chastain et al., 2016) while AIC had high levels of TNF-related genes (Luckett-Chastain et al., 2016). The high levels of TNF-related genes in AIC also point to the activation of T cells (Mehta et al., 2018). *ffar2* (free fatty acid receptor 2-like) was upregulated in AIC, and mammalian macrophages express this gene, which regulates inflammatory responses and controls intestinal epithelial integrity (Alvarez-Curto and Milligan, 2016). These results indicated the possible presence of M1-M2 phenotypes in both the adherent cells.

Dietary components and microbiota are also known to maintain intestinal epithelial integrity. Depending on stimuli from for example cytokines, microbes and other modulators (Murray et al., 2014), macrophage polarization occurs in the intestinal milieu of mammals (Belizário et al., 2018, Kim et al., 2014, Wu et al., 2020). In fish, macrophage polarization could be dependent on sensing microbial/parasite infection or other signals such as innate damage and the later amplification of macrophage phenotypes could be by cytokines produced by T-lymphocytes (Wiegertjes et al., 2016, Joerink et al., 2006a). Bain et al. (2014) reported that colonic macrophages isolated from germ-free mice had significantly lower number of macrophage subsets including Ly6C^{hi}MHCII⁻, Ly6C⁺MHCII⁺ and Ly6C⁻ cells compared to those isolated from conventionally housed control mice. This indicates that: (1) microbiota could drive constant replenishment from circulating monocytes to maintain intestinal macrophage pool and (2) the demands of local microorganisms could alter niche-specific macrophage functions. Although teleost fishes have functional analogues of the mammalian M1- and M2-macrophages, the population of fish macrophage subsets and molecular mechanisms of macrophage polarization in mucosal and systemic tissues remain unclear. Hence, I assumed that AIC express distinct tissue-specific macrophage-related genes and miRNAs that are different to those expressed in AKC. It has also been reported that mammalian intestinal macrophages play a critical role in shaping host-microbiota symbiosis to maintain intestinal homeostasis by expansion of regulatory T cells (Wang et al., 2019b). Thus, dietary components, which can modulate the

composition of microbiota, may also be involved in the regulation of the functions of intestinal macrophages.

Cell adhesion-related genes also provided evidence on macrophage activation. For example, *bcam* and *ceacam18* are equally expressed in AIC and AKC (**Paper III**) and have been linked to macrophage activation (Huang et al., 2014, Samieni et al., 2013). In addition, AIC had higher expression of mucin genes (*muc13l*, *muc1*, *cd164l2*, *muc2l* and *muc5acl*). In salmon, *muc2* and *muc5* are expressed in the distal intestine (Sveen et al., 2017). A study on gilthead sea bream (Pérez-Sánchez et al., 2013) indicated that *muc2* and *muc13* are highly expressed in the posterior intestine. In mice, *muc1* is also expressed in the intestine (McAuley et al., 2007). The presence of the mucin-like receptor, *cd164* is known to indicate the ability of adherent cells to communicate with the endothelial cells (Havens et al., 2006). Chi and Melendez (2007) reported that an interplay between monocytes and endothelial cells is mediated by intercellular or vascular cell adhesion molecules, and their interaction triggers cell migration. The targets of the upregulated miRNAs in AIC included *enc3* and *lbh* (**Paper III**), indicating the presence of epithelial cells. LBH, a stem-A-associated gene, is expressed in *Lgr5*-positive cells and is a marker of epithelial stem cells in human colon (Shiokawa et al., 2017). Furthermore, ectodermal-neural cortex 3 (ENC3) is involved in suppressing differentiation of human colonic epithelial cells during carcinogenesis (Fujita et al., 2001). Studies in mammals demonstrated that interaction between the intestinal epithelial cells and macrophages plays an important role in intestinal homeostasis (Powell et al., 2011, Al-Ghadban et al., 2016). Macrophage activation requires interaction with epithelial cells (Lee et al., 2010), and contact with endothelial cells is necessary for M2 polarization and macrophage colony maintenance (He, 2013). Furthermore, when co-cultured with enteroid monolayers, epithelium-macrophages communication occurs through the ensuing morphological changes and cytokine production (Noel et al., 2017). Thus, epithelial cells, macrophages and endothelial cells seem to act in harmony, through adherence and interaction, to maintain intestinal homeostasis. The adherent cells from salmon that are comprised of macrophages,

endothelial cells and epithelial cells could be used to understand the epithelial barrier functions triggered through external stimuli. Although I did not stimulate the adherent cells, the abovementioned mRNAs or miRNAs could be indicating that fish macrophage polarization occurred during the cell culture; this differentiation could be a result of the communication between macrophages and structural cells such as epithelial and endothelial cells (Lee et al., 2010, He, 2013). The cell culture dish that I used in **Paper I, II and IV** has a fully synthetic energy-treated surface that is appropriate for cell attachment and growth. However, this product does not constrain the adherence of only one cell type, and hence it is not suitable to specifically differentiate one cell type from another. Thus, for future studies, I plan to employ Type I collagen-coated dish to culture intestinal epithelial cells since Type I collagen, which is commonly found in connective tissues, is known to support long-term *in vitro* maintenance of mammalian intestinal epithelial cells (Jabaji et al., 2014). Mammalian studies have already indicated that type I collagen could affect epithelial cell behaviour via adhesion signalling (Provenzano and Keely, 2011, Liu et al., 2004, Wozniak et al., 2003). Thus, this could be an alternative way to separate macrophages from structural cells that could selectively attach to collagen-coated plate. The ideal way to study the characteristics of a cell type is to sort them using a monoclonal antibody and then perform single-cell sequencing. This approach will help reveal sequence information of individual cells, thereby providing a better understanding of their populations and functions. However, there are some challenges linked to sequencing of single-cells from fish intestine: (1) lack of available fish monoclonal antibodies and (2) unstandardized intestinal cell isolation protocols especially for cold water fish like salmon; for example lower temperature culture condition reduces efficacy of DTT and collagenase that helps to prevent cell clumping by removing the mucus from the harvested cells. Depending on the epitope, cross-reactivity between species of a particular antibody would allow the detection of an antigen in phylogenetically closely related species. For example, two antibodies, anti-human TCR $\gamma\delta$ and CD3 cross-react with all genera except those within the superfamily Lemuroidea, which is least linked

to humans among primates (Conrad et al., 2007). Furthermore, polyclonal anti-human CD3 cross-reacted with both salmon T-cells and Ig⁺ cells, and hence they were used for immunohistochemistry (Bakke-McKellep et al., 2007) and flow cytometry (Haugland et al., 2012) studies. Thus, antibodies developed for different species can be employed in flow cytometric studies until fish-specific monoclonal antibodies are available. It should also be noted that as an alternative approach to single-cell sequencing, single-nucleus sequencing which avoids requiring enzymatic dissociation and isolation of single-cell suspensions can be employed to classify the cell type and transcriptional state (Grindberg et al., 2013, Hu et al., 2017).

To sum up, intestinal cells have diverse cell populations that differ from those of head kidney. Adherent intestinal cells had higher phagocytic ability and apparently higher expression levels of major macrophage-related markers. The integrative analyses of mRNA and miRNA data revealed the possible existence of both M1 and M2 macrophages among the adherent intestinal cells of salmon. I also found that the intestinal macrophages could communicate with structural cells such as epithelial and endothelial cells through their adhesion molecules.

Through mapping and annotation of the salmon transcriptome (**Papers II, III and IV**), I could understand certain biological processes linked to the differentially expressed genes in the distal intestine as well as the differences in expression of macrophage-linked genes in the adherent cells from the head kidney and distal intestine of salmon. Nevertheless, there will be some shortcomings attached to any approach, and RNA-Seq is no exception. Here I mention two: (1) *Concerning sample size*: Although through power analysis we determined the sample size for the RNA-Seq study, insufficient sequence depth can reduce the sample size for the downstream analysis. This is the case, especially when multiple samples generate low read counts; this results in low statistical power and the sequencing resource use will be unfruitful (Liu et al., 2014b). In addition, the low read counts are often ignored from DE analyses (based on the algorithm), which results in inappropriate interpretation of results (Raithel et al., 2016).

Optimum number of replicates for RNA-Seq studies is still a contentious subject. A study reported that sequencing less reads and having more biological replicates can be a good strategy to increase statistical power and accuracy in RNA-Seq studies (Liu et al., 2014b). In addition, Schurch et al. (2016) suggested that at least six biological replicates per treatment should be used, and for identifying the rare DEGs, at least 12 replicates are needed. In my studies, 6 was the sample size (**Papers II, III and IV**). (2) *Verification of RNA-Seq data by qPCR*: although many studies already revealed the strong gene expression correlation between RNA-Seq and RT-qPCR data with a sample size greater than 6 (Li et al., 2016, Everaert et al., 2017), researchers are still unsure about the verification. Considering the biases due to low quality bases from mapping artefacts or contaminations (Conesa et al., 2016), I verified the transcripts of selected genes (using 6 biological replicates) by qPCR (**Paper IV**). The results showed that the mRNA levels of 15 DEGs correlated positively with the read counts from the RNA-Seq study. Fang and Cui (2011) have pointed out that verification of same RNA samples (that were used for RNA-Seq) by qPCR is not verifying biological conclusions but techniques. Thus, qPCR verification using different biological replicates is more meaningful to verify findings from RNA-Seq.

3.3. Link between inflammation and the intestinal adherent cells

Inflammation has been studied using chemical-, food- and pathogen-induced animal models. Transcriptome and cell-based approaches have been employed to understand intestinal inflammation in humans (van Baarlen et al., 2011) and mice (Beattie et al., 2013). However, there are not many publications that report inflammation-related transcriptomic or cellular responses in fish. Hence, I performed an experiment to investigate the impacts of diet-induced inflammation on the transcriptome and cells in the intestine of Atlantic salmon (**Paper IV**). Here, I hypothesized that soybean products-induced inflammation disturbs ion transport metabolism and elicits

inflammatory cytokine secretion, which may in turn influence macrophage polarization in adherent intestinal cells.

Soybean products are known to cause inflammation in carnivorous fishes (Buttle et al., 2001, Refstie et al., 2000, Gu et al., 2018, Knudsen et al., 2008). High levels of soybean meal in diets or the presence of anti-nutritional factors are reported to be the main reasons for the inflammatory condition (Hu et al., 2016, Buttle et al., 2001). In the present study, through histology, I first confirmed the inflammation characteristics in the distal intestine of Atlantic salmon fed soybean-products (**Paper IV**). In addition, this group had poor growth as shown in other fish studies (Gu et al., 2018, Wang et al., 2017). I also explored the effects of inflammation on the transcriptomic and cellular changes employing an RNA-Seq technique and IFC. The transcriptome of the distal intestine tissue was altered by diet-induced inflammation, and several of the genes (*cath1b*, *cath2*, *gal3*, *tnfrsf1b*, *lysc2*, and *anxa2*) were inflammation-associated, as discussed in **Paper IV**. It has been reported that inflammation triggers the transcriptional activation of inflammation-related genes (Ahmed et al., 2015). In addition, intestinal inflammation in salmon altered the expression of many genes linked to ion transport. Some genes connected to chloride channel proteins were down-regulated while the others encoding solute carrier families were up-regulated in the inflamed intestine. Similarly, Ramanan and Cadwell (2016) reported that intestinal inflammation in mammals can cause dysregulation of transport via epithelial barrier. Furthermore, in humans (Eisenhut, 2006) mediators of intestinal inflammation alter the epithelial ion transport system through the release of specific messengers including prostaglandins, nitric oxide and histamine. The enriched GO terms in the present study included transmembrane transporter, channel and binding activities. Soybean feeding is known to influence proteins related to transporters, tight and adherens junctions, which in turn will affect the transport of nutrients via epithelia (Hu et al., 2016).

In addition, genes associated with the intestinal adherent cells (**Papers II and III**) can be employed to study the interaction between macrophage regulators and ion

transporters during inflammation. A gene, namely lipoprotein receptor-related protein (*lrp*) is linked to *ccr7* which is involved in macrophage polarization (Mueller et al., 2018). The *ccr7* is known to control sodium absorption and colonic chloride secretion during intestinal inflammation (Schumann et al., 2012). Although *ccr7* was not expressed in the intestinal adherent cells, other possible chemokines which had higher expression could be potential markers of macrophage differentiation: *ccr9l*, *ccl20l* and *ccr6l* (**Paper II**). Furthermore, P2X purinoceptors are known to be ligand-gated Na⁺, K⁺ and Ca²⁺ channels (Burnstock et al., 2017). The expression of *p2rx8* which is one of P2X purinoceptors was significantly higher in the adherent intestinal cells as discussed in **Paper III**. The receptors that are expressed in the intestinal epithelial cells are markers of inflammation (Roberts et al., 2012). Some other genes detected in the intestinal adherent cells are also linked to ion transport, for example, two solute carrier families, monocarboxylate transporter 4-like (*slc16a3*) and choline transporter-like protein 2 (*ct12*). Intestinal inflammation in salmon disturbs ion transport mechanisms and therefore, it is not surprising that the adherent cell types we studied expressed several of the associated genes. In addition, it should be noted that there are growing evidences of interaction between commensal bacteria and ion transport (Engevik et al., 2013, Kuwahara et al., 2018, Lomasney et al., 2014). Casadei et al. (2019) reported that the olfactory organ of germ-free zebrafish and mice had higher expression levels of genes linked to sodium and potassium channels compared to those of control, suggesting that microbiota could regulate host transcriptional programs in the mucosa. Thus, future studies are needed to identify the regulatory role of gut microbiota and ion transport and their interaction with intestinal macrophages during inflammation.

Enriched pathways for the up-regulated genes in the intestine of soybean product groups included taurine and hypotaurine metabolism, drug metabolism – cytochrome P450, metabolism of xenobiotics by cytochrome P450, steroid biosynthesis and glutathione metabolism. For instance, hypotaurine is essential for the biosynthesis of the abundant free amino acid taurine, which has roles in innate immunity of mammals (Schuller-Levis and Park, 2004). High levels of this semi-essential amino acid reduce

oxidative stress due to their antioxidant properties (Oliveira et al., 2010). In addition, steroid biosynthesis and xenobiotic metabolism are characteristics of soybean products-altered metabolic pathways in salmon (De Santis et al., 2015, Kortner et al., 2012). Although in the present study cytochrome P450-related pathways were enriched based on up-regulated genes in the inflamed intestine of salmon, in a mice study, down-regulation of hepatic cytochrome P450s and other drug-metabolizing enzymes were linked to inflammation (Morgan, 2009).

The altered genes associated with adherent cells from the intestine of the soy saponin-fed salmon (**Papers II and III**) could be linked to inflammation-related macrophage phenotypes. Comparison of the expression levels of 48 macrophage-related genes in the intestine of salmon belonging to the soy saponin and control groups at 4 weeks revealed polarization of macrophage phenotypes (Figure 5). These genes were selected based on **Papers II, III** and literatures in fish and mammals (Wiegertjes et al., 2016, Wentzel et al., 2020a, Grayfer et al., 2018, Hodgkinson et al., 2015, Lu and Chen, 2019). Five genes (*il1b*, *il12b*, *il15l*, *nos1* and *cxcr3-1*) associated with M1-macrophages (Wentzel et al., 2020b, Lu et al., 2017, Martinez et al., 2008) were downregulated in the inflamed intestine of salmon. However, six genes (*gcga1*, *gcga2*, *tgfbra1*, *cxcr3-2*, *csf1r* and *eif5*) that are linked to M2-macrophages (Wan and Sun, 2019, Lu et al., 2017, Sica and Mantovani, 2012, Puleston et al., 2019, Grayfer et al., 2018, Joerink et al., 2006b) were upregulated. Wentzel et al. (2020b) suggested the candidate markers for carp M1- (*il1b*, *nos2b* and *saa*) and M2-macrophages (*timp2b*, *tgm2b* and *arg2*). Interestingly, higher expression levels of two nitric oxide synthase-related genes, *nosip* and *nostrin*, and *saal1* were found in AIC while AKC expressed the M2-macrophage markers, *tgm2* and *arg2* (**Paper III**). However, the expression of these genes did not show any significant differences in the inflamed intestine except for the expression of *il1b* (Figure 5). Future studies should employ transcriptome approach to understand the differences in genes related to M1 and M2 macrophages in adherent intestinal cells from fish fed soy saponin diet. Generally, M1 macrophages are responsible for inflammatory signaling by expressing pro-inflammatory cytokines like

il1b, while M2 macrophages are involved in tissue repair and produce anti-inflammatory cytokines (Saqib et al., 2018). It has been reported that unlike monocyte-derived macrophages and other tissue-resident macrophages, human intestinal macrophages produce more anti-inflammatory cytokines than pro-inflammatory cytokines (Smythies et al., 2005, Denning et al., 2007). In addition, the vitamin A metabolite (retinoic acid) plays important roles in maintaining intestinal immune tolerance and is also involved in shifting M1- to M2-macrophages of mice (Vellozo et al., 2017). In mice infected with *Schistosoma mansoni*, vitamin A deficiency reduced CD11b⁺MHCII⁺ macrophages in gut and liver, resulting in dysregulated inflammation. In **Paper III**, *rai1*, retinoic acid-induced protein 1-like was equally expressed in AIC and AKC. In addition, *ssa-miR-92a-3-5p* was downregulated in AIC, and miR-92a in mice modulated macrophage activation by targeting retinoic acid inducible gene-I (Sheng et al., 2018). Although intestinal macrophages are in close proximity to commensal bacteria, they are characterized by strong phagocytic ability and inflammatory anergy (Smythies et al., 2005). The co-existence with commensal bacteria without producing pro-inflammatory cytokines is due to TLR ligation of tissue-resident anti-inflammatory phenotype (Isidro and Appleyard, 2016). There are also unique CD14⁺ intestinal macrophages subsets that can induce abnormal immune responses to cause pathogenesis of Crohn disease, and this is done via IL-23/IFN- γ axis (Kamada et al., 2008).

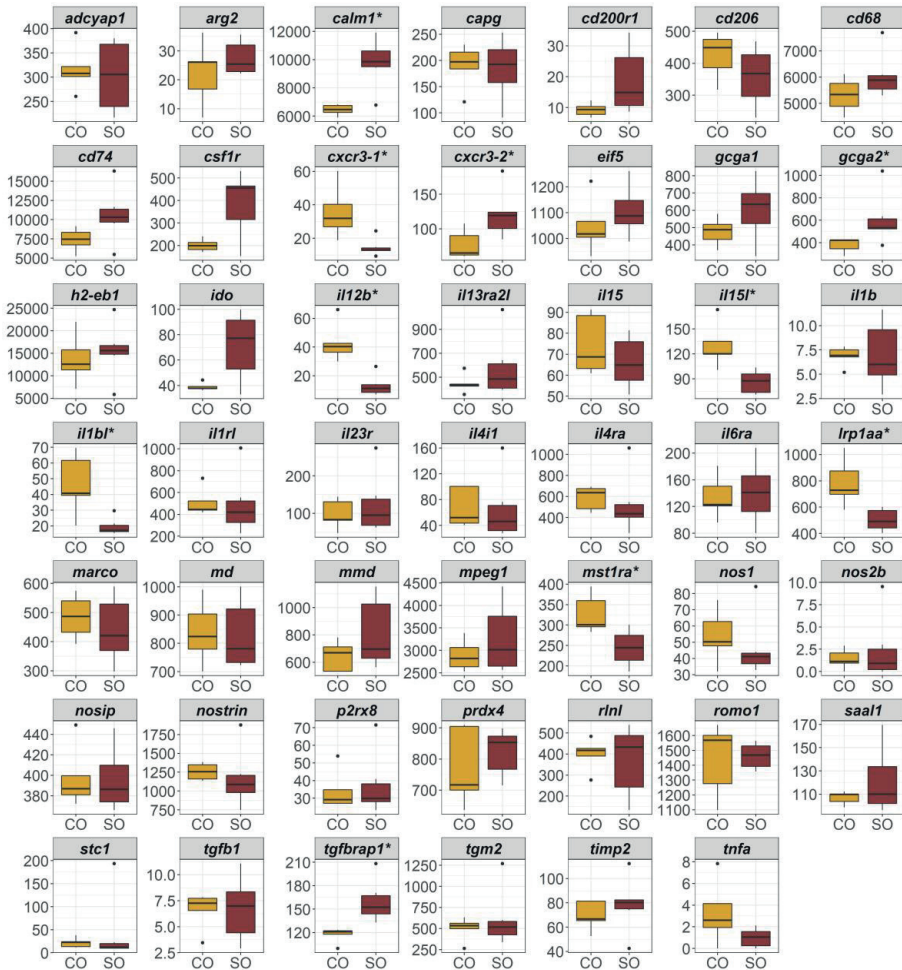


Figure 5. The expression of genes linked to macrophages in the distal intestine of salmon fed soybean products or control diets. Employing the normalized read counts from DESeq2 analyses, the expression levels of 48 selected macrophage-related genes were compared to understand the differences between soybean (SO) and control (CO) groups at 4 weeks. Statistically significant differences ($p < 0.05$) are indicated using asterisks. Boxplots show the median, minimum and maximum values in the data ($n = 6$).

Emerging evidence also points to the activation of macrophages by gut microbiota: human macrophages acquire pro-inflammatory or anti-inflammatory features by responding to bacterial LPS or microbiota-derived metabolites such as short-chain fatty acids, respectively (Wang et al., 2020). The gene *tnfrs1*, tumor necrosis factor

receptor superfamily member 1B-like that was upregulated in the inflamed intestine of salmon (**Paper IV**) is known to have critical roles in modulating inflammatory responses after binding with TNF α , which could activate macrophage via stimulation of TLR signaling by microbes or endogenous ligands (Parameswaran and Patial, 2010). It should be noted that TNF α plays a crucial role in both initiating and resolving inflammation by activating human macrophages (Michlewska et al., 2009). Several TNF-related genes were upregulated in AIC (**Paper II**): *tnfsf10a*, *tnfsf11*, *traf2*, *tnfa2* and *tnfrsf6b*. Furthermore, a study demonstrated the close relationship between M2 macrophage and ion transport during inflammation (Beceiro et al., 2017). Mice lacking TRPM2^{-/-}, a gene associated with ion channels, reduced M2-specific marker like *Arg1* but increased several M1 associated markers when chronically infected with *Helicobacter pylori*. The target gene of ssa-miR-19d-5p, *EIF5* that was downregulated in AIC compared to AKC (**Paper III**) and upregulated in the inflamed intestine of salmon (**Paper IV**) is known to have critical roles in regulating inflammatory cell activation, and eIF5A siRNA significantly reduced IL-1A and MIP1A levels (Moore et al., 2008). It should be noted that *il1b* and *mip2a* were downregulated in inflamed intestine (**Paper IV**) and AIC (**Paper III**), indicating the anti-inflammatory property of *EIF5*. Thus, these genes could be potential regulators of macrophage polarization and intestinal inflammation. Other studies have also described the different macrophage phenotypes that come into play during inflammation. In an experimental inflammation mice model, significant number of Ly6C^{Hi}CD11b⁺CD68⁺ blood monocytes expressed IL-1 β (Jones et al., 2018). The migrating monocytes that reach the lamina propria will be first converted to pro-inflammatory phenotypes, but soon it will obtain anti-inflammatory and pro-tolerogenic properties after receiving the signals from IL-10, regulatory T cells, GM-CSF (CSF2) and innate lymphoid cells (Italiani and Boraschi, 2014, Castro-Dopico et al., 2020). Reduction in CD68⁺ cells was reported to be a sign of healing mucosa in intestinal bowel disease patients (Caprioli et al., 2013). In addition, CD74 signaling is crucial in mucosal healing and barrier integrity (Farr et al., 2020). The expression of macrophage-related marker genes, namely *cd68*, *cd74* and *capg*, was the highest in

the adherent intestinal cells as pointed out in **Paper II**. In addition, the expression levels of *cd68* and *cd74* were apparently higher in the distal intestine of SO group compared to the CO group although our analysis did not indicate significant differences (Figure 5).

In the present thesis, I employed the IFC protocols to gain insight into the changes in the intestinal cell counts and their phagocytic activity under soybean products-induced inflammation (Figure 6). According to the concept of inflammation and wound healing in mammals by Koh and DiPietro (2011), Placek et al. (2019) and Feehan and Gilroy (2019), a tissue injury activates the innate immune system immediately, after which local inflammatory responses are triggered to initiate the next process. The ensuing recruitment of circulating inflammatory cells and secretion of pro-inflammatory cytokines activate local immune cells including resident macrophages to start the healing process. According to Koh and DiPietro (2011) macrophages and neutrophils are dominant during the early inflammation phase, T lymphocytes and mast cells appear from the late inflammation stage for resolution/remodeling. The percentage of lymphocyte-like cells in intestine of salmon that consumed soy products (**Paper IV**) for 8 weeks was increased compared to those of the control group (Figure 6). A study found that mice $\gamma\delta$ T cells contributed to wound healing by producing epithelial growth factors and inflammatory cytokines (Havran and Jameson, 2010), and the cells in humans are known to have the ability to phagocytose *Escherichia coli* (Wu et al., 2009). Considering the differentially expressed genes that were linked to M2-macrophages in the inflamed intestine tissue (4 weeks, Figure 5) and increased blood lymphocyte counts in the soybean group (4 weeks, **Paper IV**), I assume that the fish fed soybean products were at a phase between early and late inflammation stages. As for the 8 weeks' results, the fish might have been at the resolution/remodeling phase or the long-term accumulated inflammation stage (or chronic inflammation), as shown in Zhou et al. (2016) and Feehan and Gilroy (2019).

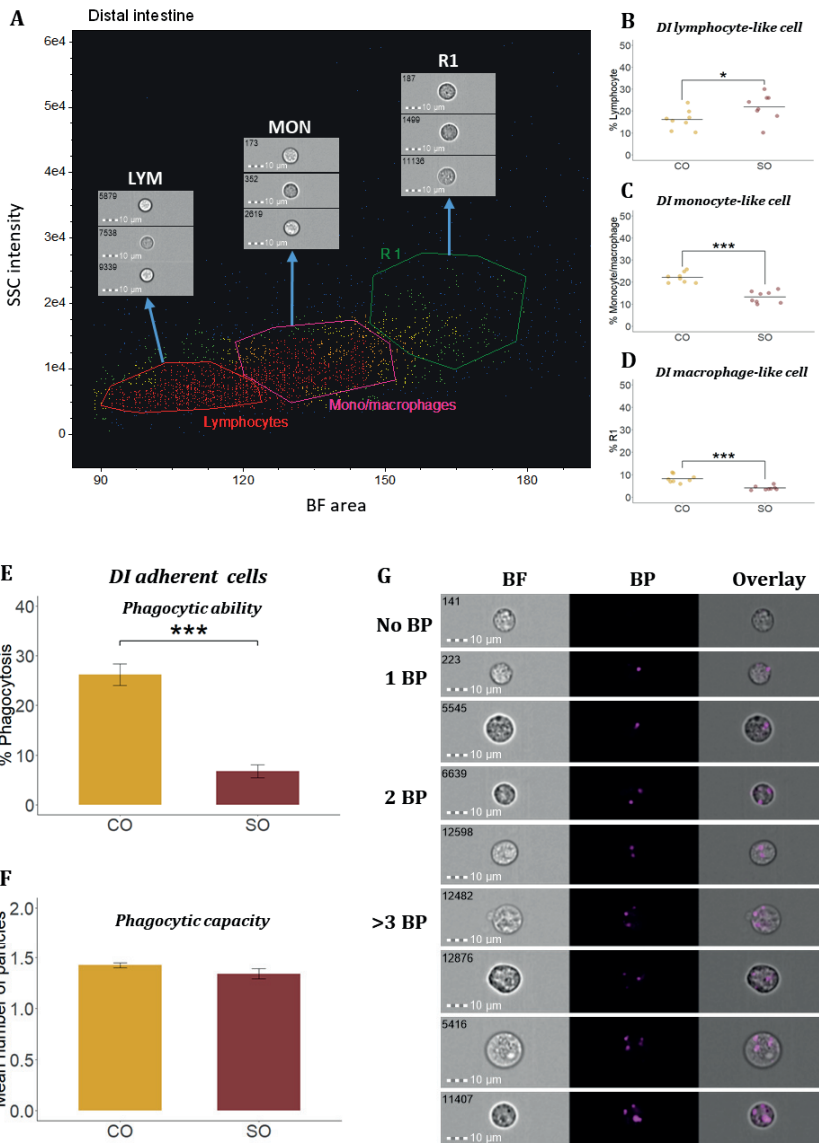


Figure 6. Diet-induced changes in intestinal cell population and phagocytic activity in salmon. After 8 weeks feeding trial, intestinal cell populations and phagocytic activity between soybean (SO) and control (CO) groups were. Three gates of the intestinal cells were identified based on viability and nuclei morphologies (A) as shown in **Papers I and II**: lymphocytes (B), monocytes/macrophages (C) and macrophage-like cells (D). Percent of phagocytic cells or phagocytic ability (E) and mean number of bio-particles (BP) ingested per phagocytic cell or phagocytic capacity (F) are shown to compare between SO and CO groups. (G) Representative cell images show cells with no BP, and 1BP, 2BP, and > 3BP. Statistically significant differences

($p < 0.05$) are indicated using asterisks. All plots show the mean \pm SD ($n = 8$). All cell images were captured with 40 \times objective. Scale bar = 10 μ m. LYM, lymphocytes; MON, monocytes/macrophages; R, region; R1, macrophage-like cells; BF, brightfield; 1 BP, 2 BP, and > 3 BP, 1–3 internalized bio-particles.

The 8-week results indicated that the phagocytic activity of adherent intestinal cells from the soybean group was reduced compared to the control group (Figure 6). It is likely that the reduced macrophage and increased lymphocyte counts could be attributed to the decreased phagocytic ability of the cells in the inflamed intestine. Likewise, bisphenol A exposure triggered inflammation and impaired macrophage phagocytic in mice (Berntsen et al., 2018). In addition, in a diabetic mice model, the impaired clearance of apoptotic cells by tissue resident macrophages increased activation of autoreactive T-cells and led to a subsequent increase in insulinitis and type 1 diabetes mellitus development (Jansen et al., 1994). Furthermore, in humans, phagocytosis of *Streptococcus pneumoniae* and *Haemophilus influenza* by macrophages isolated from chronic obstructive pulmonary disease (COPD) patients was significantly reduced compared to the control group (Taylor et al., 2010). Another study indicated that persistence of bacteria in an inflamed site could act as a chronic antigenic drive for inflammation and this could lead to an increase in T- and B-lymphocyte counts in the COPD patients (Hogg et al., 2004). From these findings, I assume that long-term soybean products feeding can cause chronic inflammation in the intestine of salmon. It should be noted that plant-based feeds can increase intestinal cancer during the first 4 months of feeding; the authors claimed that the feeds provoked first inflammation, and then dysplasia and carcinogenesis (Dale et al., 2009). Chronic inflammation against tumors in humans can increase Th2, Treg and B lymphocyte counts and these cells produce several growth factors including IL-4, IL-6, IL-10, and TGF- β and regulate M2-macrophages activation, indicating that chronic inflammation could influence the differentiation of T lymphocytes (Moro-García et al., 2018). In **Paper II**, higher expression levels of macrophages and T cells in adherent intestinal cell populations likely point to their profound roles in maintaining intestinal

homeostasis. Thus, the expression of different subsets of T lymphocytes together with M2-macrophages should be examined in future inflammation studies to reveal their effects on tissue repair.

Thus, intestinal inflammation disturbs ion transport functions and alters inflammatory cytokine expression. In addition, this condition influenced macrophage-polarization in the intestine and a tendency for M2-macrophage predominance based on their markers. The link between the inflammation study (**Paper IV**) and the adherent cell study (**Papers II and III**) points out the intricate involvement of the adherent intestinal cells in combating inflammation at the mucosal barrier.

Here, I should also mention the caveats of the IFC protocols. I stained the cell nucleus employing propidium iodide to identify the cell types (**Papers I, II and IV**). Nevertheless, the ideal way to ascertain the cell phenotypes should be through antibody labelling. The protocols and the comparisons based on cell size and complexity described in the **Paper IV** gave us evidences about the alteration in intestinal cell populations during inflammation. Caution should be taken especially when gating areas of intestinal cell populations because plasma cells or natural killer cells can be detected along with monocyte/macrophages or lymphocytes, respectively (Jeong et al., 2012, Li et al., 2013).

4. Conclusions

This study provided insights into the transcriptomic and cellular responses in the intestine tissue and cells of Atlantic salmon employing high-throughput techniques; IFC and RNA-Seq (Figure 7). I have succeeded in isolating and characterizing adherent intestinal cells of salmon, and mRNA and miRNA transcriptome analysis of the cells provided further information about their characteristics. Furthermore, I investigated the impacts of soybean products-induced intestinal inflammation on the gut transcriptome and the affected cell functions. Based on the main objectives, the following conclusions are made:

The IFC protocols developed in this PhD project enabled me to explore salmon intestinal cells. The intestine hosts diverse cell populations that are different from those in head kidney and blood, and their phagocytes include macrophages, T cells and endothelial cells. Focusing on the mRNA and miRNA transcripts of intestinal adherent cells, I observed the presumptive occurrence of macrophage phenotypes. An intestinal inflammation study pointed to the disturbances in the ion transport functions and alterations in cytokine expression. Although the cytokines were increased in salmon that developed distal intestinal inflammation, the macrophage-related mRNA levels suggested the predominant presence of M2-macrophages even though I have not examined intestinal cells *per se*. This basic information enhances our understanding of the immune components in salmon intestine, and shows that the mechanistic processes of immune defence at the intestinal level are comparable to those described in mammals.

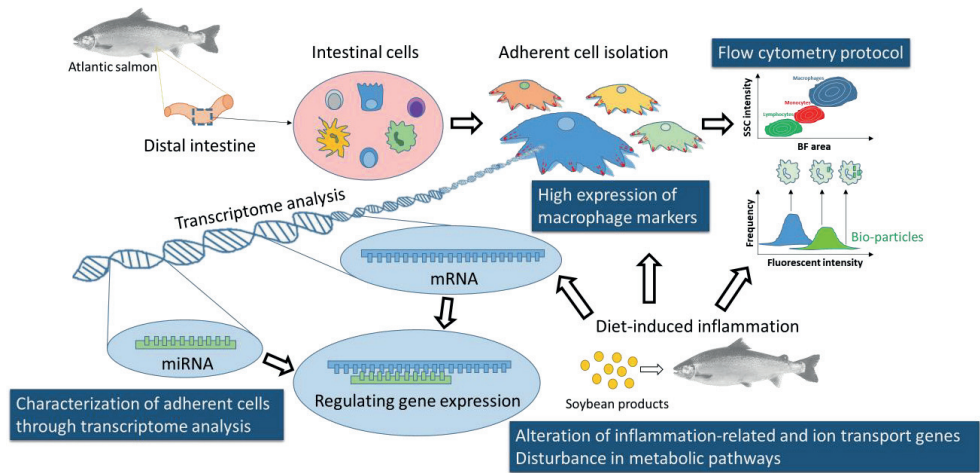


Figure 7. Graphical summary of the results presented in this dissertation.

5. Contribution to the field

Knowledge on the fish mucosal immune system and the cells that orchestrate host defence is rather limited. However, different research groups have shown great interest in this emerging topic, particularly because the aquaculture industry has a strong focus on intestinal health of farmed fish. Through my research I have made a preliminary but sound attempt to characterize the intestinal cells.

Imaging flow cytometry has several advantages over the conventional type to effectively detect dim and small particles as well as aggregates. Although IFC protocols were introduced earlier by other groups in the field of fish immunology (Rieger et al., 2012, Parra et al., 2012), I made use of the special features of IFC and refined their protocols to successfully detect fluorescent degradable and non-degradable particles in phagocytes of salmon. Then, the optimized protocol was used to isolate and characterize intestinal macrophages in salmon. I expect that the protocols applied in this thesis could open new lines of investigation in intestinal immunology.

This thesis also provided information about the presence of M1- and M2-macrophages among the adherent intestinal cell populations. The mammalian macrophage-related markers that were employed to reveal the functions and phenotypes of salmon intestinal macrophages could expand our limited knowledge of teleost intestinal macrophages. In addition, the gathered information about the interaction between macrophages and structural cells gives more understanding of mucosal barrier functions. Further studies on mRNA-miRNA interaction within a specific cell type could reveal the mechanism of gene regulation in different intestinal cells.

For the first time, RNA-Seq was employed to reveal the intestine transcriptome of salmon fed with a diet containing soybean products. I found that many ion transport-related genes were regulated in the inflamed intestine. Along with this, genes related to M2-macrophages were highly expressed. This novel information could help

researchers to focus on intestinal health when screening novel ingredients for aquafeeds.

6. Future perspectives

The present thesis provided important baseline knowledge about the characteristics of the adherent cells and tissue from the intestine of Atlantic salmon. To expand our understanding of the crosstalk between antigens and intestinal epithelium, further efforts are needed to obtain more evidence on transcriptomic responses of the intestinal cells to different antigens or changes in the resident intestinal microorganisms, which could modulate intestinal immune cell responses (Uribe-Herranz et al., 2020, Di Gangi et al., 2020). A more focused approach on specific cell types, isolated employing monoclonal antibodies will clarify the presence of various members of the cell population, including different subsets of intestinal macrophages. Considering the evidence on the presence of M1- and M2-macrophages based on mRNA and miRNA transcriptome of the cells (**Papers II and III**), future studies can explore the alteration of gene expression in these phenotypes in response to various microbes; the results could give us more knowledge of intestinal macrophage functions since gut microbiota may alter the gene expression in host immune cells (Richards et al., 2019). Furthermore, a study on the roles of cell adhesion molecules involved in the communication between macrophages and structural cells will help expand our understanding of the epithelium barrier functions in fish because the importance of such interactions has already been revealed in mammalian studies (Martin et al., 1998, Al-Ghadban et al., 2016).

This thesis also gives insight into certain relevant information on the responses of teleost intestine to inflammation. To broaden our understanding of the intestinal inflammation in fish, in-depth investigations should be conducted on the dysregulation in intestinal barrier functions. Future studies should explore the biomarker genes associated with intestinal inflammation to screen novel aqua feed ingredients. It is necessary to study immunological roles of different subsets of intestinal macrophages during the inflammation. Furthermore, profiling miRNAs in intestinal tissue affected by inflammation could give us a clear understanding of the regulation of this process at

the post-transcriptional level, particularly through interaction between miRNA and their target mRNA. While many differentially expressed genes were observed in the intestine of soy saponin-fed group, the statistical analysis did not reveal any significant differences in the transcripts of head kidney. Hence, future investigations should consider changes in the liver transcriptome to reveal systemic responses to intestinal inflammation.

7. References

- Ahmed, A.U., Williams, B.R.G. & Hannigan, G.E. (2015). Transcriptional activation of inflammatory genes: Mechanistic insight into selectivity and diversity. *Biomolecules*, 5: 3087-3111.
- Ahmed, F., Friend, S., George, T.C., Barteneva, N. & Lieberman, J. (2009). Numbers matter: quantitative and dynamic analysis of the formation of an immunological synapse using imaging flow cytometry. *Journal of Immunological Methods*, 347: 79-86.
- Al-Ghadban, S., Kaissi, S., Homaidan, F.R., Naim, H.Y. & El-Sabban, M.E. (2016). Cross-talk between intestinal epithelial cells and immune cells in inflammatory bowel disease. *Sci Rep*, 6: 29783.
- Allioli, N., Vincent, S., Vlaeminck-Guillem, V., Decaussin-Petrucci, M., Ragage, F., Ruffion, A., et al. (2011). TM4SF1, a novel primary androgen receptor target gene over-expressed in human prostate cancer and involved in cell migration. *The Prostate*, 71: 1239-1250.
- Alvarez-Curto, E. & Milligan, G. (2016). Metabolism meets immunity: The role of free fatty acid receptors in the immune system. *Biochem Pharmacol*, 114: 3-13.
- Ambros, V. (2004). The functions of animal microRNAs. *Nature*, 431: 350-355.
- Antony Jesu Prabhu, P., Stewart, T., Silva, M., Amlund, H., rnsrud, R., Lock, E.J., et al. (2018). Zinc uptake in fish intestinal epithelial model RTgutGC: Impact of media ion composition and methionine chelation. *J Trace Elem Med Biol*, 50: 377-383.
- Arts, J.a.J., Tijhaar, E.J., Chadzinska, M., Savelkoul, H.F.J. & Verburg-Van Kemenade, B.M.L. (2010). Functional analysis of carp interferon- γ : Evolutionary conservation of classical phagocyte activation. *Fish Shellfish Immunol*, 29: 793-802.
- Attaya, A., Secombes, C.J. & Wang, T. (2020). Effective isolation of GALT cells: Insights into the intestine immune response of rainbow trout (*Oncorhynchus mykiss*) to different bacterin vaccine preparations. *Fish Shellfish Immunol*, 105: 378-392.
- Attaya, A., Wang, T., Zou, J., Herath, T., Adams, A., Secombes, C.J., et al. (2018). Gene expression analysis of isolated salmonid GALT leucocytes in response to PAMPs and recombinant cytokines. *Fish & Shellfish Immunology*, 80: 426-436.
- Bain, C.C., Bravo-Blas, A., Scott, C.L., Gomez Perdiguero, E., Geissmann, F., Henri, S., et al. (2014). Constant replenishment from circulating monocytes maintains the macrophage pool in the intestine of adult mice. *Nat Immunol*, 15: 929-937.
- Bain, C.C. & Schridde, A. (2018). Origin, differentiation, and function of intestinal macrophages. *Frontiers in Immunology*, 9: 2733.
- Bakke-Mckellep, A.M., Frøystad, M.K., Lilleeng, E., Dapra, F., Refstie, S., Krogdahl, , et al. (2007). Response to soy: T-cell-like reactivity in the intestine of Atlantic salmon, *Salmo salar* L. *J Fish Dis*, 30: 13-25.
- Bakke, A. (2011). Pathophysiological and immunological characteristics of soybean meal-induced enteropathy in salmon: Contribution of recent molecular investigations. IN Cruz-Suárez, L.E., Ricque-Marie, D., Tapia-Salazar, M., Nieto-López, M.G., Villarreal-Cavazos, D.A., Gamboa-Delgado, J. & Hernández-Hernández, L. (Eds.) *Avances en Nutrición Acuícola XI - Memorias del Décimo Primer Simposio Internacional de Nutrición Acuícola*. San Nicolás de los Garza, N. L., México: Universidad Autónoma de Nuevo León, Monterrey, México. pp. 345-372.

- Banerjee, S., Xie, N., Cui, H., Tan, Z., Yang, S., Icyuz, M., et al. (2013). MicroRNA let-7c regulates macrophage polarization. *The Journal of Immunology*, 190: 6542-6549.
- Barteneva, N.S., Fasler-Kan, E. & Vorobjev, I.A. (2012). Imaging flow cytometry: Coping with heterogeneity in biological systems. *Journal of Histochemistry & Cytochemistry*, 60: 723-733.
- Barteneva, N.S. & Vorobjev, I.A. (2016). *Imaging flow cytometry*, New York: Humana Press. p. 312.
- Baumgart, D.C. & Dignass, A.U. (2002). Intestinal barrier function. *Current Opinion in Clinical Nutrition & Metabolic Care*, 5: 685-694.
- Beattie, L., Hermida, M.D.E.-R., Moore, J.W., Maroof, A., Brown, N., Lagos, D., et al. (2013). A transcriptomic network identified in uninfected macrophages responding to inflammation controls intracellular pathogen survival. *Cell Host & Microbe*, 14: 357-368.
- Beceiro, S., Radin, J.N., Chatuvedi, R., Piazuolo, M.B., Horvarth, D.J., Cortado, H., et al. (2017). TRPM2 ion channels regulate macrophage polarization and gastric inflammation during *Helicobacter pylori* infection. *Mucosal Immunol*, 10: 493-507.
- Belizário, J.E., Faintuch, J. & Garay-Malpartida, M. (2018). Gut microbiome dysbiosis and immunometabolism: New frontiers for treatment of metabolic diseases. *Mediators Inflamm*, 2018: 2037838.
- Berntsen, H.F., Bølling, A.K., Bjørklund, C.G., Zimmer, K., Ropstad, E., Zienolddiny, S., et al. (2018). Decreased macrophage phagocytic function due to xenobiotic exposures in vitro, difference in sensitivity between various macrophage models. *Food Chem Toxicol*, 112: 86-96.
- Beuvink, I., Kolb, F.A., Budach, W., Garnier, A., Lange, J., Natt, F., et al. (2007). A novel microarray approach reveals new tissue-specific signatures of known and predicted mammalian microRNAs. *Nucleic Acids Res*, 35: e52.
- Bhinder, G., Stahl, M., Sham, H.P., Crowley, S.M., Morampudi, V., Dalwadi, U., et al. (2014). Intestinal epithelium-specific MyD88 signaling impacts host susceptibility to infectious colitis by promoting protective goblet cell and antimicrobial responses. *Infection and Immunity*, 82: 3753-3763.
- Bierer, B.E. & Burakoff, S.J. (1988). T cell adhesion molecules. *The FASEB journal*, 2: 2584-2590.
- Biteau, B., Hochmuth, C.E. & Jasper, H. (2011). Maintaining tissue homeostasis: Dynamic control of somatic stem cell activity. *Cell Stem Cell*, 9: 402-411.
- Braniste, T., Tiginyanu, I., Horvath, T., Raevschi, S., Cebotari, S., Lux, M., et al. (2016). Viability and proliferation of endothelial cells upon exposure to GaN nanoparticles. *Beilstein J Nanotechnol*, 7: 1330-1337.
- Brunelleschi, S., Penengo, L., Lavagno, L., Santoro, C., Colangelo, D., Viano, I., et al. (2001). Macrophage stimulating protein (MSP) evokes superoxide anion production by human macrophages of different origin. *British Journal of Pharmacology*, 134: 1285-1295.
- Burnstock, G. (2016). P2X ion channel receptors and inflammation. *Purinergic Signalling*, 12: 59-67.
- Buttle, L.G., Burrells, A.C., Good, J.E., Williams, P.D., Southgate, P.J. & Burrells, C. (2001). The binding of soybean agglutinin (SBA) to the intestinal epithelium of Atlantic salmon, *Salmo salar* and rainbow trout, *Oncorhynchus mykiss*, fed high levels of soybean meal. *Veterinary Immunology and Immunopathology*, 80: 237-244.
- Campos, C., Sundaram, A.Y., Valente, L.M., Conceição, L.E., Engrola, S. & Fernandes, J.M. (2014). Thermal plasticity of the miRNA transcriptome during Senegalese sole development. *BMC Genomics*, 15: 525.
- Caprioli, F., Bosè, F., Rossi, R.L., Petti, L., Viganò, C., Ciafardini, C., et al. (2013). Reduction of CD68+ macrophages and decreased IL-17 expression in intestinal mucosa of patients with inflammatory bowel disease

strongly correlate with endoscopic response and mucosal healing following infliximab therapy. *Inflammatory Bowel Diseases*, 19: 729-739.

- Casadei, E., Tacchi, L., Lickwar, C.R., Espenschied, S.T., Davison, J.M., Muñoz, P., et al. (2019). Commensal bacteria regulate gene expression and differentiation in vertebrate olfactory systems through transcription factor REST. *Chem Senses*, 44: 615-630.
- Castro-Dopico, T., Fleming, A., Dennison, T.W., Ferdinand, J.R., Harcourt, K., Stewart, B.J., et al. (2020). GM-CSF calibrates macrophage defense and wound healing programs during intestinal infection and inflammation. *Cell Rep*, 32: 107857-107857.
- Cerutti, A., Chen, K. & Chorny, A. (2011). Immunoglobulin responses at the mucosal interface. *Annual Review of Immunology*, 29: 273-293.
- Chaudhuri, A.A., So, A.Y.-L., Sinha, N., Gibson, W.S., Taganov, K.D., O'connell, R.M., et al. (2011). MicroRNA-125b potentiates macrophage activation. *The Journal of Immunology*, 187: 5062-5068.
- Chi, Z. & Melendez, A.J. (2007). Role of cell adhesion molecules and immune-cell migration in the initiation, onset and development of atherosclerosis. *Cell Adhesion & Migration*, 1: 171-175.
- Chiaruttini, G., Mele, S., Opzoomer, J., Crescioli, S., Ilieva, K.M., Lacy, K.E., et al. (2017). B cells and the humoral response in melanoma: The overlooked players of the tumor microenvironment. *Oncoimmunology*, 6: e1294296.
- Conesa, A., Madrigal, P., Tarazona, S., Gomez-Cabrero, D., Cervera, A., Mcpherson, A., et al. (2016). A survey of best practices for RNA-seq data analysis. *Genome Biol*, 17: 13.
- Conrad, M.L., Davis, W.C. & Koop, B.F. (2007). TCR and CD3 antibody cross-reactivity in 44 species. *Cytometry Part A*, 71A: 925-933.
- Dale, O.B., Tørud, B., Kvellestad, A., Koppang, H.S. & Koppang, E.O. (2009). From chronic feed-induced intestinal inflammation to adenocarcinoma with metastases in salmonid fish. *Cancer Res*, 69: 4355-4362.
- Davies, L.C., Jenkins, S.J., Allen, J.E. & Taylor, P.R. (2013). Tissue-resident macrophages. *Nat Immunol*, 14: 986-995.
- De Santis, C., Bartie, K.L., Olsen, R.E., Taggart, J.B. & Tocher, D.R. (2015). Nutrigenomic profiling of transcriptional processes affected in liver and distal intestine in response to a soybean meal-induced nutritional stress in Atlantic salmon (*Salmo salar*). *Comparative Biochemistry and Physiology Part D: Genomics and Proteomics*, 15: 1-11.
- Denning, T.L., Wang, Y.-C., Patel, S.R., Williams, I.R. & Pulendran, B. (2007). Lamina propria macrophages and dendritic cells differentially induce regulatory and interleukin 17-producing T cell responses. *Nat Immunol*, 8: 1086-1094.
- Di Gangi, A., Di Cicco, M.E., Comberiati, P. & Peroni, D.G. (2020). Go with your gut: The shaping of T-cell response by gut microbiota in allergic asthma. *Front Immunol*, 11: 1485.
- Eisenhut, M. (2006). Changes in ion transport in inflammatory disease. *Journal of Inflammation*, 3: 5.
- Engevik, M.A., Aihara, E., Montrose, M.H., Shull, G.E., Hassett, D.J. & Worrell, R.T. (2013). Loss of NHE3 alters gut microbiota composition and influences *Bacteroides thetaiotaomicron* growth. *American Journal of Physiology-Gastrointestinal and Liver Physiology*, 305: G697-G711.
- Eslamloo, K., Inkpen, S.M., Rise, M.L. & Andreassen, R. (2018). Discovery of microRNAs associated with the antiviral immune response of Atlantic cod macrophages. *Mol Immunol*, 93: 152-161.

- Esteban, M.A. (2012). An overview of the immunological defenses in fish skin. *ISRN Immunology*, 2012: 853470.
- Everaert, C., Luybaert, M., Maag, J.L.V., Cheng, Q.X., Dinger, M.E., Hellems, J., et al. (2017). Benchmarking of RNA-sequencing analysis workflows using whole-transcriptome RT-qPCR expression data. *Sci Rep*, 7: 1559.
- Fang, Z. & Cui, X. (2011). Design and validation issues in RNA-seq experiments. *Brief Bioinform*, 12: 280-287.
- Farr, L., Ghosh, S., Jiang, N., Watanabe, K., Parlak, M., Bucala, R., et al. (2020). CD74 signaling links inflammation to intestinal epithelial cell regeneration and promotes mucosal healing. *Cellular and Molecular Gastroenterology and Hepatology*, 10(1): 101-112.
- Feehan, K.T. & Gilroy, D.W. (2019). Is resolution the end of inflammation? *Trends Mol Med*, 25: 198-214.
- Fischer, U., Utke, K., Ototake, M., Dijkstra, J.M. & Köllner, B. (2003). Adaptive cell-mediated cytotoxicity against allogeneic targets by CD8-positive lymphocytes of rainbow trout (*Oncorhynchus mykiss*). *Developmental & Comparative Immunology*, 27: 323-337.
- Flajnik, M.F. & Kasahara, M. (2010). Origin and evolution of the adaptive immune system: Genetic events and selective pressures. *Nature Reviews Genetics*, 11: 47-59.
- Forchielli, M.L. & Walker, W.A. (2005). The role of gut-associated lymphoid tissues and mucosal defence. *British Journal of Nutrition*, 93: S41-S48.
- Forlenza, M., Fink, I.R., Raes, G. & Wiegertjes, G.F. (2011). Heterogeneity of macrophage activation in fish. *Dev Comp Immunol*, 35: 1246-1255.
- Francis, G., Kerem, Z., Makkar, H.P. & Becker, K. (2002). The biological action of saponins in animal systems: a review. *British Journal of Nutrition*, 88: 587-605.
- Fuentes-Quesada, J.P., Viana, M.T., Rombenso, A.N., Guerrero-Rentería, Y., Nomura-Solís, M., Gomez-Calle, V., et al. (2018). Enteritis induction by soybean meal in *Totoaba macdonaldi* diets: effects on growth performance, digestive capacity, immune response and distal intestine integrity. *Aquaculture*, 495: 78-89.
- Fujita, M., Furukawa, Y., Tsunoda, T., Tanaka, T., Ogawa, M. & Nakamura, Y. (2001). Up-regulation of the ectodermal-neural cortex 1 (ENC1) gene, a downstream target of the β -catenin/T-cell factor complex, in colorectal carcinomas. *Cancer Research*, 61: 7722-7726.
- Görgens, A., Bremer, M., Ferrer-Tur, R., Murke, F., Tertel, T., Horn, P.A., et al. (2019). Optimisation of imaging flow cytometry for the analysis of single extracellular vesicles by using fluorescence-tagged vesicles as biological reference material. *Journal of Extracellular Vesicles*, 8: 1587567.
- Garrett, W.S., Gordon, J.I. & Glimcher, L.H. (2010). Homeostasis and inflammation in the intestine. *Cell*, 140: 859-870.
- Gautier, E.L., Shay, T., Miller, J., Greter, M., Jakubzick, C., Ivanov, S., et al. (2012). Gene-expression profiles and transcriptional regulatory pathways that underlie the identity and diversity of mouse tissue macrophages. *Nature Immunology*, 13: 1118-1128.
- Georgopoulou, U. & Vernier, J.-M. (1986). Local immunological response in the posterior intestinal segment of the rainbow trout after oral administration of macromolecules. *Developmental & Comparative Immunology*, 10: 529-537.
- Ginhoux, F. & Jung, S. (2014). Monocytes and macrophages: developmental pathways and tissue homeostasis. *Nature Reviews Immunology*, 14: 392-404.
- Gordon, S., Plüddemann, A. & Martinez Estrada, F. (2014). Macrophage heterogeneity in tissues: Phenotypic diversity and functions. *Immunological Reviews*, 262: 36-55.

- Gorman, O.T. & Karr, J.R. (1978). Habitat structure and stream fish communities. *Ecology*, 59: 507-515.
- Grayfer, L. & Belosevic, M. (2009). Molecular characterization, expression and functional analysis of goldfish (*Carassius auratus* L.) interferon gamma. *Dev Comp Immunol*, 33: 235-246.
- Grayfer, L., Garcia, E.G. & Belosevic, M. (2010). Comparison of macrophage antimicrobial responses induced by type II Interferons of the goldfish (*Carassius auratus* L.). *J Biol Chem*, 285: 23537-23547.
- Grayfer, L., Kerimoglu, B., Yaparla, A., Hodgkinson, J.W., Xie, J. & Belosevic, M. (2018). Mechanisms of fish macrophage antimicrobial immunity. *Front Immunol*, 9: 1105.
- Grindberg, R.V., Yee-Greenbaum, J.L., Mcconnell, M.J., Novotny, M., O'shaughnessy, A.L., Lambert, G.M., et al. (2013). RNA-sequencing from single nuclei. *Proceedings of the National Academy of Sciences*, 110: 19802-19807.
- Grove, S., Johansen, R., Reitan, L.J. & Press, C.M. (2006). Immune-and enzyme histochemical characterisation of leukocyte populations within lymphoid and mucosal tissues of Atlantic halibut (*Hippoglossus hippoglossus*). *Fish & Shellfish Immunology*, 20: 693-708.
- Gu, M., Bai, N., Zhang, Y. & Krogdahl, (2016). Soybean meal induces enteritis in turbot *Scophthalmus maximus* at high supplementation levels. *Aquaculture*, 464: 286-295.
- Gu, M., Jia, Q., Zhang, Z., Bai, N., Xu, X. & Xu, B. (2018). Soya-saponins induce intestinal inflammation and barrier dysfunction in juvenile turbot (*Scophthalmus maximus*). *Fish & Shellfish Immunology*, 77: 264-272.
- Hamuro, K., Suetake, H., Saha, N.R., Kikuchi, K. & Suzuki, Y. (2007). A teleost polymeric Ig receptor exhibiting two Ig-like domains transports tetrameric IgM into the skin. *The Journal of Immunology*, 178: 5682-5689.
- Hanaka, T., Kido, T., Noguchi, S., Yamada, S., Noguchi, H., Guo, X., et al. (2019). The overexpression of peroxiredoxin-4 affects the progression of idiopathic pulmonary fibrosis. *BMC Pulmonary Medicine*, 19: 265.
- Hashemi, N., Sharifi, M., Tolouei, S., Hashemi, M., Hashemi, C. & Hejazi, S.H. (2018). Expression of hsa Let-7a microRNA of macrophages infected by *Leishmania major*. *International Journal of Medical Research & Health Sciences*, 5: 27-32.
- Hashimoto, D., Chow, A., Noizat, C., Teo, P., Beasley, Mary b., Leboeuf, M., et al. (2013). Tissue-resident macrophages self-maintain locally throughout adult life with minimal contribution from circulating monocytes. *Immunity*, 38: 792-804.
- Haugland, G.T., Jordal, A.-E.O. & Wergeland, H.I. (2012). Characterization of small, mononuclear blood cells from salmon having high phagocytic capacity and ability to differentiate into dendritic like cells. *PLoS One*, 7: e49260.
- Havens, A.M., Jung, Y., Sun, Y.X., Wang, J., Shah, R.B., Bühring, H.J., et al. (2006). The role of sialomucin CD164 (MGC-24v or endolyn) in prostate cancer metastasis. *BMC Cancer*, 6: 195.
- Havran, W.L. & Jameson, J.M. (2010). Epidermal T cells and wound healing. *J Immunol*, 184: 5423-5428.
- He, H. (2013). The crosstalk between endothelial cells and macrophages: Biological consequences. Doctoral dissertation, The University of California, Los Angeles. p.131.
- Hedraera, M.I., Galdames, J.A., Jimenez-Reyes, M.F., Reyes, A.E., Avendaño-Herrera, R., Romero, J., et al. (2013). Soybean meal induces intestinal inflammation in zebrafish larvae. *PLoS One*, 8.

- Hiscock, K. & Tyler-Walters, H. (2006). Assessing the sensitivity of seabed species and biotopes – The Marine Life Information Network (MarLIN). *Hydrobiologia*, 555: 309-320.
- Hodgkinson, J.W., Grayfer, L. & Belosevic, M. (2015). Biology of bony fish macrophages. *Biology (Basel)*, 4: 881-906.
- Hogg, J.C., Chu, F., Utokaparch, S., Woods, R., Elliott, W.M., Buzatu, L., et al. (2004). The nature of small-airway obstruction in chronic obstructive pulmonary disease. *N Engl J Med*, 350: 2645-53.
- Hohn, C., Lee, S.-R., Pinchuk, L.M. & Petrie-Hanson, L. (2009). Zebrafish kidney phagocytes utilize macropinocytosis and Ca²⁺-dependent endocytic mechanisms. *PLoS One*, 4: e4314.
- Horton, J., Yamamoto, S. & Bryant-Greenwood, G. (2011). Relaxin modulates proinflammatory cytokine secretion from human decidual macrophages. *Biology of Reproduction*, 85: 788-797.
- Hu, H., Kortner, T.M., Gajardo, K., Chikwati, E., Tinsley, J. & Krogdahl, (2016). Intestinal fluid permeability in Atlantic salmon (*Salmo salar* L.) Is affected by dietary protein source. *PLOS ONE*, 11: e0167515.
- Hu, P., Fabyanic, E., Kwon, D.Y., Tang, S., Zhou, Z. & Wu, H. (2017). Dissecting cell-type composition and activity-dependent transcriptional state in mammalian brains by massively parallel single-nucleus RNA-seq. *Mol Cell*, 68: 1006-1015.e7.
- Huang, J., Filipe, A., Rahuel, C., Bonnin, P., Mesnard, L., Guérin, C., et al. (2014). Lutheran/basal cell adhesion molecule accelerates progression of crescentic glomerulonephritis in mice. *Kidney International*, 85: 1123-1136.
- Iliev, D.B., Jørgensen, S.M., Rode, M., Krasnov, A., Harneshaug, I. & Jørgensen, J.B. (2010). CpG-induced secretion of MHCII β and exosomes from salmon (*Salmo salar*) APCs. *Dev Comp Immunol*, 34: 29-41.
- Isidro, R.A. & Appleyard, C.B. (2016). Colonic macrophage polarization in homeostasis, inflammation, and cancer. *American journal of physiology Gastrointestinal and liver physiology*, 311: G59-G73.
- Italiani, P. & Boraschi, D. (2014). From monocytes to M1/M2 macrophages: Phenotypical vs. functional differentiation. *Front Immunol*, 5: 514.
- Jabaji, Z., Brinkley, G.J., Khalil, H.A., Sears, C.M., Lei, N.Y., Lewis, M., et al. (2014). Type I collagen as an extracellular matrix for the in vitro growth of human small intestinal epithelium. *PLoS One*, 9: e107814.
- Jansen, A., Homo-Delarche, F., Hooijkaas, H., Leenen, P.J., Dardenne, M. & Drexhage, H.A. (1994). Immunohistochemical characterization of monocytes-macrophages and dendritic cells involved in the initiation of the insulinitis and β -cell destruction in NOD mice. *Diabetes*, 43: 667-675.
- Jenberie, S., Thim, H.L., Sunyer, J.O., Skjødtt, K., Jensen, I. & Jørgensen, J.B. (2018). Profiling Atlantic salmon B cell populations: CpG-mediated TLR-ligation enhances IgM secretion and modulates immune gene expression. *Scientific Reports*, 8: 1-12.
- Joerink, M., Forlenza, M., Ribeiro, C.M.S., De Vries, B.J., Savelkoul, H.F.J. & Wiegertjes, G.F. (2006a). Differential macrophage polarisation during parasitic infections in common carp (*Cyprinus carpio* L.). *Fish Shellfish Immunol*, 21: 561-571.
- Joerink, M., Ribeiro, C.M.S., Stet, R.J.M., Hermsen, T., Savelkoul, H.F.J. & Wiegertjes, G.F. (2006b). Head kidney-derived macrophages of common carp (*Cyprinus carpio* L.) show plasticity and functional polarization upon differential stimulation. *The Journal of Immunology*, 177: 61-69.
- Johansen, F., Braathen, R. & Brandtzaeg, P. (2000). Role of J chain in secretory immunoglobulin formation. *Scandinavian Journal of Immunology*, 52: 240-248.

- Johnson, I., Gee, J.M., Price, K., Curl, C. & Fenwick, G. (1986). Influence of saponins on gut permeability and active nutrient transport in vitro. *The Journal of Nutrition*, 116: 2270-2277.
- Jones, G.-R., Bain, C.C., Fenton, T.M., Kelly, A., Brown, S.L., Ivens, A.C., et al. (2018). Dynamics of colon monocyte and macrophage activation during colitis. *Frontiers in Immunology*, 9: 2764.
- Jutras, I. & Desjardins, M. (2005). Phagocytosis: At the crossroads of innate and adaptive immunity. *Annu Rev Cell Dev Biol*, 21: 511-527.
- Kamada, N., Hisamatsu, T., Okamoto, S., Chinen, H., Kobayashi, T., Sato, T., et al. (2008). Unique CD14 intestinal macrophages contribute to the pathogenesis of Crohn disease via IL-23/IFN-gamma axis. *The Journal of Clinical Investigation*, 118: 2269-2280.
- Karl, M.O., Valtink, M., Bednarz, J. & Engelmann, K. (2006). Cell culture conditions affect RPE phagocytic function. *Graefes Archive for Clinical and Experimental Ophthalmology*, 245: 981-991.
- Kawano, A., Haiduk, C., Schirmer, K., Hanner, R., Lee, L.E.J., Dixon, B., et al. (2011). Development of a rainbow trout intestinal epithelial cell line and its response to lipopolysaccharide. *Aquac Nutr*, 17: e241-e252.
- Kihara, H., Kim, D.M., Nagai, M., Nojiri, T., Nagai, S., Chen, C.-Y., et al. (2018). Epithelial cell adhesion efficacy of a novel peptide identified by panning on a smooth titanium surface. *International Journal of Oral Science*, 10: 1-8.
- Kim, Y.-G., Udayanga, Kankanam gamage s., Totsuka, N., Weinberg, Jason b., Núñez, G. & Shibuya, A. (2014). Gut dysbiosis promotes M2 macrophage polarization and allergic airway inflammation via fungi-induced PGE2. *Cell Host Microbe*, 15: 95-102.
- Knudsen, D., Jutfelt, F., Sundh, H., Sundell, K., Koppe, W. & Frøkiær, H. (2008). Dietary soya saponins increase gut permeability and play a key role in the onset of soyabean-induced enteritis in Atlantic salmon (*Salmo salar* L.). *British Journal of Nutrition*, 100: 120-129.
- Kobayashi, K.S., Chamailard, M., Ogura, Y., Henegariu, O., Inohara, N., Nuñez, G., et al. (2005). Nod2-dependent regulation of innate and adaptive immunity in the intestinal tract. *Science*, 307: 731-734.
- Koh, T.J. & Dipietro, L.A. (2011). Inflammation and wound healing: The role of the macrophage. *Expert Reviews in Molecular Medicine*, 13: e23.
- Kong, L., Sun, M., Jiang, Z., Li, L. & Lu, B. (2018). MicroRNA-194 inhibits lipopolysaccharide-induced inflammatory response in nucleus pulposus cells of the intervertebral disc by targeting TNF receptor-associated factor 6 (TRAF6). *Medical Science Monitor : International Medical Journal of Experimental and Clinical Research*, 24: 3056-3067.
- Koppang, E.O., Fischer, U., Moore, L., Tranulis, M.A., Dijkstra, J.M., Köllner, B., et al. (2010). Salmonid T cells assemble in the thymus, spleen and in novel interbranchial lymphoid tissue. *Journal of Anatomy*, 217: 728-739.
- Kordon, A.O., Abdelhamed, H., Ahmed, H., Park, J.Y., Karsi, A. & Pinchuk, L.M. (2018). Phagocytic and bactericidal properties of channel catfish peritoneal macrophages exposed to *Edwardsiella ictaluri* live attenuated vaccine and wild-type strains. *Front Microbiol*, 8: 2638.
- Kortner, T.M., Skugor, S., Penn, M.H., Mydland, L.T., Djordjevic, B., Hillestad, M., et al. (2012). Dietary soyasaponin supplementation to pea protein concentrate reveals nutrigenomic interactions underlying enteropathy in Atlantic salmon (*Salmo salar*). *BMC Vet Res*, 8: 101.
- Król, E., Douglas, A., Tocher, D.R., Crampton, V.O., Speakman, J.R., Secombes, C.J., et al. (2016). Differential responses of the gut transcriptome to plant protein diets in farmed Atlantic salmon. *BMC Genomics*, 17: 156.

- Krogdahl, A., Bakke-Mckellep, A., Roed, K. & Baeverfjord, G. (2000). Feeding Atlantic salmon *Salmo salar* L. soybean products: effects on disease resistance (*furunculosis*), and lysozyme and IgM levels in the intestinal mucosa. *Aquaculture Nutrition*, 6: 77-84.
- Krogdahl, Gajardo, K., Kortner, T.M., Penn, M., Gu, M., Berge, G.M., et al. (2015). Soya saponins induce enteritis in Atlantic salmon (*Salmo salar* L.). *Journal of Agricultural and Food Chemistry*, 63: 3887-3902.
- Kuwahara, A., Kuwahara, Y., Inui, T. & Marunaka, Y. (2018). Regulation of ion transport in the intestine by free fatty acid receptor 2 and 3: Possible involvement of the diffuse chemosensory system. *Int J Mol Sci*, 19: 735.
- Løkka, G., Austbø, L., Falk, K., Bromage, E., Fjellidal, P.G., Hansen, T., et al. (2014). Immune parameters in the intestine of wild and reared unvaccinated and vaccinated Atlantic salmon (*Salmo salar* L.). *Developmental & Comparative Immunology*, 47: 6-16.
- Lam, R.S., O'Brien-Simpson, N.M., Holden, J.A., Lenzo, J.C., Fong, S.B. & Reynolds, E.C. (2016). Unprimed, M1 and M2 macrophages differentially interact with *Porphyromonas gingivalis*. *PLoS One*, 11: e0158629.
- Lee, B.H., Kushwah, R., Wu, J., Ng, P., Palaniyar, N., Grinstein, S., et al. (2010). Adenoviral vectors stimulate innate immune responses in macrophages through cross-talk with epithelial cells. *Immunology Letters*, 134: 93-102.
- Lee, S.H., Park, M.J., Choi, S.I., Lee, E.J., Lee, S.Y. & In, K.H. (2017). Reactive oxygen species modulator 1 (Romo1) as a novel diagnostic marker for lung cancer-related malignant effusion. *Medicine*, 96.
- Leung, C.C.T. & Wong, C.K.C. (2021). Characterization of stanniocalcin-1 expression in macrophage differentiation. *Transl Oncol*, 14: 100881.
- Li, J., Barreda, D.R., Zhang, Y.-A., Boshra, H., Gelman, A.E., Lapatra, S., et al. (2006). B lymphocytes from early vertebrates have potent phagocytic and microbicidal abilities. *Nature Immunology*, 7: 1116-1124.
- Li, W., Webster, K.A., Leblanc, M.E. & Tian, H. (2018). Secretogranin III: A diabetic retinopathy-selective angiogenic factor. *Cellular and Molecular Life Sciences*, 75: 635-647.
- Li, Y., Li, Y., Cao, X., Jin, X. & Jin, T. (2017). Pattern recognition receptors in zebrafish provide functional and evolutionary insight into innate immune signaling pathways. *Cellular & Molecular Immunology*, 14: 80-89.
- Li, Y., Zhang, L., Sun, Y., Ma, X., Wang, J., Li, R., et al. (2016). Transcriptome sequencing and comparative analysis of ovary and testis identifies potential key sex-related genes and pathways in scallop *Patinopecten yessoensis*. *Mar Biotechnol*, 18: 453-465.
- Lilleeng, E., Penn, M.H., Haugland, X., Xu, C., Bakke, A.M., Krogdahl, G., et al. (2009). Decreased expression of TGF- β , GILT and T-cell markers in the early stages of soybean enteropathy in Atlantic salmon (*Salmo salar* L.). *Fish & Shellfish Immunology*, 27: 65-72.
- Lindell, K., Fahlgren, A., Hjerde, E., Willassen, N.-P., Fällman, M. & Milton, D.L. (2012). Lipopolysaccharide O-antigen prevents phagocytosis of *Vibrio anguillarum* by rainbow trout (*Oncorhynchus mykiss*) skin epithelial cells. *PLoS One*, 7: e37678.
- Litvinov, S.V., Velders, M.P., Bakker, H., Fleuren, G.J. & Warnaar, S.O. (1994). Ep-CAM: A human epithelial antigen is a homophilic cell-cell adhesion molecule. *The Journal of Cell Biology*, 125: 437-446.
- Liu, H., Radisky, D.C., Wang, F. & Bissell, M.J. (2004). Polarity and proliferation are controlled by distinct signaling pathways downstream of PI3-kinase in breast epithelial tumor cells. *J Cell Biol*, 164: 603-612.

- Liu, Y.-C., Zou, X.-B., Chai, Y.-F. & Yao, Y.-M. (2014a). Macrophage polarization in inflammatory diseases. *Int J Biol Sci*, 10: 520-529.
- Liu, Y., Chen, Z., Dai, J., Yang, P., Hu, H., Ai, Q., et al. (2018). The protective role of glutamine on enteropathy induced by high dose of soybean meal in turbot, *Scophthalmus maximus* L. *Aquaculture*, 497: 510-519.
- Liu, Y., Zhou, J. & White, K.P. (2014b). RNA-seq differential expression studies: More sequence or more replication? *Bioinformatics (Oxford, England)*, 30: 301-304.
- Loes, A., Hinman, M., Farnsworth, D., Miller, A., Guillemin, K. & Harms, M. (2019). Identification and characterization of zebrafish Tlr4 co-receptor Md-2. *BioRxiv*.
- Lomasney, K.W., Houston, A., Shanahan, F., Dinan, T.G., Cryan, J.F. & Hyland, N.P. (2014). Selective influence of host microbiota on cAMP-mediated ion transport in mouse colon. *Neurogastroenterol Motil*, 26: 887-890.
- Lu, X.-J. & Chen, J. (2019). Specific function and modulation of teleost monocytes/macrophages: polarization and phagocytosis. *Zool Res*, 40: 146-150.
- Lu, X.-J., Chen, Q., Rong, Y.-J., Chen, F. & Chen, J. (2017). CXCR3.1 and CXCR3.2 differentially contribute to macrophage polarization in teleost fish. *The Journal of Immunology*, 198: 4692-4706.
- Luckett-Chastain, L., Calhoun, K., Scharzt, T. & Gallucci, R.M. (2016). IL-6 influences the balance between M1 and M2 macrophages in a mouse model of irritant contact dermatitis. *Am Assoc Immunol*, 2016: 196.
- Lugo-Villarino, G., Balla, K.M., Stachura, D.L., Bañuelos, K., Werneck, M.B.F. & Traver, D. (2010). Identification of dendritic antigen-presenting cells in the zebrafish. *Proceedings of the National Academy of Sciences*, 107: 15850-15855.
- Macpherson, A., McCoy, K., Johansen, F. & Brandtzaeg, P. (2008). The immune geography of IgA induction and function. *Mucosal Immunology*, 1: 11-22.
- Madsen, D.H., Leonard, D., Masedunskas, A., Moyer, A., Jürgensen, H.J., Peters, D.E., et al. (2013). M2-like macrophages are responsible for collagen degradation through a mannose receptor-mediated pathway. *J Cell Biol*, 202: 951-966.
- Maloy, K.J. & Powrie, F. (2011). Intestinal homeostasis and its breakdown in inflammatory bowel disease. *Nature*, 474: 298-306.
- Mantovani, A., Biswas, S.K., Galdiero, M.R., Sica, A. & Locati, M. (2013). Macrophage plasticity and polarization in tissue repair and remodelling. *The Journal of Pathology*, 229: 176-185.
- Mantovani, A., Sica, A. & Locati, M. (2005). Macrophage polarization comes of age. *Immunity*, 23: 344-6.
- Marjara, I.S., Chikwati, E.M., Valen, E.C., Krogdahl, & Bakke, A.M. (2012). Transcriptional regulation of IL-17A and other inflammatory markers during the development of soybean meal-induced enteropathy in the distal intestine of Atlantic salmon (*Salmo salar* L.). *Cytokine*, 60: 186-196.
- Martin, C.A., El-Sabban, M.E., Zhao, L., Burakoff, R. & Homaidan, F.R. (1998). Adhesion and cytosolic dye transfer between macrophages and intestinal epithelial cells. *Cell Adhes Commun*, 5: 83-95.
- Martin, S.a.M., Dehler, C.E. & Król, E. (2016). Transcriptomic responses in the fish intestine. *Developmental & Comparative Immunology*, 64: 103-117.
- Martinez, F.O., Sica, A., Mantovani, A. & Locati, M. (2008). Macrophage activation and polarization. *Front Biosci*, 13: 453-461.

- Mcauley, J.L., Linden, S.K., Png, C.W., King, R.M., Pennington, H.L., Gendler, S.J., et al. (2007). MUC1 cell surface mucin is a critical element of the mucosal barrier to infection. *J Clin Invest*, 117: 2313-2324.
- Mcgrath, K., Catherman, S. & Palis, J. (2017). Delineating stages of erythropoiesis using imaging flow cytometry. *Methods*, 112: 68-74.
- Mcmillan, D.N. & Secombes, C.J. (1997). Isolation of rainbow trout (*Oncorhynchus mykiss*) intestinal intraepithelial lymphocytes (IEL) and measurement of their cytotoxic activity. *Fish & Shellfish Immunology*, 7: 527-541.
- Mehta, A.K., Gracias, D.T. & Croft, M. (2018). TNF activity and T cells. *Cytokine*, 101: 14-18.
- Melton, D.W., Lei, X., Gelfond, J.A. & Shireman, P.K. (2016). Dynamic macrophage polarization-specific miRNA patterns reveal increased soluble VEGF receptor 1 by miR-125a-5p inhibition. *Physiological Genomics*, 48: 345-360.
- Miao, S., Zhao, C., Zhu, J., Hu, J., Dong, X. & Sun, L. (2018). Dietary soybean meal affects intestinal homeostasis by altering the microbiota, morphology and inflammatory cytokine gene expression in northern snakehead. *Sci Rep*, 8: 1-10.
- Michlewska, S., Dransfield, I., Megson, I.L. & Rossi, A.G. (2009). Macrophage phagocytosis of apoptotic neutrophils is critically regulated by the opposing actions of pro-inflammatory and anti-inflammatory agents: key role for TNF- α . *The FASEB Journal*, 23: 844-854.
- Montilla, N.A., Blas, M.P., Santalla, M.L. & Villa, J.M. (2004). Mucosal immune system: a brief review. *Inmunología*, 23: 207-216.
- Moore, C.C., Martin, E.N., Lee, G., Taylor, C., Dondero, R., Reznikov, L.L., et al. (2008). Eukaryotic translation initiation factor 5A small interference RNA-liposome complexes reduce inflammation and increase survival in murine models of severe sepsis and acute lung injury. *The Journal of Infectious Diseases*, 198: 1407-1414.
- Morgan, E. (2009). Impact of infectious and inflammatory disease on cytochrome P450-mediated drug metabolism and pharmacokinetics. *Clinical Pharmacology & Therapeutics*, 85: 434-438.
- Moro-García, M.A., Mayo, J.C., Sainz, R.M. & Alonso-Arias, R. (2018). Influence of inflammation in the process of T lymphocyte differentiation: Proliferative, metabolic, and oxidative changes. *Front Immunol*, 9: 339.
- Mueller, P.A., Zhu, L., Tavori, H., Huynh, K., Giunzioni, I., Stafford, J.M., et al. (2018). Deletion of macrophage low-density lipoprotein receptor-related protein 1 (LRP1) accelerates atherosclerosis regression and increases CC chemokine receptor type 7 (CCR7) expression in plaque macrophages. *Circulation*, 138: 1850-1863.
- Mulder, I., Wadsworth, S. & Secombes, C. (2007). Cytokine expression in the intestine of rainbow trout (*Oncorhynchus mykiss*) during infection with *Aeromonas salmonicida*. *Fish & Shellfish Immunology*, 23: 747-759.
- Murphy, K. & Weaver, C. (2016). *Janeway's immunobiology*, New York: Garland Science/Taylor & Francis Group, LLC. p. 904.
- Murray, P.J., Allen, J.E., Biswas, S.K., Fisher, E.A., Gilroy, D.W., Goerdts, S., et al. (2014). Macrophage activation and polarization: Nomenclature and experimental guidelines. *Immunity*, 41: 14-20.
- Murray, P.J. & Wynn, T.A. (2011). Protective and pathogenic functions of macrophage subsets. *Nature Reviews Immunology*, 11: 723-737.

- Neumann, N.F., Stafford, J.L., Barreda, D., Ainsworth, A.J. & Belosevic, M. (2001). Antimicrobial mechanisms of fish phagocytes and their role in host defense. *Developmental & Comparative Immunology*, 25: 807-825.
- Neutra, M.R., Pringault, E. & Kraehenbuhl, J.-P. (1996). Antigen sampling across epithelial barriers and induction of mucosal immune responses. *Annual Review of Immunology*, 14: 275-300.
- Nguyen-Chi, M., Laplace-Builhe, B., Travnickova, J., Luz-Crawford, P., Tejedor, G., Phan, Q.T., et al. (2015). Identification of polarized macrophage subsets in zebrafish. *Elife*, 4: e07288.
- Nie, L., Cai, S.-Y., Shao, J.-Z. & Chen, J. (2018). Toll-like receptors, associated biological roles, and signaling networks in non-mammals. *Frontiers in Immunology*, 9: 1523.
- Noel, G., Baetz, N.W., Staab, J.F., Donowitz, M., Kovbasnjuk, O., Pasetti, M.F., et al. (2017). A primary human macrophage-enteroid co-culture model to investigate mucosal gut physiology and host-pathogen interactions. *Scientific Reports*, 7: 1-14.
- Noguera, P.A., Grunow, B., Klinger, M., Lester, K., Collet, B. & Del-Pozo, J. (2017). Atlantic salmon cardiac primary cultures: An in vitro model to study viral host pathogen interactions and pathogenesis. *Plos One*, 12: e0181058.
- Oben, J.A. & Foreman, J.C. (1988). A simple quantitative fluorimetric assay of in vitro phagocytosis in human neutrophils. *J Immunol Methods*, 112: 99-103.
- Okumura, R. & Takeda, K. (2016). Maintenance of gut homeostasis by the mucosal immune system. *Proceedings of the Japan Academy, Series B*, 92: 423-435.
- Okumura, R. & Takeda, K. (2018). Maintenance of intestinal homeostasis by mucosal barriers. *Inflammation and Regeneration*, 38: 5.
- Oliveira, M.W., Minotto, J.B., De Oliveira, M.R., Zanotto-Filho, A., Behr, G.A., Rocha, R.F., et al. (2010). Scavenging and antioxidant potential of physiological taurine concentrations against different reactive oxygen/nitrogen species. *Pharmacological reports : PR*, 62: 185-93.
- Pérez-Sánchez, J., Estensoro, I., Redondo, M.J., Caldach-Giner, J.A., Kaushik, S. & Sitjà-Bobadilla, A. (2013). Mucins as diagnostic and prognostic biomarkers in a fish-parasite model: Transcriptional and functional analysis. *PLoS One*, 8: e65457.
- Palti, Y. (2011). Toll-like receptors in bony fish: From genomics to function. *Developmental & Comparative Immunology*, 35: 1263-1272.
- Parameswaran, N. & Patial, S. (2010). Tumor necrosis factor- α signaling in macrophages. *Crit Rev Eukaryot Gene Expr*, 20: 87-103.
- Parra, D., Korytář, T., Takizawa, F. & Sunyer, J.O. (2016). B cells and their role in the teleost gut. *Developmental & Comparative Immunology*, 64: 150-166.
- Parra, D., Reyes-Lopez, F.E. & Tort, L. (2015). Mucosal immunity and B cells in teleosts: Effect of vaccination and stress. *Frontiers in Immunology*, 6: 354.
- Parra, D., Rieger, A.M., Li, J., Zhang, Y.A., Randall, L.M., Hunter, C.A., et al. (2012). Pivotal advance: peritoneal cavity B-1 B cells have phagocytic and microbicidal capacities and present phagocytosed antigen to CD4⁺ T cells. *Journal of Leukocyte Biology*, 91: 525-536.
- Perdigueru, P., Martín-Martín, A., Benedicenti, O., Díaz-Rosales, P., Morel, E., Muñoz-Atienza, E., et al. (2019). Teleost IgD⁺ IgM⁻ B cells mount clonally expanded and mildly mutated intestinal IgD responses in the absence of lymphoid follicles. *Cell Reports*, 29: 4223-4235. e5.

- Peterson, L.W. & Artis, D. (2014). Intestinal epithelial cells: Regulators of barrier function and immune homeostasis. *Nature Reviews Immunology*, 14: 141-153.
- Peterson, P., Verhoef, J. & Quie, P. (1977). Influence of temperature on opsonization and phagocytosis of *staphylococci*. *Infection and Immunity*, 15: 175-179.
- Pettersen, E.F., Ingerslev, H.-C., Stavang, V., Egenberg, M. & Wergeland, H.I. (2008). A highly phagocytic cell line TO from Atlantic salmon is CD83 positive and M-CSFR negative, indicating a dendritic-like cell type. *Fish & Shellfish Immunology*, 25: 809-819.
- Picchietti, S., Fausto, A.M., Randelli, E., Carnevali, O., Taddei, A.R., Buonocore, F., et al. (2009). Early treatment with *Lactobacillus delbrueckii* strain induces an increase in intestinal T-cells and granulocytes and modulates immune-related genes of larval *Dicentrarchus labrax* (L.). *Fish & Shellfish Immunology*, 26: 368-376.
- Pipp, I., Wagner, L., Ressler, K., Budka, H. & Preusser, M. (2007). Secretogin expression in tumours of the human brain and its coverings. *APMIS*, 115: 319-326.
- Placek, K., Schultze, J.L. & Aschenbrenner, A.C. (2019). Epigenetic reprogramming of immune cells in injury, repair, and resolution. *The Journal of clinical investigation*, 129.
- Powell, A.E., Anderson, E.C., Davies, P.S., Silk, A.D., Pelz, C., Impey, S., et al. (2011). Fusion between Intestinal epithelial cells and macrophages in a cancer context results in nuclear reprogramming. *Cancer Research*, 71: 1497-1505.
- Presslauer, C., Bizuayehu, T.T., Kopp, M., Fernandes, J.M. & Babiak, I. (2017). Dynamics of miRNA transcriptome during gonadal development of zebrafish. *Scientific Reports*, 7: 43850.
- Provenzano, P.P. & Keely, P.J. (2011). Mechanical signaling through the cytoskeleton regulates cell proliferation by coordinated focal adhesion and Rho GTPase signaling. *J Cell Sci*, 124: 1195.
- Puleston, D.J., Buck, M.D., Geltink, R.I.K., Kyle, R.L., Caputa, G., O'sullivan, D., et al. (2019). Polyamines and eIF5A hypusination modulate mitochondrial respiration and macrophage activation. *Cell Metabolism*, 30: 352-363. e8.
- Qin, C.-C., Liu, Y.-N., Hu, Y., Yang, Y. & Chen, Z. (2017). Macrophage inflammatory protein-2 as mediator of inflammation in acute liver injury. *World J Gastroenterol*, 23: 3043-3052.
- Raithel, S., Johnson, L., Galliard, M., Brown, S., Shelton, J., Herndon, N., et al. (2016). Inferential considerations for low-count RNA-seq transcripts: A case study on the dominant prairie grass *Andropogon gerardii*. *BMC Genomics*, 17: 140.
- Ramachandran, R., Fausett, B.V. & Goldman, D. (2010). Ascl1a regulates Müller glia dedifferentiation and retinal regeneration through a Lin-28-dependent, let-7 microRNA signalling pathway. *Nature Cell Biology*, 12: 1101-1107.
- Ramakrishnan, S.K., Zhang, H., Ma, X., Jung, I., Schwartz, A.J., Triner, D., et al. (2019). Intestinal non-canonical NFκB signaling shapes the local and systemic immune response. *Nature Communications*, 10: 1-16.
- Ramanan, D. & Cadwell, K. (2016). Intrinsic defense mechanisms of the intestinal epithelium. *Cell Host & Microbe*, 19: 434-441.
- Refstie, S., Korsøen, J., Storebakken, T., Baevefjord, G., Lein, I. & Roem, A.J. (2000). Differing nutritional responses to dietary soybean meal in rainbow trout (*Oncorhynchus mykiss*) and Atlantic salmon (*Salmo salar*). *Aquaculture*, 190: 49-63.

- Rengarajan, M., Hayer, A. & Theriot, J.A. (2016). Endothelial cells use a formin-dependent phagocytosis-like process to internalize the bacterium *Listeria monocytogenes*. *PLoS Pathog*, 12: e1005603.
- Rességuier, J., Delaune, E., Coolen, A.-L., Levraud, J.-P., Boudinot, P., Le Guellec, D., et al. (2017). Specific and efficient uptake of surfactant-free poly (lactic acid) nanovaccine vehicles by mucosal dendritic cells in adult zebrafish after bath immersion. *Frontiers In Immunology*, 8: 190.
- Richards, A.L., Muehlbauer, A.L., Alazizi, A., Burns, M.B., Findley, A., Messina, F., et al. (2019). Gut microbiota has a widespread and modifiable effect on host gene regulation. *mSystems*, 4: e00323-18.
- Rieger, A.M., Hall, B.E. & Barreda, D.R. (2010). Macrophage activation differentially modulates particle binding, phagocytosis and downstream antimicrobial mechanisms. *Developmental & Comparative Immunology*, 34: 1144-1159.
- Rieger, A.M., Hanington, P.C., Belosevic, M. & Barreda, D.R. (2014). Control of CSF-1 induced inflammation in teleost fish by a soluble form of the CSF-1 receptor. *Fish Shellfish Immunol*, 41: 45-51.
- Rieger, A.M., Havixbeck, J.J., Belosevic, M. & Barreda, D.R. (2015). Teleost soluble CSF-1R modulates cytokine profiles at an inflammatory site, and inhibits neutrophil chemotaxis, phagocytosis, and bacterial killing. *Dev Comp Immunol*, 49: 259-266.
- Rieger, A.M., Konowalchuk, J.D., Grayfer, L., Katzenback, B.A., Havixbeck, J.J., Kiemele, M.D., et al. (2012). Fish and mammalian phagocytes differentially regulate pro-inflammatory and homeostatic responses in vivo. *PLoS One*, 7: e47070.
- Rieger, A.M., Konowalchuk, J.D., Havixbeck, J.J., Robbins, J.S., Smith, M.K., Lund, J.M., et al. (2013). A soluble form of the CSF-1 receptor contributes to the inhibition of inflammation in a teleost fish. *Dev Comp Immunol*, 39: 438-446.
- Roberts, J.A., Lukewich, M.K., Sharkey, K.A., Furness, J.B., Mawe, G.M. & Lomax, A.E. (2012). The roles of purinergic signaling during gastrointestinal inflammation. *Current Opinion in Pharmacology*, 12: 659-666.
- Rombout, J.H.W.M., Abelli, L., Picchietti, S., Scapigliati, G. & Kiron, V. (2011). Teleost intestinal immunology. *Fish & Shellfish Immunology*, 31: 616-626.
- Rombout, J.H.W.M., Joosten, P.H.M., Engelsma, M.Y., Vos, A.P., Taverne, N. & Taverne-Thiele, J.J. (1998). Indications for a distinct putative T cell population in mucosal tissue of carp (*Cyprinus carpio* L.). *Developmental & Comparative Immunology*, 22: 63-77.
- Rosales, C. & Uribe-Querol, E. (2017). Phagocytosis: A fundamental process in immunity. *BioMed Research International*, 2017: 9042851.
- Ruangsi, J., Salger, S.A., Caipang, C.M., Kiron, V. & Fernandes, J.M. (2012). Differential expression and biological activity of two piscidin paralogues and a novel splice variant in Atlantic cod (*Gadus morhua* L.). *Fish & Shellfish Immunology*, 32: 396-406.
- Sahlmann, C., Sutherland, B.J., Kortner, T.M., Koop, B.F., Krogdahl, & Bakke, A.M. (2013). Early response of gene expression in the distal intestine of Atlantic salmon (*Salmo salar* L.) during the development of soybean meal induced enteritis. *Fish & Shellfish Immunology*, 34: 599-609.
- Salinas, I. (2015). The mucosal immune system of teleost Fish. *Biology (Basel)*, 4: 525-539.
- Salinas, I., Meseguer, J. & Esteban, M. (2007). Assessment of different protocols for the isolation and purification of gut associated lymphoid cells from the gilthead seabream (*Sparus aurata* L.). *Biological Procedures Online*, 9: 43.

- Samieni, S., Zhang, Z. & Shively, J.E. (2013). CEACAM-1 negatively regulates G-CSF production by breast tumor associated macrophages that mediate tumor angiogenesis. *International Journal of Cancer*, 133.
- Santos, J.L., Montes, M.J., Gutiérrez, F. & Ruiz, C. (1995). Evaluation of phagocytic capacity with a modified flow cytometry technique. *Immunol Lett*, 45: 1-4.
- Saqib, U., Sarkar, S., Suk, K., Mohammad, O., Baig, M.S. & Savai, R. (2018). Phytochemicals as modulators of M1-M2 macrophages in inflammation. *Oncotarget*, 9: 17937-17950.
- Scapigliati, G., Fausto, A.M. & Picchiotti, S. (2018). Fish lymphocytes: An evolutionary equivalent of mammalian innate-like lymphocytes? *Frontiers in Immunology*, 9: 971.
- Schley, P. & Field, C. (2002). The immune-enhancing effects of dietary fibres and prebiotics. *British Journal of Nutrition*, 87: S221-S230.
- Schuller-Levis, G.B. & Park, E. (2004). Taurine and its chloramine: modulators of immunity. *Neurochemical research*, 29: 117-26.
- Schulz, D., Severin, Y., Zanotelli, V.R.T. & Bodenmiller, B. (2019). In-depth characterization of monocyte-derived macrophages using a mass cytometry-based phagocytosis assay. *Sci Rep*, 9: 1925.
- Schumann, M., Winter, S., Wichner, K., May, C., Kühl, A., Batra, A., et al. (2012). CCR7 deficiency causes diarrhea associated with altered ion transport in colonocytes in the absence of overt colitis. *Mucosal Immunology*, 5: 377-387.
- Schurch, N.J., Schofield, P., Gierliński, M., Cole, C., Sherstnev, A., Singh, V., et al. (2016). How many biological replicates are needed in an RNA-seq experiment and which differential expression tool should you use? *RNA (New York, NY)*, 22: 839-851.
- Selvarajan, K., Moldovan, L., Chandrakala, A.N., Litvinov, D. & Parthasarathy, S. (2011). Peritoneal macrophages are distinct from monocytes and adherent macrophages. *Atherosclerosis*, 219: 475-483.
- Sepulcre, M.P., Alcaraz-Pérez, F., López-Muñoz, A., Roca, F.J., Meseguer, J., Cayuela, M.L., et al. (2009). Evolution of lipopolysaccharide (LPS) recognition and signaling: Fish TLR4 does not recognize LPS and negatively regulates NF- κ B activation. *The Journal of Immunology*, 182: 1836-1845.
- Sheng, Y., Wang, Y., Lu, W., Zhou, Y., Dong, G., Ge, X., et al. (2018). MicroRNA-92a inhibits macrophage antiviral response by targeting retinoic acid inducible gene-I. *Microbiol Immunol*, 62: 585-593.
- Shimizu, Y., Newman, W., Gopal, T.V., Horgan, K.J., Graber, N., Beall, L.D., et al. (1991). Four molecular pathways of T cell adhesion to endothelial cells: Roles of LFA-1, VCAM-1, and ELAM-1 and changes in pathway hierarchy under different activation conditions. *The Journal of Cell Biology*, 113: 1203-1212.
- Shiokawa, D., Sato, A., Ohata, H., Mutoh, M., Sekine, S., Kato, M., et al. (2017). The induction of selected Wnt target genes by Tcf1 mediates generation of tumorigenic colon stem cells. *Cell Reports*, 19: 981-994.
- Sica, A. & Mantovani, A. (2012). Macrophage plasticity and polarization: in vivo veritas. *The Journal of Clinical Investigation*, 122: 787-795.
- Skugor, S., Grisdale-Helland, B., Refstie, S., Afanasyev, S., Vielma, J. & Krasnov, A. (2011). Gene expression responses to restricted feeding and extracted soybean meal in Atlantic salmon (*Salmo salar* L.). *Aquaculture Nutrition*, 17: 505-517.
- Smirnov, A., Solga, M.D., Lannigan, J. & Criss, A.K. (2015). An improved method for differentiating cell-bound from internalized particles by imaging flow cytometry. *Journal of Immunological Methods*, 423: 60-69.

- Smith, N.C., Christian, S.L., Woldemariam, N.T., Clow, K.A., Rise, M.L. & Andreassen, R. (2020). Characterization of miRNAs in cultured atlantic salmon head kidney monocyte-like and macrophage-like cells. *Int J Mol Sci*, 21: 3989.
- Smith, N.C., Rise, M.L. & Christian, S.L. (2019). A comparison of the innate and adaptive immune systems in cartilaginous fish, ray-finned fish, and lobe-finned fish. *Frontiers in Immunology*, 10: 2292.
- Smith, V.J. & Fernandes, J.M. (2009). Antimicrobial peptides of the innate immune system. *Fish Defenses*, 1: 241-275.
- Smythies, L.E., Sellers, M., Clements, R.H., Mosteller-Barnum, M., Meng, G., Benjamin, W.H., et al. (2005). Human intestinal macrophages display profound inflammatory anergy despite avid phagocytic and bacteriocidal activity. *The Journal of Clinical Investigation*, 115: 66-75.
- Sollid, L.M. (2002). Coeliac disease: dissecting a complex inflammatory disorder. *Nature Reviews Immunology*, 2: 647-655.
- Soza-Ried, C., Hess, I., Netuschil, N., Schorpp, M. & Boehm, T. (2010). Essential role of *c-myb* in definitive hematopoiesis is evolutionarily conserved. *Proceedings of the National Academy of Sciences*, 107: 17304.
- Stella, M.C., Vercelli, A., Repici, M., Follenzi, A. & Comoglio, P.M. (2001). Macrophage stimulating protein is a novel neurotrophic factor. *Molecular Biology of the Cell*, 12: 1341-1352.
- Subramanian, V., Nabokina, S. & Said, H. (2014). Interaction of TM4SF4 with the human thiamine (vitamin B1) transporter-2 (hTHTR-2) in human intestinal epithelial cells (896.1). *The FASEB Journal*, 28: 896.1.
- Sullivan, C., Charette, J., Catchen, J., Lage, C.R., Giasson, G., Postlethwait, J.H., et al. (2009). The gene history of zebrafish *tlr4a* and *tlr4b* is predictive of their divergent functions. *The Journal of Immunology*, 183: 5896-5908.
- Sundaram, A.Y., Kiron, V., Dopazo, J. & Fernandes, J.M. (2012). Diversification of the expanded teleost-specific toll-like receptor family in Atlantic cod, *Gadus morhua*. *BMC Evolutionary Biology*, 12: 256.
- Sveen, L.R., Grammes, F.T., Ytteborg, E., Takle, H. & Jørgensen, S.M. (2017). Genome-wide analysis of Atlantic salmon (*Salmo salar*) mucin genes and their role as biomarkers. *PLoS one*, 12: e0189103.
- Takada, S., Berezikov, E., Yamashita, Y., Lagos-Quintana, M., Kloosterman, W.P., Enomoto, M., et al. (2006). Mouse microRNA profiles determined with a new and sensitive cloning method. *Nucleic Acids Res*, 34: e115-e115.
- Tan, H.-Y., Wang, N., Li, S., Hong, M., Wang, X. & Feng, Y. (2016). The reactive oxygen species in macrophage polarization: reflecting its dual role in progression and treatment of human diseases. *Oxidative Medicine and Cellular Longevity*, 2016: 2795090.
- Taylor, A.E., Finney-Hayward, T.K., Quint, J.K., Thomas, C.M.R., Tudhope, S.J., Wedzicha, J.A., et al. (2010). Defective macrophage phagocytosis of bacteria in COPD. *Eur Respir J*, 35: 1039-1047.
- Terjung, S., Walter, T., Seitz, A., Neumann, B., Pepperkok, R. & Ellenberg, J. (2010). High-throughput microscopy using live mammalian cells. *Cold Spring Harbor Protocols*, 2010: pdb. top84.
- Thyrring, J., Rysgaard, S., Blicher, M.E. & Sejr, M.K. (2015). Metabolic cold adaptation and aerobic performance of blue mussels (*Mytilus edulis*) along a temperature gradient into the High Arctic region. *Mar Biol*, 162: 235-243.
- Tian, J., Ishibashi, K., Honda, S., Boylan, S.A., Hjelmeland, L.M. & Handa, J.T. (2005). The expression of native and cultured human retinal pigment epithelial cells grown in different culture conditions. *Br J Ophthalmol*, 89: 1510.

- Toda, H., Saito, Y., Koike, T., Takizawa, F., Araki, K., Yabu, T., et al. (2011). Conservation of characteristics and functions of CD4 positive lymphocytes in a teleost fish. *Developmental & Comparative Immunology*, 35: 650-660.
- Trapezar, M., Goropevsek, A., Gorenjak, M., Gradisnik, L. & Rupnik, M.S. (2014). A co-culture model of the developing small intestine offers new insight in the early immunomodulation of enterocytes and macrophages by *Lactobacillus* spp. through STAT1 and NF- κ B p65 translocation. *PLoS One*, 9: e86297.
- Ulvestad, J.S. (2017). Studies on the stimulation of Atlantic salmon macrophage-like cells with emphasis on respiratory burst. UiT The Arctic University of Norway. p.27.
- Urán, P., Gonçalves, A., Taverne-Thiele, J., Schrama, J., Verreth, J. & Rombout, J. (2008). Soybean meal induces intestinal inflammation in common carp (*Cyprinus carpio* L.). *Fish & Shellfish Immunology*, 25: 751-760.
- Uribe-Herranz, M., Rafail, S., Beghi, S., Gil-De-Gómez, L., Verginadis, I., Bittinger, K., et al. (2020). Gut microbiota modulate dendritic cell antigen presentation and radiotherapy-induced antitumor immune response. *The Journal of Clinical Investigation*, 130: 466-479.
- Vaishnav, S., Yamamoto, M., Severson, K.M., Ruhn, K.A., Yu, X., Koren, O., et al. (2011). The antibacterial lectin RegIII γ promotes the spatial segregation of microbiota and host in the intestine. *Science*, 334: 255-258.
- Van Baarlen, P., Troost, F., Van Der Meer, C., Hooiveld, G., Boekschoten, M., Brummer, R.J., et al. (2011). Human mucosal in vivo transcriptome responses to three lactobacilli indicate how probiotics may modulate human cellular pathways. *Proceedings of the National Academy of Sciences*, 108: 4562-4569.
- Van Furth, R., Cohn, Z.A., Hirsch, J.G., Humphrey, J.H., Spector, W.G. & Langevoort, H.L. (1972). The mononuclear phagocyte system: A new classification of macrophages, monocytes, and their precursor cells. *Bull W H O*, 46: 845-852.
- Vasanth, G., Kiron, V., Kulkarni, A., Dahle, D., Lokesh, J. & Kitani, Y. (2015). A microbial feed additive abates intestinal inflammation in Atlantic salmon. *Frontiers in Immunology*, 6: 409.
- Velu, C.S., Baktula, A.M. & Grimes, H.L. (2009). Gfi1 regulates miR-21 and miR-196b to control myelopoiesis. *Blood*, 113: 4720-4728.
- Wan, S. & Sun, H. (2019). Glucagon-like peptide-1 modulates RAW264.7 macrophage polarization by interfering with the JNK/STAT3 signaling pathway. *Exp Ther Med*, 17: 3573-3579.
- Wang, J., Chen, W.-D. & Wang, Y.-D. (2020). The relationship between gut microbiota and inflammatory Diseases: The role of macrophages. *Front Microbiol*, 11: 1065.
- Wang, J., Lei, P., Gamil, A.a.A., Lagos, L., Yue, Y., Schirmer, K., et al. (2019a). Rainbow trout (*Oncorhynchus mykiss*) intestinal epithelial cells as a model for studying gut immune function and effects of functional feed ingredients. *Front Immunol*, 10: 152.
- Wang, S., Ye, Q., Zeng, X. & Qiao, S. (2019b). Functions of macrophages in the maintenance of intestinal homeostasis. *J Immunol Res*, 2019: 1512969.
- Wang, W., Liu, Y., Guo, J., He, H., Mi, X., Chen, C., et al. (2018). miR-100 maintains phenotype of tumor-associated macrophages by targeting mTOR to promote tumor metastasis via Stat5a/IL-1ra pathway in mouse breast cancer. *Oncogenesis*, 7: 1-17.
- Wang, Y.-R., Wang, L., Zhang, C.-X. & Song, K. (2017). Effects of substituting fishmeal with soybean meal on growth performance and intestinal morphology in orange-spotted grouper (*Epinephelus coioides*). *Aquaculture Reports*, 5: 52-57.

- Wang, Z., Xu, L., Hu, Y., Huang, Y., Zhang, Y., Zheng, X., et al. (2016). miRNA let-7b modulates macrophage polarization and enhances tumor-associated macrophages to promote angiogenesis and mobility in prostate cancer. *Scientific Reports*, 6: 25602.
- Wentzel, A.S., Janssen, J.J.E., De Boer, V.C.J., Van Veen, W.G., Forlenza, M. & Wiegertjes, G.F. (2020a). Fish macrophages show distinct metabolic signatures upon polarization. *Front Immunol*, 11: 152.
- Wentzel, A.S., Petit, J., Van Veen, W.G., Fink, I.R., Scheer, M.H., Piazzon, M.C., et al. (2020b). Transcriptome sequencing supports a conservation of macrophage polarization in fish. *Sci Rep*, 10: 13470.
- Whitman, W.B., Coleman, D.C. & Wiebe, W.J. (1998). Prokaryotes: The unseen majority. *Proceedings of the National Academy of Sciences*, 95: 6578-6583.
- Wiegertjes, G.F., Wentzel, A.S., Spaink, H.P., Elks, P.M. & Fink, I.R. (2016). Polarization of immune responses in fish: The 'macrophages first' point of view. *Mol Immunol*, 69: 146-156.
- Williams, H., Brenner, S. & Venkatesh, B. (2002). Identification and analysis of additional copies of the platelet-derived growth factor receptor and colony stimulating factor 1 receptor genes in fugu. *Gene*, 295: 255-264.
- Woldemariam, N.T., Agafonov, O., Høyheim, B., Houston, R.D., Taggart, J.B. & Andreassen, R. (2019). Expanding the miRNA repertoire in Atlantic salmon; Discovery of isomiRs and miRNAs highly expressed in different tissues and developmental stages. *Cells*, 8: 42.
- Woo, H.-H., László, C.F., Greco, S. & Chambers, S.K. (2012). Regulation of colony stimulating factor-1 expression and ovarian cancer cell behavior in vitro by miR-128 and miR-152. *Mol Cancer*, 11: 58.
- Wozniak, M.A., Desai, R., Solski, P.A., Der, C.J. & Keely, P.J. (2003). ROCK-generated contractility regulates breast epithelial cell differentiation in response to the physical properties of a three-dimensional collagen matrix. *J Cell Biol*, 163: 583-595.
- Wu, K., Yuan, Y., Yu, H., Dai, X., Wang, S., Sun, Z., et al. (2020). The gut microbial metabolite trimethylamine N-oxide aggravates GVHD by inducing M1 macrophage polarization in mice. *Blood*, 136: 501-515.
- Wu, R.-Q., Zhang, D.-F., Tu, E., Chen, Q.-M. & Chen, W. (2014). The mucosal immune system in the oral cavity—An orchestra of T cell diversity. *International Journal of Oral Science*, 6: 125-132.
- Wu, Y., Wu, W., Wong, W.M., Ward, E., Thrasher, A.J., Goldblatt, D., et al. (2009). Human $\gamma\delta$ T Cells: A lymphoid lineage cell capable of professional phagocytosis. *The Journal of Immunology*, 183: 5622.
- Xiao, J., Tang, J., Chen, Q., Tang, D., Liu, M., Luo, M., et al. (2015). miR-429 regulates alveolar macrophage inflammatory cytokine production and is involved in LPS-induced acute lung injury. *Biochemical Journal*, 471: 281-291.
- Xu, C. & Zon, L.I. (2010). The zebrafish as a model for human disease. *Fish Physiology*. Elsevier. pp. 345-365.
- Yan, B., Guo, J.-T., Zhu, C.-D., Zhao, L.-H. & Zhao, J.-L. (2013). miR-203b: A novel regulator of MyoD expression in tilapia skeletal muscle. *Journal of Experimental Biology*, 216: 447-451.
- Yi, H.-J. & Lu, G.-X. (2012). Adherent and non-adherent dendritic cells are equivalently qualified in GM-CSF, IL-4 and TNF- α culture system. *Cellular Immunology*, 277: 44-48.
- Yi, S., Gao, Z.-X., Zhao, H., Zeng, C., Luo, W., Chen, B., et al. (2013). Identification and characterization of microRNAs involved in growth of blunt snout bream (*Megalobrama amblycephala*) by Solexa sequencing. *BMC Genomics*, 14: 754.

- Yona, S., Kim, K.-W., Wolf, Y., Mildner, A., Varol, D., Breker, M., et al. (2013). Fate mapping reveals origins and dynamics of monocytes and tissue macrophages under homeostasis. *Immunity*, 38: 79-91.
- Yuan, Y., Lin, D., Feng, L., Huang, M., Yan, H., Li, Y., et al. (2018). Upregulation of miR-196b-5p attenuates BCG uptake via targeting SOCS3 and activating STAT3 in macrophages from patients with long-term cigarette smoking-related active pulmonary tuberculosis. *Journal of Translational Medicine*, 16: 284.
- Zhang, B., Shan, H., Li, D., Li, Z.-R., Zhu, K.-S., Jiang, Z.-B., et al. (2012). Different methods of detaching adherent cells significantly affect the detection of TRAIL receptors. *Tumori Journal*, 98: 800-803.
- Zhang, C., Rahimnejad, S., Wang, Y.-R., Lu, K., Song, K., Wang, L., et al. (2018). Substituting fish meal with soybean meal in diets for Japanese seabass (*Lateolabrax japonicus*): effects on growth, digestive enzymes activity, gut histology, and expression of gut inflammatory and transporter genes. *Aquaculture*, 483: 173-182.
- Zhang, M., Sun, K., Wu, Y., Yang, Y., Tso, P. & Wu, Z. (2017a). Interactions between intestinal microbiota and host immune response in inflammatory bowel disease. *Frontiers in Immunology*, 8: 942.
- Zhang, X., Guo, L., Collage, R.D., Stripay, J.L., Tsung, A., Lee, J.S., et al. (2011). Calcium/calmodulin-dependent protein kinase (CaMK) α mediates the macrophage inflammatory response to sepsis. *Journal of Leukocyte Biology*, 90: 249-261.
- Zhang, Y.-A., Salinas, I., Li, J., Parra, D., Bjork, S., Xu, Z., et al. (2010). IgT, a primitive immunoglobulin class specialized in mucosal immunity. *Nature Immunology*, 11: 827.
- Zhang, Y., Li, X., Wang, C., Zhang, M., Yang, H. & Lv, K. (2020). lncRNA AK085865 promotes macrophage M2 polarization in CVB3-induced VM by regulating ILF2-ILF3 complex-mediated miRNA-192 biogenesis. *Molecular Therapy - Nucleic Acids*, 21: 441-451.
- Zhang, Y., Olson, R.M. & Brown, C.R. (2017b). Macrophage LTB₄ drives efficient phagocytosis of *Borrelia burgdorferi* via BLT1 or BLT2. *J Lipid Res*, 58: 494-503.
- Zhang, Y., Zhang, M., Zhong, M., Suo, Q. & Lv, K. (2013). Expression profiles of miRNAs in polarized macrophages. *Int J Mol Med*, 31: 797-802.
- Zhang, Z., Lei, B., Wu, H., Zhang, X. & Zheng, N. (2017c). Tumor suppressive role of miR-194-5p in glioblastoma multiforme. *Molecular Medicine Reports*, 16: 9317-9322.
- Zhao, W., Minderman, H. & Russell, M.W. (2014). Identification and characterization of intestinal antigen-presenting cells involved in uptake and processing of a nontoxic recombinant chimeric mucosal immunogen based on cholera toxin using imaging flow cytometry. *Clinical and Vaccine Immunology*, 21: 74-84.
- Zhou, D., Huang, C., Lin, Z., Zhan, S., Kong, L., Fang, C., et al. (2014). Macrophage polarization and function with emphasis on the evolving roles of coordinated regulation of cellular signaling pathways. *Cell Signal*, 26: 192-197.
- Zhou, Y., Hong, Y. & Huang, H. (2016). Triptolide attenuates inflammatory response in membranous glomerulonephritis rat via downregulation of NF- κ B signaling pathway. *Kidney Blood Press Res*, 41: 901-910.

Paper I

This is an open-access article, reproduced and distributed under the terms of the Creative Commons Attribution License (CC BY)



Imaging Flow Cytometry Protocols for Examining Phagocytosis of Microplastics and Bioparticles by Immune Cells of Aquatic Animals

Youngjin Park¹, Isabel S. Abihssira-García¹, Sebastian Thalmann², Geert F. Wiegertjes³, Daniel R. Barreda⁴, Pål A. Olsvik¹ and Viswanath Kiron^{1*}

¹ Faculty of Biosciences and Aquaculture, Nord University, Bodo, Norway, ² Luminex B.V., 's-Hertogenbosch, Netherlands, ³ Aquaculture and Fisheries Group, Wageningen University & Research, Wageningen, Netherlands, ⁴ Department of Biological Sciences, University of Alberta, Edmonton, AB, Canada

OPEN ACCESS

Edited by:

Kim Dawn Thompson,
Moredun Research Institute,
United Kingdom

Reviewed by:

Sebastian Reyes-Cerpa,
Universidad Mayor, Chile
Caroline Fossum,
Swedish University of Agricultural
Sciences, Sweden

*Correspondence:

Viswanath Kiron
kiron.viswanath@nord.no

Specialty section:

This article was submitted to
Comparative Immunology,
a section of the journal
Frontiers in Immunology

Received: 20 October 2019

Accepted: 27 January 2020

Published: 18 February 2020

Citation:

Park Y, Abihssira-García IS, Thalmann S, Wiegertjes GF, Barreda DR, Olsvik PA and Kiron V (2020) Imaging Flow Cytometry Protocols for Examining Phagocytosis of Microplastics and Bioparticles by Immune Cells of Aquatic Animals. *Front. Immunol.* 11:203. doi: 10.3389/fimmu.2020.00203

Imaging flow cytometry (IFC) is a powerful tool which combines flow cytometry with digital microscopy to generate quantitative high-throughput imaging data. Despite various advantages of IFC over standard flow cytometry, widespread adoption of this technology for studies in aquatic sciences is limited, probably due to the relatively high equipment cost, complexity of image analysis-based data interpretation and lack of core facilities with trained personnel. Here, we describe the application of IFC to examine phagocytosis of particles including microplastics by cells from aquatic animals. For this purpose, we studied (1) live/dead cell assays and identification of cell types, (2) phagocytosis of degradable and non-degradable particles by Atlantic salmon head kidney cells and (3) the effect of incubation temperature on phagocytosis of degradable particles in three aquatic animals—Atlantic salmon, Nile tilapia, and blue mussel. The usefulness of the developed method was assessed by evaluating the effect of incubation temperature on phagocytosis. Our studies demonstrate that IFC provides significant benefits over standard flow cytometry in phagocytosis measurement by allowing integration of morphometric parameters, especially while identifying cell populations and distinguishing between different types of fluorescent particles and detecting their localization.

Keywords: ImageStream[®], IFC, Atlantic salmon, Nile tilapia, blue mussel, phagocytosis

INTRODUCTION

Flow cytometry (FC) is widely employed for studying mammalian cells in particular and detecting biomarkers in clinical studies. FC systems quantify cell data within seconds and can provide information on cell phenotypes and functions. However, conventional FC is not designed to measure morphological and spatial information of single cells, and the technology is not able to efficiently detect dim and small particles (<300 nm) (1) as well as to distinguish aggregates of these small particles. Furthermore, although conventional FC can measure intra- and extra-cellular marker expressions, it does not provide information on marker localization. Another obstacle connected to conventional FC is auto-fluorescence. While the system cannot always precisely distinguish between false-positive and false-negative events (2), fine-tuning of instrument settings and protocol optimization can minimize the problem (3). Nevertheless, cell phenotype identification and functional analyses using conventional FC cannot be entirely objective as the equipment lacks image-capturing features. To overcome inaccuracies in acquiring cell data,

quantitative studies preferably rely on both conventional FC and fluorescent cell imaging.

Imaging flow cytometry (IFC), also called multispectral imaging flow cytometry, is a powerful tool that enables us to collect information from single cells, including those from fluorescent images. Major advantages of IFC are (1) high fluorescence sensitivity, (2) high image resolution capability, (3) high speed processing, (4) ability to analyse changes in cell or nuclear morphology, (5) rare cell detection ability, and (6) capacity to understand cell-cell interaction (2). Certain disciplines of biology, namely hematology (4), immunology (5), cell biology (6), and microbiology (7) have already benefited from IFC. However, application of IFC is still in its infancy when it comes to studies in aquatic sciences.

Researchers have reported IFC-based analyses of fish cells, using nucleus staining to understand cell morphology and employing fluorescent particles to determine phagocytic activity in goldfish (8, 9). Different particles such as fluorescent latex beads (10), zymosan-APC (8), and nanoparticles (11) have been used to analyse phagocytosis using IFC. These methods can be further optimized, depending on the characteristics of the particles, e.g., latex beads that are not degraded vis-à-vis pHrodo™ BioParticles® that emit fluorescent light upon acidification following ingestion by the target cells (10). Researchers have also improved the protocol for measuring particles' intensity in IFC (12). Overall, these studies provide the first information on the use of IFC to identify different cells and understand cell functions such as phagocytosis and the localization of markers of interest in cells from aquatic animals.

Though previous studies on aquatic animals have reported phagocytosis, here we present (1) basic, but optimized protocols for live/dead cell assay and identification of cell types (2), an improved protocol for examining phagocytosis of non-degradable (microplastic) and degradable (bioparticles) particles by immune cell types of fish, and (3) an optimized phagocytosis assay using cells harvested from three very different aquatic animals: cold water-adapted carnivorous marine fish (Atlantic salmon, *Salmo salar*), warm water-adapted omnivorous, freshwater fish (Nile tilapia, *Oreochromis niloticus*) and a cold water-adapted detritivorous/planktivorous marine mollusc (blue mussel, *Mytilus edulis*). Effect of incubation temperature was studied to verify the sensitivity and usefulness of the optimized phagocytosis assay.

METHODS

Ethics Statement

The studies were approved (Atlantic salmon: FOTS ID 10050, Nile tilapia: FOTS ID 1042) by the National Animal Research Authority in Norway (Mattilsynet). The fish rearing and handling procedures were according to the approved protocols of FDU.

Animals

Atlantic salmon (*S. salar*) in the weight range 700–900 g were used in this experiment. They were purchased from a commercial producer (Sundsford Smolt, Nygårdsoen, Norway) and maintained at the Research Station of Nord University,

Bodø, Norway. Fish were fed a commercial feed (Ewos AS, Bergen, Norway) and reared in a flow-through sea water system (temperature: 7–8°C, dissolved oxygen saturation: 87–92%, 24-h light cycle).

Nile tilapia (*O. niloticus*, 400–600 g) were bred and reared at the Research Station of Nord University in a freshwater recirculating aquaculture system (temperature: 28°C, pH: 7.6, dissolved oxygen saturation: 80% in outlet and 115% in inlet, 11 h dark/13 h light cycle). The fish were fed commercial feeds (Skretting, Stavanger, Norway) during the rearing period.

Adult blue mussels (*M. edulis*) were collected from a beach along the Saltenfjorden, Bodø, Norway (67°12'01" N 14°37'56" E) and transported to the Research Station, Nord University. Prior to isolation of hemocytes, they were kept for 2 days in running seawater at 7–8°C.

Cell Isolation

Cells from salmon and tilapia head kidney (HK) were grown in Leibovitz's L-15 Medium (L-15; Sigma-Aldrich, Oslo, Norway), supplemented with 100 µg/mL gentamicin sulfate (Sigma), 2 mM L-glutamine (Sigma) and 15 mM HEPES (Sigma). Osmolality of medium was adjusted by adding a solution consisting of 5% (v/v) 0.41 M NaCl, 0.33 M NaHCO₃, and 0.66 (w/v) D-glucose. Cell culture media were adjusted to 380 mOsm for salmon and 320 mOsm for tilapia. To culture the mussel hemocytes, filtered (through a 0.2 µm mesh) sea water was used as the medium.

Head kidney from salmon ($n = 6$) were sampled after the fish were killed with an overdose of MS-222 (Tricaine methane sulphonate; Argent Chemical Laboratories, Redmond, USA; 80 mg/L). Thereafter, the HK cells were isolated as described previously (13) with minor modifications. Briefly, HK was dissected out, and the tissues were transferred to 15 mL centrifuge tubes to make a total volume of 4 mL in ice-cold L-15+ (L-15 medium with 50 U/mL penicillin, 50 µg/mL streptomycin, 2% fetal bovine serum (FBS) and 10 U/mL heparin). The tissue was placed on a sterile 100 µm cell strainer (Falcon) and the cells were disrupted with the help of a syringe plunger. The harvested cells were washed twice in ice-cold L-15+. The cell suspension from salmon HK was then layered on 40/60% Percoll (Sigma) to separate HK leukocytes for magnetic-activated cell sorting (MACS) or layered on 34/51% Percoll to separate monocytes/macrophages for subsequent phagocytosis assays. After centrifugation (500 × g, 30 min, 4°C), the cells at the interface between the two Percoll gradients were collected and washed twice with ice-cold L-15-FBS free (L-15 medium with 50 U/mL penicillin, 50 µg/mL streptomycin) by centrifugation (500 × g, 5 min, 4°C). Cells were then kept in L-15+. HK phagocytic cells that were separated based on 34/51% Percoll gradient, were allowed to adhere on a petri dish for 3 days at 12°C. After removing the supernatant containing non-adherent cells, the petri dish with the adherent cells was placed on ice for 10 min, and the cells were collected by washing three times with 1.5 mL ice-cold PBS supplemented with 5 mM EDTA. Next, these collected cells were centrifuged (500 × g, 5 min, 4°C) and used for further analyses.

Head kidney from tilapia ($n = 6$) were collected after killing the fish with an overdose of clove oil (Sigma Aldrich, St. Louis,

MO, USA), and cells were harvested as described previously (14, 15), with minor modifications. Briefly, the HK tissues were transferred to 15 mL centrifuge tubes to make a total volume of 4 mL in ice-cold L-15+. The cells were harvested from the HK and washed twice as described for salmon. The cell suspension was layered on 34/51% Percoll to separate phagocytic cells, and then after centrifugation, cells at the interface were collected and washed twice in L-15-FBS free. The cells in the suspension were allowed to adhere on a petri dish containing L-15+ for 3 days at 25°C. After removing the supernatant containing non-adherent cells, the petri dish with the adherent cells was placed on ice for 10 min, and the cells were collected by washing three times with 1.5 mL ice-cold PBS supplemented with 5 mM EDTA. Next, the collected cells were centrifuged (500 × g, 5 min, 4°C) and used for further analyses.

In the fish experiments, the cells were counted using a portable cell counter (Scepter™ 2.0 cell counter, EMD Millipore, Darmstadt, Germany).

Hemocytes from adult mussels ($n = 6$) were isolated as described previously (16) with minor modifications. Briefly, hemolymph was drawn from the posterior adductor muscle using a 2 mL syringe equipped with a 23G-needle. The hemocytes from each mussel were counted using a Neubauer chamber, and 0.2×10^6 cells per sample were collected and re-suspended in 1 mL of filtered sea water to avoid formation of clumps.

Magnetic-Activated Cell Sorting (MACS) of Salmon IgM⁺ Cells

The isolated salmon HK leukocytes (2×10^6 cells) were incubated with mouse anti-trout/salmon IgM (6.06 μg/mL; Aquatic Diagnostics Ltd, Sterling, UK) for 60 min at 4°C. After two washes with L-15+, the cells were incubated for 15 min at 4°C in a cocktail with a total volume of 100 μL, which contained L-15+, 1 μL of goat anti-mouse IgG-FITC (0.75 mg/mL; Thermo Fisher Scientific, Oslo, Norway) and 40 μL of goat anti-mouse IgG microbeads as per the instructions of the manufacturer (Miltenyi Biotec, Bergisch Gladbach, Germany). First, MACS LD columns (Miltenyi Biotec) that were placed in a magnetic separator of the multistand were washed using L-15+. The cell suspension was then transferred into the LD column. Following cell sorting, the positive cells were harvested and re-suspended in L-15+.

Live/Dead Cell Assay

In the studies on cells from salmon and tilapia, aliquots containing 1×10^6 cells in 50 μL PBS were transferred to 1.5 mL microcentrifuge tubes. Then 1 μL of propidium iodide (PI; 1 mg/mL, Sigma) was added to each sample to detect the dead cells in the cell suspension. In the case of mussel, aliquots containing 0.2×10^6 cells in 50 μL filtered sea water were transferred to 1.5 mL microcentrifuge tubes, and then 1 μL of DRAQ5™ (25 mM, Thermo Fisher Scientific) was added to each sample to detect the dead cells in the cell suspension. The tubes were gently mixed before the samples were run through the ImageStream®^X Mk II Imaging Flow Cytometer (Luminex Corporation, Austin, TX, USA). Cell analyses were performed on 10,000 cells acquired at a rate of 300 objects/second at low speed and a magnification of

40×. Dead cells were estimated as the percent of cells positive for either PI or DRAQ5™ (red fluorescent cells). After excluding the dead cells, viable cells were analyzed to generate brightfield (BF) area (size) vs. side scatter (SSC) intensity (complexity) dot plots. Instrument settings were kept identical throughout the study.

Phagocytosis Assay

In the first phagocytosis experiment, phagocytic cells from salmon HK were employed to study the uptake of two types of particles; non-degradable fluorescent polystyrene microplastic beads (2.1 μm; Magsphere Inc., California, USA) and degradable fluorescent bio-particles (>0.2 μm; pHrodo™ Red *Escherichia coli* Bioparticles, Thermo Fisher Scientific). In the second experiment, we used degradable fluorescent bio-particles only; to determine phagocytic ability and capacity of the cells from salmon, tilapia and mussel at two different incubation temperatures. Phagocytic ability was measured as the percent of phagocytic cells among the total macrophage-like cells or hemocytes. On the other hand, phagocytic capacity was measured as the mean number of particles per phagocytic cell. Phagocytic index (PI) or phagocytic activity was determined employing the equation (17, 18):

Phagocytic index (PI) = [% phagocytic cells containing at least one particle] × [mean particle count per phagocytic cell].

Briefly, fluorescent bio-particles were added at a cell:particle ratio of 1:5 per sample, both in the case of HK macrophages (0.5×10^6 cells) and hemocytes (0.2×10^6 cells). Cells suspensions and bio-particles were mixed and incubated for 2 h at different temperatures. Following incubation, cell suspensions were washed twice with 500 μL L-15+ by centrifugation (500 × g, 5 min, 4°C). The supernatant was discarded, and the resulting cell pellets were re-suspended in 50 μL PBS. The cell samples were run in an imaging flow cytometer (Luminex), equipped with a 10 mW 488 nm argon-ion laser, to detect the bio-particle fluorescence (577/35 nm bandpass; Channel 3). Thereafter, the images were analyzed using IDEAS 6.1.822.0 software (Luminex).

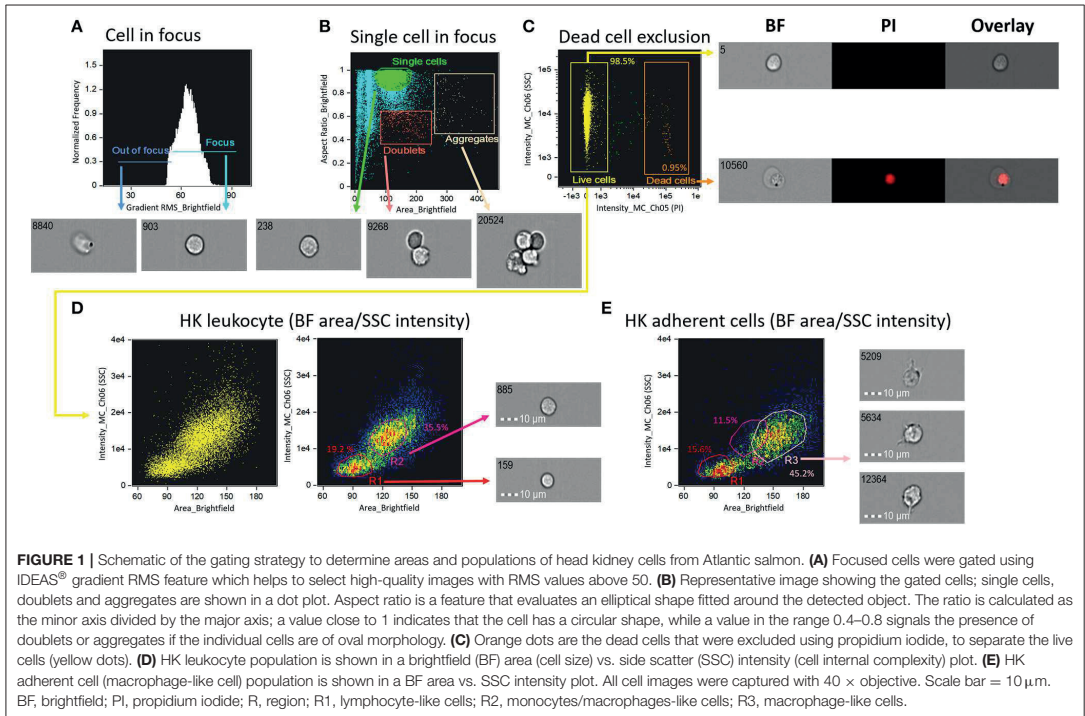
Data and Statistical Analyses

Statistical analysis was performed in RStudio version 1.1.463. Normality of the data was tested by Shapiro-Wilk Test, and the assumption of equal variance was checked by Bartlett's Test. Comparisons between the two groups were performed using unpaired Student's *t*-test. Statistically significant differences ($p < 0.05$) are reported for the phagocytosis data.

RESULTS

Live/Dead Cells and Leukocyte Populations From Salmon Head Kidney

To determine single cell area and to identify cell populations, we employed a basic gating strategy using the Brightfield Gradient Root Mean Square (RMS) feature of the imaging flow cytometer (see **Figure 1**). This strategy helped us to select the cells in best focus, i.e., this allowed us to obtain high quality images with RMS values >50 (**Figure 1A**). Next, we separated single cells from others (debris, doublets and aggregates; **Figure 1B**). Dead cells were excluded based on



positivity for PI (Figure 1C). The percentage of live cells were 98.5%. The brightfield (BF) area and side scatter (SSC) intensity of the live, single cells were assessed. We prepared a BF area vs. SSC intensity dot plot to show the salmon HK leukocyte populations (Figure 1D). Cells with smaller size (low BF area) and low SSC intensity were possibly lymphocyte-like cells (19.2%; R1 in Figure 1D) while those with larger size (BF area) and higher SSC intensity compared to lymphocyte-like cells were considered as monocytes/macrophages (35.5%; R2 in Figure 1D). Figure 1E shows salmon HK adherent cell populations in a BF area vs. SSC intensity dot plot; here, R3 is probably HK macrophage-like cells (45.2%). We conclude that using IFC, dead cells can be excluded, and different single cell populations can be better detected than in conventional FC.

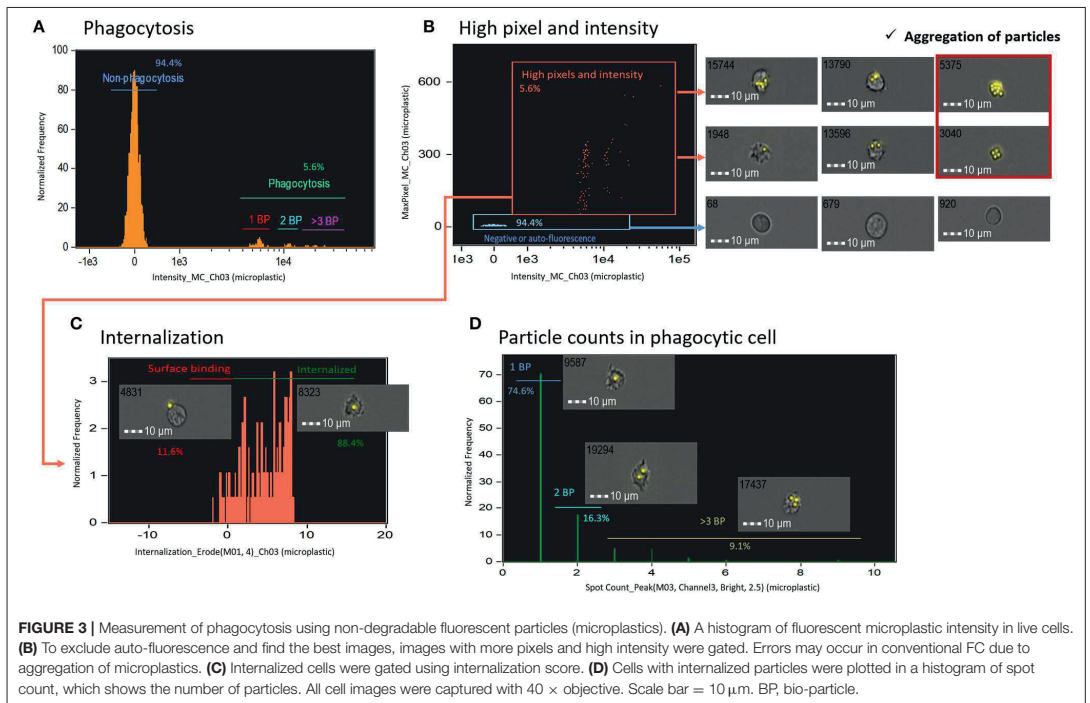
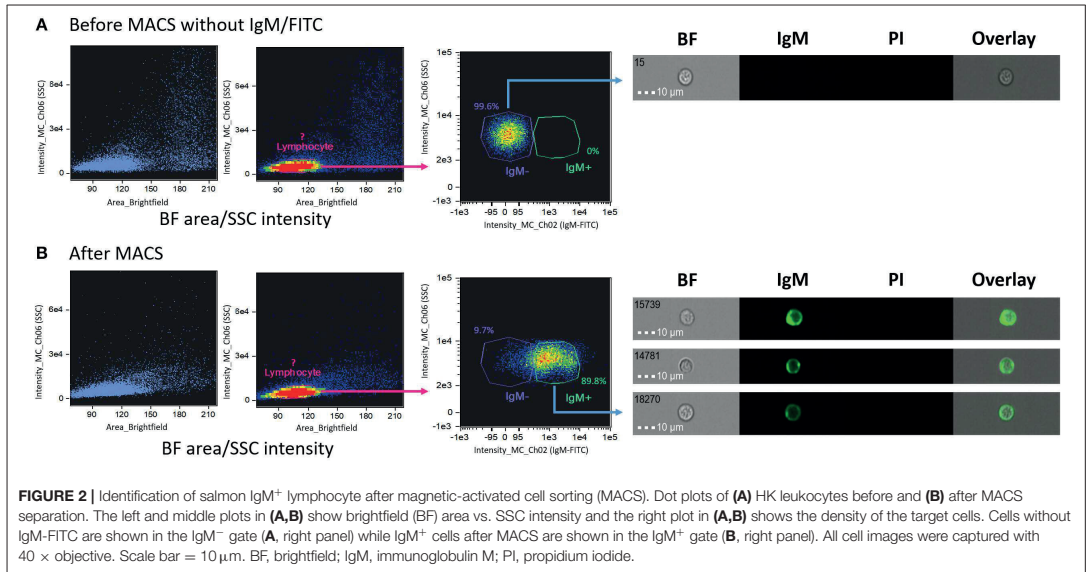
Salmon Head Kidney IgM⁺ Lymphocyte Identification

Salmon head kidney IgM⁺ lymphocytes separated using MACS were used to ascertain their localization in a BF area vs. SSC intensity dot plot (Figure 2). For this purpose, cells were extracellularly stained with IgM-FITC, which enabled us to identify areas of negatively- and positively-stained B lymphocyte populations. Before MACS (Figure 2A), all cells were located in the IgM⁻ area (right panel Figure 2A). After staining with

IgM-FITC and performing MACS (Figure 2B), most cells were located in the IgM⁺ area (89.8%; right panel Figure 2B). These data confirmed that the IgM⁺ cells matched the location of the lymphocyte-like cells (R1 population in Figure 1D). Thus, we confirmed the localization of salmon IgM⁺ cells using IFC.

Examining Phagocytosis Using Non-degradable Fluorescent Microplastic Beads

To determine the phagocytosis of microplastics by salmon HK cells, first, we plotted histograms of fluorescence intensity of non-degradable fluorescent polystyrene microplastic beads in live cells (Figure 3A). Because all the polystyrene beads were of similar size, we assumed that fluorescence intensity is proportional to the number of beads taken up by each phagocytic cell. Using IFC, we could exclude auto-fluorescence and could gate images with more pixels and higher intensity (phagocytic images with pixel value > 30 were considered to be of high quality) (Figure 3B). Caution was taken to exclude aggregates; addition of many microplastic beads can cause bead aggregation, leading to false identification of aggregates as phagocytic cells, especially in conventional FC. Next, we gated phagocytic cells that engulfed microplastic beads using an internalization score (Figure 3C). This score is the ratio of the particle intensity inside a cell to the intensity of the whole cell, and it is calculated after masking (which selects pixels



within an image based on their intensity and localization) with the following mask function [Erode (M01, 4)_Ch03]. The ratio indicated the proximity of microplastic to the center of the cell; cells with a score of > 0.3 were considered to have internalized particles and those with a score of < 0.3 were considered to have surface-bound particles (11). Finally, only cells with internalized particles were presented in a histogram of spot count feature, which is an ideal approach to quantify the masked spots in the cell (Figure 3D). Overall, IFC can be applied for detecting non-degradable microplastic beads inside the phagocytic cells and quantifying the number of beads. In addition, salmon HK phagocytic cells could recognize microplastics as foreign bodies although we observed only few phagocytosed particles.

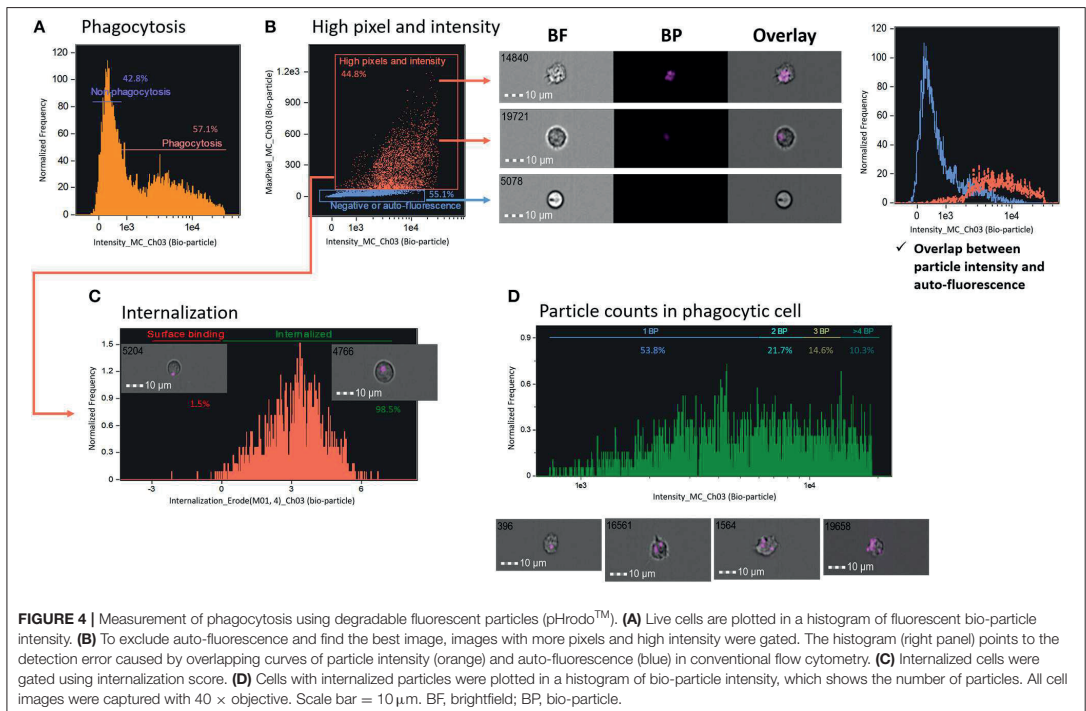
Examining Phagocytosis Using Degradable Fluorescent Bio-particles

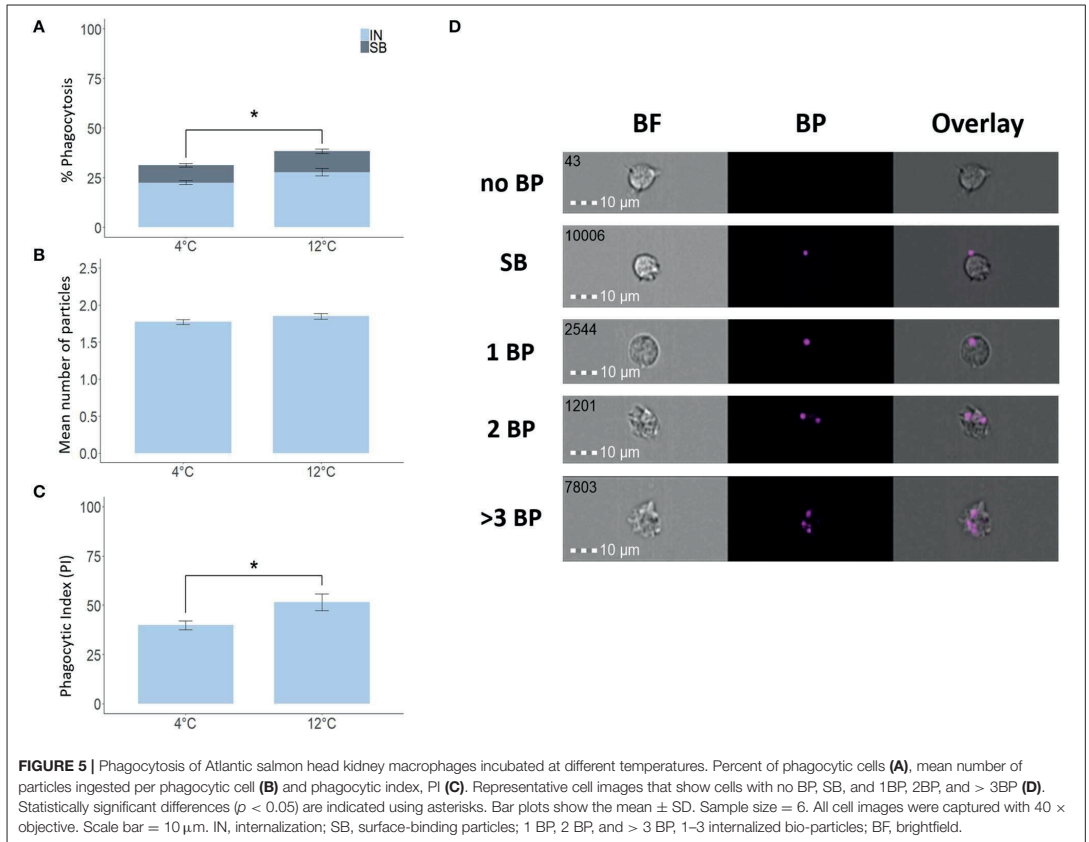
To determine phagocytosis of degradable bio-particles by salmon HK cells compared with non-degradable microplastics, first, we plotted histograms of fluorescence intensity of degradable bio-particles (Figure 4A). In comparison to the histogram of the non-degradable microplastic beads described above (Figure 3), it was more difficult to distinguish the number of bio-particles in this histogram. To exclude auto-fluorescence and obtain high-quality images, we adopted a gating strategy based on high pixel (pixel value > 30) and intensity of images (Figure 4B). We created

two gates, one to include particles with high pixel and high intensity and the other one with negative or auto-fluorescence (histogram in Figure 4B). From the histogram, it is clear that overlapping particle intensity (orange) and auto-fluorescence (blue) curves can cause detection errors. Cells that had engulfed the bio-particles were gated using the internalization score as described in the previous section (Figure 4C). Finally, only cells with internalized particles are presented in a histogram of particle intensity to understand the number of particles in the phagocytic cells (Figure 4D). We found that to quantify the number of degradable particles, particle intensity-based protocol is a better strategy compared to the method employing spot count feature.

Optimizing IFC-Based Method for Phagocytosis Assay

To verify the validity of our IFC-based method, we used degradable fluorescent bio-particles from *E. coli* to assess the effect of incubation temperature on the phagocytic activity and capacity of phagocytic cells from three aquatic animals. The phagocytic ability of HK phagocytic cells from salmon (Figure 5A) and tilapia (Figure 6A) incubated at 12 and 25°C, respectively, was significantly higher compared to cells incubated at 4°C, but temperature did not significantly affect the phagocytic ability of hemocytes from blue mussel (Figure 7A). In contrast, the phagocytic capacity of none of the aquatic species tested





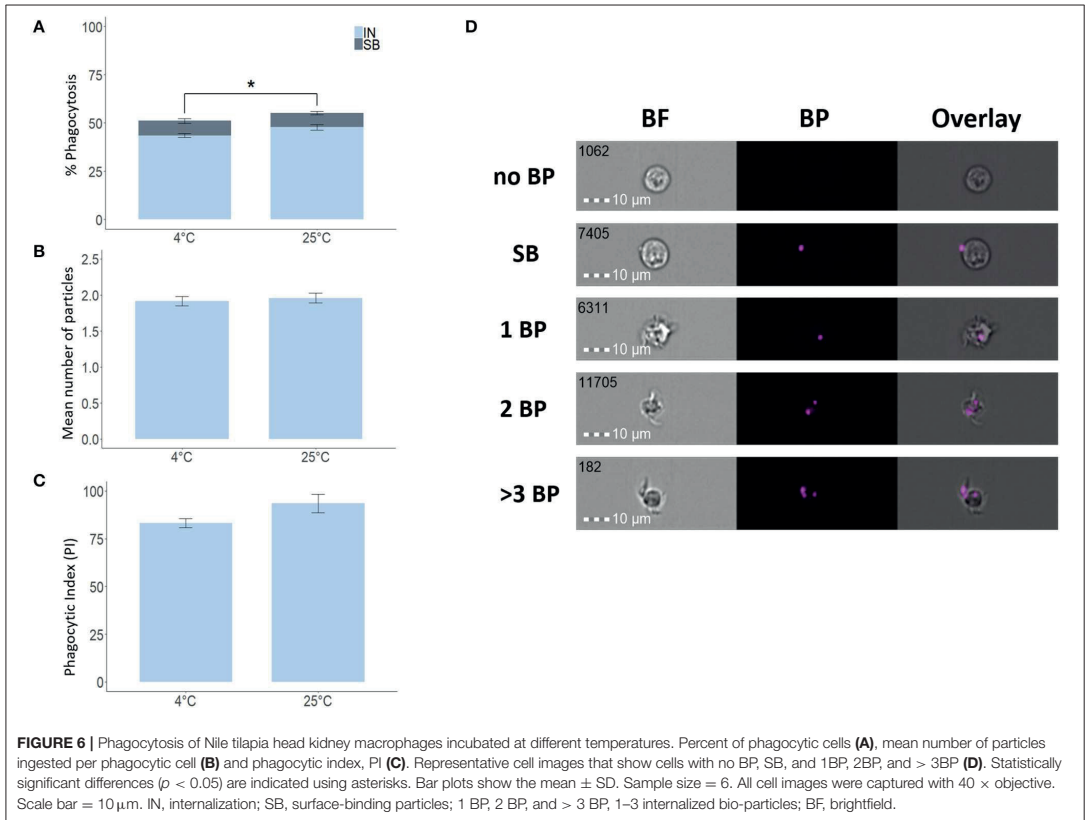
was significantly affected by temperature (**Figures 5B,D, 6B,D, 7B,D**). The phagocytic index of only the salmon cells incubated at 12°C was significantly higher compared to cells incubated at 4°C (**Figure 5C**). This temperature effect could not be detected for the phagocytic index of tilapia HK cells (**Figure 6C**) and blue mussel hemocytes (**Figure 7C**) although the cells were incubated at higher values, i.e., 12 and 25°C, respectively. The optimized method for phagocytosis assay was well-applied to phagocytic cells from three aquatic animals. The results showed that unlike that of phagocytic cells from fishes, phagocytosis of the cells from mussel was not significantly affected by incubation temperature.

DISCUSSION

The major advantage of imaging flow cytometry (IFC) over conventional flow cytometry (FC) is its ability to distinguish between false-positive and false-negative events by considering additional features of the captured cellular images (2). The two systems share the basic principle (19). Although IFC has been widely adopted to study mammalian cell types, it is not yet

commonly employed to investigate other organisms, including aquatic animals. There is a paucity of appropriate tools such as cell-specific markers, which hampers the wider adoption of new technologies like IFC. Furthermore, the associated protocols require thorough refining before IFC can be used to study cell types from aquatic animals. For example, as the weak and small fluorescence cannot be detected by the system, we employ masking and features within IDEAS software to accurately select the area of interest during image analysis (20). Our study describes procedures to accurately identify cellular phenotypes and quantify phagocytosis by cells from three very different aquatic animals.

In the present IFC study, we could successfully exclude dead cells and cell aggregates and could identify single leukocytes from Atlantic salmon HK based on bright field (BF) area and SSC intensity. We observed two distinct populations: cells located in the low BF area and low SSC intensity, and cells located in the high BF area and high SSC intensity. Our IFC results are in agreement with conventional FC data on HK leukocytes from salmon (21). A study on goldfish primary kidney macrophages



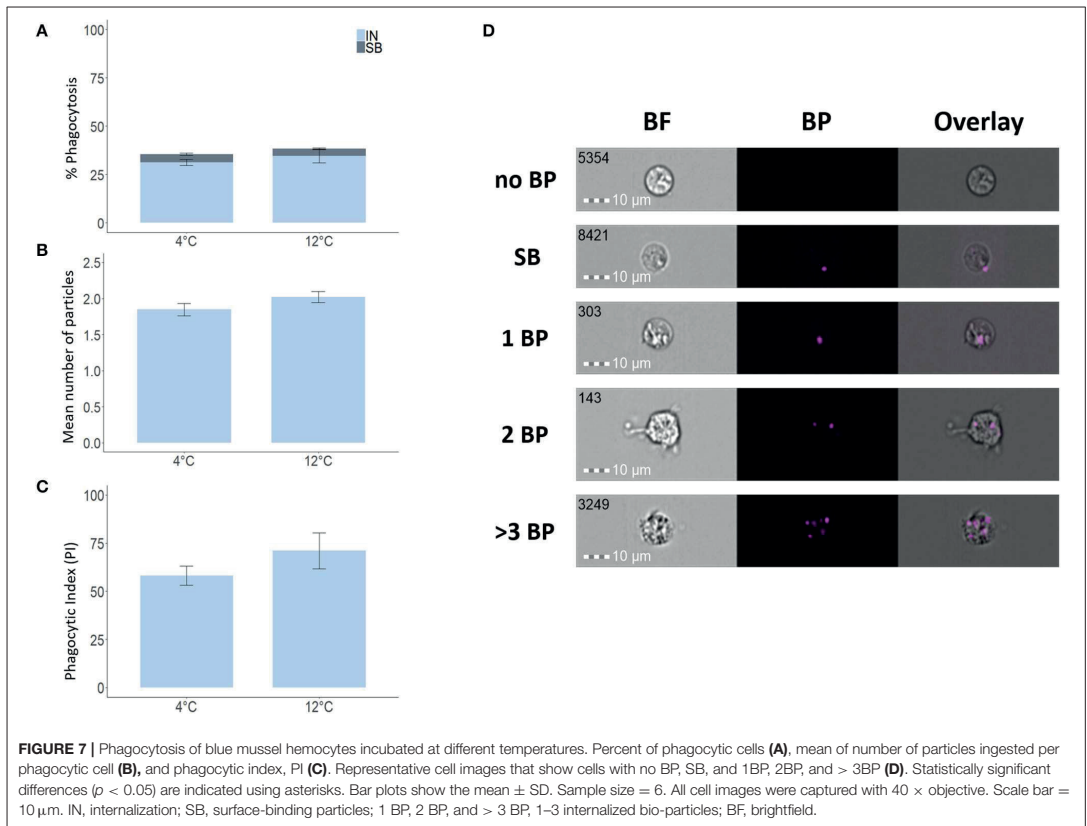
also compared IFC results with those from conventional FC data; both systems were used to identify cell sub-populations. Similar dot plots were generated for both flow cytometry systems, indicating that the replacement of forward scatter (FSC) which measures cell size in conventional FC by BF area in IFC (22) is a reliable approach, independent of fish species.

Interestingly, adherent cells from Atlantic salmon HK (R3, macrophage-like cells) were located in a higher BF area than R2 cells from the same organ (Figures 1D,E). The proportion of macrophage-like cells was approximately 45.2%. The macrophage-like cells in the R3 region displayed a similar morphology to that of the adherent TO cells, a cell line originating from salmon HK leukocytes (23). Furthermore, in another study that employed conventional FC, salmon macrophage-like cells were presented in an FSC vs. SSC plot (24). Similar to our gating, the author gated three regions in the plot and assumed that the two higher FSC regions contained macrophage-like cells which was \sim 56% out of the total number of cells.

After optimizing the method to distinguish between lymphocytes from monocytes/macrophages, magnetic cell

sorting (MACS) was performed to sort target lymphocytes using an IgM-specific antibody. The purity of IgM⁺ cells after MACS was 89.8% which is similar to 92% in a salmon study (25). MACS enabled us to ascertain the area of lymphocyte-like cells as defined/interpreted from the BF area vs. SSC intensity plots. The sorted salmon IgM⁺ cells were located in the low BF area and low SSC intensity gate, confirming a close area match to that of the lymphocyte-like cells. Similarly, a previous study on trout HK confirmed lymphocyte localization (low FSC and low SSC) using conventional FC, based on CD4⁺T cell markers (26). In addition, employing conventional FC, percentage of IgM⁺ and IgT⁺ B cells in salmon HK cells were determined by gating the same area (25). The gate areas in Figures 1, 2 confirm the presence of lymphocytes.

After confirming the identity of the B lymphocytes in the low BF area vs. low SSC intensity gate, we explored the phagocytosis of the adherent monocytes/macrophages HK fraction. Phagocytosis is an important initial immune response with final entry of antigens into the phagosomes/lysosomes that stimulates the production of reactive oxygen species (27). Phagocytic activity is influenced by many factors such as cell



maturity, cytokine response, antigen presenting cell activation status (28) and the characteristics of phagocytosed antigens or particles (29). We explored the phagocytic activity of salmon HK cells using IFC, which allowed for not only quantification of the number of cells with internalized particles but also the localization of particles inside the cells. The IFC methods for assessing phagocytosis are complex, and researchers are yet to standardize them for different particle types. In the present study, we tested two different types of particles, non-degradable and degradable particles. This is the first IFC study that reports the use of microplastic as non-degradable particles and bio-particles from *E. coli* as degradable particles. Considering the growing debate on microplastic pollution of the marine ecosystem, studying phagocytosis of microplastics by immune cells from aquatic animals can be of particular interest from an environmental perspective. In our studies, with our sensitive IFC methodology, we could clearly detect microplastic particles engulfed by salmon macrophages, although only few particles were detected inside these cells. We, therefore, assume that these cell types can phagocytose microplastics as (foreign) particles. It should be pointed out that the salmon HK phagocytic cells

were not able to uptake more microplastics; the reason could be that the cells can efficiently recognize microbe-derived particles (bio particle from *E. coli*) due to their natural antigenicity and phagocytose it more easily than an “unknown particle” such as the microplastic. Furthermore, the microplastic beads are not coated with any compound recognizable by the phagocytic cells, and they are larger compared to the bioparticles.

Compared to microplastic particles, the bio-particles are known to emit fluorescence within cells. However, this occurs only upon acidification, i.e., they emit fluorescence of a particular wavelength, depending on the pH level that the particle encounters. Hence, we suggest the use of fluorescent intensity feature rather than spot count feature to accurately assess the counts of degradable particles in phagocytes. Although a different feature was used to count the number of particles per phagocytic cell, a publication (12) has reported an IFC method for counting internalized fluorescent-labeled bacteria. The author succeeded in distinguishing between cells with high bright detail similarity score and those with low bright detail similarity score; the former one had internalized particles while other cells had external particles. Although the method of Smirnov et al. (12) gives

information on the overall degree of phagocytosis in phagocytic cells, it cannot accurately count the internalized particles. Thus, the bright detail similarity score and fluorescent intensity feature are effective in detecting and counting (as in this report) the mean number of internalized particles per phagocytic cell.

Although we did not perform a direct comparison between IFC and conventional FC, from our results we understand that false events such as auto-fluorescence and aggregated particles can be misinterpreted in the case of conventional FC. Pixel and intensity features were adjusted carefully in the present study to exclude the false-positive events. Caution should be exercised when gating phagocytic cells using these features because in IFC, cell size is measured based on pixels, and the sensitivity of the measurement is dependent on the cell size (19). Thus, in order to include the region of interest for analysis, the mask that identifies the intracellular compartment has to be adjusted for different types of cells and particles.

After standardizing the protocols for monocytes/macrophage phagocytosis, we optimized the methods for measuring phagocytosis, using degradable bio-particles, by cells from three very different aquatic animals—two fishes, Atlantic salmon and Nile tilapia and a mollusc, blue mussel—to evaluate the effect of incubation temperature on their phagocytic abilities and capacities. Our results indicated that phagocytosis of cells from the fishes can be affected by the incubation temperature. Although not directly comparable, phagocytosis of human leukocytes was reduced at higher and lower temperature compared to the normal host temperature range (30). Interestingly, the phagocytosis by hemocytes from blue mussel, a eurythermal species that can tolerate a broad temperature range from -1 to 20°C (31, 32), was not affected by incubation temperature.

In summary, IFC was used to study phagocytosis in fish and mussel cells. We were able to identify cell populations and determine the phagocytosis of different kinds of particles by quantifying the number of internalized particles and detecting the localization of particles in the phagocytes. This study provides important information about how IFC can be used in the field of fish immunology and ecotoxicology. Furthermore, the

procedures described in this report may have wider application in aquatic sciences, to unravel the effects of microplastic-ingestion by living organisms in the oceans.

DATA AVAILABILITY STATEMENT

All datasets generated for this study are included in the article/supplementary material.

ETHICS STATEMENT

The animal study was reviewed and approved by National Animal Research Authority in Norway (Mattilsynet).

AUTHOR CONTRIBUTIONS

YP and VK conceived and designed the study. YP and IA-G performed the experiments. YP analyzed the data and wrote the first draft of the manuscript while IA-G wrote a section of it. ST, GW and DB provided suggestions to improve the IFC protocols. YP, IA-G, ST, GW, DB, PO, and VK read, revised, and approved the manuscript for submission.

FUNDING

This study was supported by the INFISH project (272004) funded by Regional Forskningsfond Nord-Norge (RFF Nord-Norge). YP was financially supported by Korean Government Scholarship—National Institute for International Education, South Korea.

ACKNOWLEDGMENTS

The support of the staff at the Research Station, Nord University, Norway is acknowledged. YP is grateful to the members of the Cell Biology and Immunology Group, Wageningen University, the Netherlands for teaching him the principles of flow cytometry. Bisa Saraswathy is thanked for her support in data analysis, helpful discussion, and manuscript preparation.

REFERENCES

- Görgens A, Bremer M, Ferrer-Tur R, Murke F, Tertel T, Horn PA, et al. Optimisation of imaging flow cytometry for the analysis of single extracellular vesicles by using fluorescence-tagged vesicles as biological reference material. *J Extracell Vesicles*. (2019) 8:1587567. doi: 10.1080/20013078.2019.1587567
- Barteneva NS, Fasler-Kan E, Vorobjev IA. Imaging flow cytometry: coping with heterogeneity in biological systems. *J Histochem Cytochem*. (2012) 60:723–33. doi: 10.1369/0022155412453052
- Hulspas R, O'gorman MR, Wood BL, Gratama JW, Sutherland DR. Considerations for the control of background fluorescence in clinical flow cytometry. *Cytom B Clin Cytom*. (2009) 76:355–64. doi: 10.1002/cyto.b.20485
- Van Beers EJ, Samsel L, Mendelsohn L, Saiyed R, Fertrin KY, Brantner CA, et al. Imaging flow cytometry for automated detection of hypoxia-induced erythrocyte shape change in sickle cell disease. *Am J Hematol*. (2014) 89:598–603. doi: 10.1002/ajh.23699
- Ofir-Birin Y, Abou Karam P, Rudik A, Giladi T, Porat Z, Regev-Rudski N. Monitoring extracellular vesicle cargo active uptake by imaging flow cytometry. *Front Immunol*. (2018) 9:1011. doi: 10.3389/fimmu.2018.01011
- Piancone F, Saresella M, Marventano I, La Rosa F, Santangelo MA, Caputo D, et al. Monosodium urate crystals activate the inflammasome in primary progressive multiple sclerosis. *Front Immunol*. (2018) 9:983. doi: 10.3389/fimmu.2018.00983
- Jenner D, Ducker C, Clark G, Prior J, Rowland CA. Using multispectral imaging flow cytometry to assess an *in vitro* intracellular *Burkholderia thailandensis* infection model. *Cytom A*. (2016) 89:328–37. doi: 10.1002/cyto.a.22809
- Rieger AM, Konowalchuk JD, Grayfer L, Katzenback BA, Havixbeck JJ, Kiemle MD, et al. Fish and mammalian phagocytes differentially regulate pro-inflammatory and homeostatic responses *in vivo*. *PLoS ONE*. (2012) 7:e47070. doi: 10.1371/journal.pone.0047070
- Rességuier J, Delaune E, Coolen A-L, Levraud J-P, Boudinot P, Le Guellec D, et al. Specific and efficient uptake of surfactant-free poly (lactic acid)

- nanovaccine vehicles by mucosal dendritic cells in adult zebrafish after bath immersion. *Front Immunol.* (2017) 8:190. doi: 10.3389/fimmu.2017.00190
10. Parra D, Rieger AM, Li J, Zhang YA, Randall LM, Hunter CA, et al. Pivotal advance: peritoneal cavity B-1 B cells have phagocytic and microbicidal capacities and present phagocytosed antigen to CD4+ T cells. *J Leukocyte Biol.* (2012) 91:525–36. doi: 10.1189/jlb.0711372
 11. Phanse Y, Ramer-Tait AE, Friend SL, Carrillo-Conde B, Lueth P, Oster CJ, et al. Analyzing cellular internalization of nanoparticles and bacteria by multi-spectral imaging flow cytometry. *J Visual Exp.* (2012) 64:e3884. doi: 10.3791/3884
 12. Smirnov A, Solga MD, Lannigan J, Criss AK. An improved method for differentiating cell-bound from internalized particles by imaging flow cytometry. *J Immunol Methods.* (2015) 423:60–9. doi: 10.1016/j.jim.2015.04.028
 13. Paulsen SM, Engstad RE, Robertsen B. Enhanced lysozyme production in Atlantic salmon (*Salmo salar* L.) macrophages treated with yeast β -glucan and bacterial lipopolysaccharide. *Fish Shellfish Immunol.* (2001) 11:23–37. doi: 10.1006/fsim.2000.0291
 14. Pirarat N, Pinpimai K, Endo M, Katagiri T, Ponpornpisit A, Chansue N, et al. Modulation of intestinal morphology and immunity in Nile tilapia (*Oreochromis niloticus*) by *Lactobacillus rhamnosus* GG. *Res Vet Sci.* (2011) 91:e92–7. doi: 10.1016/j.rvsc.2011.02.014
 15. Wen C-M. Development and characterization of a cell line from tilapia head kidney with melanomacrophage characteristics. *Fish Shellfish Immunol.* (2016) 49:442–9. doi: 10.1016/j.fsi.2016.01.013
 16. Antoun SW. *Mussel (Mytilus edulis) hemocytes for in vitro testing* (dissertation/master's thesis). University of Oslo, Oslo, Norway (2011).
 17. Barbudde SB, Malik SVS, Gupta LK. Effect of *in vitro* monocyte activation by *Listeria Monocytogenes* antigens on phagocytosis and production of reactive oxygen and nitrogen radicals in bovines. *Vet Immunol Immunopathol.* (1998) 64:149–59. doi: 10.1016/S0165-2427(98)00129-9
 18. Fuentes A-L, Millis L, Vapenik J, Sigola L. Lipopolysaccharide-mediated enhancement of zymosan phagocytosis by RAW 264.7 macrophages is independent of opsonins, laminarin, mannan, and complement receptor 3. *J Surg Res.* (2014) 189:304–12. doi: 10.1016/j.jss.2014.03.024
 19. Basiji DA. *Principles of Amnis Imaging Flow Cytometry in Imaging Flow Cytometry*. Berlin: Springer (2016) 13–21. doi: 10.1007/978-1-4939-3302-0_2
 20. Grimwade LF, Fuller KA, Erber WN. Applications of imaging flow cytometry in the diagnostic assessment of acute leukaemia. *Methods.* (2017) 112:39–45. doi: 10.1016/j.ymeth.2016.06.023
 21. Kalgraff CA, Wergeland HI, Pettersen EF. Flow cytometry assays of respiratory burst in Atlantic salmon (*Salmo salar* L.) and in Atlantic cod (*Gadus morhua* L.) leucocytes. *Fish Shellfish Immunol.* (2011) 31:381–8. doi: 10.1016/j.fsi.2011.05.028
 22. Rieger AM, Hall BE, Barreda DR. Macrophage activation differentially modulates particle binding, phagocytosis and downstream antimicrobial mechanisms. *Dev Compar Immunol.* (2010) 34:1144–59. doi: 10.1016/j.dci.2010.06.006
 23. Pettersen EF, Ingerslev H-C, Stavang V, Egenberg M, Wergeland HI. A highly phagocytic cell line TO from Atlantic salmon is CD83 positive and M-CSFR negative, indicating a dendritic-like cell type. *Fish Shellfish Immunol.* (2008) 25:809–19. doi: 10.1016/j.fsi.2008.08.014
 24. Ulvestad JS. *Studies on the stimulation of Atlantic salmon macrophage-like cells with emphasis on respiratory burst* (dissertation/master's thesis). UiT The Arctic University of Norway, Tromsø, Norway (2017).
 25. Jenberie S, Thim HL, Sunyer JO, Skjødt K, Jensen I, Jørgensen JB. Profiling Atlantic salmon B cell populations: CpG-mediated TLR-ligation enhances IgM secretion and modulates immune gene expression. *Sci Rep.* (2018) 8:3565. doi: 10.1038/s41598-018-21895-9
 26. Maisey K, Montero R, Corripio-Miyar Y, Toro-Ascuay D, Valenzuela B, Reyes-Cerpa S, et al. Isolation and characterization of salmonid CD4+ T cells. *J Immunol.* (2016) 196:4150–63. doi: 10.4049/jimmunol.1500439
 27. Gartlan KH, Krashias G, Wegmann F, Hillson WR, Scherer EM, Greenberg PD, et al. Sterile inflammation induced by Carbopol elicits robust adaptive immune responses in the absence of pathogen-associated molecular patterns. *Vaccine.* (2016) 34:2188–96. doi: 10.1016/j.vaccine.2016.03.025
 28. Gordon S. Phagocytosis: an immunobiologic process. *Immunity.* (2016) 44:463–75. doi: 10.1016/j.immuni.2016.02.026
 29. Underhill DM, Goodridge HS. Information processing during phagocytosis. *Nat Rev Immunol.* (2012) 12:492. doi: 10.1038/nri3244
 30. Peterson P, Verhoef J, Quie P. Influence of temperature on opsonization and phagocytosis of staphylococci. *Infect Immun.* (1977) 15:175–9. doi: 10.1128/IAI.15.1.175-179.1977
 31. Hiscock K, Tyler-Walters H. Assessing the sensitivity of seabed species and biotopes—the Marine Life Information Network (MarLIN). *Hydrobiologia.* (2006) 555:309–20. doi: 10.1007/s10750-005-1127-z
 32. Thyrring J, Rysgaard S, Blicher ME, Sejr MK. Metabolic cold adaptation and aerobic performance of blue mussels (*Mytilus edulis*) along a temperature gradient into the high Arctic region. *Marine Biol.* (2015) 162:235–43. doi: 10.1007/s00227-014-2575-7

Conflict of Interest: ST is an employee of Luminox B.V., which is a subsidiary of Luminox Corporation. Luminox Corporation is the manufacturer of the ImageStream[®] Mk II Imaging Flow Cytometer.

The remaining authors declare that the research was conducted in the absence of any commercial or financial relationships that could be construed as a potential conflict of interest.

Copyright © 2020 Park, Abihssira-García, Thalmann, Wiegertjes, Barreda, Olsvik and Kiron. This is an open-access article distributed under the terms of the Creative Commons Attribution License (CC BY). The use, distribution or reproduction in other forums is permitted, provided the original author(s) and the copyright owner(s) are credited and that the original publication in this journal is cited, in accordance with accepted academic practice. No use, distribution or reproduction is permitted which does not comply with these terms.

Paper II

This is an open-access article, reproduced and distributed under the terms of the Creative Commons Attribution License (CC BY)



Adherent Intestinal Cells From Atlantic Salmon Show Phagocytic Ability and Express Macrophage-Specific Genes

Youngjin Park¹, Qirui Zhang², Geert F. Wiegertjes³, Jorge M.O. Fernandes¹ and Viswanath Kiron^{1*}

¹ Faculty of Biosciences and Aquaculture, Nord University, Bodo, Norway, ² Division of Clinical Genetics, Lund University, Lund, Sweden, ³ Aquaculture and Fisheries Group, Wageningen University & Research, Wageningen, Netherlands

OPEN ACCESS

Edited by:

Yi Feng,
The University of Edinburgh,
United Kingdom

Reviewed by:

Dimitar Borisov Iliev,
Institute of Molecular Biology (BAS),
Bulgaria
Sherri L. Christian,
Memorial University of Newfoundland,
Canada

*Correspondence:

Viswanath Kiron
kiron.viswanath@nord.no

Specialty section:

This article was submitted to
Cell Death and Survival,
a section of the journal
Frontiers in Cell and Developmental
Biology

Received: 07 July 2020

Accepted: 22 September 2020

Published: 15 October 2020

Citation:

Park Y, Zhang Q, Wiegertjes GF,
Fernandes JMO and Kiron V (2020)
Adherent Intestinal Cells From Atlantic
Salmon Show Phagocytic Ability
and Express Macrophage-Specific
Genes.
Front. Cell Dev. Biol. 8:580848.
doi: 10.3389/fcell.2020.580848

Our knowledge of the intestinal immune system of fish is rather limited compared to mammals. Very little is known about the immune cells including the phagocytic cells in fish intestine. Hence, employing imaging flow cytometry and RNA sequencing, we studied adherent cells isolated from healthy Atlantic salmon. Phagocytic activity and selected gene expression of adherent cells from the distal intestine (adherent intestinal cells, or AIC) were compared with those from head kidney (adherent kidney cells, or AKC). Phagocytic activity of the two cell types was assessed based on the uptake of *Escherichia coli* BioParticlesTM. AIC showed phagocytic ability but the phagocytes were of different morphology compared to AKC. Transcriptomic analysis revealed that AIC expressed genes associated with macrophages, T cells, and endothelial cells. Heatmap analysis of selected genes indicated that the adherent cells from the two organs had apparently higher expression of macrophage-related genes. We believe that the adherent intestinal cells have phagocytic characteristics and high expression of genes commonly associated with macrophages. We envisage the possibilities for future studies on enriched populations of adherent intestinal cells.

Keywords: adherent, intestinal cells, ImageStream[®]X, Atlantic salmon, phagocytosis, RNA-Seq, macrophages

INTRODUCTION

Teleost fishes have both organized and diffuse lymphoid tissues. However, these tissues differ from those of mammals morphologically and functionally. Fish lack bone marrow and lymph nodes found in mammals. Therefore, they rely on thymus, (head) kidney and spleen as their key lymphoid organs. The head kidney (or anterior kidney), is the main source of cytokine-producing lymphoid cells (Geven and Klaren, 2017), macrophages, and plasma cells, which find their way to specific sites, including those in the intestine, to replenish tissue-resident cell populations (Kratofil et al., 2017). Furthermore, the head kidney recruits specific cell types during disease conditions like inflammation (Parra et al., 2015). The head kidney is also a well-known primary B cell organ in fishes (Li et al., 2006; Parra et al., 2015).

This makes the head kidney the main hematopoietic organ in teleost fish. In addition, fish possess mucosa-associated lymphoid tissues (MALTs), but these tissues are more diffuse compared to those in mammals (Parra et al., 2015). Among these MALTs, gut-associated lymphoid tissues (GALTs) contain two main populations of immune cells: (1) intraepithelial lymphocytes, which include mainly T cells located between the epithelial cells; and (2) lamina propria leukocytes, which are comprised of lymphocytes, macrophages, granulocytes and plasma cells (Rombout et al., 2011). In-depth knowledge of these immune cells present in GALT is necessary to understand the crosstalk between antigens and the epithelium as well as the immunological functions of both the key lymphoid organs and GALT. However, the lack of appropriate cell markers and complexity of isolation protocols are still hampering the progress of research on leukocyte cell populations in the fish intestine.

The most common practice is to collect adherent cells from specific organs in order to characterize them through further analysis. Cell adhesion refers to the ability of cells to adhere to other cells or extracellular matrix (Khalili and Ahmad, 2015). This process not only stimulates communication between cells but also helps to retain the tissue structure and functions (Khalili and Ahmad, 2015). The cells isolated from tissues or organs are mostly adherent types, and the known mammalian adherent cells are macrophages (Selvarajan et al., 2011), T cells (Bierer and Burakoff, 1988; Shimizu et al., 1991), endothelial cells (Braniste et al., 2016), epithelial cells (Kihara et al., 2018) and dendritic cells (DC, only upon antigen exposure) (Yi and Lu, 2012). Mammalian cell culture methods are frequently adopted to culture and study monocyte-derived macrophage-like cells from fish immunological tissues such as spleen (Iliev et al., 2013) and head kidney (Joerink et al., 2006; Iliev et al., 2019). However, our knowledge of the cell types including phagocytic cells that are involved in the fish intestinal immune response is rather limited compared to mammals.

As for the intestinal cells of fish, McMillan and Secombes (1997) were the first researchers to describe protocols to isolate them from rainbow trout, *Oncorhynchus mykiss*. After a decade, several research groups put in effort to effectively isolate and characterize intestinal immune cells from different fish species such as rainbow trout (Bernard et al., 2006), gilthead seabream, *Sparus aurata* (Salinas et al., 2007) and Atlantic salmon, *Salmo salar* (Attaya et al., 2018). Although there is ample information about the adherent cells from the head kidney in teleost fishes, knowledge about the intestinal cells has to be gathered by employing next generation techniques.

Therefore, this study investigated the adherent cells isolated from the distal intestine by employing the cells from the head kidney of Atlantic salmon as reference. We adopted two high-throughput techniques, imaging flow cytometry (IFC) and RNA sequencing. First, using IFC we explored the adherent cells from the aforementioned organs to decipher the characteristics of the populations and their phagocytic activity. Subsequently, a transcriptomic study was carried out to profile the expression of (1) cell type (macrophage, dendritic cell, endothelial cell, T and B cells)-related genes and (2) other immune genes (cytokines,

chemokines, mucins and toll-like receptors) to delineate if the adherent cells expressed genes associated with phagocytes.

MATERIALS AND METHODS

Experimental Fish and Sampling Procedure

Atlantic salmon post smolts of about 70 g were purchased from a commercial producer (Sundsford Smolt, Nygårdsjøen, Norway) and maintained at the Research Station of Nord University, Bodø, Norway. Fish were fed a commercial feed (Ewos Micro, Ewos AS, Bergen, Norway) to satiation, and reared in a flow-through sea water system (temperature: 7–8°C, dissolved oxygen saturation: 87–92%, 24-h light cycle). Fish (of the weight range 510–590 g) was used in this study. The fish were starved for 24 h and were killed with an over dose of MS-222 (Tricaine methane sulfonate; Argent Chemical Laboratories, Redmond, United States; 80 mg/L). Head kidney (HK) and distal intestine (DI) samples were then collected.

Cell Isolation and Culture

Immune cells from the head kidney (HK) and distal intestine (DI) were isolated and grown at 12°C in Leibovitz's L-15 Medium (L-15; Sigma-Aldrich, Oslo, Norway) as described previously by Park et al. (2020) and Salinas et al. (2007), respectively. The osmolality of cell culture media was adjusted to 380 mOsm by adding a solution consisting of 5% (v/v) 0.41 M NaCl, 0.33 M NaHCO₃ and 0.66 (w/v) D-glucose (Sigma).

Briefly, HK from salmon ($n = 6$) were sampled and transferred to 15 mL centrifuge tubes to make a total volume of 4 mL in ice-cold L-15 + [L-15 medium with 50 U/mL penicillin (Sigma), 50 µg/mL streptomycin (Sigma), 2% fetal bovine serum (FBS; Sigma) and 10 U/mL heparin (Sigma)]. The tissues were passed through a sterile 100-µm cell strainer (Falcon, New York, United States) with ice-cold L-15 + . Thereafter, the cell suspensions were layered on 40%/60% Percoll (Sigma) to separate HK leukocytes and centrifuged at 500 × g for 30 min, at 4°C. Cells at the interface were collected and washed twice with ice-cold L-15-FBS free (L-15 medium with 50 U/mL penicillin, 50 µg/mL streptomycin) by centrifugation (500 × g, 5 min, 4°C).

For intestinal cell isolation, DI samples from salmon ($n = 6$) were transferred to a cell culture dish (Nunc EasyDish, Thermo Fisher Scientific, Oslo, Norway) with 2 mL ice-cold PBS. The tissues were cut open longitudinally and washed with ice-cold PBS to remove gut contents. After washing they were cut into small pieces (1–2 cm fragments) and transferred to 15 mL centrifuge tubes to make a total volume of 4 mL in DTT solution (0.145 mg/mL dithiothreitol + 0.37 mg/mL EDTA in Ca²⁺ and Mg²⁺ free HBSS, Sigma) at room temperature for 20 min to break disulfide bonds in the mucus. Next, the tissue fragments were washed with L-15 + supplemented with DNase (0.05 mg/ml; Sigma) to prevent cell clumping and wash out excess DTT. Thereafter, the washed fragments were transferred to 15 mL centrifuge tubes to make a total volume of 6 mL in the digestive solution (0.37 mg/mL collagenase IV, Thermo Fisher Scientific). The centrifuge tubes

were incubated in a shaking incubator (200 rpm) at RT for 60 min. The tissue fragments and supernatants were then passed through a sterile 100- μ M cell strainer with ice-cold L-15 + , and the cell suspensions were layered on 25%/75% Percoll. The tubes containing the cells and Percoll were centrifuged at $500 \times g$ for 30 min, at 4°C to separate DI leukocytes. Cells at the interface were collected and washed twice with ice-cold L-15-FBS free by centrifugation ($500 \times g$, 5 min, 4°C).

Both HK and DI leukocytes (mentioned under flow cytometry studies) were allowed to adhere on a cell culture dish with 2 mL L-15 + for 2 days at 12°C. After collecting the supernatant containing non-adherent cells, the dish with the adherent cells was placed on ice for 10 min, and the cells were detached by washing three times with 1.5 mL ice-cold PBS supplemented with 5 mM EDTA. The cells obtained were centrifuged ($500 \times g$, 5 min, 4°C) and resuspended in 1 mL L-15 + . Then, the cells were counted using a portable cell counter (Scepter 2.0 cell counter, EMD Millipore, Darmstadt, Germany). To confirm the quality of the harvested cells, we observed the cells using a live cell imager (ZOE Fluorescent Cell imager, Bio-Rad, Oslo, Norway). With our improved protocols, we were able to harvest many cells with high viability. We checked the quality of the isolated cells by observing them through microscope and with the help of live/dead cell assays using propidium iodide.

Flow Cytometry Studies

To understand the cell populations and their functions we isolated and cultured cells from HK and DI. These cells were studied employing the ImageStream[®] Mk II Imaging Flow Cytometer (Luminex Corporation, Austin, TX, United States) equipped with two argon-ion lasers (488 and 642 nm) and a side scatter laser (785 nm). The acquired cell data were analyzed using IDEAS 6.1.822.0 software (Luminex). All flow cytometry assays were performed as described previously (Park et al., 2020).

Cell Population

To study the cell populations – (i) whole leukocytes, (ii) supernatants and (iii) adherent cells – from three cell suspensions from HK or DI, aliquots containing $> 5 \times 10^5$ cells were washed with 500 μ L PBS by centrifugation ($500 \times g$, 5 min, 4°C) and resuspended in 50 μ L PBS. Prior to loading the tubes containing the cells in the flow cytometer, 1 μ L of propidium iodide (PI, 1 mg/mL, Sigma) was added to differentiate between the dead and live cells as well as to estimate the cell types based on the morphology of their nucleus. From each sample, more than 10,000 cell images were acquired using two lasers with optimized voltage levels, 488 nm (1 mW) and 785 nm (0.47 mW). Thereafter, using IDEAS software, dead cells were excluded based on PI positivity; both are shown in a brightfield (BF) area (cell size) vs. side scatter (SSC) intensity (cell granularity) plot.

Phagocytosis Assay

To compare the phagocytic activity of whole leukocytes and adherent cells (i and iii mentioned under flow cytometry studies), aliquots containing 0.5×10^5 cells in 100 μ L L-15 + were incubated with fluorescent bio-particles (pHrodo[™] Red *Escherichia coli* Bioparticles, Thermo Fisher Scientific), at a cell and particle ratio of 1:5 for 2 h at 12°C. After incubation, the cells were washed once with 500 μ L PBS by centrifugation ($500 \times g$, 5 min, 4°C) and resuspended in 50 μ L PBS. Thereafter, the tubes containing cells were loaded in the flow cytometer and more than 10,000 cell images were acquired using two lasers with optimized voltage levels, 488 nm (50 mW) and 785 nm (0.47 mW). Data analyses were performed following our previous protocol (Park et al., 2020). Phagocytic ability was measured as the percent of phagocytic cells in total cells while phagocytic capacity was calculated as the mean number of particles in each phagocyte as described previously (Park et al., 2020).

Transcriptomic Analysis

The main aim of the RNA-Seq analysis was to obtain a snapshot of the expression profiles of selected genes. To compare the expression of genes linked to the adherent cells from HK and DI, 12 libraries were prepared ($n = 6$). The list of selected genes used in this study is comprised of (1) 34 cell type (macrophage, dendritic cell, endothelial cell, T and B cells)-related genes and (2) 42 other immune-related (cytokines, chemokines, mucins and toll-like receptors) genes, as shown in Tables 1 and 2, respectively.

RNA Isolation, Library Preparation and Illumina Sequencing

Total RNA was extracted from the adherent cells that were isolated from HK and DI ($< 500,000$ cells) using the PicoPure RNA isolation kit (Thermo Fisher Scientific) according to the manufacturer's protocol. The quality and quantity of total RNA were assessed using Agilent RNA high sensitivity screen tape kits and Bioanalyzer 2200 TapeStation system (Agilent Technologies, Santa Clara, CA, United States). RNA sequencing libraries were prepared using the NEBNext Ultra II Directional RNA library preparation kit with poly (A) mRNA magnetic isolation module (NEB #E7490; New England BioLabs[®], Herts, United Kingdom), according to the manufacturer's protocol. For the first and second strand cDNA synthesis, 50 ng of total RNA having high RNA integrity number (RIN > 8) was enriched with Oligo(dT)-conjugated magnetic beads and fragmented to ~ 200 nt. Thereafter, the resulting cDNA were end-repaired for adaptor ligation. The ligated cDNAs were amplified with barcoded primers on a thermal cycler for 14 cycles. The PCR products were purified using AMPure XP beads (Beckman Coulter Inc., Brea, CA, United States) to avoid contamination from residual adapter dimers and unwanted (smaller) fragments. After library preparation, the quality and quantity of individual libraries were assessed using Agilent DNA high sensitivity screen tape kits and Bioanalyzer 2200 TapeStation system. These barcoded individual libraries were pooled at equimolar ratios and sequenced as single-end reads (75 bp) on an Illumina NextSeq 500 sequencer (Illumina, San Diego, CA, United States) with

TABLE 1 | List of abbreviations and details of genes expressed in macrophages, dendritic cells, endothelial cells, T and B cells.

Abbreviations	Gene name	Ensembl/GenBank ID
<i>cd68</i>	CD68	ENSSSAG00000002993
<i>cd200r1</i>	CD200 receptor 1A-like	ENSSSAG00000039924
<i>mmf</i>	monocyte to macrophage differentiation protein	ENSSSAG00000001828
<i>csf1r</i>	macrophage receptor MARCO-like	ENSSSAG000000063051
<i>marco</i>	macrophage colony stimulating factor receptor-like protein	ENSSSAG000000061479
<i>mpeg1</i>	macrophage expressed 1	ENSSSAG000000076214
<i>capg</i>	macrophage-capping protein-like	ENSSSAG000000003660
<i>h2-eb1</i>	H-2 class II histocompatibility antigen, I-E beta chain	XM_014133067
<i>cd74</i>	HLA class II histocompatibility antigen gamma chain-like	ENSSSAG000000004635
<i>cd80</i>	CD80-like	ENSSSAG000000056420
<i>cd83</i>	CD83 antigen	ENSSSAG000000057240
<i>cd209</i>	CD209 antigen-like	XM_014194638
<i>cd3gda</i>	CD3gamdelta-A	ENSSSAG00000009995
<i>cd3z</i>	CD3zeta-1	ENSSSAG000000055061
<i>cd42al</i>	truncated CD4-2A-like protein	ENSSSAG000000076595
<i>cd8a</i>	CD8 alpha	ENSSSAG000000065860
<i>cd8b</i>	CD8 beta	ENSSSAG000000045680
<i>cd28</i>	T-cell-specific surface glycoprotein CD28-like	ENSSSAG000000060163
<i>cd2l</i>	T-cell surface antigen CD2-like	XM_014129565
<i>cd96</i>	T-cell surface protein tactile-like	XM_014129863
<i>trbc1</i>	T-cell receptor beta-1 chain C region-like	NC_027300
<i>trgc2</i>	T-cell receptor gamma chain C region C10.5-like	NC_027319
<i>cd6l</i>	T-cell differentiation antigen CD6-like	ENSSSAG000000057293
<i>tcd80l</i>	T-lymphocyte activation antigen CD80-like	ENSSSAG000000056420
<i>tagap</i>	T-cell activation GTPase activating protein	ENSSSAG000000061533
<i>igm</i>	IgM	XM_014203125
<i>cd48l</i>	CD48 antigen-like	ENSSSAG000000064252
<i>cd79a</i>	B-cell antigen receptor complex-associated protein alpha chain-like	ENSSSAG000000003014
<i>blnk</i>	B-cell linker	ENSSSAG000000065613
<i>bcap29</i>	B cell receptor associated protein 29	ENSSSAG000000074312
<i>bcl9l</i>	B-cell CLL/lymphoma 9 protein-like	ENSSSAG000000063108
<i>ecscr</i>	endothelial cell-specific chemotaxis regulator-like	XM_014129374
<i>cd151al</i>	CD151 antigen-like	ENSSSAG000000065694
<i>pecam</i>	platelet endothelial cell adhesion molecule-like	ENSSSAG000000001458

NextSeq 500/550 high output v2 reagents kit (Illumina) at the sequencing facility of Nord University, Bodø, Norway.

Bioinformatics Analyses

All bioinformatics analyses of RNA-Seq data were performed as described previously by Zhang et al. (2018). The obtained raw sequencing data was deposited in the Gene Expression Omnibus (GEO, NCBI); the accession number is GSE154142. Briefly, raw sequence data were converted to FASTQ format with bcl2fastq2 (v2.17, Illumina). The adapter sequences were removed using cutadapt (version 1.12) with the following parameters: -q 20 -quality-base = 33 -m 20 -trim-n. The quality of the trimmed fastq files (clean reads) was then assessed using FastQC (Andrews, 2010), and the reads with quality > Q30 were mapped to the Atlantic salmon genome ICSASG_v2 from RefSeq¹. The mapped reads were quantified and then annotated using gff3 annotation

¹https://www.ncbi.nlm.nih.gov/assembly/GCF_000233375.1/

file. The generated data was normalized using DESeq2 (Love et al., 2014), and the normalized data was used for statistical comparisons, i.e., to determine the differences in the expression of selected immune-related genes in AIC and AKC. The package, DESeq2 employs shrinkage estimation for dispersions and fold changes. The R packages ggplot2 version 3.1.1 (Wickham, 2016) were employed to prepare and format the graphs. A heatmap was prepared using the functions from the package ComplexHeatmap (Gu, 2015).

Statistical Analyses

Statistical analysis was performed using RStudio version 1.1.463. Normality of the flow cytometry and gene expression data was tested by Shapiro-Wilk Test, and the assumption of equal variance was checked by Bartlett's Test. Comparisons between groups were performed using unpaired Student's *t*-test. The differences were considered significant at $p < 0.05$.

TABLE 2 | List of abbreviations and details of genes coding for selected cytokines, chemokines, mucins, and toll-like receptors.

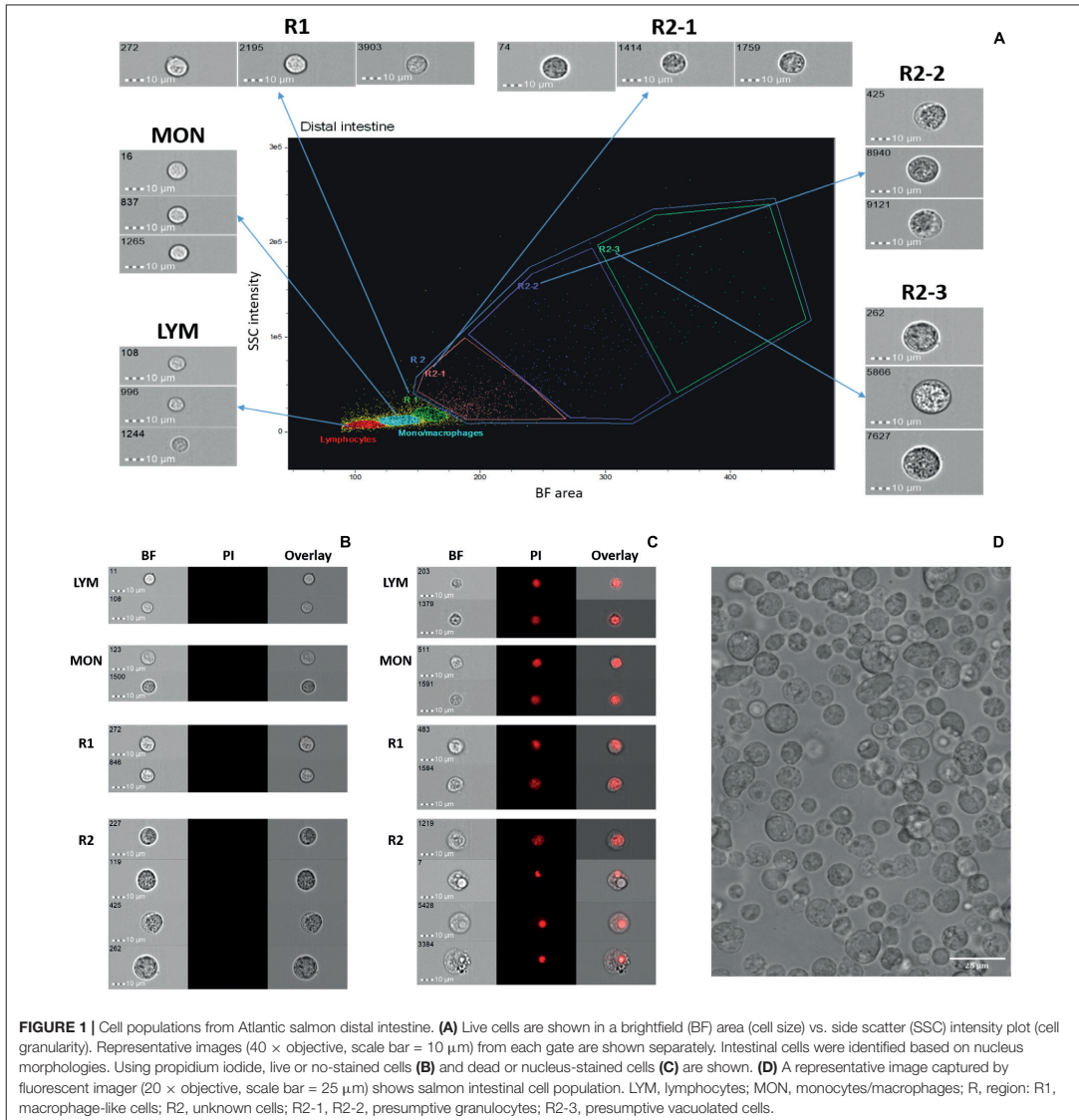
Abbreviations	Gene name	Ensembl/GenBank ID
<i>tgfbr1</i>	Transforming growth factor beta receptor type-1-like	ENSSSAG00000079756
<i>tgfbr2</i>	Transforming growth factor beta receptor type-2	ENSSSAG00000071570
<i>tab2</i>	Transforming growth factor beta-activated kinase 1 and MAP3K7-binding protein 2-like	ENSSSAG00000074549
<i>traf2</i>	Tumor necrosis factor receptor associated factor 2	ENSSSAG00000046864
<i>tnfa2</i>	Tumor necrosis factor alpha-2 precursor	ENSSSAG00000053783
<i>tnfaip2</i>	Tumor necrosis factor alpha-induced protein 2-like	XM_014143804
<i>tnfrsf6b</i>	Tumor necrosis factor receptor superfamily member 6b	ENSSSAG00000044783
<i>tnfrsf10a</i>	Tumor necrosis factor receptor superfamily member 10A-like	ENSSSAG00000049387
<i>tnfrsf11</i>	Tumor necrosis factor superfamily member 11	ENSSSAG00000053734
<i>tnfrsf13b</i>	Tumor necrosis factor receptor superfamily member 13B-like	ENSSSAG00000079103
<i>il1b-like</i>	Interleukin-1 beta-like	ENSSSAG00000060993
<i>irak3-like</i>	Interleukin-1 receptor-associated kinase 3-like	ENSSSAG00000051931
<i>il1r1</i>	Interleukin-1 receptor-like protein	ENSSSAG00000069876
<i>il1rap</i>	Interleukin 1 receptor accessory protein	ENSSSAG00000043510
<i>il6r</i>	Interleukin-6 receptor subunit alpha	ENSSSAG00000052467
<i>il6rb</i>	Interleukin-6 receptor subunit beta-like	ENSSSAG00000061284
<i>il8</i>	Interleukin 8	ENSSSAG0000006498
<i>il12rb2</i>	Interleukin-12 receptor beta-2 chain	ENSSSAG00000042273
<i>il17rc1</i>	Interleukin-17 receptor C-like	ENSSSAG0000007189
<i>il17rel</i>	Interleukin-17 receptor E-like	XM_014134812
<i>il31ra</i>	Interleukin-31 receptor A	ENSSSAG00000062925
<i>cxcr11</i>	C-X-C chemokine receptor type 1-like	ENSSSAG00000042001
<i>cc12l</i>	C-C motif chemokine 2-like	XM_014191804
<i>cxcr3l</i>	C-X-C chemokine receptor type 3-like	ENSSSAG00000051147
<i>ccr3</i>	C-C chemokine receptor type 3	ENSSSAG00000042484
<i>cxcr4l</i>	C-X-C chemokine receptor type 4-like	ENSSSAG00000050781
<i>cxcr5l</i>	C-X-C chemokine receptor type 5-like	ENSSSAG00000040121
<i>ccr5l</i>	C-C chemokine receptor type 5-like	ENSSSAG00000072678
<i>ccr6l</i>	C-C chemokine receptor type 6	ENSSSAG00000076547
<i>ccr9l</i>	C-C chemokine receptor type 9-like	ENSSSAG00000070198
<i>cc119l</i>	C-C motif chemokine 19-like	ENSSSAG00000002773
<i>cc120l</i>	C-C motif chemokine 20-like	ENSSSAG00000051350
<i>cc125</i>	C-C motif chemokine 25	ENSSSAG00000071212
<i>muc1</i>	mucin 1, cell surface associated	XM_014160723
<i>muc5acl</i>	Mucin-5AC-like	ENSSSAG00000080927
<i>muc13l</i>	Mucin-13-like	ENSSSAG00000069082
<i>muc17l</i>	Mucin-17-like	ENSSSAG00000047784
<i>cd164l2</i>	CD164 sialomucin-like 2 protein	XM_014143111
<i>tlr2</i>	Toll-like receptor 2	ENSSSAG00000003781
<i>tlr6</i>	Toll-like receptor 6	ENSSSAG00000079217
<i>tlr8</i>	Toll-like receptor 8	ENSSSAG00000074528
<i>tlr13</i>	Toll-like receptor 13	ENSSSAG00000077966

RESULTS

Diverse Cells Among Salmon Distal Intestine Cell Population

We explored the cell populations from salmon DI by employing IFC. After dead cell exclusion, approximately 90% of viable cells (negative for PI) were obtained; shown in a BF area (cell size) vs. SSC intensity (cell granularity) plot (**Figure 1A**). Because we have already revealed the identity of the HK cell population in our previous study (Park et al., 2020) here we show only

the DI cell population in **Figure 1**. The gating strategy that was developed previously by Park et al. (2020) was employed for DI cell populations (**Figure 1A**: LYM, lymphocyte; MON, monocyte/macrophage; R1, macrophage-like cells). Nucleus morphologies were revealed through PI staining (**Figures 1B,C**). Only PI negative live cells (**Figure 1B**) were considered for the gating shown in **Figure 1A**; cells in the gates LYM, MON, and R1 had spherical and fairly rigid nuclei while those in the gate R2 had relatively smaller and different shaped nuclei. We found that there are diverse cells in the isolated salmon DI cell population.

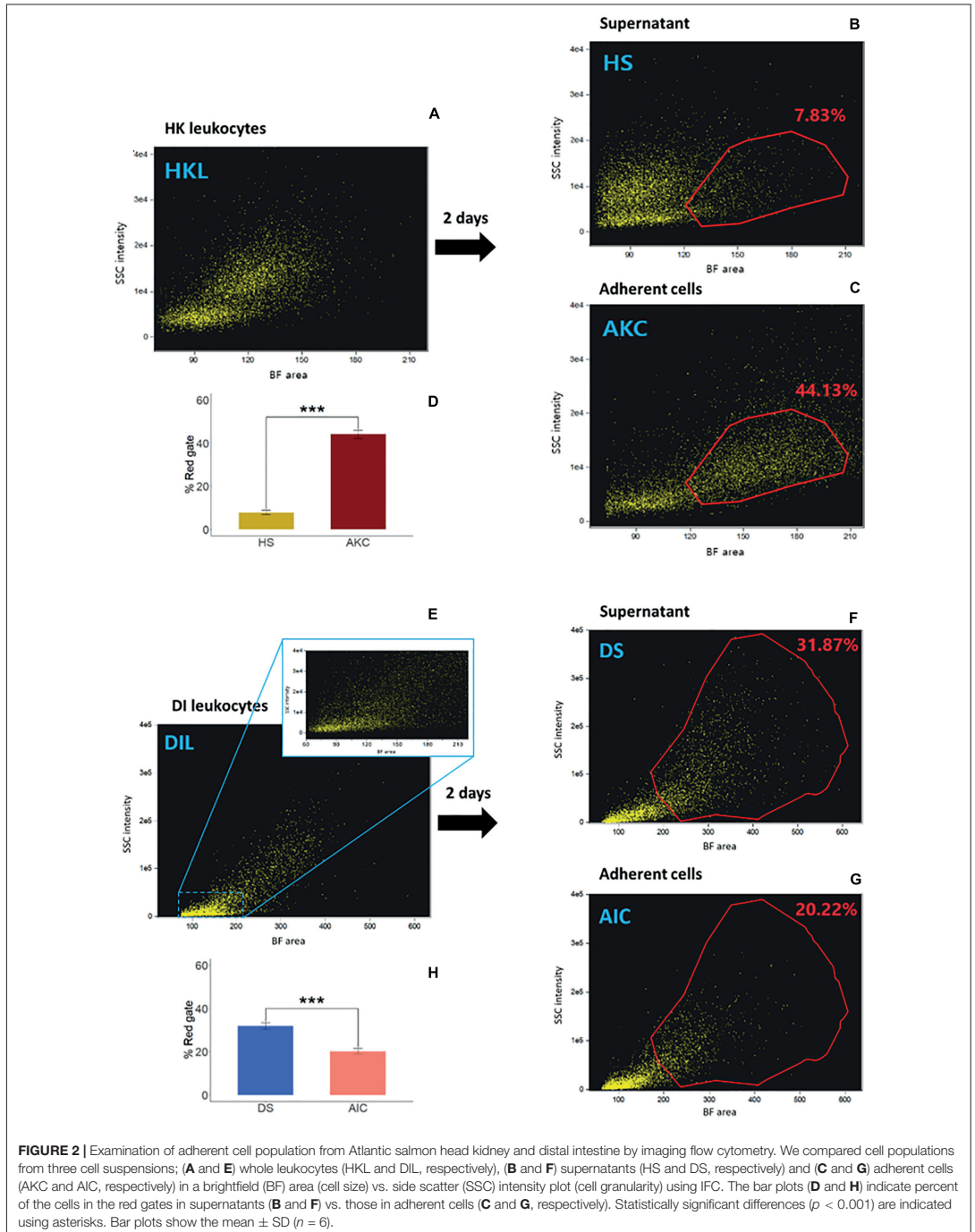


A representative image of the DI cell images from among 6 images captured (to confirm the quality of the harvested DI cells) by the fluorescent imager is shown in **Figure 1D**.

Adherent Cells From Salmon Distal Intestine Exhibit Phagocytic Ability

The cell populations – whole leukocytes (HKL and DIL, respectively), supernatants (HS and DS, respectively) and adherent cells (AKC and AIC, respectively) – from three cell

suspensions from HK or DI are shown in **Figures 2A–C** and **Figures 2E–G**, respectively. The reference AKC had macrophage population, located in higher BF area and higher SSC intensity compared to those of head kidney supernatant-derived cells (HS, red gates; **Figures 2B–D**). In the DI cells, the cell populations were more scattered, as evident in the dotplot (considering the BF area values). However, AIC apparently had a lower percentage of the cells in the gated area compared to those of distal intestine supernatant-derived cells (DS, red gates; **Figures 2F–H**).



To compare the phagocytic activity of whole leukocytes and adherent cells from HK (Figures 3A–C) and DI (Figures 4A–C), we quantified the uptake of *E. coli* BioParticles™ by the cells (Park et al., 2020). The phagocytic abilities of AKC and AIC were significantly higher than those of HKL and DIL (Figures 3A, 4A), respectively. The phagocytes from AIC had different morphologies compared to AKC (Figures 3C, 4C). Among AICs, along with single and round shaped phagocytes, we found oval shaped (5.69% of total phagocytes, Figure 4D) and doublets consisting of a phagocytic cell and an interacting cell (1.15% of total phagocytes, Figure 4E).

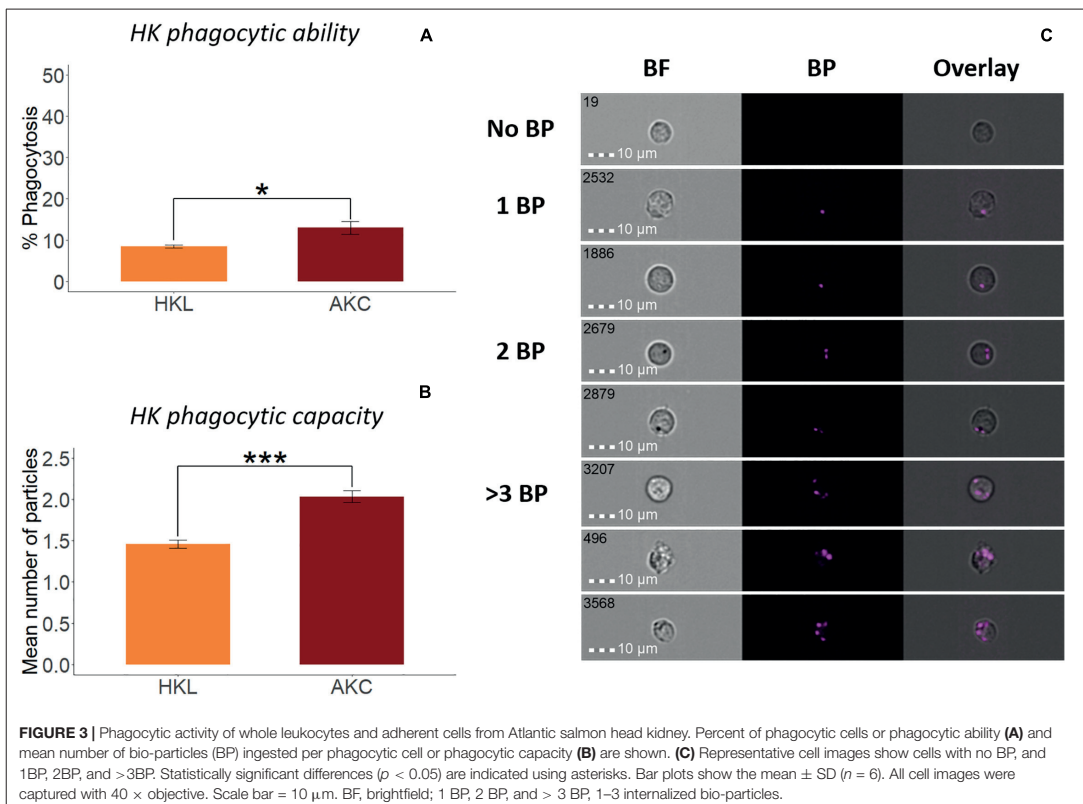
Adherent Cells From Distal Intestine of Salmon Express Macrophage and Immune-Related Genes

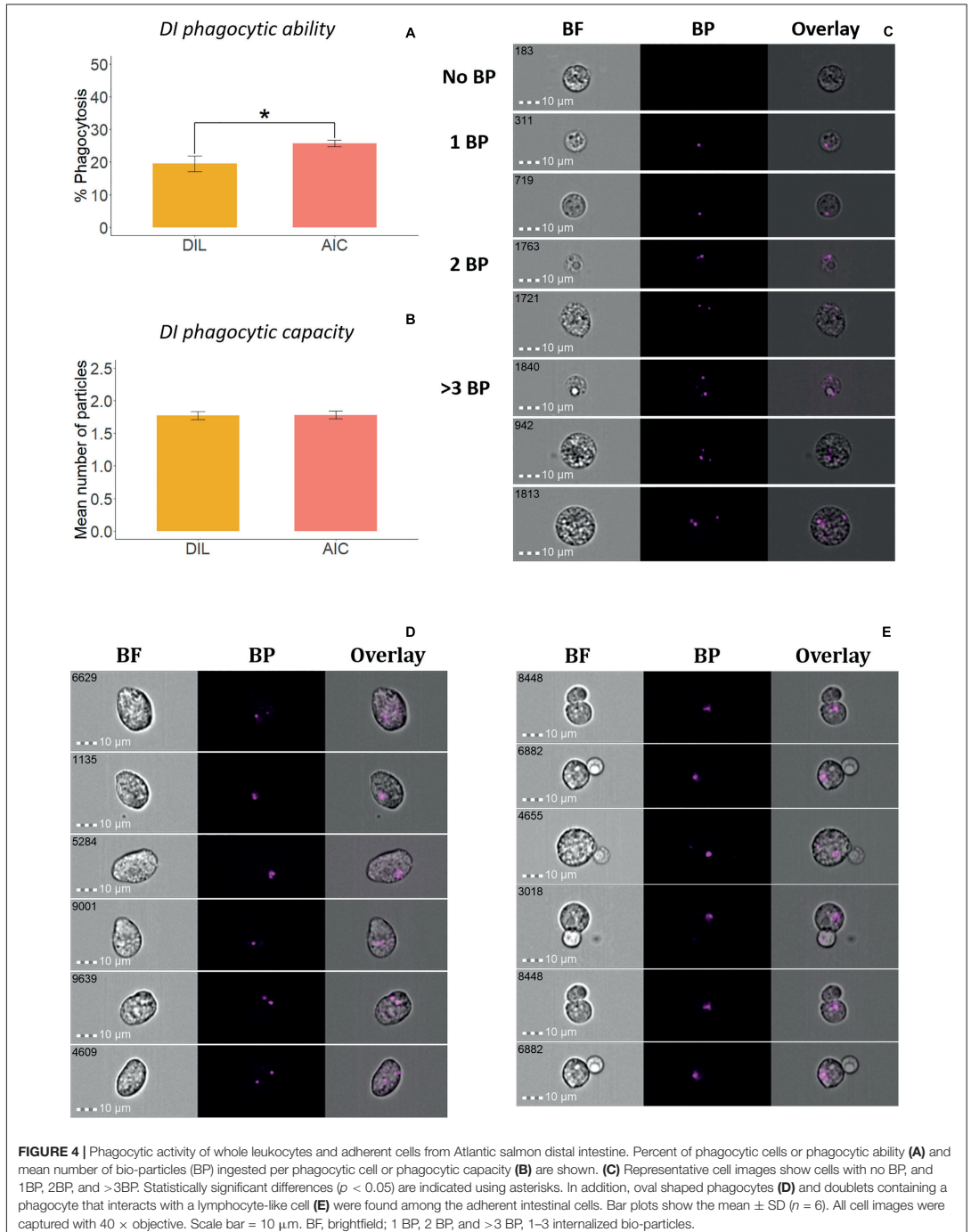
To understand the identity of cell types in AIC, the expression of selected genes in AIC was compared with those of AKC. We obtained over 312 million cleaned reads from 12 (6 from AIC and 6 from AKC) samples after adapter trimming and quality filtering. Of them, over 285 million reads were mapped to Atlantic salmon genome. Average mapping percentage among samples was 91.36% (Supplementary Table 1). The dispersion of the

genes decreased with increase in mean of normalized counts (Supplementary Figure 1).

Employing the normalized read counts from DESeq2 analyses, we describe the expression of 34 cell-specific (macrophage, dendritic cell, endothelial cell, T and B cells) genes and 42 immune-related (cytokines, chemokines, mucins and toll-like receptors) genes in AIC compared to AKC. Lack of appropriate cell markers and unavailability of easy intestinal cell isolation techniques hamper the characterization of adherent cells. Therefore, we adopted the targeted analysis strategy to delineate the cell types by linking them to known genes.

The expression of 34 genes associated with macrophages, dendritic cells (DC), endothelial cells, T and B cells in AIC were compared to those in AKC (Figures 5, 6). Among the 9 macrophage-related genes, the expression of 8 genes (*h2-eb1*, *cd74*, *cd68*, *marco*, *capg*, *mpeg1*, *cd200r1*, and *csflr*) was significantly lower in AIC compared to AKC (Figure 5A). As for the DC specific genes (Figure 5B), AIC had significantly lower expression of *cd209* and *cd83* than those of AKC. As for the endothelial cell-related genes, the expression of *ecscr* and *cd151l* was significantly higher in AIC than in AKC though this was not the case for the *pecam* gene (Figure 5C).





Regarding the T and B cell-specific gene profile (Figure 6), AIC had significantly higher expression of most T cell-related genes (*cd96*, *tagap*, *cd3gda*, *cd8b*, *cd8a*, *cd6l*, *cd42al*, *cd28*, *trbc1*, *cd2l*, and *trgc2*), but significantly lower expression of B cell-related genes (*igm*, *blnk*, and *cd79a*).

The expression of 21 immune-related cytokine genes were also considered for the AIC vs. AKC comparisons (Figure 7). AIC had significantly lower expression of interleukin 1 and 6 receptors (*il1rap* and *il6r*) while the expression of tumor necrosis factor (TNF)-related genes (*tnfrsf10a*, *tnfrsf11*, *traf2*, and *tnfrsf6b*) was significantly higher. Among the transforming growth factor (TGF)-related genes, the expression of TGF β receptors (*tgfb1* and *tgfb2*) were significantly higher, while the expression of TGF β activated kinase binding protein (*tab2*) was significantly lower in AIC.

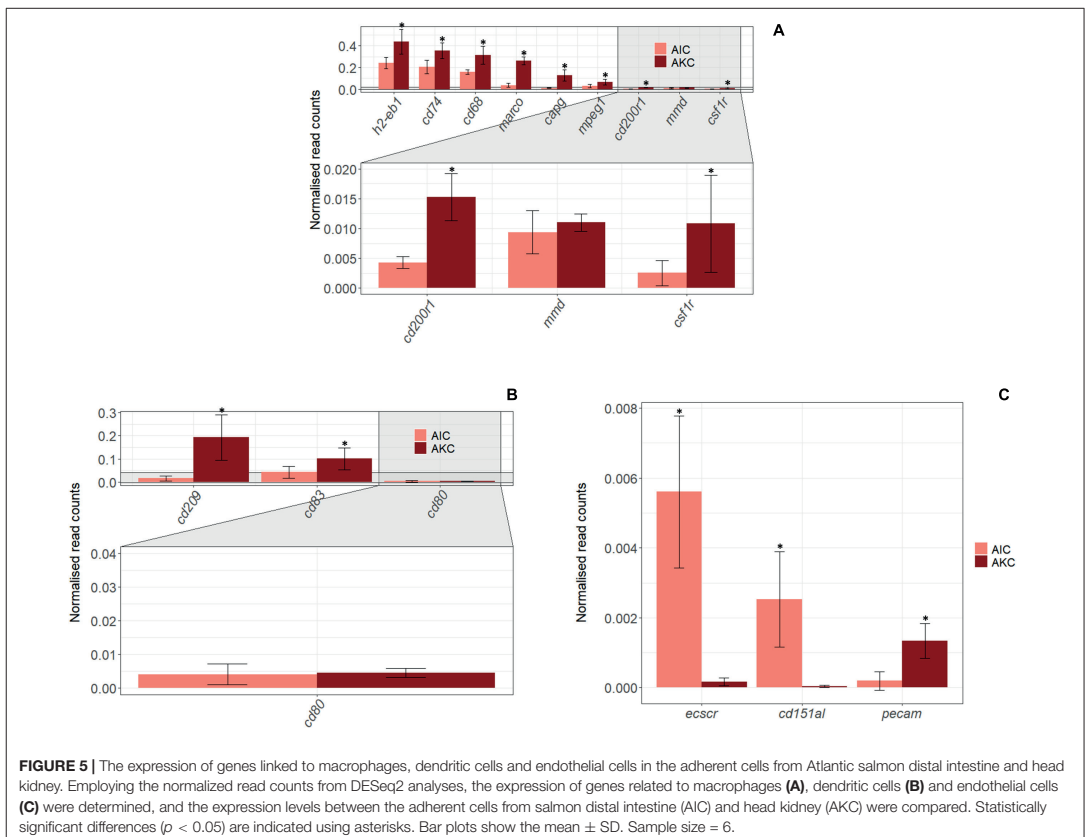
Twelve immune-related genes of chemokines were also studied in AIC and AKC (Figure 8A). The expression levels of *ccr9l*, *ccl20l*, *ccr6l*, and *ccr5l* were significantly higher, while the expression of *cxcr3l*, *ccr3*, *ccl25*, *cxcr4l*, *cxcr1l*, and *cxcr5l* was significantly lower in AIC.

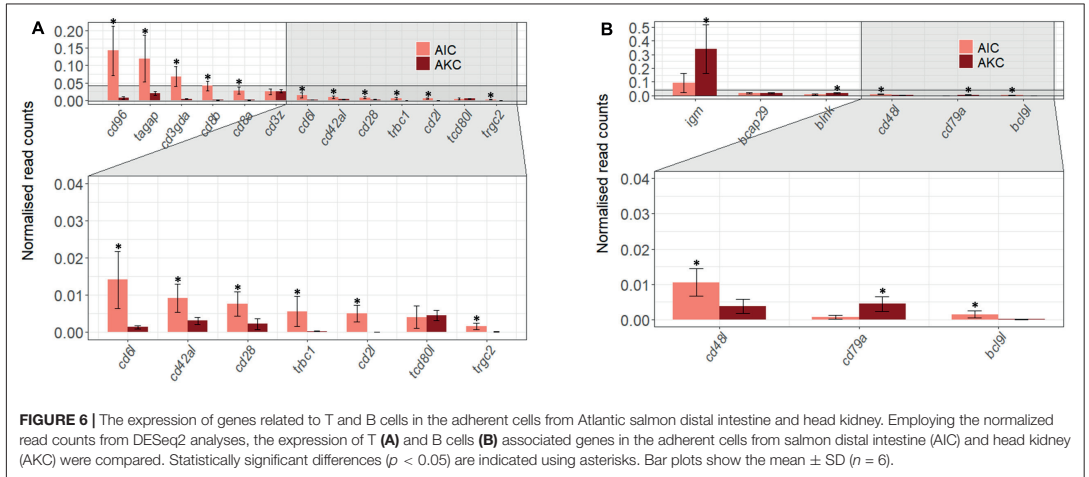
The expression of 9 immune-related genes for mucin and toll-like receptor (TLR) were also compared to understand the differences in AIC and AKC (Figures 8B,C). Mucin-related genes (*muc13l*, *muc1*, *cd164l2*, and *muc5acl*) were mainly expressed in AIC but several TLR genes (*tlr13*, *tlr8*, *tlr2* and *tlr6*) were not predominantly expressed in AIC.

Hierarchical clustering-based heatmap along with the boxplot annotation shown in Figure 9 reveals the gene profiles associated with AIC and AKC. Although the expression of the genes associated with AKC macrophages was significantly higher than those of AIC, both showed predominantly higher expression of the macrophage-specific genes than those of other cell types such as T and B cells.

DISCUSSION

The intestine has a key role in sustaining the health of fishes. Various cells in the intestine act in harmony to maintain the local (Okumura and Takeda, 2016) as well as systemic homeostasis (Biteau et al., 2011; Ramakrishnan et al., 2019). Of these cells,



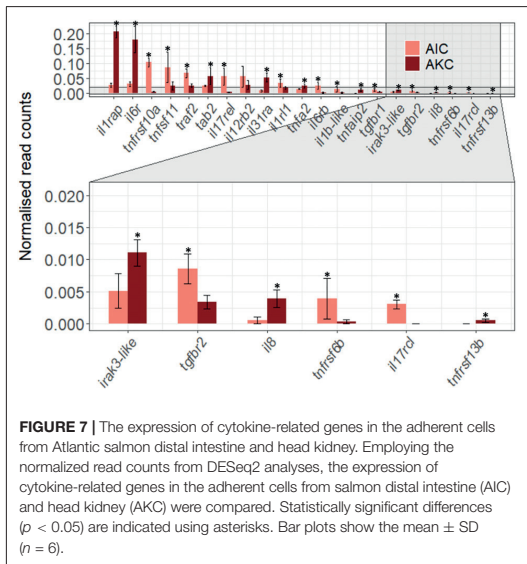


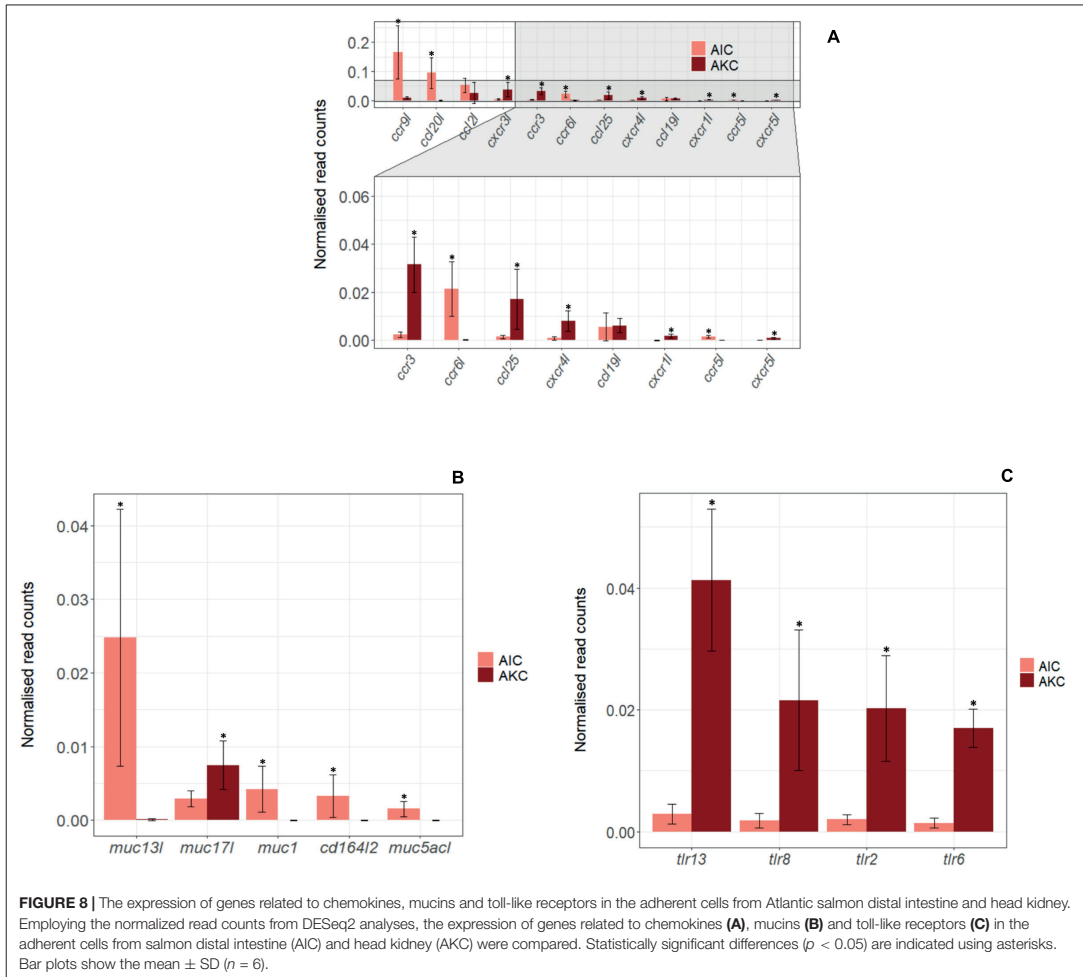
the GALT cells are imperative in responding to antigens, both benign and pathogenic. The immune cells that are developed in the main lymphoid site enter the circulation, and along with the GALT cells they surveil the host immune status. In the present study, we obtained leukocytes from DI and HK of Atlantic salmon and then separated the adherent cells from the two cell populations.

Employing IFC, we examined the phagocytic activity of the adherent intestine cells and compared it with those of adherent head kidney cells. We also examined the expression of

immunologically relevant genes through RNA-Seq of the cells from the two key immune organs of Atlantic salmon.

AIC had distinct cell population; the cells were less diverse than the whole leukocyte population. Other researchers were also able to isolate cells from the intestine of Atlantic salmon (Attaya et al., 2018) and gilthead seabream (Salinas et al., 2007), but they did not specifically examine adherent cells. The major phagocytes in vertebrates are neutrophils, monocytes, macrophages, mast cells, and immature dendritic cells (Robinson and Babcock, 1998). In the present study, we confirmed the phagocytic ability of AIC, which had different shapes compared with those of AKC. Unlike monocyte-derived macrophages which have mainly stretched shapes, the AIC appeared larger and rounded as shown in a mice study (Vereyken et al., 2011). Rombout et al. (1998) reported that the carp intestinal cells are diverse compared to the cells from other immunological tissues such as spleen and head kidney. In addition to many round-shaped cells, the oval shaped phagocytes, similar to the ones we observed, are reported as endothelial cells in mammals, and they were shown to have the ability to internalize pathogenic bacteria (Rengarajan et al., 2016). Furthermore, Lindell et al. (2012) showed that oval-shaped skin epithelial cells in trout can perform phagocytosis of *Vibrio anguillarum*. However, their identity has to be validated by employing specific cell markers. As for the doublets in the adherent cells, the phagocytes in them resembled macrophage-like cells (R1, Figure 1A) while the interacting small cells had a morphology similar to that of lymphocytes. A study that investigated mouse intestinal cells using imaging flow cytometry (Zhao et al., 2014) indicated that similar doublets consisted of CD103⁺ intestinal dendritic cells and CD4⁺ T cells. From our results, we infer that the oval-shaped cells similar to endothelial cells or epithelial cells with phagocytic ability may have special roles in mucosal immune system. In addition, the presence of the doublets indicates the interaction between

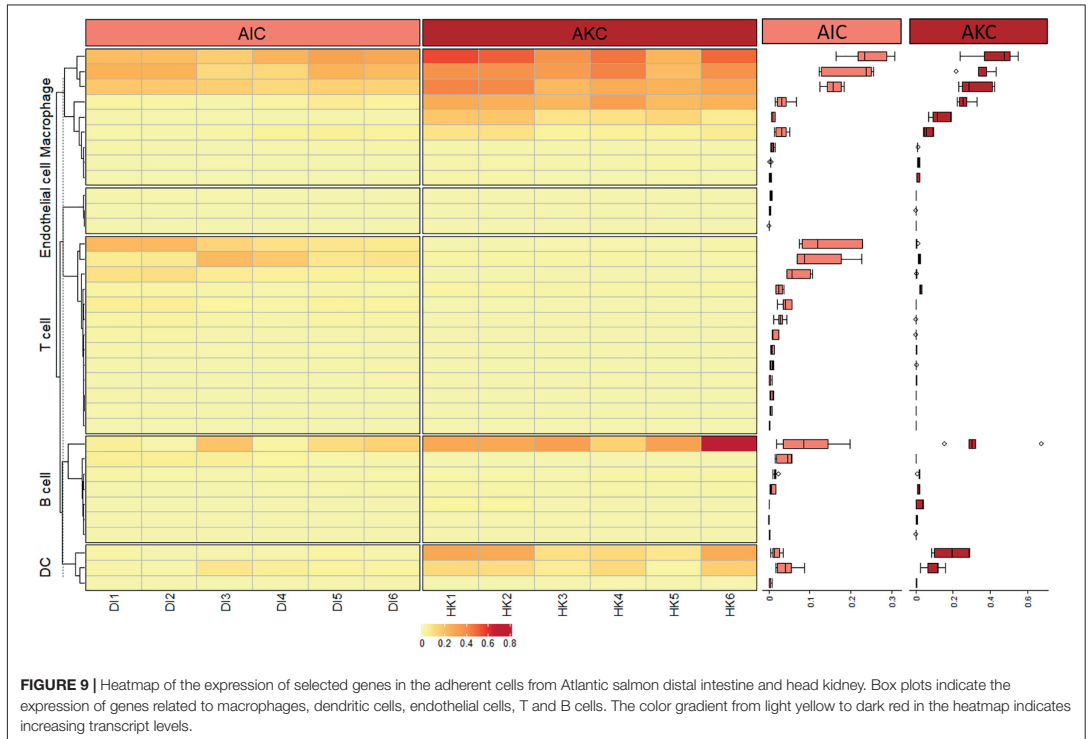




phagocytes and lymphocyte-like cells that cooperate with them in immune defense.

In the present study, considering the phagocytic ability and high expression levels of macrophage genes in AIC we presume that majority of cell types in AIC are macrophages. Salmon macrophages can be effectively harvested after culturing adherent cells from HK (Paulsen et al., 2001). The presence of macrophages in adherent cells from fish intestine and their phagocytic properties have not been reported yet. In the present study, high levels of TNF-related genes (*tnfrsf10a*, *tnfsf11*, *traf2* and *tnfsf6b*) and TGF β receptors (*tgfb1* and *tgfb2*) in AIC can be linked to activation and proliferation of macrophages (Luckett-Chastain et al., 2016; Yu et al., 2017) and T cells (McKarns and Schwartz, 2005; Mehta et al., 2018) while high levels of *il1* and *il6* in AKC can be linked to the classical activation of

macrophages (Luckett-Chastain et al., 2016). We have also found that the expression of eight macrophage-related genes (*h2-eb1*, *cd74*, *cd68*, *marco*, *capg*, *mpeg1*, *cd200r1*, and *csf1r*) was highest in AIC among selected cell type linked genes (Figure 9) although the expression in AKC was significantly higher than those of AIC (Figure 5). Our results are in agreement with another HK transcriptomic study; carp HK macrophage-like cells had higher expression of *cd68* and *mcsfr* compared to those of HK leukocytes (Hu et al., 2018). Furthermore, a study conducted by Jenberie et al. (2018) revealed the higher expressions of *csf1r* and *marco* in HK macrophage-like cells. Another salmon study indicated the higher expression of MHCII β in the adherent cells from the head kidney (Iliev et al., 2019), and we found that the expression of *h2-eb1* gene was higher in AKC. This gene in association with MHC class II plays a role in the



processing and presentation of antigens (Adamus et al., 2012), and teleost mucosa has major T cells receptors (TCR) such as TCR $\alpha\beta$ and TCR $\gamma\delta$, and their respective co-receptors, namely CD4 and CD8, which facilitate antigen recognition (Toda et al., 2011). The presence of T cells in fish intestine was reported years ago by Rombout et al. (1998). Another study (Romano et al., 2007) also indicated the abundance of T cells and TCR β^+ lymphocytes in the posterior intestine and mid-intestine of seabass, respectively. In addition, CD3e $^+$ cells are abundant in salmonid immune organs including intestine (Koppang et al., 2010). Our results about the higher expression of T cell-related genes and *h2-eb1* in AIC and the doublets could be pointing to the cooperation between the adherent cell populations. AIC had higher expression of chemokines, probably those related to T cells. Furthermore, three chemokines (*ccr9l*, *ccl20l*, and *ccr6l*) were dominantly expressed in AIC. It has been reported that mammalian CD4 $^+$ T cells express *ccr9* (Cosorich et al., 2019) while *ccl20* and *ccr6* are expressed on CD8 $^+$ T cell (Kondo et al., 2007; Kish, 2015). The chemokines that are highly expressed in AKC are related to macrophage activation: teleost macrophage-like cells express *cxc3l* (Lu et al., 2017), *ccl25* (Aquilino et al., 2016) and *cxc4l* (Chia et al., 2018) while mammalian macrophages express *ccr3* (Park et al., 1999). In present study, higher expression levels of *ccr9l*, *ccl20l*, and *ccr6l* may be indicating the presence of T cells in AIC. Furthermore,

considering our hypothesis that the adherent cells could be mainly phagocytes, the expression of T cell-related genes in the intestine could be suggestive of their critical role in mucosal immune system. A study on zebrafish (Wan et al., 2017) showed that $\gamma\delta$ T cells which are generally abundant in the intestinal epithelium have potent phagocytic ability. In addition, the phagocytic activity of AIC and the finding of a previous study on the ability of oval-shaped mammalian endothelial cells to internalize pathogens (Rengarajan et al., 2016) likely indicate the phagocytic property of endothelial cells in AIC. We found that AIC had significantly higher expression of endothelial genes (*ecscr* and *cd151l*) while AKC had higher expression of *pecam* gene. Both *ecscr* and *cd151* are known as general signatures of mammalian endothelial cells (Verma et al., 2010; Yang et al., 2017) though they have not yet been reported in fish. On the other hand, *pecam* (or *cd31*) is a gene associated with endothelial cell adhesion molecule and it was highly expressed within blood vascular compartment (Privratsky and Newman, 2014). Furthermore, the presence of the mucin-like receptor, *cd164* could be an indication of the ability of certain cells in AIC to adhere to endothelial cells (Havens et al., 2006).

In summary, employing IFC and transcriptomics, we were able to characterize the adherent cell populations from DI, based on the genes reported as specific to certain cell types.

AIC had different-shaped phagocytes and expressed genes associated with macrophages, T cells, and endothelial-like cells. Overall (selected) gene profiles show that AIC predominantly express macrophage-related genes. Further investigation on the transcriptomic responses of the intestinal cells to different antigens will help to expand our understanding of their crosstalk at the mucosal surfaces in teleosts.

DATA AVAILABILITY STATEMENT

The obtained raw sequencing data was deposited in the Gene Expression Omnibus (GEO, NCBI); the accession number is GSE154142.

ETHICS STATEMENT

The animal study was reviewed and approved by National Animal Research Authority in Norway (Mattilsynet; FOTS ID 10050).

AUTHOR CONTRIBUTIONS

YP, JF, and VK conceived and designed the study. YP performed the experiments on the cells and wrote the first draft of the manuscript. YP and QZ conducted RNA sequencing and data analysis. GW provided suggestions to improve the manuscript. YP, QZ, GW, JF, and VK read, revised and approved the

manuscript for submission. All authors contributed to the article and approved the submitted version.

FUNDING

The INFISH project (272004) funded by the Regionale Forskningsfond Nord-Norge partly supported this study. YP is a recipient of the Korean Government Scholarship—National Institute for International Education, South Korea.

ACKNOWLEDGMENTS

The authors, especially YP, is grateful to Bisa Saraswathy for her valuable support in data analyses, discussions and comments on the manuscript. The authors would like to thank the staff at the Research Station, Nord University for their help in the laboratory.

SUPPLEMENTARY MATERIAL

The Supplementary Material for this article can be found online at: <https://www.frontiersin.org/articles/10.3389/fcell.2020.580848/full#supplementary-material>

Supplementary Figure 1 | Dispersion estimation plot. The plot indicates the shrinkage of the gene-wise dispersions.

Supplementary Table 1 | Details of raw reads, cleaned reads and mapped reads from different samples.

REFERENCES

- Adamus, G., Brown, L., Andrew, S., Meza-Romero, R., Burrows, G. G., and Vandenbark, A. A. (2012). Neuroprotective effects of recombinant T-cell receptor ligand in autoimmune optic neuritis in HLA-DR2 mice. *Invest. Ophthalmol. Vis. Sci.* 53, 406–412. doi: 10.1167/iovs.11-8419
- Andrews, S. (2010). *FastQC: A Quality Control Tool for High Throughput Sequence Data*. Babraham Bioinformatics. Cambridge: Babraham Institute.
- Aquilino, C., Granja, A. G., Castro, R., Wang, T., Abos, B., Parra, D., et al. (2016). Rainbow trout CK9, a CCL25-like ancient chemokine that attracts and regulates B cells and macrophages, the main antigen presenting cells in fish. *Oncotarget* 7, 17547–17564. doi: 10.18632/oncotarget.t.8163
- Attaya, A., Wang, T., Zou, J., Herath, T., Adams, A., Secombes, C. J., et al. (2018). Gene expression analysis of isolated salmonid GALT leucocytes in response to PAMPs and recombinant cytokines. *Fish Shellf. Immunol.* 80, 426–436. doi: 10.1016/j.fsi.2018.06.022
- Bernard, D., Six, A., Rigottier-Gois, L., Messiaen, S., Chilmonczyk, S., Quillet, E., et al. (2006). Phenotypic and functional similarity of gut intraepithelial and systemic T cells in a teleost fish. *J. Immunol.* 176, 3942–3949. doi: 10.4049/jimmunol.176.7.3942
- Bierer, B. E., and Burakoff, S. J. (1988). T cell adhesion molecules. *FASEB J.* 2, 2584–2590.
- Biteau, B., Hochmuth, C. E., and Jasper, H. (2011). Maintaining tissue homeostasis: dynamic control of somatic stem cell activity. *Cell Stem Cell* 9, 402–411. doi: 10.1016/j.stem.2011.10.004
- Braniste, T., Tiginyanu, I., Horvath, T., Raevschi, S., Cebotari, S., Lux, M., et al. (2016). Viability and proliferation of endothelial cells upon exposure to GaN nanoparticles. *Beilstein J. Nanotechnol.* 7, 1330–1337. doi: 10.3762/bjnano.7.124
- Chia, K., Mazzolini, J., Mione, M., and Sieger, D. (2018). Tumor initiating cells induce Cxcr4-mediated infiltration of pro-tumoral macrophages into the brain. *eLife* 7:e31918.
- Cosorich, I., Mcguire, H. M., Warren, J., Danta, M., and King, C. (2019). CCR9 expressing T helper and T follicular helper cells exhibit site-specific identities during inflammatory disease. *Front. Immunol.* 9:2899. doi: 10.3389/fimmu.2018.02899
- Geven, E. J., and Klaren, P. H. (2017). The teleost head kidney: integrating thyroid and immune signalling. *Dev. Compar. Immunol.* 66, 73–83. doi: 10.1016/j.dci.2016.06.025
- Gu, Z. (2015). *Complexheatmap: Making Complex Heatmaps. R Package Version 1*.
- Havens, A. M., Jung, Y., Sun, Y. X., Wang, J., Shah, R. B., Bühring, H. J., et al. (2006). The role of sialomucin CD164 (MGC-24v or endolyn) in prostate cancer metastasis. *BMC Cancer* 6:195. doi: 10.1186/1471-2407-6-195
- Hu, Y., Wei, X., Liao, Z., Gao, Y., Liu, X., Su, J., et al. (2018). Transcriptome analysis provides insights into the markers of resting and LPS-activated macrophages in grass carp (*Ctenopharyngodon idella*). *Intern. J. Mol. Sci.* 19:3562. doi: 10.3390/ijms19113562
- Iliev, D. B., Lagos, L., Thim, H. L., Jørgensen, S. M., Krasnov, A., and Jørgensen, J. B. (2019). CpGs induce differentiation of Atlantic salmon mononuclear phagocytes into cells with dendritic morphology and a proinflammatory transcriptional profile but an exhausted allostimulatory activity. *Front. Immunol.* 10:378. doi: 10.3389/fimmu.2019.0378
- Iliev, D. B., Thim, H., Lagos, L., Olsen, R., and Jørgensen, J. (2013). Homing of antigen-presenting cells in head kidney and spleen-salmon head kidney hosts diverse APC types. *Front. Immunol.* 4:137. doi: 10.3389/fimmu.2013.00137

- Jenberie, S., Thim, H. L., Sunyer, J. O., Skjødt, K., Jensen, I., and Jørgensen, J. B. (2018). Profiling Atlantic salmon B cell populations: CpG-mediated TLR-ligation enhances IgM secretion and modulates immune gene expression. *Sci. Rep.* 8, 1–12. doi: 10.1038/s41598-018-21895-9
- Joerink, M., Ribeiro, C. M., Stet, R. J., Hermesen, T., Savelkoul, H. F., and Wiegertjes, G. F. (2006). Head kidney-derived macrophages of common carp (*Cyprinus carpio* L.) show plasticity and functional polarization upon differential stimulation. *J. Immunol.* 177, 61–69. doi: 10.4049/jimmunol.177.1.61
- Khalili, A. A., and Ahmad, M. R. (2015). A review of cell adhesion studies for biomedical and biological applications. *Intern. J. Mol. Sci.* 16, 18149–18184. doi: 10.3390/ijms160818149
- Kihara, H., Kim, D. M., Nagai, M., Nojiri, T., Nagai, S., Chen, C.-Y., et al. (2018). Epithelial cell adhesion efficacy of a novel peptide identified by panning on a smooth titanium surface. *Intern. J. Oral Sci.* 10, 1–8. doi: 10.1038/s41368-018-0022-1
- Kish, D. (2015). Roles of the CCL20-CCR6 axis and CXCR3 in CD8 T cell-mediated contact hypersensitivity (CCR5P. 211). *J. Immunol.* 194:186.13.
- Kondo, T., Takata, H., and Takiguchi, M. (2007). Functional expression of chemokine receptor CCR6 on human effector memory CD8+ T cells. *Eur. J. Immunol.* 37, 54–65. doi: 10.1002/eji.200636251
- Koppang, E. O., Fischer, U., Moore, L., Tranulis, M. A., Dijkstra, J. M., Köllner, B., et al. (2010). Salmonid T cells assemble in the thymus, spleen and in novel interbranchial lymphoid tissue. *J. Anat.* 217, 728–739. doi: 10.1111/j.1469-7580.2010.01305.x
- Kratofil, R. M., Kubes, P., and Deniset, J. F. (2017). Monocyte conversion during inflammation and injury. *Arterioscler. Thromb. Vasc. Biol.* 37, 35–42. doi: 10.1161/atvaha.116.308198
- Li, J., Barreda, D. R., Zhang, Y.-A., Boshra, H., Gelman, A. E., Lapatra, S., et al. (2006). B lymphocytes from early vertebrates have potent phagocytic and microbicidal abilities. *Nat. Immunol.* 7, 1116–1124. doi: 10.1038/ni1389
- Lindell, K., Fahlgren, A., Hjerde, E., Willassen, N.-P., Fällman, M., and Milton, D. L. (2012). Lipopolysaccharide O-antigen prevents phagocytosis of *Vibrio anguillarum* by rainbow trout (*Oncorhynchus mykiss*) skin epithelial cells. *PLoS One* 7:e37678. doi: 10.1371/journal.pone.0037678
- Love, M. I., Huber, W., and Anders, S. (2014). Moderated estimation of fold change and dispersion for RNA-seq data with DESeq2. *Genome Biol.* 15:550. doi: 10.1186/s13059-014-0550-8
- Lu, X.-J., Chen, Q., Rong, Y.-J., Chen, F., and Chen, J. (2017). CXCR3. 1 and CXCR3. 2 differentially contribute to macrophage polarization in teleost fish. *J. Immunol.* 198, 4692–4706. doi: 10.4049/jimmunol.1700101
- Luckett-Chastain, L., Calhoun, K., Schartz, T., and Gallucci, R. M. (2016). IL-6 influences the balance between M1 and M2 macrophages in a mouse model of irritant contact dermatitis. *J. Immunol.* 196:196.17.
- McKarns, S. C., and Schwartz, R. H. (2005). Distinct effects of TGF- β 1 on CD4+ and CD8+ T cell survival, division, and IL-2 production: a role for T cell intrinsic Smad3. *J. Immunol.* 174, 2071–2083. doi: 10.4049/jimmunol.174.4.2071
- McMillan, D. N., and Secombes, C. J. (1997). Isolation of rainbow trout (*Oncorhynchus mykiss*) intestinal intraepithelial lymphocytes (IEL) and measurement of their cytotoxic activity. *Fish Shellf. Immunol.* 7, 527–541. doi: 10.1006/fsim.1997.0099
- Mehta, A. K., Gracias, D. T., and Croft, M. (2018). TNF activity and T cells. *Cytokine* 101, 14–18. doi: 10.1016/j.cyt.2016.08.003
- Okumura, R., and Takeda, K. (2016). Maintenance of gut homeostasis by the mucosal immune system. *Proc. Jpn. Acad. Ser. B* 92, 423–435. doi: 10.2183/pjab.92.423
- Park, I.-W., Koziel, H., Hatch, W., Li, X., Du, B., and Groopman, J. E. (1999). CD4 receptor-dependent entry of human immunodeficiency virus type-1 env-pseudotypes into CCR5-, CCR3-, and CXCR4-expressing human alveolar macrophages is preferentially mediated by the CCR5 coreceptor. *Am. J. Respir. Cell Mol. Biol.* 20, 864–871. doi: 10.1165/ajrcmb.20.5.3547
- Park, Y., Abihssira-Garcia, I. S., Thalmann, S., Wiegertjes, G. F., Barreda, D. R., Olsvik, P. A., et al. (2020). Imaging flow cytometry protocols for examining phagocytosis of microplastics and bioparticles by immune cells of aquatic animals. *Front. Immunol.* 11:203. doi: 10.3389/fimmu.2018.00203
- Parra, D., Reyes-Lopez, F. E., and Tort, L. (2015). Mucosal immunity and B cells in teleosts: Effect of vaccination and stress. *Front. Immunol.* 6:354. doi: 10.3389/fimmu.2018.00354
- Paulsen, S. M., Engstad, R. E., and Robertsen, B. (2001). Enhanced lysozyme production in Atlantic salmon (*Salmo salar* L.) macrophages treated with yeast β -glucan and bacterial lipopolysaccharide. *Fish Shellf. Immunol.* 11, 23–37. doi: 10.1006/fsim.2000.0291
- Privratsky, J. R., and Newman, P. J. (2014). PECAM-1: regulator of endothelial junctional integrity. *Cell Tissue Res.* 355, 607–619. doi: 10.1007/s00441-013-1779-3
- Ramakrishnan, S. K., Zhang, H., Ma, X., Jung, I., Schwartz, A. J., Triner, D., et al. (2019). Intestinal non-canonical NF κ B signaling shapes the local and systemic immune response. *Nat. Commun.* 10, 1–16. doi: 10.1038/s41467-019-08581-8
- Rengarajan, M., Hayer, A., and Theriot, J. A. (2016). Endothelial cells use a formin-dependent phagocytosis-like process to internalize the bacterium *Listeria monocytogenes*. *PLoS Pathog.* 12:e1005603. doi: 10.1371/journal.pone.0100560
- Robinson, J. P., and Babcock, G. F. (1998). *Phagocyte Function: A Guide for Research and Clinical Evaluation*. New York, NY: Wiley-Liss.
- Romano, N., Rossi, F., Abelli, L., Caccia, E., Piergentili, R., Mastrolia, L., et al. (2007). Majority of TcR β + T-lymphocytes located in thymus and midgut of the bony fish, *Dicentrarchus labrax* (L.). *Cell Tissue Res.* 329, 479–489. doi: 10.1007/s00441-007-0429-z
- Rombout, J., Joosten, P., Engelsma, M., Vos, A., Taverne, N., and Taverne-Thiele, J. (1998). Indications for a distinct putative T cell population in mucosal tissue of carp (*Cyprinus carpio* L.). *Dev. Compar. Immunol.* 22, 63–77. doi: 10.1016/s0145-305x(97)00048-7
- Rombout, J. H., Abelli, L., Picchietti, S., Scapiigliati, G., and Kiron, V. (2011). Teleost intestinal immunology. *Fish Shellf. Immunol.* 31, 616–626. doi: 10.1016/j.fsi.2010.09.001
- Salinas, I., Meseguer, J., and Esteban, M. (2007). Assessment of different protocols for the isolation and purification of gut associated lymphoid cells from the gilthead seabream (*Sparus aurata* L.). *Biol. Proc.* 9:43. doi: 10.1251/bpo132
- Selvarajan, K., Moldovan, L., Chandrakala, A. N., Litvinov, D., and Parthasarathy, S. (2011). Peritoneal macrophages are distinct from monocytes and adherent macrophages. *Atherosclerosis* 219, 475–483. doi: 10.1016/j.atherosclerosis.2011.09.014
- Shimizu, Y., Newman, W., Gopal, T. V., Horgan, K. J., Graber, N., Beall, L. D., et al. (1991). Four molecular pathways of T cell adhesion to endothelial cells: Roles of LFA-1, VCAM-1, and ELAM-1 and changes in pathway hierarchy under different activation conditions. *J. Cell Biol.* 113, 1203–1212. doi: 10.1083/jcb.113.5.1203
- Toda, H., Saito, Y., Koike, T., Takizawa, F., Araki, K., Yabu, T., et al. (2011). Conservation of characteristics and functions of CD4 positive lymphocytes in a teleost fish. *Dev. Compar. Immunol.* 35, 650–660. doi: 10.1016/j.dci.2011.01.013
- Vereyken, E. J., Heijnen, P. D., Baron, W., De Vries, E. H., Dijkstra, C. D., and Teunissen, C. E. (2011). Classically and alternatively activated bone marrow derived macrophages differ in cytoskeletal functions and migration towards specific CNS cell types. *J. Neuroinflamm.* 8:58. doi: 10.1186/1742-2094-8-58
- Verma, A., Bhattacharya, R., Remadevi, I., Li, K., Pramanik, K., Samant, G. V., et al. (2010). Endothelial cell-specific chemotaxis receptor (ecscr) promotes angioblast migration during vasculogenesis and enhances VEGF receptor sensitivity. *Blood J. Am. Soc. Hematol.* 115, 4614–4622. doi: 10.1182/blood-2009-10-248856
- Wan, F., Hu, C.-B., Ma, J.-X., Gao, K., Xiang, L.-X., and Shao, J.-Z. (2017). Characterization of $\gamma\delta$ T cells from zebrafish provides insights into their important role in adaptive humoral immunity. *Front. Immunol.* 7:675. doi: 10.3389/fimmu.2018.00675
- Wickham, H. (2016). *ggplot2: Elegant Graphics for Data Analysis*. Berlin: Springer.
- Yang, X., Li, S., Zhong, J., Zhang, W., Hua, X., Li, B., et al. (2017). CD151 mediates netrin-1-induced angiogenesis through the Src-FAK-Paxillin pathway. *J. Cell. Mol. Med.* 21, 72–80. doi: 10.1111/jcmm.12939
- Yi, H.-J., and Lu, G.-X. (2012). Adherent and non-adherent dendritic cells are equivalently qualified in GM-CSF, IL-4 and TNF- α culture system. *Cell. Immunol.* 277, 44–48. doi: 10.1016/j.cellimm.2012.05.014

- Yu, X., Buttgereit, A., Lelios, I., Utz, S. G., Cansever, D., Becher, B., et al. (2017). The cytokine TGF- β promotes the development and homeostasis of alveolar macrophages. *Immunity* 47, 903–912. doi: 10.1016/j.immuni.2017.10.007
- Zhang, Q., Kopp, M., Babiak, I., and Fernandes, J. M. (2018). Low incubation temperature during early development negatively affects survival and related innate immune processes in zebrafish larvae exposed to lipopolysaccharide. *Sci. Rep.* 8, 1–14. doi: 10.1038/s41598-018-22288-8
- Zhao, W., Minderman, H., and Russell, M. W. (2014). Identification and characterization of intestinal antigen-presenting cells involved in uptake and processing of a nontoxic recombinant chimeric mucosal immunogen based on cholera toxin using imaging flow cytometry. *Clin. Vaccine Immunol.* 21, 74–84. doi: 10.1128/COVI.00452-13

Conflict of Interest: The authors declare that the research was conducted in the absence of any commercial or financial relationships that could be construed as a potential conflict of interest.

Copyright © 2020 Park, Zhang, Wiegertjes, Fernandes and Kiron. This is an open-access article distributed under the terms of the Creative Commons Attribution License (CC BY). The use, distribution or reproduction in other forums is permitted, provided the original author(s) and the copyright owner(s) are credited and that the original publication in this journal is cited, in accordance with accepted academic practice. No use, distribution or reproduction is permitted which does not comply with these terms.

Paper III

1 **miRNA and mRNA profiles unveil macrophage heterogeneity among**
2 **intestinal cells of Atlantic salmon**

3
4 Youngjin Park ^{1,a}, Qirui Zhang ^{1,a,b}, Jorge M.O. Fernandes ¹, Geert F. Wiegertjes ², and
5 Viswanath Kiron ^{1*}
6

7 ¹ Faculty of Biosciences and Aquaculture, Nord University, Bodø, Norway

8 ² Aquaculture and Fisheries Group, Wageningen University & Research, Wageningen,
9 Netherlands
10

11 Running title: (5 words): Macrophage heterogeneity in salmon intestinal cells
12

13 * **Correspondence:** Viswanath Kiron

14 Telephone: +47 755 17399

15 E-mail: kiron.viswanath@nord.no
16

17 ^a These authors contributed equally to this study

18 ^b Present address: Division of Clinical Genetics, Lund University, Lund, Sweden
19

20 **Abstract**

21 The intestine has many types of cells that are present mostly in the epithelium and
22 lamina propria. The importance of the intestinal cells for the mammalian mucosal
23 immune system is well-established. However, there is no in-depth information about
24 many of the intestinal cells in teleosts. In our previous study, we reported that
25 adherent intestinal cells (AIC) predominantly express macrophage-related genes. To
26 gather further evidence to demonstrate that AIC are macrophage-like, we compared
27 the equally abundant as well as differentially expressed mRNAs and miRNAs in AIC with
28 those in adherent head kidney cells (AKC), which have been previously characterized
29 as macrophage-like cells. There were 18309 mRNAs, and 59 miRNAs that were equally
30 abundant between AIC and AKC. Integrative analysis of the mRNA and miRNA
31 transcriptomes revealed 5 pairs with significant negative correlations that are linked to
32 macrophages and epithelial cells. The integrated analysis revealed that AIC is
33 comprised of macrophages and structural cells such as endothelial cells and epithelial
34 cells. Based on the abundance of macrophage-specific mRNAs and miRNAs in AIC and
35 AKC, we suggest macrophage heterogeneity in adherent intestinal cells.

36

37 **Keywords: adherent cells; intestinal cells; macrophages; RNA-Seq; miRNAs;**
38 **Atlantic salmon**

39

40

41 **1. Introduction**

42 Gut-associated lymphoid tissue (GALT) has a significant role in host defence and
43 accounts for almost 70% of cellular components of the entire immune system.
44 Furthermore, about 80% of plasma cells are found in GALT, at least in mammals (Vighi
45 et al., 2008). Fish GALT consists of various immune cell types such as macrophages,
46 dendritic-like cells, B and T cells, and intraepithelial lymphocytes; they are present
47 either between the epithelial cells or in the lamina propria of the intestine (Martin et
48 al., 2016). The cells of the GALT are assumed to work together as a mucosal barrier,
49 supporting the immune system in the intestine (Turner, 2009), which is the largest
50 interface between the external environment and the host.

51
52 Cell adhesion is one of the inherent functions of intestinal cells. This fundamental
53 characteristic is essential for stimulating cell-cell communication and sustaining tissue
54 structure (Bachir et al., 2017). The ability of cells to adhere to one another can be
55 exploited to obtain a highly enriched cell population. In mammals, this characteristic
56 has been used to study adherent cell types, such as macrophages (Golder and Doe,
57 1983), epithelial cells (Ren et al., 2017) and endothelial cells (Margiotta et al., 1995). In
58 fish, the head kidney is a key immune organ and adherent cells from this tissue (AKC)
59 of Atlantic salmon (*Salmo salar*) were previously described as monocyte-derived
60 macrophages (Park et al., 2020a). Recently, we also reported that the adherent cells
61 from the intestine (AIC) of Atlantic salmon express a number of genes typical of
62 macrophages and the cells have phagocytic ability (Park et al., 2020b), suggesting that
63 AIC contain macrophages.

64
65 MicroRNAs are a group of small RNAs that are able to bind to the 3' UTR of messenger
66 RNAs (mRNAs) and negatively regulate target transcripts by silencing mRNA translation
67 or promoting their degradation (Ambros, 2004). Studies have revealed the negative
68 correlations between the expression of miRNA and mRNA in mammals, based on the
69 fact that up/downregulated miRNAs give rise to down/upregulated mRNA (De Cecco
70 et al., 2017; Diaz et al., 2015). miRNA-mRNA interactions have also been studied to
71 understand the miRNA targeting specificity in other organisms such as insects (Fu et
72 al., 2020). A recent study profiled the miRNAs from different tissues and
73 developmental stages of Atlantic salmon (Woldemariam et al., 2019). Furthermore,
74 Smith et al. (2020) reported that miRNA expressions in adherent head kidney cells
75 could influence macrophage differentiation. However, corresponding observations on
76 fish intestine cells do not exist.

77
78 Macrophages can display different activation states, reflecting different phenotypes
79 acquired in response to distinct environmental signals. Macrophage heterogeneity can

80 be influenced by dietary components and microbiota (Belizário et al., 2018; Kim et al.,
81 2014; Wu et al., 2020), among other factors. The degree to which macrophages can be
82 polarized is based on various stimuli such as cytokines, microbes and other modulators
83 (Kim et al., 2016; Mohammadi et al., 2019). It has also been reported that the local
84 environment of intestine could imprint the phenotypes and functions of human
85 macrophages (Bain and Schridde, 2018). The demands of local microorganisms can
86 alter niche-specific macrophage functions since microbiota could drive constant
87 replenishment from circulating monocytes to maintain the intestinal macrophage pool
88 (Bain et al., 2014). Furthermore, self-replenishment of tissue-resident macrophages is
89 considered as a conserved process (Soza-Ried et al., 2010). On the other hand, it is also
90 known that miRNAs have roles in differentiation of intestinal epithelial cells, dendritic
91 cells and macrophages, and even polarization of macrophages (McKenna et al., 2010;
92 Peng et al., 2016; Zhou et al., 2015). We suggest that the capacity of fish macrophages
93 to differentiate into extremes such as M1 or M2-like macrophage types can be
94 influenced by initial immune responses and danger signals, and that this polarization is
95 amplified via positive feedback from T-lymphocytes, especially later in evolution of the
96 macrophages (Wiegertjes et al., 2016). Fish M1 and M2-like macrophages, examples of
97 heterogeneous macrophages polarized into extreme phenotypes, are believed to
98 produce antimicrobials (nitric oxide and pro-inflammatory cytokines)(M1) or
99 molecules associated with tissue regeneration (arginase and anti-inflammatory
100 cytokines)(M2) similar to their mammalian counterparts (Wentzel et al., 2020a;
101 Wentzel et al., 2020b; Wiegertjes et al., 2016). Although we reported the presence of
102 macrophages in AIC in our previous study (Park et al., 2020b), we could not ascertain
103 conclusively the macrophage heterogeneity in AIC.

104
105 Here, we investigated both mRNA and miRNA transcriptomes in adherent cells from
106 the intestine (AIC) of Atlantic salmon and adherent cells from the head kidney (AKC).
107 We examined (1) equally abundant macrophage-related mRNAs and miRNAs in AIC and
108 AKC, (2) differentially expressed mRNAs (DEGs) and miRNAs (DE miRNAs) in AIC
109 compared to AKC, and (3) negative correlations between DE miRNA and DE target
110 mRNAs. We discuss the observation that adherent cells from the intestine display gene
111 profiles that fit with the presence of heterogeneous macrophage phenotypes.

112
113

114 **2. Materials and methods**

115 **2.1. Ethics statement**

116 The present study was approved by the National Animal Research Authority in Norway
117 (Mattilsynet; FOTS ID 10050) and executed according to its guidelines.

118

119 **2.2. Experimental fish and sample collection**

120 In this study, Atlantic salmon (*Salmo salar*) post smolts were purchased from a
121 commercial producer (Sundsford Smolt, Nygårdstjøen, Norway). These fish were raised
122 in a flow-through sea water system (temperature: 7-8°C, dissolved oxygen saturation:
123 87-92 %, 24-h light cycle) at the Research Station of Nord University, Bodø, Norway,
124 and fed a commercial feed (Ewos Micro, Ewos AS, Bergen, Norway) at 1.2% of their
125 body weight daily. Samples were collected from fish (n = 6) of weight range 510-590 g.
126 They were starved for 24 h and were sacrificed with an overdose of tricaine methane
127 sulphate (Argent Chemical Laboratories, Redmond, USA; 200 mg/L). Then, distal
128 intestine (DI) and head kidney (HK) were dissected under sterile conditions and they
129 were used for cell isolation.

130

131 **2.3. Cell isolation and culture**

132 Cells from DI and HK were harvested and grown at 12°C in Leibovitz's L-15 Medium (L-
133 15; Sigma, Oslo, Norway) as described previously by (Park et al., 2020b). Briefly, the
134 isolated DI or HK leukocytes were allowed to adhere on a cell culture dish (Nunc
135 EasYDish, Thermo Fisher Scientific, Oslo, Norway) with 2 mL L-15+ (L-15 medium with
136 50 U/mL penicillin, 50 µg/mL streptomycin, 2% fetal bovine serum and 10 U/mL
137 heparin) for 2 days at 12°C. Thereafter the media was removed and the adherent cells
138 on the culture dish were detached by washing three times with 1.5 mL ice-cold PBS
139 (Sigma) supplemented with 5 mM EDTA (Sigma). The cells were centrifuged (500 × g, 5
140 min, 4°C) and re-suspended with 2 mL L-15+. Then, the adherent cells, AIC or AKC were
141 counted using a portable cell counter (Scepter™ 2.0 cell counter, EMD Millipore,
142 Darmstadt, Germany) for further analysis.

143

144 **2.4. mRNA and small RNA profiling**

145 We performed mRNA and small RNA sequencing to profile the gene expression of AIC
146 and AKC (reference cell type). Six biological replicates were used for the study.

147

148 **2.4.1. RNA isolation**

149 Total RNA was extracted from AIC or AKC (500,000 cells) using PicoPure RNA isolation
150 kit (Thermo Fisher Scientific) according to the manufacturer's protocol. The quality and
151 quantity of the isolated total RNA were assessed using Agilent RNA high sensitivity
152 screen tape kits and Bioanalyzer 2200 TapeStation system (Agilent Technologies, Santa
153 Clara, CA, USA).

154

155 **2.4.2. Library preparation and Illumina sequencing**

156 **2.4.2.1. mRNA sequencing**

157 High quality RNA (RNA Integrity Number > 8) from each sample (50 ng) was used for
158 library construction using the NEBNext Ultra II Directional RNA library preparation kit
159 with poly (A) mRNA magnetic isolation module (NEB #E7490; New England BioLabs®,
160 Herts, UK) as described previously by Park et al. (2020b). The quality and quantity of
161 sequencing-ready libraries were examined using Agilent DNA high sensitivity screen
162 tape kits and Bioanalyzer 2200 TapeStation system. These individual libraries were
163 pooled at equimolar ratio and sequenced on a NextSeq 500 sequencer (Illumina, San
164 Diego, CA, USA) with a high throughput flow cell (single-end, 75 bp) at the sequencing
165 facility of Nord University, Bodø, Norway.

166

167 **2.4.2.2. Small RNA sequencing**

168 From the extracted RNA that was used for mRNA sequencing, 50 ng was used for library
169 preparation using the NEXTflex Small RNA-Seq Kit v3 (Bioo Scientific, Austin, TX, USA)
170 following the manufacturer's protocol. Briefly, RNA was ligated with the NEXTflex 3' 4N
171 and 5' 4N Adenylated adapters. Then, the RNA was reverse transcribed into first-strand
172 cDNA and amplified with NEXTflex universal and barcoded primers on a thermocycler
173 (Applied Biosystem, NY, USA) for 25 cycles. The conditions for each cycle were: 95 °C
174 for 2 min; 95 °C for 20 s, 60 °C for 30 s, 72 °C for 15 s; 72 °C for 2 min. For PAGE size
175 selection, 5 µL of 6X gel loading dye was added to each PCR product and the mixture
176 was loaded on 10 % TBE-PAGE gel (Thermo Fisher Scientific). Then, the cDNA was
177 isolated from the ~150 bp gel band. After size selection, the quality and quantity of
178 individual libraries were assessed using Agilent RNA high sensitivity screen tape kits
179 and Bioanalyzer 2200 TapeStation system. These individual libraries were pooled at
180 equimolar ratio and sequenced as mentioned in the above section.

181

182 **2.4.3. Bioinformatics analyses and statistics**

183 In the related study on AIC (Park et al., 2020b), we profiled the expression of selected
184 cell specific genes (macrophages, dendritic cells, T and B cells and endothelial cells) and
185 genes related to cytokines and chemokines. In the present study we reanalysed the
186 mRNA transcriptome data recently published in the aforementioned paper and
187 integrated it with the newly generated small RNA-Seq dataset. In particular, i) we
188 filtered out top thirty equally abundant macrophage-related genes (with $|\text{Log}_2\text{FC}| <$
189 0.005) and miRNAs (with $|\text{Log}_2\text{FC}| < 1$) in AIC and AKC, ii) determined differentially
190 expressed genes and miRNAs between AIC and AKC, and iii) analysed the association
191 between mRNAs and miRNAs (i.e., correlation analysis between miRNA and their target
192 gene). The overall workflow of the mRNA-Seq and small RNA-Seq data analysis is shown
193 in Supplementary Figure 1.

194

195 **2.4.3.1. mRNA-Seq and small RNA-Seq analysis**

196 All bioinformatic analyses of mRNA-Seq data were performed as previously described
197 by Zhang et al. (2018). Briefly, raw data were converted to fastq format with bcl2fastq2
198 (v2.17, illumina), followed by adapter trimming using Cutadapt (Martin, 2011) and
199 filtering low-quality reads with fastq_quality_filter “-q 20 -p 80”. The clean reads were
200 then aligned against ICSASG_v2 assembly of Atlantic salmon genome using STAR
201 (Dobin et al., 2013) with following parameters: “--outSAMtype BAM
202 SortedByCoordinate --quantMode TranscriptomeSAM GeneCounts”. Read counts
203 were extracted from the alignment file ReadsPerGene.out.tab, the fourth column of
204 which refers to the read counts from the “2nd read strand”. Raw read counts of the 12
205 samples were merged to create a matrix, which was used for the differential expression
206 analysis. For small RNA-Seq analysis, the quality of raw reads was assessed using
207 FastQC (Andrews, 2010), followed by adapter trimming using Cutadapt and removal of
208 low quality reads using FASTX-Toolkit as described above. Clean reads were aligned to
209 Atlantic salmon genome ICSASG_v2 using miRDeep2 package (Friedländer et al., 2012)
210 command mapper.pl with parameters: “-e -d -h -i -j -l 18 -m -n -o 16”, and were
211 quantified using command quantifier.pl with salmon hairpin and mature miRNAs from
212 miRbase (Griffiths-Jones et al., 2007) as input. The filtered miRNAs were subjected to
213 differential expression analysis by comparing AIC to AKC. DESeq2 (Love et al., 2014)
214 was employed to determine differentially expressed mRNAs and miRNAs between AIC
215 and AKC. An absolute fold change (FC) ≥ 2 and Benjamini-Hochberg adjusted p value $<$
216 0.05 were considered for the analyses. The R packages ggplot2 (Wickham, 2016) and
217 pheatmap (Kolde and Kolde, 2015) were employed for data visualization.

218

219 **2.4.3.2. *In silico* analysis to determine the target genes of miRNAs**

220 To study the correlation between DE miRNAs and their target transcripts found in the
221 DEGs, we used two target prediction algorithms: miRanda “-sc 140 -en -20 -scale 4 -
222 strict -go -4 -ge -9 -quiet” (Enright et al., 2003) and RNAhybrid “-b 1 -c -m 5000 -u 1 -v
223 1 -e -20 -p 0.05 -s 3utr_human -q” (Krüger and Rehmsmeier, 2006). Only genes that
224 were identified by both algorithms were selected as potential targets. We focused on
225 miRNAs and their target pairs that were inversely correlated, since miRNAs are
226 negative regulators of gene expression (Moraes et al., 2017). Using Pearson’s
227 correlation analysis, negative correlations between DE miRNA and their target mRNAs
228 among DEGs were determined according to the following three criteria: (1) normality
229 of the data and homoscedasticity of residuals, (2) correlation coefficient $r < 0$ and (3)
230 p-value < 0.05 . Here we considered two types of negative correlation pairs: (1)
231 upregulated DE miRNAs and downregulated target genes among DEGs, (2)
232 downregulated DE miRNAs and upregulated target genes among DEGs.

233

234

235 **3. Results**

236 We employed RNA-Seq and small RNA-Seq to profile the top thirty macrophage-related
237 genes (Table 1) and miRNAs (Table 2) that are equally abundant in AIC and AKC, and to
238 reveal the DEGs (Tables 3 and 4) and DE miRNAs (Tables 5 and 6) in AIC compared to
239 AKC. In addition, a correlation study was performed to decipher the negative
240 correlation between DE miRNAs and their target genes in the DEGs (Table 7).

241 **3.1. Library characterization and overview of the mRNA and miRNA** 242 **transcriptome in adherent intestinal cells**

243 We obtained over 312 million clean reads from 12 mRNA libraries (6 from AIC and 6
244 from AKC), and more than 285 million (91.4%) were mapped to the Atlantic salmon
245 genome. Additional library details are reported in Park et al. (2020b). As for the small
246 RNA-Seq data, over 390 million raw reads were obtained by high-throughput
247 sequencing of miRNA. After adapter trimming and removal of low-quality reads, over
248 323 million clean reads were retained, and more than 98 million of them (32.0%) were
249 aligned to mature miRNAs from Atlantic salmon (Supplementary Table 1).

250 The overall quality of the mRNA and miRNA expression data can be observed in the
251 dispersion plots (Supplementary Figures 2A and 3A). Minus over average and volcano
252 plots show the differentially expressed mRNAs (Supplementary Figures 2B) and
253 miRNAs (Supplementary Figures 3B). The principal component analysis plots of mRNA
254 (Figure 1A) and miRNA (Figure 2A) sequence data show two clear clusters
255 corresponding to AIC and AKC. They are clearly separated along the first component,
256 which represents 91 and 75 % of the variance in mRNA and small RNA data,
257 respectively.
258

259 **3.2. Top thirty macrophage-related mRNA and miRNA genes that are equally** 260 **abundant in adherent intestinal and head kidney cells**

261 While the number of common mRNA in AIC and AKC is 18309 (Figure 1B), the
262 corresponding number for the miRNA (Figure 2B) is 59. The top 30 macrophage-related
263 mRNAs and miRNAs that were expressed at similar levels in AIC and AKC are shown in
264 Tables 1 and 2, respectively. Of the genes that had similar normalised read counts in
265 AIC and AKC (Table 1), *serbp1a*, *ran1* and *cnbp* were the most abundant (with high base
266 mean) genes in AIC. There were four major genes that are associated with
267 macrophages as well as phagocytosis (*mst1ra*, *romo1*, *prdx4* and *calm1*) and two cell
268 adhesion-related genes, namely *bcam* and *ceacam18*. Among the similarly expressed
269 miRNAs in the two types of adherent cells (Table 2), *ssa-let-7b-5p* and *ssa-miR-150-5p*
270 were the most abundant miRNA genes in AIC.
271

272

273 **3.3. Expression levels of potential gene markers of macrophage heterogeneity**
274 **in adherent intestinal and head kidney cells**

275 As a first exploration, we examined heterogeneity amongst the phenotypes of
276 macrophages in AIC and AKC. Five candidate markers for carp M1- and M2-
277 macrophages as identified by Wentzel et al. (2020b) were also found in the
278 transcriptome of AIC and AKC in the present study (Figure 3). AIC had higher expression
279 of M1-macrophage markers (*nosip*, *nostrin* and *saal1*) (Figure 3A) while AKC had higher
280 expression of M2-macrophage markers (*tgm2* and *arg2*) (Figure 3B).

281

282 **3.4. Differentially expressed genes and miRNAs in adherent intestinal cells**

283 In total, 11051 DEGs were identified in AIC compared to AKC; 6821 up and 4230
284 downregulated DEGs (Figure 1C). The top 30 up and downregulated mRNAs in AIC
285 compared to AKC are shown in Tables 3 and 4, respectively. In addition, 37 DE miRNAs
286 were identified in AIC compared to AKC; 20 up and 17 downregulated DE miRNAs
287 (Figure 2C, Tables 5 and 6).

288

289 Among the upregulated DEGs (Table 3), there were two highly regulated genes (\log_2FC
290 ≥ 13.5) in AIC compared to AKC; *adcyp1* and *epcam*. In addition, *gcga1*, *stc1*, *segn*,
291 *tm4sf4*, *t4s1*, *ffar2*, *gcga2*, *rln1* and *scg3* that were detected as upregulated DEGs in AIC
292 also had high fold changes (> 12). As for the downregulated DEGs (Table 4), two genes
293 that were highly downregulated in AIC compared to AKC are *acsl3l* and *p2ry12l* (\log_2FC
294 ≤ -8.9). Furthermore, some genes that were linked to macrophages were also
295 downregulated; *cd147l*, *mrc2l*, *mip2a*, and *ltb4rl* ($\log_2FC \leq -6.7$).

296

297 The three most upregulated miRNAs ($\log_2FC \geq 12$) in AIC compared to AKC were ssa-
298 miR-192b-5p, ssa-miR-196b-5p and ssa-miR-2188-5p. The 20 DE miRNAs that had
299 \log_2FC in the range 1-13 include ssa-miR-429-3p, ssa-miR-192a-5p, ssa-miR-196a-5p,
300 ssa-miR-194a-5p, ssa-miR-210-5p, ssa-miR-10b-5p, ssa-miR-125a-5p, ssa-miR-100a-5p,
301 ssa-miR-23a-3p, ssa-miR-23b-3p and ssa-let-7a-5p (Table 5). The three most
302 downregulated miRNAs ($\log_2FC \leq -4.3$) in AIC compared to AKC were ssa-miR-19d-5p,
303 ssa-miR-17-5p and ssa-miR-92a-5p. The 17 downregulated DE miRNAs that had \log_2FC
304 in the range between -1 and -9.7 include ssa-miR-155-5p, ssa-miR-128-1-5p, ssa-miR-
305 181c-5p, ssa-miR-21b-5p, ssa-miR-731-5p and ssa-miR-181a-5p (Table 6).

306

307 **3.5. Integrative analysis of DE miRNA and their target genes in DEGs**

308 Integrative analysis of DE miRNAs and their target genes among DEGs revealed 15
309 negative correlation pairs (Table 7). Of them, 5 pairs were significantly correlated ($p <$
310 0.05; 4 pairs: downregulated DE miRNA—upregulated target gene, and 1 pair:
311 upregulated DE miRNA—downregulated target gene); ssa-miR-19d-5p—*EIF5*, ssa-miR-

312 92a-3-5p—*enc3*, ssa-miR-128-1-5p—*lbh*, ssa-miR-181c-5p—*p2rx8* and saa-let-7a-5p—
313 *lrplaa* (Figure 4).

314
315

316 **4. Discussion**

317 In-depth studies and characterization of teleost intestinal immune cell types are few
318 and deserve more detailed studies. Hence, we have been characterising the intestinal
319 cells employing a novel approach: by exploiting the ability of some of the intestinal
320 cells to adhere to surfaces, we examined adherent cells specifically, isolated from the
321 distal intestine (AIC) of Atlantic salmon. In our previous study (Park et al., 2020b), we
322 found that they expressed macrophage-specific genes. To characterize these cells, we
323 identified the equally abundant transcripts as well as differentially expressed mRNAs
324 and miRNAs in AIC by comparing them with those in the adherent cells from head
325 kidney (AKC or macrophage-like reference cells). In addition, analysis of DE miRNAs and
326 DE mRNAs revealed the negatively correlated pairs associated with the adherent
327 intestinal cells of salmon.

328

329 **Similarities and differences between macrophage-linked gene expression in** 330 **AIC and AKC**

331 Adherent HK cells from Atlantic salmon contain monocyte-derived macrophages
332 (Paulsen et al., 2001). The genes *serbp1a* and *cnbp* were observed to be equally
333 abundant in AIC and AKC. The former gene is known to recruit macrophages and
334 polarize them to M2 forms (Kubala et al., 2018) and the latter is associated with the
335 cytosol of macrophages (Chen et al., 2018). Among the other mRNAs that had equal
336 abundance in both AIC and AKC, namely *mst1ra*, *romo1*, *prdx4* and *calm1* are
337 macrophage- and phagocytosis-linked genes (Brunelleschi et al., 2001; Hanaka et al.,
338 2019; Lee et al., 2017; Stella et al., 2001; Tan et al., 2016; Zhang et al., 2011).

339 Expressed miRNAs that were equally abundant in AIC and AKC included ssa-let-7b-5p,
340 ssa-miR-125b-5p and ssa-let-7c-5p. In mammals, let-7b (Wang et al., 2016), let-7c-5p
341 (Banerjee et al., 2013) and miR-125b (Chaudhuri et al., 2011) have been associated
342 with macrophage polarization. In salmon, ssa-miR-462a-5p was expressed during head
343 kidney monocyte-to-macrophage differentiation (Smith et al., 2020).

344 Differences in expression of macrophage-related genes in AIC and AKC that we noted
345 could be attributed to the organ-linked diversity of macrophages (Gautier et al., 2012).
346 A recent study has reported the abundant expression of ssa-miR-192a-5p and ssa-miR-
347 194a-5p in Atlantic salmon intestine (Woldemariam et al., 2019); these miRNAs had
348 higher expression in AIC too. In addition, ssa-miR-192a/b-5p were upregulated in AIC.
349 miR-192 is known to be a tumor suppressor and M1 macrophages are known to prime
350 anti-tumor responses (Gordon, 2003; Shang et al., 2018). Two other miRNAs, ssa-miR-

351 155-5p and ssa-miR-21b-5p, that were downregulated in AIC, were detected in salmon
352 HK macrophage-like cells (Smith et al., 2020) while a teleost specific miRNA ssa-miR-
353 731-5p downregulated in AIC was found in cod HK macrophages (Eslamloo et al., 2018).
354 Yet another miRNA downregulated in AIC was ssa-miR-128-1-5p. Woo et al. (2012)
355 have reported that miR-128 downregulated colony stimulating factor-1 (CSF-1), a
356 secreted cytokine that induces monocyte differentiation into macrophages, in human
357 ovarian cancer cells. Studies have indicated that in cyprinid fish, CSF-1 stimulation will
358 induce the production of soluble CSF-1 receptors by macrophages (Rieger et al., 2014;
359 Rieger et al., 2013), and these receptors are expressed by mature macrophages
360 through M2-polarizing responses (Rieger et al., 2013). In our previous study, we
361 reported higher expression levels of *csf1r* in AKC compared to those in AIC (Park et al.,
362 2020b). Considering the expression levels of miR-128-1-5p and *csf1r* in the
363 aforementioned study as well as in the present study, we speculate that macrophage
364 differentiation takes place in AKC, and comparison of the genes in AIC and AKC gives
365 fundamental information about polarization in AIC.

366 Some miRNAs that were upregulated in AIC are linked to macrophages; as examples
367 from mammals, miR-23a-3p was involved in macrophage polarization (Ma et al., 2016).
368 miR-196b-5p (Yuan et al., 2018), and miR-196 (Velu et al., 2009) were associated with
369 macrophage activation. miR-194a-5p (Zhang et al., 2017b) and miR-10b-5p (Wang et
370 al., 2018a) modulated apoptosis in macrophages. Like the disparities in the miRNA
371 abundances in AIC and AKC, certain genes also had differential expression in the two
372 adherent cell types. For example, *mip2a* (macrophage inflammatory protein 2) was
373 downregulated in AIC, and its expression on human macrophages stimulated
374 neutrophil recruitment and activation by binding to their specific receptors, *cxcr1* and
375 *cxcr2*, during acute inflammation (Qin et al., 2017). *ffar2* (free fatty acid receptor 2-like)
376 that was upregulated in AIC is expressed on mammalian macrophages and known to
377 have a role in regulating inflammatory responses by controlling gut epithelial integrity
378 and neutrophil chemotaxis (Alvarez-Curto and Milligan, 2016).

379
380 Interaction between host microRNA and microbes could modulate macrophage
381 functions, at least in mice. It was reported that while *Listeria monocytogenes* reduced
382 the expression of mice miR-192, *Lactobacillus* sp. induced its expression, suggesting
383 the ability of microbes to restore intestinal homeostasis through miRNA regulation
384 (Riaz Rajoka et al., 2018). Also in mice, miR-194-5p and let-7c-5p that were equally
385 abundant in AIC and AKC were found to have a strong connection with certain bacterial
386 families like *Enterobacteriaceae* (Viennois et al., 2019). One of these miRNAs, miR-194-
387 5p, is also associated with inflammatory responses (Meng et al., 2019; Wang et al.,
388 2017). It has been reported that mammalian intestinal macrophages, which lack the

389 surface receptor that helps recognize LPS (CD14) do not produce pro-inflammatory
390 cytokines, but instead produce more anti-inflammatory cytokines (Denning et al., 2007;
391 Smythies et al., 2005). Monocyte-derived macrophages that have initial pro-
392 inflammatory features are soon converted to anti-inflammatory and tolerogenic
393 phenotypes through the signals from IL-10, regulatory T cells, GM-CSF (CSF2) and
394 innate lymphoid cells (Castro-Dopico et al., 2020; Italiani and Boraschi, 2014).
395 Furthermore, the vitamin A metabolite (retinoic acid) is required for maintaining
396 intestinal immune tolerance and to promote M1- to M2-macrophage conversion in
397 mice (Vellozo et al., 2017). In the present study, *rai1*, retinoic acid-induced protein 1-
398 like was equally expressed in AIC and AKC. In addition, *ssa-miR-92a-3-5p* was
399 downregulated in AIC, and *miR-92a* in mice modulated macrophage activation by
400 targeting retinoic acid inducible gene-1 (Sheng et al., 2018). The target gene of *ssa-miR-*
401 *92a-3-5p*, *enc3* that was upregulated in AIC is linked to activation of human colonic
402 epithelial cells (Fujita et al., 2001). Accumulating evidences on interaction between
403 miRNAs and microbes also provide valuable information about the macrophage
404 phenotypes. The miRNA, *miR-196* (upregulated in AIC) present in bovine
405 gastrointestinal tract, was correlated to the abundance of *Bifidobacterium* or
406 *Lactobacillus* species or both, and is also considered as a modulator of lymphoid tissue
407 development (Liang et al., 2014).

408
409 Several genes that were found in AIC and AKC were linked to macrophage activation.
410 Two cell adhesion-related genes, namely *bcam* and *ceacam18* were expressed in AIC
411 and AKC. In mice, basal cell adhesion molecule (*bcam*) plays crucial roles in facilitating
412 the accumulation of monocytes and macrophages (Huang et al., 2014). It has been
413 reported that carcinoembryonic antigen-related cell adhesion molecule (*ceacam*), a
414 major negative regulator of inflammation, could modulate G-CSF production in mice
415 macrophages, and their expression in M1 was higher than in M2 macrophages (Samieni
416 et al., 2013). A recent study demonstrated that carp macrophages express G-CSF
417 paralogs (*g-csfa1* and *g-csfa2*) at high levels (Katakura et al., 2019). In this context, it
418 should be stated that CSF-1 stimulation causes the polarization to M2 form in fishes
419 (Rieger et al., 2013) while GM-CSF-1 is an M1 stimulus in mammals (Mills and Ley,
420 2014). Considering the expression of genes related to macrophages and cell adhesion
421 in both AIC and AKC, we believe that adhesion molecules can modulate macrophage
422 functions and this action may be mediated by the interaction with structural cells from
423 epithelium and endothelium. The top DEGs in AIC included genes associated with
424 endothelial (*segn* and *scg3*) and epithelial cells (*epcam1*, *tm4sf4* and *t4s1*). It has been
425 reported that *segn*, secretagoin-like (Pipp et al., 2007) and *scg3*, secretogranin III (Li
426 et al., 2018) are involved in modulating endothelial cell function. The gene *epcam1* is

427 an epithelial cell adhesion molecule that mediates Ca²⁺-independent homotypic
428 epithelial cell–cell adhesion (Litvinov et al., 1994). Chi and Melendez (2007) reported
429 that an interplay between monocytes and endothelial cells is mediated by intercellular
430 or vascular cell adhesion molecules, and their interaction triggers cell migration.
431 Furthermore, Prieto et al. (1994) reported that the maturation of monocytes to
432 macrophages is regulated by the cell adhesion molecules.

433 In the present study, *enc3* and *lbh* were the targets of the upregulated miRNAs in AIC.
434 *lbh*, a stem-A-associated gene, is expressed in *Lgr5*-positive cells and is a marker of
435 epithelial stem cells in human colon (Shiokawa et al., 2017) and had higher expression
436 in AIC. Furthermore, ectodermal-neural cortex 3 (ENC3) is involved in suppressing
437 differentiation of human colonic epithelial cells during carcinogenesis (Fujita et al.,
438 2001). Interaction between mammalian intestinal epithelial cells and macrophages
439 play an important role in intestinal homeostasis (Al-Ghadban et al., 2016; Powell et al.,
440 2011). Macrophage activation requires interaction with epithelial cells (Lee et al., 2010),
441 and contact with endothelial cells is necessary for M2 polarization and macrophage
442 colony maintenance (He, 2013). Taken together, we believe that mucosal and systemic
443 macrophages are of different phenotypes and their responses may be influenced by
444 the tissue environment such as diet and composition of microbiota, as reviewed by
445 Alvarez-Curto and Milligan (2016).

446

447 **miRNA and mRNA-based evidences on macrophage heterogeneity**

448 Although we have not actively stimulated the macrophages in adherent cells, based on
449 the genes specific to particular phenotypes, we speculate the presence of macrophage
450 heterogeneity and maybe even presence of M1 and M2 macrophages. A recent study
451 has reported the potential markers for M1-macrophages (*il1b*, *nos2b* and *saa*) and M2-
452 macrophages (*timp2b*, *tgm2b* and *arg2*) by LPS and cAMP stimulation, respectively; the
453 authors also observed differences in nitric oxide production and arginase activity of
454 these phenotypes (Wentzel et al., 2020b). In the present study, we also found the
455 expressions of the macrophage marker genes in AIC and AKC. The higher expression of
456 M1-macrophage marker genes—two nitric oxide synthase-related genes, *nosip* and
457 *nostrin*, and *saal1*—were noted in AIC. On the other hand, AKC had the higher
458 expression of the marker genes for M2 macrophages—*tgm2* and *arg2*. It is known that
459 the two genes, *nosip* (nitric oxide synthase interacting protein) and *nostrin* (nitric oxide
460 synthase trafficking) were associated with modulating nitric oxide synthesis
461 (Chakraborty and Ain, 2017; Mukherjee et al., 2018). Human studies showed that the
462 expression levels of transglutaminases 2 (TG2) known as a marker for M2-macrophages
463 increased during the monocyte-to-macrophages differentiation (Mehta et al., 1987;

464 Murtaugh et al., 1984). Furthermore, in our previous study, the gene *il1b1* was highly
465 expressed in AIC compared to AKC (Park et al., 2020b).

466 Two other genes that were upregulated in AIC in the present study, namely *stc1* and
467 *rln1* point to the existence of M1 macrophages. A recent study reported that
468 lipopolysaccharide (LPS)/IFN γ -induced M1 human macrophages had higher expression
469 levels of STC1 compared to phorbol myristate acetate-induced M0- and IL-4/IL-13-
470 induced M2-macrophages (Leung and Wong, 2021). The other gene reported here, *rln1*
471 (relaxin-like protein), is known to significantly increase pro-inflammatory cytokine IL-6
472 in human M1 macrophages (Horton et al., 2011).

473 On the contrary, *cd147* was down regulated in AIC, even though they have been
474 associated with murine and human M1 macrophages and such cells induced Th17
475 differentiation (Geng et al., 2014). This variance in *cd147* expression in AIC warrants
476 additional investigation. As regards the miRNAs, Zhang et al. (2013) reported that miR-
477 181 and miR-155 (downregulated in AIC) were highly expressed in M1-macrophages of
478 mice. On the other hand, miR-210-5p and miR-125a-5p were upregulated in AIC, and
479 these miRNAs are known to be highly expressed in mice M1-macrophages (Melton et
480 al., 2016). In addition, miR-429 that was expressed in AIC is reported to be associated
481 with LPS-induced pro-inflammatory cytokine in mice macrophage (Xiao et al., 2015).
482 Another miRNA, *ssa-miR-194a-5p* was upregulated in AIC, and in rats, miR-194 in LPS-
483 induced nucleus pulposus cells modulated the expression of inflammatory cytokines-
484 associated genes (*tnfa*, *il1* and *il6*) (Kong et al., 2018), which could be linked to the
485 characteristics of mammalian M1-macrophage polarization (Genard et al. (2017).
486 Mammalian M1 macrophages play a critical role in host defense against infection (Liu
487 et al., 2014). P2X purinoceptor 5-like is the target gene (*p2rx*) of *ssa-miR-181c-5p* that
488 was upregulated in AIC. During inflammatory response, P2X purinoceptors are
489 upregulated in macrophages, indicating that the gene could act as a danger signal
490 sensor (Burnstock, 2016). In a report on mice, miR-17-5p upregulation in the peritoneal
491 macrophages of ApoE^{-/-} mice fed with a high-cholesterol diet, indicates that the miRNA
492 regulates inflammation and lipid accumulation by repressing the expression of a
493 cholesterol transporter gene, ABCA1 (Tan et al., 2019). *p2rx* and ABCA1 that were
494 highly expressed in mammalian macrophages during inflammation could be linked to
495 M1-macrophages. Thus, from these results we assume that teleost M1 macrophages
496 have different roles when responding at different mucosal and systemic tissues.

497
498 In Atlantic salmon, *mst1ra* had similar expression in both AIC and AKC. This gene,
499 encoding macrophage-stimulating protein receptor, is expressed on mammalian
500 peritoneal macrophages (Stella et al., 2001) and regulates their biological functions,
501 including phagocytosis and the M1-M2 macrophage balance (Brunelleschi et al., 2001).

502 The gene encoding adenylate cyclase activating polypeptide 1, *adcyap1*, was
503 upregulated in AIC. This cytoprotective peptide modulates murine macrophage
504 polarization during chronic inflammation—increased M2 polarization but reduced M1
505 polarization by interfering with JNK/STAT3 signalling pathway (Wan and Sun, 2019).
506 Two other genes were downregulated in AIC, namely *mrc2l* (C-type mannose receptor
507 2-like) and *ltb4rl* (leukotriene B4 receptor 1-like). The former is known to be expressed
508 on mice M2-like macrophages (Madsen et al., 2013), while *ltb4rl* expressed on mouse
509 macrophages favours M2 polarization (Zhang et al., 2017a). Among the miRNAs
510 studied, two upregulated ones in AIC are associated with M2 polarization. miR-100
511 induced the M2-polarization of macrophages (Wang et al., 2018b) and high expression
512 of let-7a upregulated the anti-inflammatory factors and promoted the switch from M1
513 to M2 phenotype (Hashemi et al., 2018). *ssa-miR-125a-5p* was among the top
514 upregulated miRNAs in AIC and high expression of miR-125 has been reported in mice
515 M2-macrophages (Zhang et al., 2013). In addition, *ssa-miR-192a-5p* was upregulated
516 in AIC, as observed for bone marrow-derived macrophages of mice, the expression of
517 miR-192 promoted M2-macrophage differentiation in vitro (Zhang et al., 2020).
518 Eukaryotic translation initiation factor-5 (*eif5*) is the target gene of *ssa-miR-19d-5p* that
519 was downregulated in AIC, and *eif5* is known to modulate mitochondrial respiration
520 and indirectly affect alternative (M2) macrophage activation in humans (Puleston et
521 al., 2019). Yet another miRNA upregulated in AIC is *ssa-let-7a-5p* and its target gene is
522 *lrp1aa*. Mueller et al. (2018) found that low-density lipoprotein receptor-related
523 protein (*Irp*) controls the expression of C-C chemokine receptor type 7 (*ccr7*, a
524 macrophage polarization marker) in mice macrophages. LRP1-mediated signalling
525 helps in resolution of the active inflammatory response and promotes the conversion
526 to anti-inflammatory M2 functional phenotype (Potere et al., 2019). In addition, LDL
527 receptor-related protein-1 is known to regulate miR155 (Mantuano et al., 2016). It
528 should be noted that *ssa-miR-155-5p* was downregulated in AIC. Summing up, we
529 believe that intestinal-resident macrophages have more M2-macrophage
530 characteristics than monocyte-derived ones, and the miRNAs described here could be
531 involved in switching of macrophage phenotypes in salmon.

532
533

534 **5. Conclusion**

535 The present transcriptomic study has provided new molecular insights on the intestinal
536 adherent cells of Atlantic salmon. Taken together, these multiple analyses based on
537 the transcriptomic data suggest that the adherent intestinal cells contain macrophages,
538 epithelial cells and endothelial cells, and their interaction could be pointing to the
539 presence of a heterogeneous population of macrophages. Possibly, the expression of

540 specific miRNA and mRNA could indicate the existence of both M1 and M2
541 macrophages in the adherent intestinal cells of salmon. This adherent cell population
542 should be further studied to understand their contribution to intestinal immunity in
543 Atlantic salmon, and other teleosts. Furthermore, miRNA and mRNA pair searching
544 studies employing M1 and M2 macrophage populations should be conducted to clarify
545 the functions of intestinal macrophages.

546

547 **Data Availability**

548 mRNA-Seq and small RNA-Seq data can be found in Gene Expression Omnibus (GEO,
549 NCBI) under the accession numbers GSE154142 and GSE154147, respectively. All in-
550 house scripts can be obtained from the authors on request.

551

552 **AUTHOR CONTRIBUTIONS**

553 YP, JF and VK conceived and designed the study. YP and QZ performed the experiment,
554 RNA sequencing and data analysis. YP wrote the first draft of this manuscript. YP, QZ,
555 JF and VK read, revised and approved this manuscript for submission.

556

557 **ACKNOWLEDGMENTS**

558 We thank the staff at the Research Station, Nord University, Norway for their support
559 for this experiment. We (especially YP) appreciate the help from Bisa Saraswathy for
560 data analysis, manuscript preparation and valuable discussions.

561

562 **FUNDING**

563 This study was partially supported by INFISH project (272004) funded by the Regionale
564 Forskningsfond Nord-Norge. YP was a recipient of the Korean Government
565 Scholarship—National Institute for International Education, South Korea.

566

567 **Conflict of Interest Statement:**

568 The authors declare no conflict of interest.

569

570 **REFERENCES**

- 571 Al-Ghadban, S., Kaissi, S., Homaidan, F.R., Naim, H.Y., and El-Sabban, M.E. (2016). Cross-talk
572 between intestinal epithelial cells and immune cells in inflammatory bowel disease.
573 *Scientific Reports* 6, 1-13.
- 574 Alvarez-Curto, E., and Milligan, G. (2016). Metabolism meets immunity: The role of free fatty
575 acid receptors in the immune system. *Biochem Pharmacol* 114, 3-13.
- 576 Ambros, V. (2004). The functions of animal microRNAs. *Nature* 431, 350-355.
- 577 Andrews, S. (2010). FastQC: A quality control tool for high throughput sequence data
578 (Babraham Bioinformatics, Babraham Institute, Cambridge, United Kingdom).

579 Bachir, A.I., Horwitz, A.R., Nelson, W.J., and Bianchini, J.M. (2017). Actin-based adhesion
580 modules mediate cell interactions with the extracellular matrix and neighboring cells.
581 Cold Spring Harbor Perspectives in Biology 9, a023234.

582 Bain, C.C., Bravo-Blas, A., Scott, C.L., Gomez Perdiguero, E., Geissmann, F., Henri, S., Malissen,
583 B., Osborne, L.C., Artis, D., and Mowat, A.M. (2014). Constant replenishment from
584 circulating monocytes maintains the macrophage pool in the intestine of adult mice.
585 Nat Immunol 15, 929-937.

586 Bain, C.C., and Schridde, A. (2018). Origin, differentiation, and function of intestinal
587 macrophages. Front Immunol 9, 2733.

588 Banerjee, S., Xie, N., Cui, H., Tan, Z., Yang, S., Icyuz, M., Abraham, E., and Liu, G. (2013).
589 MicroRNA let-7c regulates macrophage polarization. The Journal of Immunology 190,
590 6542-6549.

591 Belizário, J.E., Faintuch, J., and Garay-Malpartida, M. (2018). Gut microbiome dysbiosis and
592 immunometabolism: New frontiers for treatment of metabolic diseases. Mediators
593 Inflamm 2018, 2037838.

594 Brunelleschi, S., Penengo, L., Lavagno, L., Santoro, C., Colangelo, D., Viano, I., and Gaudino, G.
595 (2001). Macrophage stimulating protein (MSP) evokes superoxide anion production
596 by human macrophages of different origin. British Journal of Pharmacology 134, 1285-
597 1295.

598 Burnstock, G. (2016). P2X ion channel receptors and inflammation. Purinergic Signalling 12,
599 59-67.

600 Castro-Dopico, T., Fleming, A., Dennison, T.W., Ferdinand, J.R., Harcourt, K., Stewart, B.J.,
601 Cader, Z., Tuong, Z.K., Jing, C., Lok, L.S.C., *et al.* (2020). GM-CSF calibrates macrophage
602 defense and wound healing programs during intestinal infection and inflammation.
603 Cell Rep 32, 107857-107857.

604 Chakraborty, S., and Ain, R. (2017). Nitric-oxide synthase trafficking inducer is a pleiotropic
605 regulator of endothelial cell function and signaling. The Journal of Biological
606 Chemistry 292, 6600-6620.

607 Chaudhuri, A.A., So, A.Y.-L., Sinha, N., Gibson, W.S., Taganov, K.D., O'Connell, R.M., and
608 Baltimore, D. (2011). MicroRNA-125b potentiates macrophage activation. The Journal
609 of Immunology 187, 5062-5068.

610 Chen, Y., Sharma, S., Assis, P.A., Jiang, Z., Elling, R., Olive, A.J., Hang, S., Bernier, J., Huh, J.R.,
611 Sasseti, C.M., *et al.* (2018). CNBP controls IL-12 gene transcription and Th1 immunity.
612 J Exp Med 215, 3136-3150.

613 Chi, Z., and Melendez, A.J. (2007). Role of cell adhesion molecules and immune-cell migration
614 in the initiation, onset and development of atherosclerosis. Cell Adhesion & Migration
615 1, 171-175.

616 De Cecco, L., Giannoccaro, M., Marchesi, E., Bossi, P., Favales, F., Locati, L.D., Licitra, L., Pilotti,
617 S., and Canevari, S. (2017). Integrative miRNA-gene expression analysis enables
618 refinement of associated biology and prediction of response to cetuximab in head and
619 neck squamous cell cancer. Genes 8, 35.

620 Denning, T.L., Wang, Y.-c., Patel, S.R., Williams, I.R., and Pulendran, B. (2007). Lamina propria
621 macrophages and dendritic cells differentially induce regulatory and interleukin 17-
622 producing T cell responses. Nat Immunol 8, 1086-1094.

623 Diaz, G., Zamboni, F., Tice, A., and Farci, P. (2015). Integrated ordination of miRNA and mRNA
624 expression profiles. BMC Genomics 16, 1-13.

625 Dobin, A., Davis, C.A., Schlesinger, F., Drenkow, J., Zaleski, C., Jha, S., Batut, P., Chaisson, M.,
626 and Gingeras, T.R. (2013). STAR: Ultrafast universal RNA-seq aligner. *Bioinformatics*
627 *29*, 15-21.

628 Enright, A.J., John, B., Gaul, U., Tuschl, T., Sander, C., and Marks, D.S. (2003). MicroRNA targets
629 in *Drosophila*. *Genome Biology* *5*, R1.

630 Eslamloo, K., Inkpen, S.M., Rise, M.L., and Andreassen, R. (2018). Discovery of microRNAs
631 associated with the antiviral immune response of Atlantic cod macrophages. *Mol*
632 *Immunol* *93*, 152-161.

633 Friedländer, M.R., Mackowiak, S.D., Li, N., Chen, W., and Rajewsky, N. (2012). miRDeep2
634 accurately identifies known and hundreds of novel microRNA genes in seven animal
635 clades. *Nucleic Acids Research* *40*, 37-52.

636 Fu, X., Liu, P., Dimopoulos, G., and Zhu, J. (2020). Dynamic miRNA-mRNA interactions
637 coordinate gene expression in adult *Anopheles gambiae*. *PLoS Genetics* *16*, e1008765.

638 Fujita, M., Furukawa, Y., Tsunoda, T., Tanaka, T., Ogawa, M., and Nakamura, Y. (2001). Up-
639 regulation of the ectodermal-neural cortex 1 (ENC1) gene, a downstream target of the
640 β -catenin/T-cell factor complex, in colorectal carcinomas. *Cancer Research* *61*, 7722-
641 7726.

642 Gautier, E.L., Shay, T., Miller, J., Greter, M., Jakubzick, C., Ivanov, S., Helft, J., Chow, A., Elpek,
643 K.G., and Gordonov, S. (2012). Gene-expression profiles and transcriptional regulatory
644 pathways that underlie the identity and diversity of mouse tissue macrophages.
645 *Nature Immunology* *13*, 1118-1128.

646 Genard, G., Lucas, S., and Michiels, C. (2017). Reprogramming of tumor-associated
647 macrophages with anticancer therapies: Radiotherapy versus chemo- and
648 immunotherapies. *Front Immunol* *8*, 828.

649 Geng, J.-j., Zhang, K., Chen, L.-n., Miao, J.-l., Yao, M., Ren, Y., Fu, Z.-g., Chen, Z.-n., and Zhu, P.
650 (2014). Enhancement of CD147 on M1 macrophages induces differentiation of Th17
651 cells in the lung interstitial fibrosis. *Biochimica et Biophysica Acta (BBA) - Molecular*
652 *Basis of Disease* *1842*, 1770-1782.

653 Golder, J.P., and Doe, W.F. (1983). Isolation and preliminary characterization of human
654 intestinal macrophages. *Gastroenterology* *84*, 795-802.

655 Gordon, S. (2003). Alternative activation of macrophages. *Nature Reviews Immunology* *3*, 23-
656 35.

657 Griffiths-Jones, S., Saini, H.K., Van Dongen, S., and Enright, A.J. (2007). miRBase: Tools for
658 microRNA genomics. *Nucleic Acids Research* *36*, D154-D158.

659 Hanaka, T., Kido, T., Noguchi, S., Yamada, S., Noguchi, H., Guo, X., Nawata, A., Wang, K.-Y.,
660 Oda, K., and Takaki, T. (2019). The overexpression of peroxiredoxin-4 affects the
661 progression of idiopathic pulmonary fibrosis. *BMC Pulmonary Medicine* *19*, 265.

662 Hashemi, N., Sharifi, M., Tolouei, S., Hashemi, M., Hashemi, C., and Hejazi, S.H. (2018).
663 Expression of hsa Let-7a microRNA of macrophages infected by *Leishmania major*.
664 *International Journal of Medical Research & Health Sciences* *5*, 27-32.

665 He, H. (2013). The crosstalk between endothelial cells and macrophages: Biological
666 consequences. Doctoral dissertation, The University of California, Los Angeles. p.131.

667 Horton, J., Yamamoto, S., and Bryant-Greenwood, G. (2011). Relaxin modulates
668 proinflammatory cytokine secretion from human decidual macrophages. *Biology of*
669 *Reproduction* *85*, 788-797.

670 Huang, J., Filipe, A., Rahuel, C., Bonnin, P., Mesnard, L., Guérin, C., Wang, Y., Le Van Kim, C.,
671 Colin, Y., and Tharaux, P.-L. (2014). Lutheran/basal cell adhesion molecule accelerates

672 progression of crescentic glomerulonephritis in mice. *Kidney International* 85, 1123-
673 1136.

674 Italiani, P., and Boraschi, D. (2014). From monocytes to M1/M2 macrophages: phenotypical
675 vs. functional differentiation. *Front Immunol* 5, 514.

676 Katakura, F., Nishiya, K., Wentzel, A.S., Hino, E., Miyamae, J., Okano, M., Wiegertjes, G.F., and
677 Moritomo, T. (2019). Paralogs of common carp granulocyte colony-stimulating factor
678 (G-CSF) have different functions regarding development, trafficking and activation of
679 neutrophils. *Front Immunol* 10, 255.

680 Kim, C.-S., Choi, H.-S., Joe, Y., Chung, H.T., and Yu, R. (2016). Induction of heme oxygenase-1
681 with dietary quercetin reduces obesity-induced hepatic inflammation through
682 macrophage phenotype switching. *Nutr Res Pract* 10, 623-628.

683 Kim, Y.-G., Udayanga, Kankanam Gamage S., Totsuka, N., Weinberg, Jason B., Núñez, G., and
684 Shibuya, A. (2014). Gut dysbiosis promotes M2 macrophage polarization and allergic
685 airway inflammation via fungi-induced PGE2. *Cell Host Microbe* 15, 95-102.

686 Kolde, R., and Kolde, M.R. (2015). Package ‘pheatmap’. *R Package* 1, 790.

687 Kong, L., Sun, M., Jiang, Z., Li, L., and Lu, B. (2018). MicroRNA-194 inhibits lipopolysaccharide-
688 induced inflammatory response in nucleus pulposus cells of the intervertebral disc by
689 targeting TNF receptor-associated factor 6 (TRAF6). *Medical Science Monitor :
690 International Medical Journal of Experimental and Clinical Research* 24, 3056-3067.

691 Krüger, J., and Rehmsmeier, M. (2006). RNAhybrid: microRNA target prediction easy, fast and
692 flexible. *Nucleic Acids Research* 34, W451-W454.

693 Kubala, M.H., Punj, V., Placencio-Hickok, V.R., Fang, H., Fernandez, G.E., Sposto, R., and
694 DeClerck, Y.A. (2018). Plasminogen activator inhibitor-1 promotes the recruitment
695 and polarization of macrophages in xancer. *Cell Rep* 25, 2177-2191.e2177.

696 Lee, B.H., Kushwah, R., Wu, J., Ng, P., Palaniyar, N., Grinstein, S., Philpott, D.J., and Hu, J. (2010).
697 Adenoviral vectors stimulate innate immune responses in macrophages through
698 cross-talk with epithelial cells. *Immunology Letters* 134, 93-102.

699 Lee, S.H., Park, M.J., Choi, S.I., Lee, E.J., Lee, S.Y., and In, K.H. (2017). Reactive oxygen species
700 modulator 1 (Romo1) as a novel diagnostic marker for lung cancer-related malignant
701 effusion. *Medicine* 96.

702 Leung, C.C.T., and Wong, C.K.C. (2021). Characterization of stanniocalcin-1 expression in
703 macrophage differentiation. *Transl Oncol* 14, 100881.

704 Li, W., Webster, K.A., LeBlanc, M.E., and Tian, H. (2018). Secretogranin III: A diabetic
705 retinopathy-selective angiogenic factor. *Cellular and Molecular Life Sciences* 75, 635-
706 647.

707 Liang, G., Malmuthuge, N., McFadden, T.B., Bao, H., Griebel, P.J., Stothard, P., and Guan, L.L.
708 (2014). Potential regulatory role of microRNAs in the development of bovine
709 gastrointestinal tract during early life. *PLoS One* 9, e92592.

710 Litvinov, S.V., Velders, M.P., Bakker, H., Fleuren, G.J., and Warnaar, S.O. (1994). Ep-CAM: A
711 human epithelial antigen is a homophilic cell-cell adhesion molecule. *The Journal of
712 Cell Biology* 125, 437-446.

713 Liu, Y.-C., Zou, X.-B., Chai, Y.-F., and Yao, Y.-M. (2014). Macrophage polarization in
714 inflammatory diseases. *Int J Biol Sci* 10, 520-529.

715 Love, M.I., Huber, W., and Anders, S. (2014). Moderated estimation of fold change and
716 dispersion for RNA-seq data with DESeq2. *Genome Biol* 15, 550.

717 Ma, S., Liu, M., Xu, Z., Li, Y., Guo, H., Ge, Y., Liu, Y., Zheng, D., and Shi, J. (2016). A double
718 feedback loop mediated by microRNA-23a/27a/24-2 regulates M1 versus M2
719 macrophage polarization and thus regulates cancer progression. *Oncotarget* 7, 13502.
720 Madsen, D.H., Leonard, D., Masedunskas, A., Moyer, A., Jürgensen, H.J., Peters, D.E.,
721 Amornphimoltham, P., Selvaraj, A., Yamada, S.S., Brenner, D.A., *et al.* (2013). M2-like
722 macrophages are responsible for collagen degradation through a mannose receptor–
723 mediated pathway. *J Cell Biol* 202, 951-966.
724 Mantuano, E., Brifault, C., Lam, M.S., Azmoon, P., Gilder, A.S., and Gonias, S.L. (2016). LDL
725 receptor-related protein-1 regulates NFκB and microRNA-155 in macrophages to
726 control the inflammatory response. *Proceedings of the National Academy of Sciences*
727 113, 1369.
728 Margiotta, M.S., Benton, L., and Greco, R.S. (1995). Endothelial cells adherent to expanded
729 polytetrafluoroethylene express the intercellular adhesion molecule-1. *Journal of the*
730 *American College of Surgeons* 181, 215.
731 Martin, M. (2011). Cutadapt removes adapter sequences from high-throughput sequencing
732 reads. *EMBnet Journal* 17, 10-12.
733 Martin, S.A., Dehler, C.E., and Król, E. (2016). Transcriptomic responses in the fish intestine.
734 *Developmental & Comparative Immunology* 64, 103-117.
735 McKenna, L.B., Schug, J., Vourekas, A., McKenna, J.B., Bramswig, N.C., Friedman, J.R., and
736 Kaestner, K.H. (2010). MicroRNAs control intestinal epithelial differentiation,
737 architecture, and barrier function. *Gastroenterology* 139, 1654-1664. e1651.
738 Mehta, K., Turpin, J., and Lopez-Berestein, G. (1987). Induction of tissue transglutaminase in
739 human peripheral blood monocytes by intracellular delivery of retinoids. *J Leukoc Biol*
740 41, 341-348.
741 Melton, D.W., Lei, X., Gelfond, J.A., and Shireman, P.K. (2016). Dynamic macrophage
742 polarization-specific miRNA patterns reveal increased soluble VEGF receptor 1 by miR-
743 125a-5p inhibition. *Physiological Genomics* 48, 345-360.
744 Meng, L., Li, M., Gao, Z., Ren, H., Chen, J., Liu, X., Cai, Q., Jiang, L., Ren, X., Yu, Q., *et al.* (2019).
745 Possible role of hsa-miR-194-5p, via regulation of HS3ST2, in the pathogenesis of
746 atopic dermatitis in children. *Eur J Dermatol* 29, 603-613.
747 Mills, C.D., and Ley, K. (2014). M1 and M2 macrophages: The chicken and the egg of immunity.
748 *J Innate Immun* 6, 716-726.
749 Mohammadi, A., Blesso, C.N., Barreto, G.E., Banach, M., Majeed, M., and Sahebkar, A. (2019).
750 Macrophage plasticity, polarization and function in response to curcumin, a diet-
751 derived polyphenol, as an immunomodulatory agent. *J Nutr Biochem* 66, 1-16.
752 Moraes, L.N., Fernandez, G.J., Vechetti-Júnior, I.J., Freire, P.P., Souza, R.W., Villacis, R.A.,
753 Rogatto, S.R., Reis, P.P., Dal-Pai-Silva, M., and Carvalho, R.F. (2017). Integration of
754 miRNA and mRNA expression profiles reveals microRNA-regulated networks during
755 muscle wasting in cardiac cachexia. *Scientific Reports* 7, 1-13.
756 Mueller, P.A., Zhu, L., Tavori, H., Huynh, K., Giunzioni, I., Stafford, J.M., Linton, M.F., and Fazio,
757 S. (2018). Deletion of macrophage low-density lipoprotein receptor-related protein 1
758 (LRP1) accelerates atherosclerosis regression and increases CC chemokine receptor
759 type 7 (CCR7) expression in plaque macrophages. *Circulation* 138, 1850-1863.
760 Mukherjee, R., Singh, D.K., Barman, P.K., Prusty, B.K., Thatoi, P., Tripathy, R., Das, B.K., and
761 Ravindran, B. (2018). A novel polymorphism in nitric oxide synthase interacting
762 protein (NOSIP) modulates nitric oxide synthesis and influences mortality in human
763 sepsis. *BioRxiv*, 038398.

764 Murtaugh, M.P., Arend, W.P., and Davies, P.J. (1984). Induction of tissue transglutaminase in
765 human peripheral blood monocytes. *J Exp Med* *159*, 114-125.

766 Park, Y., Abihssira-García, I.S., Thalmann, S., Wiegertjes, G.F., Barreda, D.R., Olsvik, P.A., and
767 Kiron, V. (2020a). Imaging flow cytometry protocols for examining phagocytosis of
768 microplastics and bioparticles by immune cells of aquatic animals. *Frontiers in*
769 *Immunology* *11*, 203.

770 Park, Y., Zhang, Q., Wiegertjes, G.F., Fernandes, J.M.O., and Kiron, V. (2020b). Adherent
771 intestinal cells from Atlantic salmon show phagocytic ability and express macrophage-
772 specific genes. *Front Cell Dev Biol* *8*, 580848.

773 Paulsen, S.M., Engstad, R.E., and Robertsen, B. (2001). Enhanced lysozyme production in
774 Atlantic salmon (*Salmo salar* L.) macrophages treated with yeast β -glucan and
775 bacterial lipopolysaccharide. *Fish & Shellfish Immunology* *11*, 23-37.

776 Peng, L., Zhang, H., Hao, Y., Xu, F., Yang, J., Zhang, R., Lu, G., Zheng, Z., Cui, M., and Qi, C.-F.
777 (2016). Reprogramming macrophage orientation by microRNA 146b targeting
778 transcription factor IRF5. *EBioMedicine* *14*, 83-96.

779 Pipp, I., Wagner, L., Rössler, K., Budka, H., and Preusser, M. (2007). Secretagogin expression
780 in tumours of the human brain and its coverings. *APMIS* *115*, 319-326.

781 Potere, N., Del Buono, M.G., Mauro, A.G., Abbate, A., and Toldo, S. (2019). Low density
782 lipoprotein receptor-related protein-1 in cardiac inflammation and infarct healing.
783 *Frontiers in Cardiovascular Medicine* *6*, 51.

784 Powell, A.E., Anderson, E.C., Davies, P.S., Silk, A.D., Pelz, C., Impey, S., and Wong, M.H. (2011).
785 Fusion between Intestinal epithelial cells and macrophages in a cancer context results
786 in nuclear reprogramming. *Cancer Research* *71*, 1497-1505.

787 Prieto, J., Eklund, A., and Patarroyo, M. (1994). Regulated expression of integrins and other
788 adhesion molecules during differentiation of monocytes into macrophages. *Cellular*
789 *Immunology* *156*, 191-211.

790 Puleston, D.J., Buck, M.D., Geltink, R.I.K., Kyle, R.L., Caputa, G., O'Sullivan, D., Cameron, A.M.,
791 Castoldi, A., Musa, Y., and Kabat, A.M. (2019). Polyamines and eIF5A hypusination
792 modulate mitochondrial respiration and macrophage activation. *Cell Metabolism* *30*,
793 352-363. e358.

794 Qin, C.-C., Liu, Y.-N., Hu, Y., Yang, Y., and Chen, Z. (2017). Macrophage inflammatory protein-
795 2 as mediator of inflammation in acute liver injury. *World J Gastroenterol* *23*, 3043-
796 3052.

797 Ren, H., Zhang, C., Liu, R., Li, N., Li, X., Xue, H., Guo, Y., Wang, Z., Cui, J., and Ming, L. (2017).
798 Primary cultures of mouse small intestinal epithelial cells using the dissociating
799 enzyme type I collagenase and hyaluronidase. *Brazilian Journal of Medical and*
800 *Biological Research* *50*.

801 Riaz Rajoka, M.S., Jin, M., Haobin, Z., Li, Q., Shao, D., Huang, Q., and Shi, J. (2018). Impact of
802 dietary compounds on cancer-related gut microbiota and microRNA. *Appl Microbiol*
803 *Biotechnol* *102*, 4291-4303.

804 Rieger, A.M., Hanington, P.C., Belosevic, M., and Barreda, D.R. (2014). Control of CSF-1
805 induced inflammation in teleost fish by a soluble form of the CSF-1 receptor. *Fish*
806 *Shellfish Immunol* *41*, 45-51.

807 Rieger, A.M., Konowalchuk, J.D., Havixbeck, J.J., Robbins, J.S., Smith, M.K., Lund, J.M., and
808 Barreda, D.R. (2013). A soluble form of the CSF-1 receptor contributes to the inhibition
809 of inflammation in a teleost fish. *Dev Comp Immunol* *39*, 438-446.

810 Samieni, S., Zhang, Z., and Shively, J.E. (2013). CEACAM-1 negatively regulates G-CSF
811 production by breast tumor associated macrophages that mediate tumor
812 angiogenesis. *International Journal of Cancer* *133*.

813 Shang, G., Mi, Y., Mei, Y., Wang, G., Wang, Y., Li, X., Wang, Y., Li, Y., and Zhao, G. (2018).
814 MicroRNA-192 inhibits the proliferation, migration and invasion of osteosarcoma cells
815 and promotes apoptosis by targeting matrix metalloproteinase-11. *Oncol Lett* *15*,
816 7265-7272.

817 Sheng, Y., Wang, Y., Lu, W., Zhou, Y., Dong, G., Ge, X., Song, Y., and Zhang, Y. (2018). MicroRNA-
818 92a inhibits macrophage antiviral response by targeting retinoic acid inducible gene-
819 I. *Microbiol Immunol* *62*, 585-593.

820 Shiokawa, D., Sato, A., Ohata, H., Mutoh, M., Sekine, S., Kato, M., Shibata, T., Nakagama, H.,
821 and Okamoto, K. (2017). The induction of selected Wnt target genes by Tcf1 mediates
822 generation of tumorigenic colon stem cells. *Cell Reports* *19*, 981-994.

823 Smith, N.C., Christian, S.L., Woldemariam, N.T., Clow, K.A., Rise, M.L., and Andreassen, R.
824 (2020). Characterization of miRNAs in cultured atlantic salmon head kidney
825 monocyte-like and macrophage-like cells. *Int J Mol Sci* *21*, 3989.

826 Smythies, L.E., Sellers, M., Clements, R.H., Mosteller-Barnum, M., Meng, G., Benjamin, W.H.,
827 Orenstein, J.M., and Smith, P.D. (2005). Human intestinal macrophages display
828 profound inflammatory anergy despite avid phagocytic and bacteriocidal activity. *The*
829 *Journal of Clinical Investigation* *115*, 66-75.

830 Soza-Ried, C., Hess, I., Netuschil, N., Schorpp, M., and Boehm, T. (2010). Essential role of *c-*
831 *myb* in definitive hematopoiesis is evolutionarily conserved. *Proceedings of the*
832 *National Academy of Sciences* *107*, 17304.

833 Stella, M.C., Vercelli, A., Repici, M., Follenzi, A., and Comoglio, P.M. (2001). Macrophage
834 stimulating protein is a novel neurotrophic factor. *Molecular Biology of the Cell* *12*,
835 1341-1352.

836 Tan, H.-Y., Wang, N., Li, S., Hong, M., Wang, X., and Feng, Y. (2016). The reactive oxygen
837 species in macrophage polarization: reflecting its dual role in progression and
838 treatment of human diseases. *Oxidative Medicine and Cellular Longevity* *2016*.

839 Tan, L., Liu, L., Jiang, Z., and Hao, X. (2019). Inhibition of microRNA-17-5p reduces the
840 inflammation and lipid accumulation, and up-regulates ATP-binding cassette
841 transporterA1 in atherosclerosis. *J Pharmacol Sci* *139*, 280-288.

842 Turner, J.R. (2009). Intestinal mucosal barrier function in health and disease. *Nature Reviews*
843 *Immunology* *9*, 799-809.

844 Vellozo, N.S., Pereira-Marques, S.T., Cabral-Piccin, M.P., Filardy, A.A., Ribeiro-Gomes, F.L.,
845 Rigoni, T.S., DosReis, G.A., and Lopes, M.F. (2017). All-trans retinoic acid promotes an
846 M1- to M2-phenotype shift and inhibits macrophage-mediated immunity to
847 *Leishmania major*. *Front Immunol* *8*, 1560.

848 Velu, C.S., Baktula, A.M., and Grimes, H.L. (2009). Gfi1 regulates miR-21 and miR-196b to
849 control myelopoiesis. *Blood* *113*, 4720-4728.

850 Viennois, E., Chassaing, B., Tahsin, A., Pujada, A., Wang, L., Gewirtz, A.T., and Merlin, D. (2019).
851 Host-derived fecal microRNAs can indicate gut microbiota healthiness and ability to
852 induce inflammation. *Theranostics* *9*, 4542-4557.

853 Vighi, G., Marcucci, F., Sensi, L., Di Cara, G., and Frati, F. (2008). Allergy and the gastrointestinal
854 system. *Clin Exp Immunol* *153 Suppl 1*, 3-6.

855 Wan, S., and Sun, H. (2019). Glucagon-like peptide-1 modulates RAW264.7 macrophage
856 polarization by interfering with the JNK/STAT3 signaling pathway. *Exp Ther Med* *17*,
857 3573-3579.

858 Wang, D., Wang, W., Lin, W., Yang, W., Zhang, P., Chen, M., Ding, D., Liu, C., Zheng, J., and Ling,
859 W. (2018a). Apoptotic cell induction of miR-10b in macrophages contributes to
860 advanced atherosclerosis progression in ApoE^{-/-} mice. *Cardiovascular Research* *114*,
861 1794-1805.

862 Wang, K., Lai, C., Gu, H., Zhao, L., Xia, M., Yang, P., and Wang, X. (2017). miR-194 inhibits innate
863 antiviral immunity by targeting FGF2 in influenza H1N1 virus infection. *Front Microbiol*
864 *8*, 2187.

865 Wang, W., Liu, Y., Guo, J., He, H., Mi, X., Chen, C., Xie, J., Wang, S., Wu, P., and Cao, F. (2018b).
866 miR-100 maintains phenotype of tumor-associated macrophages by targeting mTOR
867 to promote tumor metastasis via Stat5a/IL-1ra pathway in mouse breast cancer.
868 *Oncogenesis* *7*, 1-17.

869 Wang, Z., Xu, L., Hu, Y., Huang, Y., Zhang, Y., Zheng, X., Wang, S., Wang, Y., Yu, Y., and Zhang,
870 M. (2016). miRNA let-7b modulates macrophage polarization and enhances tumor-
871 associated macrophages to promote angiogenesis and mobility in prostate cancer.
872 *Scientific Reports* *6*, 25602.

873 Wentzel, A.S., Janssen, J.J.E., de Boer, V.C.J., van Veen, W.G., Forlenza, M., and Wiegertjes,
874 G.F. (2020a). Fish macrophages show distinct metabolic signatures upon polarization.
875 *Front Immunol* *11*, 152.

876 Wentzel, A.S., Petit, J., van Veen, W.G., Fink, I.R., Scheer, M.H., Piazzon, M.C., Forlenza, M.,
877 Spaik, H.P., and Wiegertjes, G.F. (2020b). Transcriptome sequencing supports a
878 conservation of macrophage polarization in fish. *Sci Rep* *10*, 13470.

879 Wickham, H. (2016). *ggplot2: Elegant graphics for data analysis*. Springer International
880 Publishing New York, p.260.

881 Wiegertjes, G.F., Wentzel, A.S., Spaik, H.P., Elks, P.M., and Fink, I.R. (2016). Polarization of
882 immune responses in fish: The 'macrophages first' point of view. *Mol Immunol* *69*,
883 146-156.

884 Woldemariam, N.T., Agafonov, O., Høyheim, B., Houston, R.D., Taggart, J.B., and Andreassen,
885 R. (2019). Expanding the miRNA repertoire in Atlantic salmon; Discovery of isomiRs
886 and miRNAs highly expressed in different tissues and developmental stages. *Cells* *8*,
887 42.

888 Woo, H.-H., László, C.F., Greco, S., and Chambers, S.K. (2012). Regulation of colony stimulating
889 factor-1 expression and ovarian cancer cell behavior in vitro by miR-128 and miR-152.
890 *Mol Cancer* *11*, 58.

891 Wu, K., Yuan, Y., Yu, H., Dai, X., Wang, S., Sun, Z., Wang, F., Fei, H., Lin, Q., Jiang, H., *et al.*
892 (2020). The gut microbial metabolite trimethylamine N-oxide aggravates GVHD by
893 inducing M1 macrophage polarization in mice. *Blood* *136*, 501-515.

894 Xiao, J., Tang, J., Chen, Q., Tang, D., Liu, M., Luo, M., Wang, Y., Wang, J., Zhao, Z., Tang, C., *et al.*
895 (2015). miR-429 regulates alveolar macrophage inflammatory cytokine production
896 and is involved in LPS-induced acute lung injury. *Biochem J* *471*, 281-291.

897 Yuan, Y., Lin, D., Feng, L., Huang, M., Yan, H., Li, Y., Chen, Y., Lin, B., Ma, Y., and Ye, Z. (2018).
898 Upregulation of miR-196b-5p attenuates BCG uptake via targeting SOCS3 and
899 activating STAT3 in macrophages from patients with long-term cigarette smoking-
900 related active pulmonary tuberculosis. *Journal of Translational Medicine* *16*, 284.

901 Zhang, Q., Kopp, M., Babiak, I., and Fernandes, J.M. (2018). Low incubation temperature
902 during early development negatively affects survival and related innate immune
903 processes in zebrafish larvae exposed to lipopolysaccharide. *Scientific Reports* 8, 1-14.
904 Zhang, X., Guo, L., Collage, R.D., Stripay, J.L., Tsung, A., Lee, J.S., and Rosengart, M.R. (2011).
905 Calcium/calmodulin-dependent protein kinase (CaMK) I α mediates the macrophage
906 inflammatory response to sepsis. *Journal of Leukocyte Biology* 90, 249-261.
907 Zhang, Y., Li, X., Wang, C., Zhang, M., Yang, H., and Lv, K. (2020). lncRNA AK085865 promotes
908 macrophage M2 polarization in CVB3-induced VM by regulating ILF2-ILF3 complex-
909 mediated miRNA-192 biogenesis. *Molecular Therapy - Nucleic Acids* 21, 441-451.
910 Zhang, Y., Olson, R.M., and Brown, C.R. (2017a). Macrophage LTB(4) drives efficient
911 phagocytosis of *Borrelia burgdorferi* via BLT1 or BLT2. *J Lipid Res* 58, 494-503.
912 Zhang, Y., Zhang, M., Zhong, M., Suo, Q., and Lv, K. (2013). Expression profiles of miRNAs in
913 polarized macrophages. *Int J Mol Med* 31, 797-802.
914 Zhang, Z., Lei, B., Wu, H., Zhang, X., and Zheng, N. (2017b). Tumor suppressive role of miR-
915 194-5p in glioblastoma multiforme. *Molecular Medicine Reports* 16, 9317-9322.
916 Zhou, H., Xiao, J., Wu, N., Liu, C., Xu, J., Liu, F., and Wu, L. (2015). MicroRNA-223 regulates the
917 differentiation and function of intestinal dendritic cells and macrophages by targeting
918 C/EBP β . *Cell Reports* 13, 1149-1160.
919
920

921 **Table 1.** Top thirty macrophage-related genes that are equally abundant in adherent
 922 cells from distal intestine and head kidney.

Gene ID	Symbol	Description	BaseMean ¹	Log ₂ FC ²
LOC106560288	<i>serbp1a</i>	Plasminogen activator inhibitor 1 RNA-binding protein-like	4829	0.004
LOC100136528	<i>ran1</i>	Ran protein	3237	-0.004
LOC100194661	<i>cnbp</i>	CCHC-type zinc finger, nucleic acid binding protein	2012	0.003
LOC106611171	<i>calm1</i>	Calmodulin 1	1361	-0.002
LOC106606196	<i>slc16a3</i>	Monocarboxylate transporter 4-like	1345	-0.001
LOC100196549	<i>romo1</i>	Reactive oxygen species modulator 1	1034	0.000
LOC106566174	<i>sp1</i>	Sp1 transcription factor	845	0.003
LOC100194901	<i>rab6c</i>	Ras-related protein Rab-6C	623	0.001
LOC106570994	<i>rab10</i>	Ras-related protein Rab-10 pseudogene	613	0.002
LOC106572095	<i>ccn2</i>	Cyclin-I-like	549	0.003
LOC106608187	<i>zfan3</i>	AN1-type zinc finger protein 3-like	540	-0.001
LOC106580924	<i>sorl1</i>	Sortilin related receptor 1	510	-0.002
LOC106589503	<i>rai1</i>	Retinoic acid-induced protein 1-like	487	-0.002
LOC106576790	<i>znf518a</i>	Zinc finger protein 518A-like	396	0.002
LOC106575550	<i>ddx3x</i>	ATP-dependent RNA helicase DDX3X-like	353	0.002
LOC106582756	<i>mst1ra</i>	Macrophage-stimulating protein receptor-like	349	0.001
LOC106612069	<i>dpf2l</i>	Zinc finger protein ubi-d4-like	332	-0.001
LOC100380559	<i>myef2</i>	Myelin expression factor 2	323	-0.002
LOC106563587	<i>prdx4</i>	Peroxiredoxin-4-like	276	-0.002
LOC106589519	<i>znf420</i>	Zinc finger protein 420-like	248	0.002
LOC106575781	<i>tuba8l2</i>	Tubulin alpha chain-like	212	0.004
LOC106605589	<i>ceacam18</i>	Carcinoembryonic antigen-related cell adhesion molecule 18-like	157	0.000
LOC106613791	<i>cks2</i>	Cyclin-dependent kinases regulatory subunit 1-like	127	-0.001
LOC100195338	<i>ctl2</i>	Choline transporter-like protein 2	125	-0.002
LOC100286477	<i>myo1e</i>	Myosin IE	59	0.004
LOC100195309	<i>zn214</i>	Zinc finger protein 214	58	-0.003
LOC106575882	<i>znf146</i>	Zinc finger protein OZF-like	52	0.004
LOC106595099	<i>zcwpw2</i>	Zinc finger CW-type PWWP domain protein 2-like	35	0.001
LOC106577531	<i>bcam</i>	Basal cell adhesion molecule-like	20	0.004
LOC106573576	<i>pip5k1c</i>	Phosphatidylinositol 4-phosphate 5-kinase type-1 gamma-like	18	-0.001

923 ¹ BaseMean = average of the normalized read counts in all libraries.

924 ² Log₂ fold change between AIC and AKC.

925

926 **Table 2.** Top thirty equally abundant macrophage-related miRNAs in adherent cells
 927 from distal intestine and head kidney and their potential target mRNAs.

miRNA	BaseMean ¹	LOG ₂ FC ²	Target number
ssa-let-7b-5p	711968	0.905	1
ssa-miR-150-5p	81792	-0.56	2
ssa-miR-30b-5p	59008	0.448	0
ssa-let-7j-5p	52386	-0.275	0
ssa-let-7e-5p	38601	0.16	0
ssa-miR-462a-5p	34375	-0.5	0
ssa-let-7g-5p	31523	0.491	0
ssa-let-7c-5p	14848	-0.613	0
ssa-let-7h-5p	13739	0.384	1
ssa-miR-128-3p	8917	0.082	1
ssa-miR-125b-5p	8346	-0.094	2
ssa-miR-16a-5p	6581	-0.909	0
ssa-let-7f-5p	5489	0.376	0
ssa-let-7i-5p	3941	-0.192	1
ssa-miR-15a-5p	3335	-0.429	0
ssa-miR-26a-5p	3200	-0.137	1
ssa-miR-146a-5p	1633	-0.71	0
ssa-let-7d-5p	1621	0.097	1
ssa-miR-129-5p	1036	0.771	2
ssa-miR-139-5p	604	-0.788	7
ssa-miR-103-3p	555	0.493	3
ssa-miR-24b-3p	512	0.847	0
ssa-miR-181b-5p	395	-0.906	5
ssa-miR-128-3-5p	364	-0.542	3
ssa-miR-33b-3p	179	0.883	1
ssa-miR-16c-5p	168	0.648	0
ssa-miR-29a-5p	127	-0.016	1
ssa-miR-462a-3p	117	-0.663	6
ssa-miR-455-3p	71	-0.159	5
ssa-miR-30a-3-3p	64	-0.703	17

928 ¹ BaseMean = average of the normalized read counts in all libraries.

929 ² Log₂ fold change between AIC and AKC

930

931

932 **Table 3.** Top twenty upregulated genes in adherent cells from distal intestine compared
 933 to those from head kidney.

Gene ID	Symbol	Description	Log ₂ FC ¹
LOC106578701	<i>adcyap1</i>	Glucagon family neuropeptides-like	13.9
LOC106576762	<i>epcam</i>	Epithelial cell adhesion molecule	13.5
LOC106574454	<i>gcga1</i>	Glucagon-1	13.4
LOC106579860	<i>stc1</i>	Stanniocalcin 1	13.2
LOC106569925	<i>segn</i>	Secretagogen-like	13.0
LOC100194779	<i>ndf1</i>	Neurogenic differentiation factor 1	12.9
LOC106583415	<i>pcsk1</i>	Neuroendocrine convertase 1-like	12.9
LOC106580802	<i>cylc1</i>	Cylicin-1-like	12.9
LOC106609020	<i>tm4sf4</i>	Transmembrane 4 L6 family member 4-like	12.8
LOC106581833	<i>fev</i>	Protein FEV	12.7
LOC100286464	<i>insl5a</i>	Insulin-like 5a	12.5
LOC106563244	<i>pktspi</i>	Putative Kunitz-type serine protease inhibitor	12.5
LOC100195566	<i>t4s1</i>	Transmembrane 4 L6 family member 1	12.4
LOC106561864	<i>ktspik1l</i>	Kunitz-type serine protease inhibitor Kunitz-1-like	12.4
LOC106588240	<i>ffar2</i>	Free fatty acid receptor 2-like	12.3
LOC106575340	<i>gcga2</i>	Glucagon-2	12.2
LOC106588285	<i>mtss1</i>	Metastasis suppressor protein 1 isoform X5	12.2
LOC106608662	<i>gpr78b</i>	G-protein coupled receptor 26-like	12.2
LOC106598496	<i>rlnl</i>	Relaxin-like	12.2
LOC106562528	<i>scg3</i>	Secretogranin III	12.2

934 ¹Log₂ fold change between AIC and AKC

935

936

937 **Table 4.** Top twenty downregulated genes in adherent cells from distal intestine
 938 compared to head kidney adherent cells.

Gene ID	Symbol	Description	Log2FC ¹
LOC106613121	<i>acsl3l</i>	Long-chain-fatty-acid--CoA ligase 3-like	-10.8
LOC106581495	<i>p2ry12l</i>	P2Y purinoceptor 12-like	-8.9
LOC106572147	<i>wfdc2l</i>	WAP four-disulfide core domain protein 2-like	-8.5
LOC106572149	<i>wfdc18l</i>	WAP four-disulfide core domain protein 18-like	-8.4
LOC106592337	<i>ropa70l</i>	Replication protein A 70 kDa DNA-binding subunit-like	-8.2
LOC100136492	<i>star</i>	Steroidogenic acute regulatory protein, mitochondrial	-8.0
LOC106606380	<i>cd147l</i>	Basigin-like	-7.5
LOC106605190	<i>siglec5l</i>	Sialic acid-binding Ig-like lectin 5	-7.4
LOC106562884	<i>ier5l</i>	Immediate early response gene 5-like protein	-7.4
LOC106577929	<i>mrc2l</i>	C-type mannose receptor 2-like	-7.3
LOC106587084	<i>tspan4l</i>	Tetraspanin-4-like	-7.3
LOC106587258	<i>cdh15l</i>	Cadherin-15-like	-7.1
LOC106583235	<i>cyp1b1l</i>	Cytochrome P450 1B1 pseudogene	-7.0
LOC106565670	<i>gnal2l</i>	Guanine nucleotide-binding protein G(t) subunit alpha-2-like	-7.0
LOC100196393	<i>mip2a</i>	Macrophage inflammatory protein 2-alpha	-6.9
LOC106610444	<i>cllec4fl</i>	C-type lectin domain family 4 member F-like	-6.8
LOC106568001	<i>ropgap7l</i>	Rho GTPase-activating protein 7-like	-6.8
LOC106582339	<i>tsg6l</i>	Tumor necrosis factor-inducible gene 6 protein-like	-6.8
LOC106582554	<i>irgc</i>	Interferon-inducible GTPase 5-like	-6.7
LOC106587608	<i>ltb4rl</i>	Leukotriene B4 receptor 1-like	-6.7

939 ¹Log2 fold change between AIC and AKC

940

941 **Table 5.** Top twenty upregulated miRNAs in adherent cells from distal intestine
 942 compared to those from head kidney and the number of their potential target mRNAs.

miRNA	BaseMean ¹	log2FC ²	Adjusted p-value	Target number
ssa-miR-192b-5p	5282	13.2	<0.001	0
ssa-miR-196b-5p	517	13.2	<0.001	0
ssa-miR-2188-5p	243	12.0	<0.001	1
ssa-miR-429-3p	186	11.6	<0.001	0
ssa-miR-375-3p	998576	11.5	<0.001	0
ssa-miR-194a-3p	106	10.9	<0.001	6
ssa-miR-192a-5p	9921	9.4	<0.001	0
ssa-miR-196a-5p	3036	9.0	<0.001	0
ssa-miR-194a-5p	2227	7.7	<0.001	0
ssa-miR-10d-5p	1788	3.9	<0.001	0
ssa-miR-210-5p	496	3.8	0.0170	1
ssa-miR-10b-5p	6108	3.5	<0.001	0
ssa-miR-7a-5p	792	3.5	0.0297	2
ssa-miR-1338-3p	1663	3.3	0.0045	0
ssa-miR-125a-5p	21846	2.4	<0.001	0
ssa-miR-1338-5p	607	2.3	0.0105	2
ssa-miR-100a-5p	13148	2.1	<0.001	0
ssa-miR-23a-3p	1755	1.4	0.0079	1
ssa-miR-23b-3p	10223	1.4	0.0013	0
ssa-let-7a-5p	2941685	1.0	0.0063	1

943 ¹ BaseMean = average of the normalized read counts in all libraries.

944 ² Log2 fold change between AIC and AKC

945

946 **Table 6.** Top seventeen downregulated miRNAs in adherent cells from distal intestine
 947 compared to head kidney adherent cells, and the number of their potential target
 948 mRNAs.

miRNA	BaseMean ¹	log ₂ FC ²	Adjusted p-value	Target number
ssa-miR-19d-5p	395	-9.7	<0.001	4
ssa-miR-17-5p	53	-8.4	0.0011	0
ssa-miR-92a-5p	944	-4.3	0.0045	2
ssa-miR-93a-5p	133	-4.0	0.0248	2
ssa-miR-92a-4-5p	401	-3.7	0.0379	15
ssa-miR-92a-3-5p	627	-3.5	0.0021	28
ssa-miR-155-5p	6230	-3.4	<0.001	0
ssa-miR-128-1-5p	854	-2.8	0.0088	12
ssa-miR-21a-5p	18442	-2.6	<0.001	0
ssa-miR-181c-5p	10845	-1.7	<0.001	1
ssa-miR-462b-5p	19706	-1.4	<0.001	0
ssa-miR-21b-5p	231373	-1.3	0.0345	0
ssa-miR-92a-3p	1068097	-1.2	<0.001	0
ssa-miR-731-5p	37193	-1.2	0.0335	1
ssa-miR-15c-5p	13391	-1.1	0.0116	1
ssa-miR-25-3p	2910	-1.1	0.0045	6
ssa-miR-181a-5p	104721	-1.0	0.0144	0

949 ¹ BaseMean = average of the normalized read counts in all libraries.

950 ² Log₂ fold change between AIC and AKC

951

952

953

954

955 **Table 7.** Negative correlations between differentially expressed miRNAs and their
 956 potential target mRNAs among DEGs.

MicroRNA	Target gene	Symbol	Description	Correlation coefficient (r)	P value
AIC—downregulated miRNA & upregulated target gene					
ssa-miR-181c-5p	LOC106612812	<i>p2rx8</i>	P2X purinoceptor 5-like	-0.8927	<0.001
ssa-miR-19d-5p	LOC106607644	<i>EIF5</i>	Eukaryotic translation initiation factor 5-like	-0.7989	0.0018
ssa-miR-128-1-5p	LOC106571118	<i>LBH</i>	Protein LBH-like	-0.7321	0.0067
ssa-miR-92a-3-5p	LOC106560599	<i>ENC3</i>	Ectodermal-neural cortex 3	-0.6739	0.0162
ssa-miR-92a-3-5p	LOC106589523	<i>eef2k</i>	Eukaryotic elongation factor 2 kinase-like	-0.6015	0.0385
ssa-miR-128-1-5p	LOC106574722	<i>CU051</i>	Small integral membrane protein 11-like	-0.5774	0.0492
ssa-miR-92a-4-5p	LOC106611553	<i>QDPR</i>	Dihydropteridine reductase-like	-0.5728	0.0515
ssa-miR-93a-5p	LOC106576270	<i>SPIC</i>	Transcription factor Spi-C-like	-0.5566	0.0601
ssa-miR-92a-3-5p	LOC106603902	<i>FAM53C</i>	Family with sequence similarity 53 member C	-0.5525	0.0624
ssa-miR-92a-3-5p	LOC106612663	<i>FAM83B</i>	Protein FAM83B-like	-0.5459	0.0663
ssa-miR-92a-4-5p	LOC106562770	<i>CALL4</i>	Calmodulin-like protein 4	-0.4746	0.119
ssa-miR-92a-3-5p	LOC106607421	<i>PBX4</i>	Pre-B-cell leukemia transcription factor 1-like	-0.4538	0.1384
ssa-miR-92a-4-5p	LOC106601006	<i>FBXL20</i>	F-box/LRR-repeat protein 20	-0.3896	0.2105
ssa-miR-92a-4-5p	LOC106572667	<i>LMBR1</i>	Limb region 1 homolog-like protein	-0.3423	0.2761
AIC—upregulated miRNA & downregulated target gene					
ssa-let-7a-5p	LOC106565466	<i>LRP1AA</i>	Low-density lipoprotein receptor-related protein 1-like	-0.7014	0.0110

957
 958

959 **Figure Legends:**

960

961 **Figure 1. Comparison between mRNA transcriptomes of the adherent cells from**
962 **intestine and those from head kidney of Atlantic salmon.** (A) Principal component
963 analysis of mRNA transcriptome data, (B) Venn diagram showing common and unique
964 genes and (C) heatmap of DEGs ($|\text{fold change}| \geq 2$ and adjusted p value < 0.05 ; $n = 6$).
965 AIC: Adherent cells from the distal intestine, AKC: Adherent cells from the head kidney.

966

967 **Figure 2. Comparison between miRNA transcriptomes of the adherent cells from**
968 **intestine and those from head kidney of Atlantic salmon.** (A) Principal component
969 analysis of miRNA transcriptome, (B) Venn diagram showing common and unique
970 genes and (C) heatmap of DE miRNAs ($|\text{fold change}| \geq 2$ and adjusted p value < 0.05 ;
971 $n = 6$). AIC: Adherent cells from the distal intestine, AKC: Adherent cells from the head
972 kidney.

973

974 **Figure 3. The expression of genes linked to fish macrophage polarization between**
975 **AIC and AKC.** Employing the normalized read counts from DESeq2 analyses, the
976 expression levels of the potential gene markers for fish M1- (A) and M2-macrophages
977 (B) were compared to understand the differences between AIC and AKC. Statistically
978 significant differences ($p < 0.05$) are indicated using asterisks. Boxplots show the
979 median, minimum and maximum values in the data ($n = 6$). AIC: Adherent cells from
980 the distal intestine; AKC: Adherent cells from the head kidney; *nosip*: nitric oxide
981 synthase interacting protein; *nostrin*: nitric oxide synthase trafficking; *saal1*: serum
982 amyloid A-like 1; *tgm2*: transglutaminase 2, like; *arg2*: arginase 2.

983

984 **Figure 4. Negative correlation between miRNAs in AIC and AKC and their target**
985 **mRNAs.** Correlation of (A) ssa-miR-19d-5p with *eif5*, (B) ssa-miR-92a-3-5p with *enc3*,
986 (C) ssa-miR-128-1-5p with *lbh*, (D) ssa-miR-181c-5p with *p2rx8* and (E) ssa-let-7a-5p
987 with *lrp1aa*. Negative correlations between them were determined with the following
988 three criteria: (1) normality of the data and homoscedasticity of residuals, (2)
989 correlation coefficient $r < 0$ and (3) p-value < 0.05 . AIC: Adherent cells from the distal
990 intestine; AKC: Adherent cells from the head kidney; *eif*: eukaryotic translation factor
991 5-like; *enc3*: ectodermal-neural cortex 3; *lbh*: protein LBH-like; *p2rx8*: P2X purinoceptor
992 5-like; *lrplaa*: low-density lipoprotein receptor-related protein 1-like.

993

994

995 **Supplementary Table and Figure Legends:**

996

997 **Supplementary Table 1.** Details of raw, clean and mapped reads in microRNA dataset.

998

999 **Supplementary Figure 1.** Workflow of the bioinformatic analysis of mRNA and small
1000 RNA sequencing datasets.

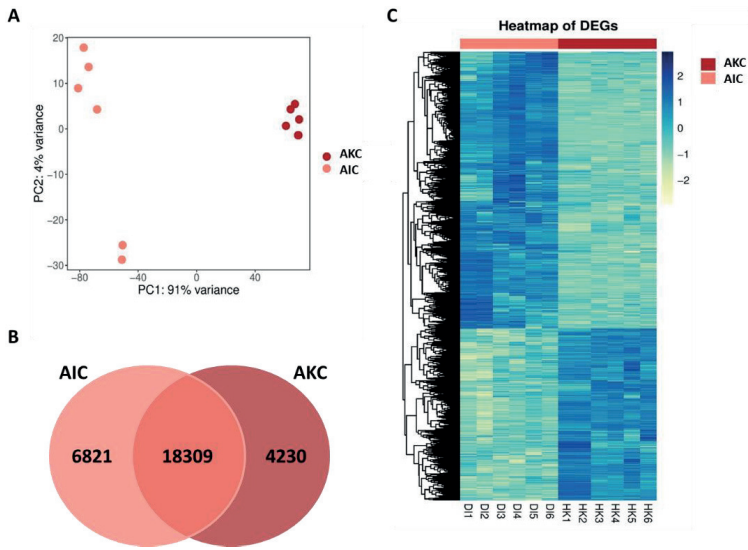
1001

1002 **Supplementary Figure 2.** Dispersion estimates (A) and minus over average expression
1003 (B) of the mRNA-Seq dataset. AIC: Adherent cells from the distal intestine, AKC:
1004 Adherent cells from the head kidney.

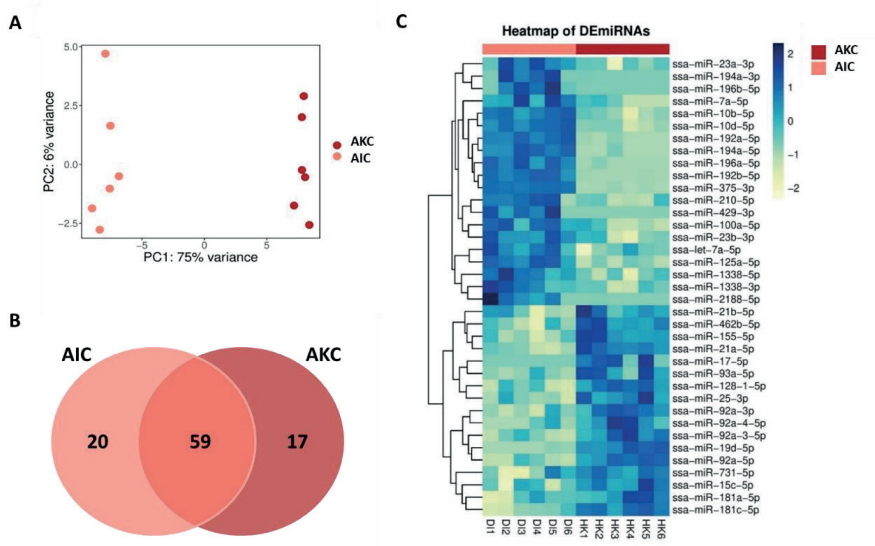
1005

1006 **Supplementary Figure 3.** Dispersion estimates (A) and minus over average expression
1007 (B) of the small RNA-Seq dataset. AIC: Adherent cells from the distal intestine, AKC:
1008 Adherent cells from the head kidney.

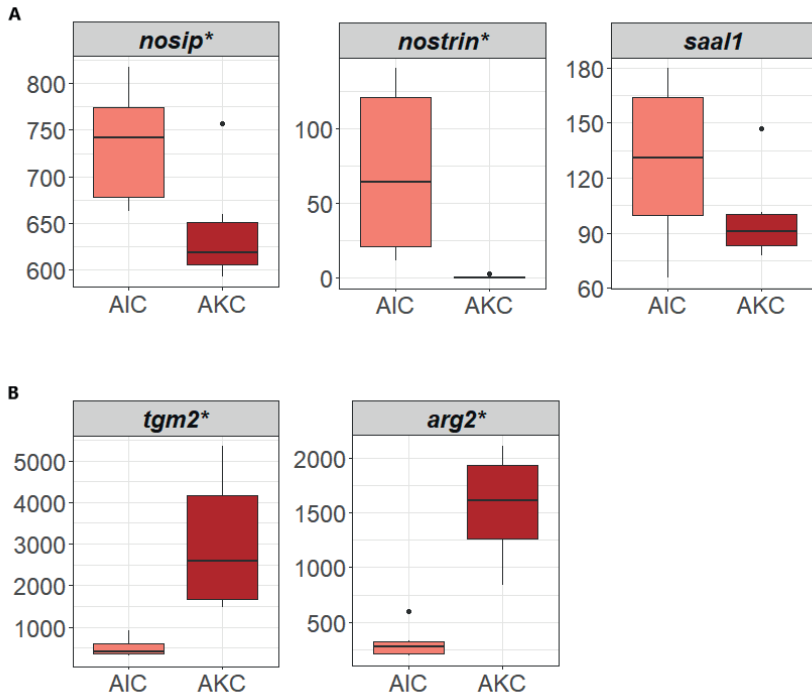
1009



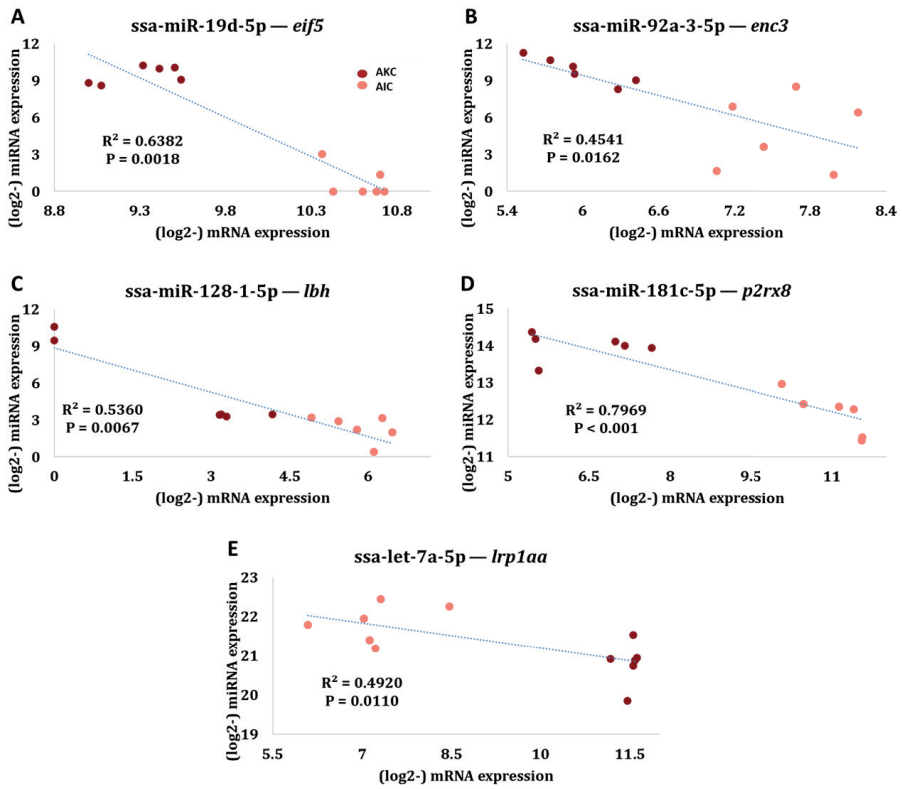
1010
 1011 **Figure 1.**
 1012
 1013
 1014
 1015



1016
 1017 **Figure 2.**



1018
1019 **Figure 3.**
1020



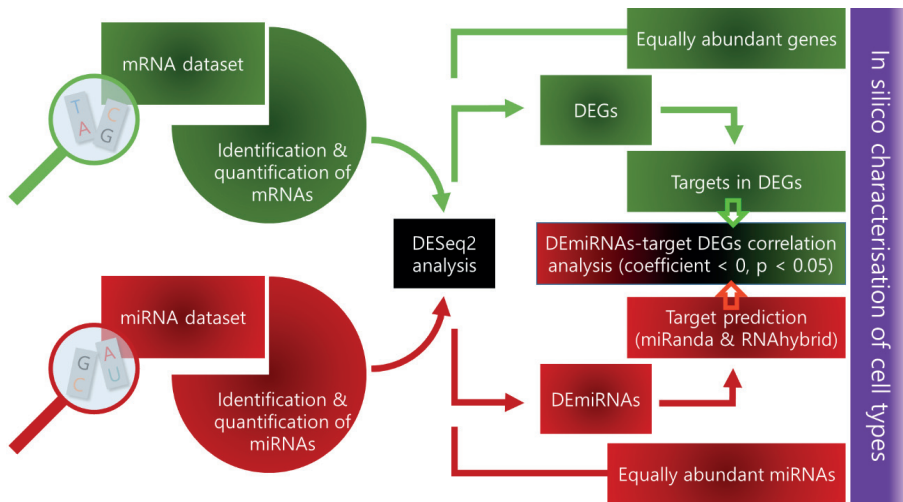
1021
 1022 **Figure 4.**
 1023

1024 **Supplementary Table 1.** Details of raw, clean and mapped reads in microRNA dataset.

Groups*	Sample codes	Raw reads	Clean reads	Mapped reads	Mapped %
AIC	AIC1	26608890	21463160	3726222	18.8%
AIC	AIC2	27535079	23957743	5263643	24.3%
AIC	AIC3	33968889	29440202	6884530	26.4%
AIC	AIC4	39962327	35165417	11407860	34.1%
AIC	AIC5	33239412	24700980	4545988	19.3%
AIC	AIC6	27344360	20106792	4089693	21.5%
AKC	AKC1	36439656	31870692	15934581	53.9%
AKC	AKC2	29458328	25088829	10204611	44.5%
AKC	AKC3	37069631	32441338	11422923	38.9%
AKC	AKC4	35144755	28290815	5465346	23.3%
AKC	AKC5	28278201	21026958	7567940	37.0%
AKC	AKC6	35631141	29604234	11709694	41.6%

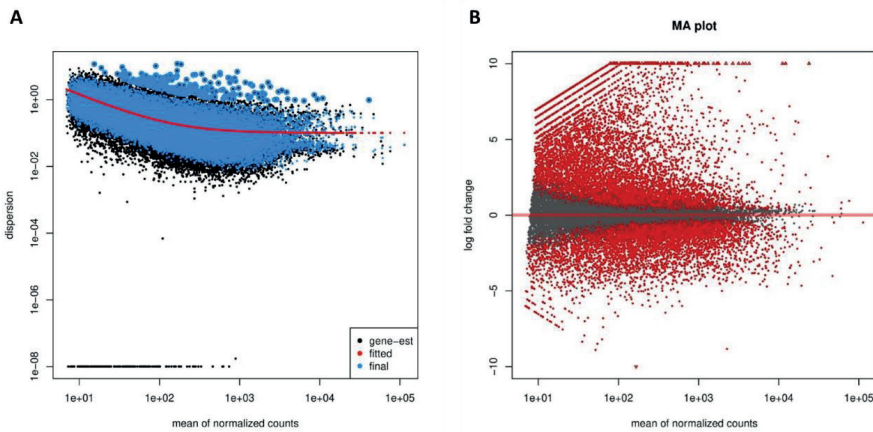
1025 * AIC: Adherent cells from distal intestine, AKC: Adherent cells from head kidney.

1026



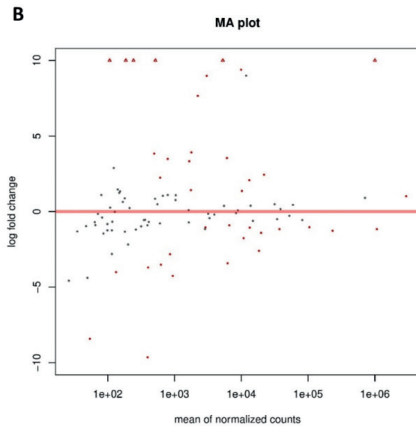
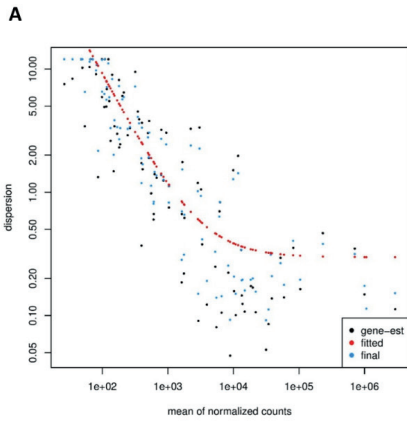
1027
1028 **Supplementary Figure 1.**

1029
1030
1031



1032
1033 **Supplementary Figure 2.**

1034



1035
1036
1037

Supplementary Figure 3.

Paper IV

This is an open-access article, reproduced and distributed under the terms of the Creative Commons Attribution License (CC BY)



Intestinal Transcriptome Analysis Reveals Soy Derivative-Linked Changes in Atlantic Salmon

Viswanath Kiron^{1*}, Youngjin Park¹, Prabhugouda Siriypagouda¹, Dalia Dahle¹, Ghana K. Vasanth¹, Jorge Dias², Jorge M. O. Fernandes¹, Mette Sorensen¹ and Viviane Verlhac Trichet^{3*}

¹ Faculty of Biosciences and Aquaculture, Nord University, Bodø, Norway, ² SPAROS Lda., Olhão, Portugal,

³ DSM Nutritional Products, Global Innovation, Kaiseraugst, Switzerland

OPEN ACCESS

Edited by:

Min Wan,
Ocean University of China, China

Reviewed by:

Javier Santander,
Memorial University of Newfoundland,
Canada
M. Carla Piazzon,
Torre de la Sal Aquaculture Institute
(IATS), Spain

*Correspondence:

Viswanath Kiron
kiron.viswanath@nord.no
Viviane Verlhac Trichet
v.verlhac@me.com

Specialty section:

This article was submitted to
Comparative Immunology,
a section of the journal
Frontiers in Immunology

Received: 19 August 2020

Accepted: 23 October 2020

Published: 11 December 2020

Citation:

Kiron V, Park Y, Siriypagouda P,
Dahle D, Vasanth GK, Dias J,
Fernandes JMO, Sorensen M and
Trichet VV (2020) Intestinal
Transcriptome Analysis
Reveals Soy Derivative-Linked
Changes in Atlantic Salmon.
Front. Immunol. 11:596514.
doi: 10.3389/fimmu.2020.596514

Intestinal inflammation in farmed fish is a non-infectious disease that deserves attention because it is a major issue linked to carnivorous fishes. The current norm is to formulate feeds based on plant-derived substances, and the ingredients that have antinutritional factors are known to cause intestinal inflammation in fishes such as Atlantic salmon. Hence, we studied inflammatory responses in the distal intestine of Atlantic salmon that received a feed rich in soybean derivatives, employing histology, transcriptomic and flow cytometry techniques. The fish fed on soy products had altered intestinal morphology as well as upregulated inflammation-associated genes and aberrated ion transport-linked genes. The enriched pathways for the upregulated genes were among others taurine and hypotaurine metabolism, drug metabolism—cytochrome P450 and steroid biosynthesis. The enriched gene ontology terms belonged to transmembrane transporter- and channel-activities. Furthermore, soybean products altered the immune cell counts; lymphocyte-like cell populations were significantly higher in the whole blood of fish fed soy products than those of control fish. Interestingly, the transcriptome of the head kidney did not reveal any differential gene expression, unlike the observations in the distal intestine. The present study demonstrated that soybean derivatives could evoke marked changes in intestinal transport mechanisms and metabolic pathways, and these responses are likely to have a significant impact on the intestine of Atlantic salmon. Hence, soybean-induced enteritis in Atlantic salmon is an ideal model to investigate the inflammatory responses at the cellular and molecular levels.

Keywords: aquafeed, *Salmo salar*, soy saponin, intestinal inflammation, flow cytometry

INTRODUCTION

The quality of high-value farmed fishes such as Atlantic salmon (*Salmo salar*) depends to a great extent on the ingredients in their feeds. Furthermore, the increase in the demand for farmed salmon necessitates intensive farming and the adoption of sustainable feed ingredients. Awareness about sustainability and limited availability of finite marine sources has led to the replacement of fishmeal and fish oil in aquafeeds with plant derivatives. The current norm is to incorporate considerable

amounts of plant-derived components—proteins from pea, soybean, horse beans, oil from rapeseed, starch and gluten from wheat and maize gluten—in aquafeeds (1). However, carnivorous fishes are known to develop intestinal inflammation, e.g. when they consume high levels of terrestrial plant components such as the products from soybean. This undesirable health condition is mainly caused by antinutritional factors in soybean such as soyasaponin, β -conglycinin and glycinin (2–4).

Feeding fish with high levels of full-fat soybean products or low levels of the soybean meal with other legumes is known to not only affect their growth and nutrient utilization but also can disturb the integrity of the distal intestine. Plant-derived ingredients may shift the intestinal microbial community composition (5, 6), which in turn can affect the overall intestinal health, including immunity (7). Inflammation is the first sign of intolerance to dietary components, and fishes that develop the non-infectious disease will have widened lamina propria with many inflammatory cells, less absorptive vacuoles, and shortened brush border microvilli in their distal intestine (4). Fish with inflamed distal intestine will be characterized by poor nutrient digestibility and disturbances in transcellular water transport, especially when their feeds contain >30% soybean meal (8–10). Furthermore, the combination of soybean (even defatted meal) and other legumes can affect the metabolism and gut functions in Atlantic salmon; aberrations in epithelial barrier and major transcriptome changes are already reported (11–13). Studies that employed other fish species have also indicated the adverse effects of soybean meal or soy saponins on growth, nutrient utilization, antioxidant status, and intestinal morphology (14, 15). Thus, it is evident that plant-derived ingredients with antinutritional factors can affect the health of farmed fish, leading to undesirable fish welfare issues. Although the aforementioned studies have described soy-related inflammation in Atlantic salmon, it is imperative to further understand the molecular changes in the intestine of fish that develop intestinal inflammation. Identification of appropriate markers of inflammation would not only enable effective screening of new feed ingredients, but also enhance our understanding of the processes that are affected during inflammation in a lower vertebrate.

We employed a well-studied fish model, Atlantic salmon, to examine the dietary soy products-linked disturbances in the intestine. This study describes the changes in micromorphology, transcriptome of the distal intestine, and whole blood cells in the inflammation (SO) group compared to the control (CO) group. The novelty of the current study lies in the adoption of RNA-Seq to clearly delineate the molecular changes evoked during inflammation.

MATERIALS AND METHODS

Experimental Design

In this study, we examined the intestinal transcriptome of a carnivorous fish that developed inflammation. For this, Atlantic salmon post-smolts procured from a local commercial producer (Sundsford Smolt, Nygårdsoen, Norway) were maintained at the Research Station of Nord University, Bodø, Norway, for 4

months. For the experiment, 120 fish (128.66 ± 13.29 g; mean \pm SD) were randomly distributed to replicate tanks of the two study groups, i.e. CO and SO groups. During a 2-week acclimation period, all the fish were fed a commercial feed (Ewos AS, Bergen, Norway). The 800 L tanks were part of a flow-through seawater system at the Research Station. Water from a depth of 250 m in Saltenfjorden was pumped, filtered, and aerated, and then used for rearing the fish. The water flow rate was maintained at 1,000 L per h, and the average temperature and salinity of the rearing water were 7.6°C and 34 g L⁻¹, respectively. The dissolved oxygen saturation values, measured at the water outlet of the tanks was in the range 87–92%, and throughout the experimental period, we employed a 24-h light photoperiod.

The two feeds for the study were prepared as 3 mm extruded pellets by SPAROS Lda (Olhão, Portugal); a control feed for the CO group, and a soybean and soy saponin-containing feed for the SO group (**Supplementary Table 1**). The feeds contained only around 25% ingredients that were of marine origin; 15% fishmeal and 9.4–9.6% sardine oil. All other ingredients were from different plants: soybean, wheat, corn, and rapeseed. Although both the feeds contained soy protein concentrate and soy lecithin powder, only the SO feed contained soybean meal, soybean meal full fat and soy saponins (40% purity). The latter two ingredients were included in the SO feed to induce distal intestinal inflammation in the fish. These feeds were fed *ad libitum* to the respective fish groups, using automatic feeders (Arvo Tech, Huutokoshi, Finland). The feeders delivered the feeds twice a day, 08:00–09:00 and 14:00–15:00, and the daily feeding rate was 1.2% of the fish weight.

Sampling

After 36 days of feeding, the fish were euthanized with an overdose (160 mg L⁻¹) of MS222 tricaine methanesulfonate (Argent Chemical Laboratories, Redmond, WA, USA) to collect the blood, distal intestine, and head kidney. The distal segment (DI) of the intestine was chosen as it is affected by dietary soy products. On the other hand, the head kidney (HK) was selected because it is a key organ involved in the systemic immune responses. First, 2 ml of whole blood (WB) was drawn from *vena caudalis* of fish (n = 10) using heparinized syringe and transferred to 15 ml centrifuge tubes containing 4 ml of culture medium (described later). Thereafter, the fish were dissected under aseptic conditions to collect the DI (after removing the contents) and HK samples (n = 6) which were then transferred to cryotubes, snap-frozen in liquid nitrogen and stored at -80°C. In addition, we had collected the DI samples on day 4 (n = 6); this sample was employed only to understand the histological changes at an early time point. The anterior most portion of the DI segment collected on day 36 was also used for the histology study. DI obtained on day 36 was used for the RNA-Seq and qPCR studies, and HK was employed for the RNA-Seq.

Intestine Tissue Histomorphology

To understand the morphological changes in the distal intestine, samples of the segment were processed, and 5 μ m sections of the tissues from the CO and SO groups were prepared as reported in

Vasanth et al. (16). Alcian Blue-Periodic Acid Schiff's reagent (AB-PAS, pH 1.0) (17) was used to stain the sections for mucins. Thereafter, the sections were viewed using a microscope (Olympus BX51, Olympus Europa GmbH, Hamburg, Germany) with a maximum magnification of 200×. The photomicrographs were captured employing a Camera (SC180, Olympus) and processed with the imaging software CellEntry (Soft Imaging System GmbH, Munster, Germany).

Intestine/Head Kidney Transcriptome—RNA Isolation, Library Preparation, and Sequencing

To delineate the changes of the respective transcriptomes, total RNA was extracted from DI and HK samples following the QIAzol protocol (Qiagen, Hilden, Germany). RNA purity and quantity were determined using the NanoDrop 1000 (Thermo Fisher Scientific, Waltham, MA, USA). Furthermore, the integrity of the RNA isolated from the two organs was assessed using Agilent RNA screen tapes, following manufacturer's protocol, on the 2200 TapeStation system (Agilent Technologies, Santa Clara, CA, USA). Only samples with RIN > 7.5 were used for library preparation.

RNA sequencing libraries were prepared according to the protocols of Siriyyappagounder et al. (18) by using NEBNext ultra II directional RNA library preparation kit with poly (A) mRNA magnetic isolation module (NEB #E7490; New England BioLabs®, Herts, UK). Briefly, 1 µg of total RNA was used as the starting material for the library preparation. The mRNA was enriched using oligo-dT magnetic beads and fragmented to ~100–200 nt, prior to synthesis of the first and second cDNA strands. The resulting cDNA was purified and 3' end repaired for adapter ligation. Further PCR enrichment (8 cycles) was performed, and PCR products were cleaned with AMPure XP beads (Beckman Coulter Inc., Brea, CA, USA) to ensure that the libraries were free from residual adapter dimers and unwanted (smaller) fragments. In total, 24 libraries were prepared (12 for DI and 12 for HK); there were six replicates per treatment group. Individual libraries were quantified, normalized and pooled at equimolar ratio and sequenced as single-end reads (75 bp) on an illumina NextSeq 500 sequencer (illumina, San Diego, CA, USA) with NextSeq 500/550 high output v2 reagents kit (illumina). Libraries from the DI and HK samples were sequenced separately by using two flow cells. The obtained raw sequencing data was deposited in the Sequence Read Archive, National Center for Biotechnology Information (NCBI) database under the accession number PRJNA640734.

Intestine/Head Kidney Transcriptome—Data Processing and Statistical Analyses

Adapter sequences from the raw reads were removed using cutadapt (version 1.12) (19), employing the following parameters: -q 25, 20 -quality-base = 33 -trim-n -m 20. The quality of the clean reads was further assessed using FastQC (Andrews, 2010) and reads with quality <30 were removed. Reference genome of Atlantic salmon (assembly ICSASG_v2) and gene model annotation files were downloaded from NCBI to

annotate the sequences. The software STAR (version 2.5.3a) was used to build the index, and cleaned reads were mapped to reference genome with default parameters.

We employed DESeq2 version 1.22.2, which uses shrinkage estimates for both dispersion and fold change to identify the differentially expressed genes (DEGs) (20). An organism database with Entrez geneID was prepared using AnnotationHub version 2.14.5 (21). Pathway enrichment and gene ontology (GO) over-representation of DEGs were assessed with clusterProfiler version 3.10.1 (22). Furthermore, the association of the enriched objects was delineated using the same package. Based on the report by Hong et al. (23), we performed separate enrichment analyses for up- and downregulated genes. The functions of the packages ggplot2 version 3.1.1 (24) and ggraph (25) were used to format the graphs.

Intestine Transcriptome—Verifying the Expression of DEGs by Real-Time PCR

qPCR was performed to verify the mRNA levels of selected DEGs identified from the RNA-Seq study; here we employed the same samples that were used for the RNA-Seq study. Briefly, 1 µg of total RNA from each sample was reverse transcribed using the QuantiTect reverse transcription kit (Qiagen), according to the manufacturer's instructions. The obtained cDNA was further diluted 10 times with nuclease free water and used as PCR template. The PCR reactions were conducted using the SYBR green in LightCycler® 96 Real-Time PCR System (Roche Holding AG, Basel, Switzerland), following the method previously described by Vasanth et al. (16). The reactions were performed in duplicate on samples from six fish per group.

Primers for the selected genes were designed using the Primer-BLAST tool in NCBI. The primer secondary structures such as hairpin, repeats, self and cross dimer were accessed with NetPrimer (Premier Biosoft, Palo Alto, USA). The primers for the reference and target genes are given in **Table 1**. Using geNorm (26), a geometric normalization factor was computed for each of the samples based on the relative quantities of the two most stable genes (*rps29* and *ubi*) from among the set of four reference genes—elongation factor 1A (*ef1ab*), ribosomal protein L13 (*rpl13*), ribosomal protein S29 (*rps29*), and ubiquitin (*ubi*). The expression levels of all the target genes were then calculated relative to the normalization factor.

Cytological Studies—Cell Isolation and Culture

To further understand the feed-induced inflammatory responses, we examined the immune cell population in WB. The cell isolation and culture procedures for the WB samples have been described in Park et al. (27). Briefly, the collected WB was kept in 4 ml of ice-cold L-15 medium. To isolate the WB leucocytes (WBLs), we employed Percoll (Sigma-Aldrich, Oslo, Norway) 40%/60%. After centrifugation (500 × g, 30 min, 4°C), the cells that were separated at the interface of the Percoll gradients were carefully collected and washed twice with 4 ml of ice-cold L-15 by centrifugation (500 × g, 5 min, 4°C).

TABLE 1 | Details of primers used for the qPCR verification study.

Gene	Primer sequence	PCR efficiency (%)	Amplicon size (bp)	GenBank accession numbers
<i>anxa2</i>	CATTGCAGAAAGAAATACAAAGGGG-F CCAGCGTGACAATACTGTG-R	92.1	96	XM_014161401.1
<i>cath1b</i>	GTCCTCTGAAGAAAAATGGGAAAC-F GCATAGCATCTTCTGCCTC-R	88.5	135	NM_001123586.1
<i>cath2</i>	CCGATTCTGGAGACTGGCAA-F TGTCCGAATCTTCTGAGTGC-R	96.5	111	NM_001123573.1
<i>clcn1</i>	TCAGCAACAACAGTCTCT-F GCTGTGGATGGTGTGTT-R	93.0	82	XM_014152555.1
<i>clcn2</i>	CTCGGACACATCAGTAAG-F TGAGGGAGGTGGAGTCTAGC-R	90.8	123	XM_014184291.1
<i>csad</i>	CGGTCTGGCTGACATAAT-F AGTTGACTCGTCCACCCCTGA-R	88.2	127	NC_027317.1
<i>gal3</i>	CGGAGCTACTAACAGATA-F GTTGGCTGGTGGGTTGC-R	90.1	127	NM_001140833.1
<i>gsto1</i>	GCTTCATGCCAAGGGGAT-F TCTCCAATGTCGGAACAGG-R	89.9	107	NM_001141472.1
<i>lysc2</i>	ATGAGAGCTGTTGTGTTG-F AGACAGGCACCCAGTT-R	97.0	144	XM_014145497.1
<i>mta</i>	TGAATGCTCCAAAACCTGG-F CCTGAGGCACACTTGCTG-R	88.3	130	NM_001123677.1
<i>rbp2</i>	GACCTGCTACACCTGGACATC-F TCTCAAATGGCCCTACCTG-R	104.0	147	NM_001146482.1
<i>slc26a6</i>	TGGGCATGGAACACCTGA-F CACCAACTGTTAACTCG-R	91.1	124	NC_027312.1
<i>slc6a19</i>	ATGGAGGAGGAGCGTTTA-F CGATGCCAACACCTGTGAGA-R	100.5	158	NM_001141815.1
<i>slc6a6</i>	GGTGTAAATTCATTTCCGATGC-F CTCTTTCTGTGCCATGCTGC-R	95.8	109	XM_014134772.1
<i>tnfrsf1b</i>	TCGGAGGTGTTATCGGAG-F CCTGGACCCTGTGAAGACTTT-R	91.7	80	XM_014133111.1
Reference genes				
<i>ef1ab</i>	TGCCCTCCAGGATGTCTAC-F CACGGCCACAGGACTG-R	94.5	59	BG933853
<i>rpl13</i>	CGCTCCAAAGCTCCTCTTCCC-F CCATCTTGAGTTCCTCCTCAGTGC-R	95.5	79	BT048949.1
<i>rps29</i>	GGGTATCAGCAGCTCTATTGG-F AGTCCAGCTTAAACAAGCCGATG-R	93.3	167	BT043522.1
<i>ubi</i>	AGCTGGCCCAAGTACAACCTGTG-F CCACAAAAGCACCAGCCAAC-R	94.9	162	AB036060.1

Annexin 2-like (anxa2), cathelicidin 1-B (cath1b), cathelicidin 2 (cath2), chloride channel protein 1-like (clcn1), chloride channel protein 2-like (clcn2), cysteine sulfinate decarboxylase-like (csad), galectin-3 (gal3), glutathione S-transferase omega-1 (gsto1), lysozyme C II (lysc2), metallothionein A (mta), retinol binding protein II (rbp2), solute carrier family 26 member 6-like (slc26a6), solute carrier family 6 member 19 (slc6a19), solute carrier family 6 (neurotransmitter transporter, taurine) member 6 (slc6a6), and tumor necrosis factor receptor superfamily member 1B-like (tnfrsf1b).

Cytological Studies—Flow Cytometric Assay

ImageStream[®]X Mk II Imaging Flow Cytometer (Luminex Corporation, Austin, TX, USA) equipped with two argon-ion lasers (488 and 642 nm) and a side scatter laser (785 nm) was used for the flow cytometric assays. The acquired cell data was analyzed using IDEAS 6.1.822.0 software (Luminex Corporation). The protocols for the flow cytometric assays were previously described in Park et al. (27).

WB Lymphocyte-Like Cell Population

To compare the percentage of lymphocyte-like cells of fish from the CO and SO groups, aliquots containing 1×10^6 cells of WBL in 50 μ l PBS were prepared in 1.5 ml microcentrifuge tubes. Before every sample was run through the flow cytometer, 1 μ l of

propidium iodide (PI; 1 mg/ml, Sigma-Aldrich) was added to stain dead cells. Next, 1 mW 488 nm argon-ion laser and 0.47 mW 785 nm side scatter laser in the imaging flow cytometer were set to detect the dead cells (702/86 nm bandpass; Channel 5) and cell complexity (772/55 nm bandpass; Channel 6), respectively. Cell analyses were performed on 10,000 cells acquired at low speed (300 objects/s) and at a magnification of 40 \times . Dead cells were estimated as the percent of cells that were positive for PI (red fluorescent cells). After excluding the dead cells, viable cells were analyzed by generating brightfield (BF) area (size) vs. side scatter (SSC) intensity (complexity) dot plots. The settings of the cytometer were kept identical during the analysis of all the samples. We adopted a gating strategy based on our IFC protocols (27); using HK IgM⁺ cells isolated by magnetic-activated cell sorting, lymphocyte localization (low BF area and low SSC intensity) was determined employing a BF area vs. SSC

intensity plot. In the present study, the percentages of cells in the lymphocyte localization gates were compared to determine the differences in the CO and SO groups.

Data Handling and Statistical Analyses—Flow Cytometry and qPCR Studies

The data analyses were performed in RStudio. Normality of the qPCR and flow cytometry data was tested by Shapiro–Wilk Test, and the assumption of equal variance was checked by the Bartlett’s Test. Unpaired Student’s t-test was employed to compare the statistically significant difference between the two groups. Mann–Whitney U test was used for non-parametric data. The differences were considered significant at $p < 0.05$.

RESULTS

Soybean Products Induced Inflammation in the Distal Intestine of Atlantic Salmon

On the 4th day after the start of the trial, the DI of the SO group did not exhibit any characteristic morphological changes associated with inflammation (**Figure 1A, Supplementary Figure 1A**). However, at this time point, we could observe a reduction in absorptive vacuoles and more intraepithelial lymphocytes compared to those in the CO group. The morphological differences in the SO group were clearly discernible on the 36th day (**Figure 1B, Supplementary Figure 1B**); the SO group had fused villi, fewer supranuclear vacuoles,

widened lamina propria, infiltration of inflammatory cells, and enlarged stratum compactum.

Transcriptome of the Distal Intestine Revealed DEGs Induced by the Soybean Products

The transcriptomes of DI and HK were collected on day 36 when the fish intestine exhibited distinct features of inflammation. A total of over 563 million cleaned reads from 24 (12 from distal intestine and 12 from head kidney) samples were obtained after adapter trimming and quality filtering; of these over 435 million reads were mapped to Atlantic salmon transcriptome and genome. However, one biological replicate of the DI from the CO group was removed from the downstream analysis due to lower (22.83%) mapping percentage (**Supplementary Table 2**). An illustration of the bioinformatics pipeline is provided in **Supplementary Figure 2**.

The principal component analyses of the normalized counts pointed to the differential clustering of the CO and SO groups in the DI (**Figure 2A**), but not in the HK (**Figure 2B**). The dispersions of the gene expression data, as expected, decreased with increasing mean, and the MA (minus over average) plot revealed the differentially expressed genes after shrinking the dispersions and logarithmic fold changes (DI: **Supplementary Figures 3A, B**; HK: **Supplementary Figures 4A, B**). We identified 53 upregulated and 38 downregulated genes in the DI at a logarithmic fold change threshold of 0.75 and an adjusted p-value of 0.05 (**Figures 3A, B; Supplementary Figure 5**). However, DEGs were not detected in the case of HK ($p > 0.05$).

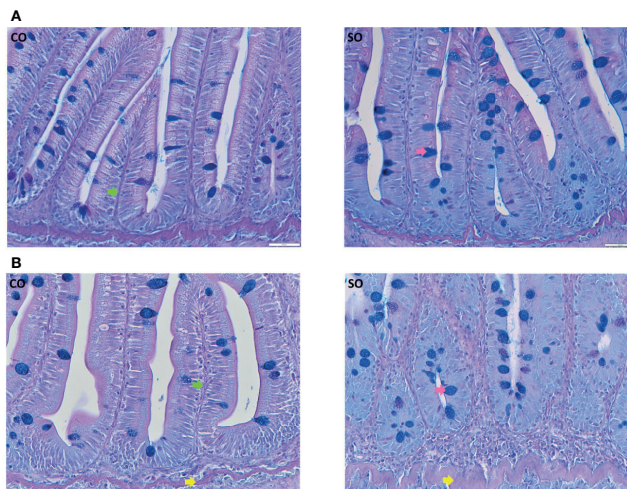


FIGURE 1 | Photomicrographs of the distal intestine of Atlantic salmon from the CO and SO groups. **(A)** Inflammatory features are not visible in the SO group on day 4 after the start of the feeding trial. **(B)** Saponin-induced inflammatory characteristics are evident at day 36 of the trial. Control group—CO, and soy-derivatives fed group—SO. Pink arrow—goblet cells, green arrow: lamina propria, yellow arrow—stratum compactum. Scale bar: 50 μ m.

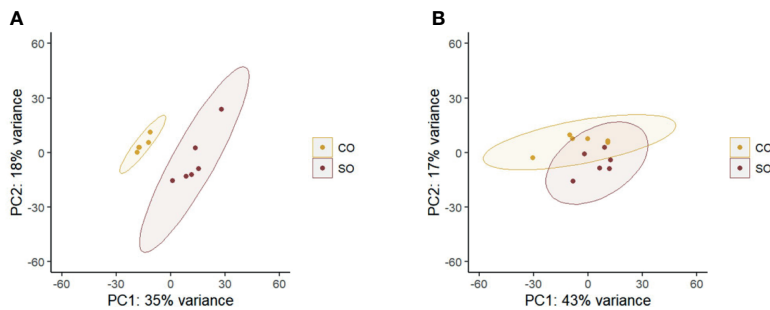


FIGURE 2 | Principal component analysis plot shows the clustering of the CO and SO fish groups. **(A)** The distal intestine and **(B)** head kidney. Control group—CO, and soy-derivatives fed group—SO. Note that from the intestine data, one replicate was removed from the CO group because the reads did not yield a good mapping result.

The upregulated genes in the DI included inflammation-associated genes such as *cathelicidins*, *galectin*, *tumor necrosis factor receptor superfamily member 1B-like*, *lysozyme CII*, *annexin A2-like* (**Supplementary Tables 3, 5**). Some solute carrier families were upregulated while others were downregulated in the SO group (**Supplementary Tables 4, 5**). Genes connected to chloride channel proteins (*clcn1*, *clcn2*) were downregulated in the SO group. In addition, sodium-associated transporters were altered in the same group (*sodium/glucose co-transporter 1-like*, *slc5a1*, and *sodium- and chloride-dependent taurine transporter*, *slc6a6* were upregulated and *sodium-dependent neutral amino acid transporter B(0)AT1-like*, *slc6a19* and *potassium voltage-gated channel subfamily A regulatory beta subunit 2*, *kcnab2* were downregulated). Another anion exchanger, *solute carrier family 26 member 6*, *slc26a6* and the mitochondrial amino acid transporter, *slc25a48* were upregulated in the SO group.

The expression of 15 DEGs was verified by qPCR. The bar plots in **Supplementary Figure 6** show the mRNA levels of the selected genes. The mRNA levels correlated positively with the read counts from the RNA-Seq study (**Supplementary Figure 7**).

Soybean Products Affected the Biological Pathways

The enriched pathways for the upregulated genes were taurine and hypotaurine metabolism, beta-alanine metabolism, pantothenate and coenzyme (CoA) biosynthesis, drug metabolism—cytochrome P450, drug metabolism—other enzymes, metabolism of xenobiotics by cytochrome P450, steroid biosynthesis, and glutathione metabolism (**Figure 4A**). All these enriched pathways had common genes; the exception was steroid biosynthesis (**Figure 4B**). The package clusterProfiler did not detect any enriched pathways for the downregulated genes. The enriched GO terms based on the upregulated genes were among others, oxidoreductase activity, some binding and lyase activities (**Figure 4C**). More GO terms based on the downregulated genes were enriched; many belonged to transmembrane transporter activity, channel activity and some binding activity (**Figure 4D**). For the upregulated genes, NADP, vitamins, pyridoxal phosphate, flavin adenine dinucleotide,

and coenzyme binding were enriched (**Figure 4C**). On the other hand, for the downregulated genes, tetrapyrrole, iron ion, oxygen, heme, and amino acid binding were the enriched GO terms (**Figure 4D**).

Soybean Products Induced Inflammation Was Marked by an Increase in WB Lymphocyte-Like Cells

To compare the percentage of WB lymphocyte-like cells from the CO and SO groups, WBL population was presented on a brightfield area (cell size) vs side scatter intensity (cell complexity) dot plot (**Figures 5A, B**). The gate for lymphocyte-like cells was determined based on salmon IgM⁺ cell area, as previously described by Park et al. (27). From **Figure 5C**, it is evident that the SO group (77.64%) had higher percentage of WBL-like cells compared to the CO group (74.35%; $p < 0.05$).

DISCUSSION

Diet-induced intestinal inflammation is a common clinical issue that has to be tackled by understanding the associated mechanisms because the disease has pervaded all classes of the global population. In humans, Crohn's disease and ulcerative colitis are inflammatory bowel diseases. These non-communicable diseases are assumed to be early adulthood diseases caused by genetic and environmental factors which disturb immunity and weaken epithelial barrier (28). Like humans, carnivorous farmed fish are prone to diet-linked allergies that can affect their growth (4, 8–10). Here we describe the soybean/soy saponin-induced inflammation primarily based on the changes in the transcriptome of the DI of Atlantic salmon. The results indicate the alteration of around 90 genes and disturbance of associated pathways and GO terms in the DI of fish. Furthermore, the differential counts of the immune cells also point to possible changes in the immune status of this fish group.

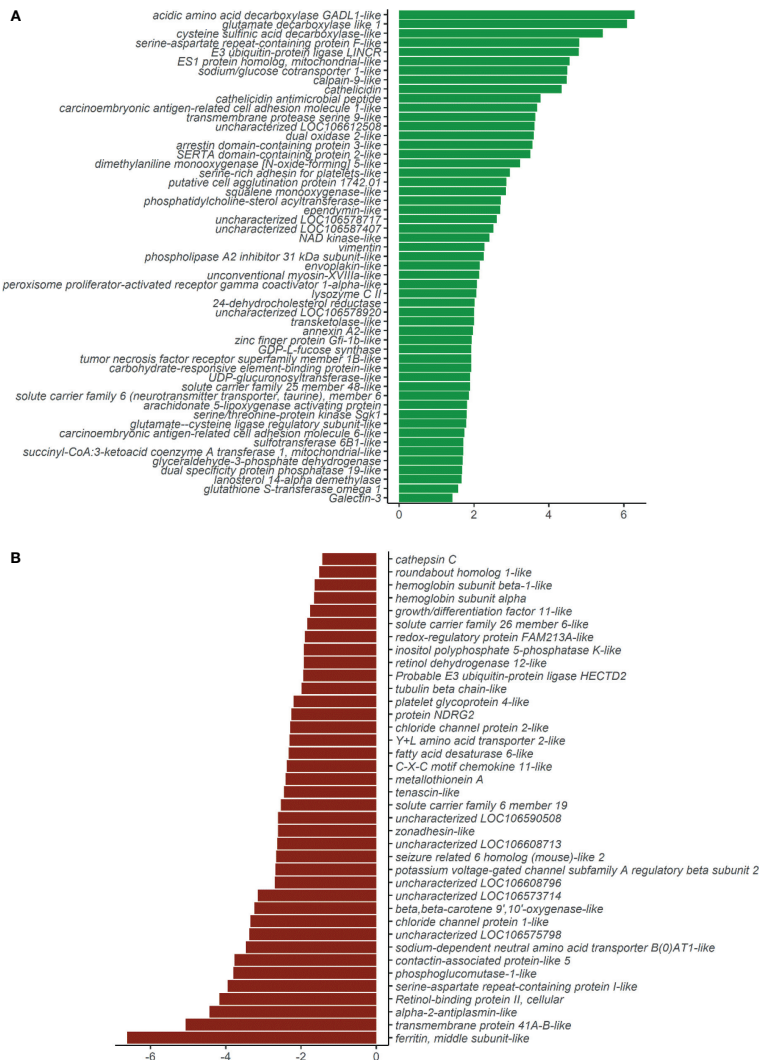
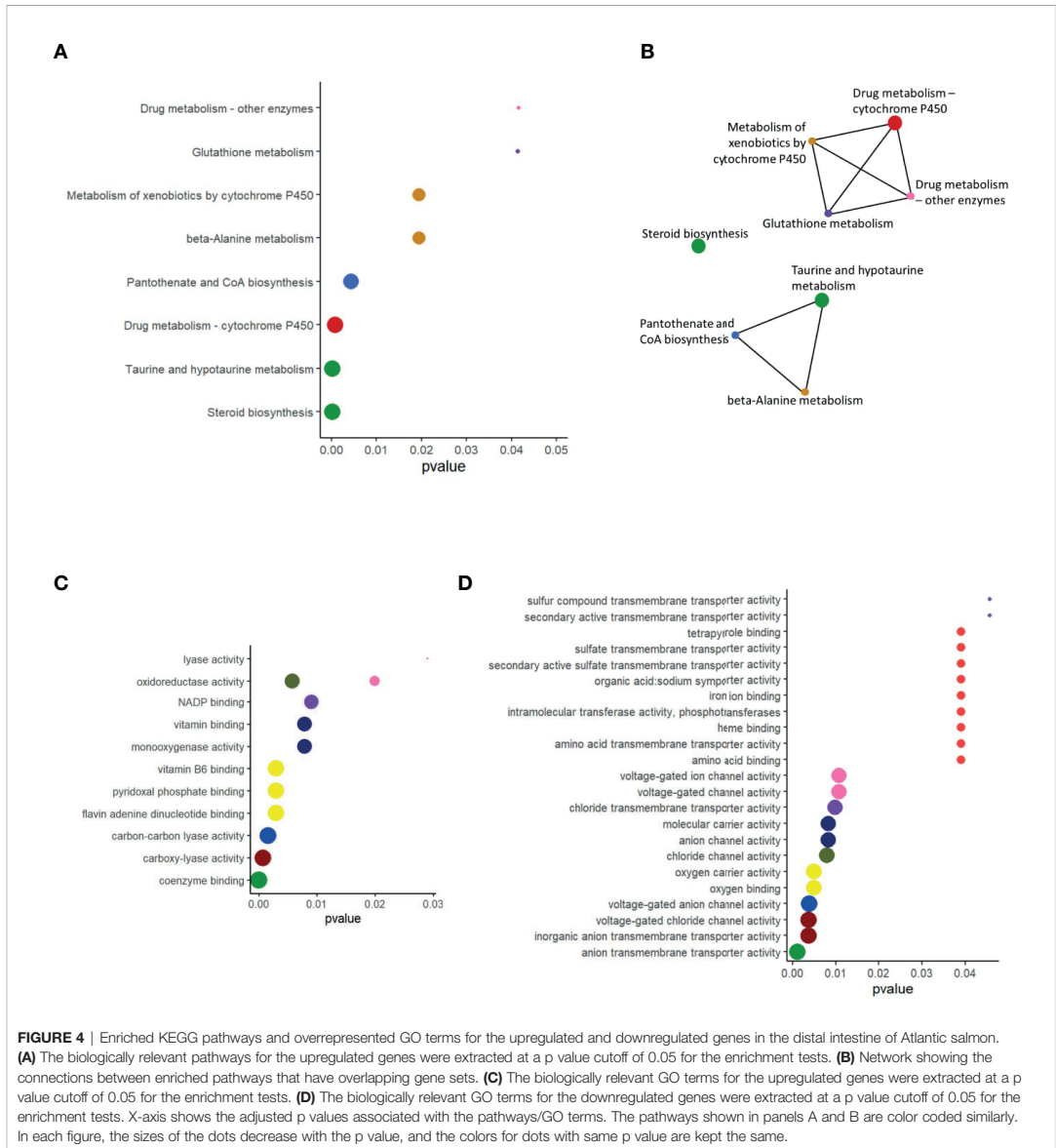


FIGURE 3 | Plot showing the differentially expressed genes in the distal intestine of Atlantic salmon. **(A)** Fifty-three genes were upregulated in the SO group (green bars). **(B)** Thirty-eight genes were downregulated in the SO group (red bars). X-axis labels show the log₂foldchange, and the y-axis shows the differentially expressed genes.

High Fat Soybean Products and Soy Saponin Induced Inflammation in the Distal Intestine of Atlantic Salmon

Certain soybean products are known to cause inflammation in the intestine of carnivorous fishes (2, 4, 9, 12, 14). High levels of soybean meal in diets or the presence of antinutritional factors is reported to be the main reasons for the inflammatory

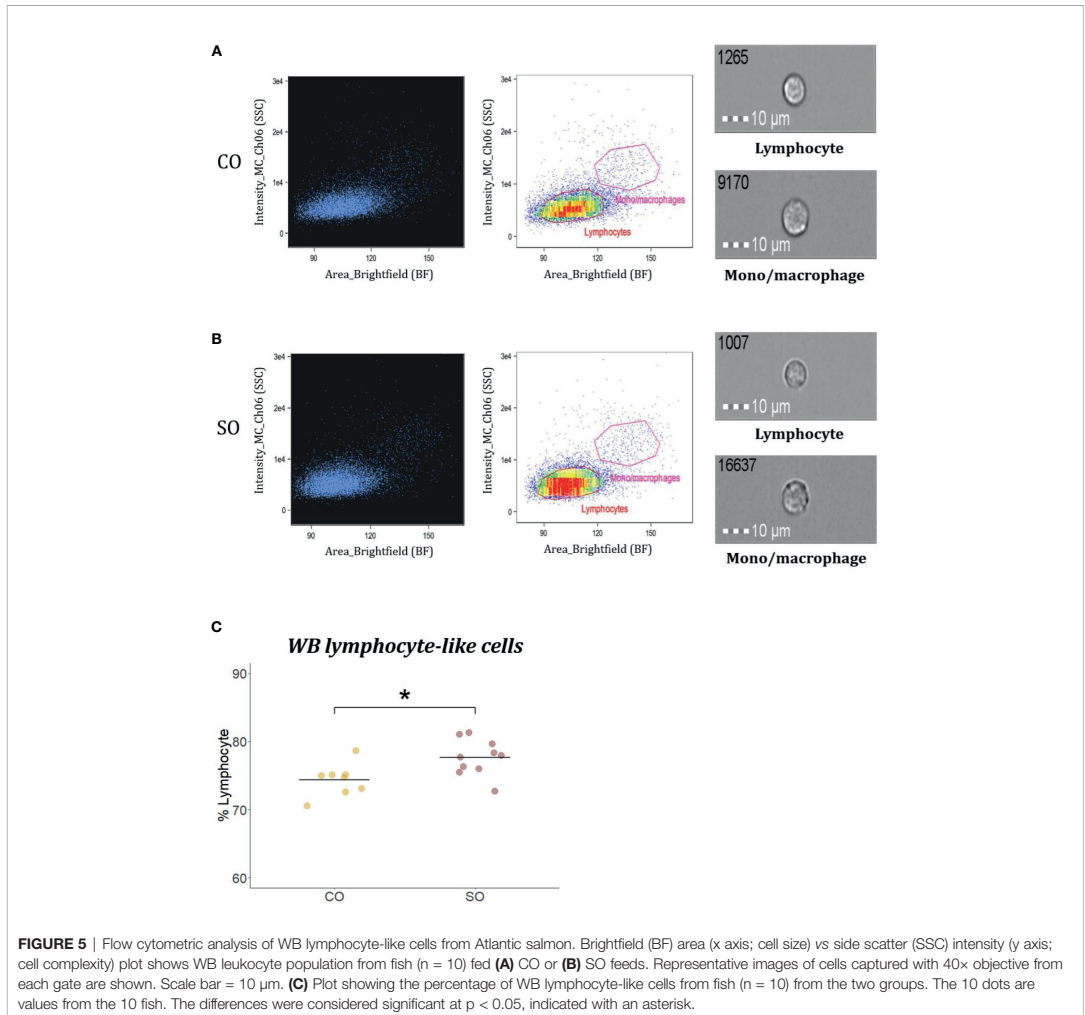
condition (2, 10). Feeding even 10% of solvent extracted soybean meal or 25% defatted soybean meal can give rise to pathological changes in Atlantic salmon (12, 29). Furthermore, the severity of inflammation in the DI of this fish is dependent on the content of the antinutritional factor (30). A study points out that the impact of soy saponin concentrate (of 69% purity) feeding for 53 days is relatively



benign in terms of inflammatory signs (12). In the present study, 36 days of feeding soy products (meal, full fat, and soy saponin) led to the development of inflammation in the DI of salmon. The inflammation characteristics were similar to that described previously by others (4, 12, 30) but not as intense as reported earlier in a chemically-induced inflammation model that employed a direct application method (16).

Distinct Effects of Soy Products in the Intestine Transcriptome

In this study, in addition to local responses to soybean products in the DI, we anticipated that changes may occur in the HK, a key immune organ. Most transcriptome studies focusing on HK have registered responses to bacterial/viral pathogens or parasites, while some studies have shown that functional feeds could



alter expression of genes in the organ, as described in a review article (31). In the present study, we did not detect any DEGs in the head kidney similar to the transcriptome investigation by Tacchi et al. (32) that compared marine protein- and plant protein-based diets; no common genes were expressed in the intestine, muscle, and liver. Diet-induced inflammation may affect systemic response as reported for salmon fed soybean based on 44 common genes expressed in the intestine and liver (33). Furthermore, diets did not alter the HK transcripts in fish, but the responses became evident 24 h after injection with the viral mimic polyriboinosinic polyribocytidylic acid (34). In the present study, we did not find a significant impact of the soy products on the HK transcriptome. The lack of response in HK seems to indicate that it is not the optimal organ to check the

diet-induced changes in transcriptome. However, future studies should consider the changes in the liver transcriptome, a metabolically active organ.

Soy Products Evoked Inflammation-Associated Signals in the Intestine

Bacterial entry through a breach in the epithelial barrier due to defective functions and aberrant innate immune responses are accountable for evoking intestinal inflammation in humans (35). Such an inflammation triggers the transcriptional activation of selected immune-related genes (36).

Cathelicidin genes, *cath11* and *cath12*, are known to be expressed in the DI of salmon and were stimulated by pathogenic bacteria; in our study they were upregulated in the

DI of fish from the SO group (**Supplementary Figure 6**). Human cathelicidin, LL-37 mRNA, was increased significantly in the inflamed mucosa of ulcerative colitis and Crohn's disease (37). In addition, it is interesting to note that both *lysozyme CII* and *tumor necrosis factor receptor superfamily member 1B-like* were upregulated. Based on mammalian studies, it is known that pathogen associated molecular patterns are recognized by toll-like receptors that activate the MyD88-independent pathway including the TNF (Tumor necrosis factor) receptor associated factor 6 (TRAF6), which is associated with TNF receptor superfamily (38). Tafalla and Granja (39) have reviewed the involvement of mammalian TNF receptor superfamily 1B (TNFRSF1B) in human T cell activation, and they have suggested the same function in fishes. Another pro-inflammatory mediator, Galectin 3 (40), was altered in inflamed tissues of humans (41), as reported here. A study on striped murrel *Channa striatus* revealed the ability of a galectin, CsGal-1, to agglutinate Gram-negative bacteria (42). Galectin-3 in mammals is known to recognize 'self' glycans generally but can interact with the lipopolysaccharide (LPS) of bacteria (43). Galectin-3 is secreted by inflammatory macrophages, and its induced secretion is perceived as a danger signal by the innate immune system (44, 45). The intestinal epithelial breach in the SO group, probably resulting from the unwanted reaction, may have possibly facilitated the entry of bacteria through the mucosal barriers and altered the expression of *gal3*.

Metallothionein is an anti-inflammatory mediator. After LPS treatment, metallothionein knock-out mice showed inflammatory responses in the lung epithelial cells suggesting that metallothionein is involved in cytoprotection during LPS-related inflammation (46). In the present study, metallothionein A was downregulated in the SO group, indicating a possible connection between metallothionein A and intestinal inflammation.

Retinol-binding protein transports vitamin A from the liver to other tissues like the intestine (47). It has been reported that tissue injury during inflammation causes a reduction in the synthesis of retinol-binding protein (48). In our study, the mRNA level of retinol binding protein II in the SO group was significantly downregulated. Notably, a study on humans reported that its concentration in serum decreases during the acute-phase stage of inflammation (49).

As observed in the salmon intestine, the mRNA levels of Annexin A2 were higher in the inflamed mucosa of patients with Crohn's disease (50). Intestinal epithelial cell turnover prevents pathogen colonization (51), and the actin-binding protein, Annexin A2, is necessary for the movement of intestinal epithelial cells during wound resealing (52). A link between *anxa1* and gastroprotection was suggested in an earlier study on Atlantic salmon (16).

Soy Products Also Impaired the Transport Mechanisms and Metabolism in the Intestine

Intestinal junctional molecules play key roles in sustaining epithelial integrity (35). Dysregulation of epithelial transport or entry of opportunistic microbes through the breaches in epithelial barrier can cause intestinal inflammation (51). The characteristic selective permeability of the epithelial barrier to ions, through

gating of ion channels, enables directional transport of ions (53). Chloride channel proteins form gated pores for the passage of anions, and this process is dependent on transmembrane voltage, pH, cell-swelling and phosphorylation (54). The Cl^- exits basolaterally, among other means, *via* K^+/Cl^- cotransport, Cl^- channel (55), and genes associated with chloride channel proteins were downregulated in the fish fed the soy products. In addition, solute carrier families are involved in ion transport across the apical membrane of fish intestine (55). *Slc6a6* is a sodium and chloride-ion dependent transporter that transports taurine and beta-alanine *via* intestinal brush border (56), and this gene was upregulated in the SO group, and the associated pathways that were enriched were taurine and beta-alanine pathways. Furthermore, $\text{Cl}^-/\text{HCO}_3^-$ exchange and active transport of most neutral amino acids at the apical membrane of the fish intestine are performed by *slc26a6* and *slc6a19*, respectively (55). These solute carrier families were downregulated in salmon that were prone to the unwanted reaction. Furthermore, the enriched GO terms included chloride channel activity, voltage-gated channel activity, voltage-gated anion activity, anion channel activity *etc.* We also observed a dysregulation in other activities, *viz.* transmembrane transporter activity and symporter activity in the SO group. In addition, *slc5a1*, the key mediator of glucose and galactose uptake from the lumen, and *slc25a48*, mitochondrial amino acid transporter were upregulated, and *kcnab2* (*Potassium voltage-gated channel subfamily A regulatory beta subunit 2*), which has a role in electrolyte transport, was downregulated in the SO group. Such aberrations in humans can lead to irregular nutrient absorption (57) and disturbances in the luminal fluid microenvironment (53). The alterations in iron ion, oxygen, heme, and amino acid binding GO terms, based on the downregulated genes, and NADP, vitamins, and coenzyme binding, based on upregulated genes, also point to the impaired transport mechanisms across the epithelial layer in the SO group. Other studies have also reported the effect of soybean feeding on transporter proteins, which eventually may have a bearing on the transport of nutrients *via* epithelia. In one of them, the soybean meal-wheat gluten combination affected the expression of aquaporins, ion transporters, tight junction, and adherens junction proteins in the DI of Atlantic salmon, although the genes associated with chloride channels remained unchanged (10). Furthermore, Atlantic salmon fed soy saponins alone and soy saponin in combination with soybean meal had aberrations in intestinal permeability (12). The transcriptional changes of the genes linked to the transporter proteins may be indicating disturbances in the transport of essential nutrients and the associated pathways.

Although we identified some enriched pathways linked to the upregulated genes, there was not much overlap in the pathways we obtained and those reported previously. Based on current as well as earlier studies, steroid biosynthesis and xenobiotic metabolism (13, 33) can be highlighted as the two metabolic pathways altered by dietary soybean products. Downregulation of hepatic cytochrome P450s and other drug-metabolizing enzymes are linked to inflammation (58). Furthermore, CYP1A1, an enzyme in the phase I of the reactions which helps in the excretion of endogenous (*e.g.* steroids) and exogenous (*e.g.* drugs) substances

(59), was lower in the colonic enterocytes of patients suffering from Crohn's disease and ulcerative colitis (60). Our observation on Atlantic salmon also corroborates with this finding. The biosynthesis of steroids was enriched in the SO group, and the enrichment of two cytochrome P450-associated pathways could be indicating the need to alleviate the toxicity of steroids and soy saponin.

Hypotaurine is essential for the biosynthesis of the abundant free amino acid taurine, which has roles in innate immunity of mammals (61). High levels of this semi-essential amino acid reduce oxidative stress due to its antioxidant properties (62). In humans, taurine and β -alanine transport in the intestine takes place with the help of transporters like Na^+ - and Cl^- -dependent TauT (SLC6A6) (56). Taurine is linked to growth and health of fish (63). A gene that is related to biosynthesis of taurine, *csad*, was upregulated in the distal intestine of fish from the SO group. It seems that *slc6a6*, *csad*, taurine, and hypotaurine metabolism pathways are associated with the inflammatory condition.

Dietary Soy Components Affect Blood Lymphocyte Counts

The head kidney is the major hematopoietic organ in teleost fish, having roles similar to those of the mammalian bone marrow. Hematopoietic stem cells in the organ are capable of self-renewal and differentiating into cells of erythroid, myeloid, and lymphoid lineages (64). Injuries during inflammation or metabolic changes are known to influence the size and fate of hematopoietic stem cells (65). It has also been reported that systemic response during inflammation increased the number of granulocytes and monocytes in mice bone marrow (66). In the present study, we observed a significant increase in blood lymphocyte-like cell counts in fish fed the inflammation-causing soybean products compared to those of control. It is reported that in humans, the patrolling naive lymphocytes enter the gut and undergo activation and priming based on the condition in the intestine (67). The increase in blood lymphocyte counts of fish that developed inflammation is possibly indicative of the cell recruitment to quell the localised intestinal inflammation.

CONCLUSIONS

The soybean–soy saponin combination induced DI inflammation in Atlantic salmon. The transcriptional changes associated with inflammation could be linked to disturbances in transport mechanisms as well as drug and taurine and hypotaurine metabolisms and steroid biosynthesis in the DI of the fish. The HK transcriptome was largely unaffected during intestinal injury. However, this needs to be verified as the increased lymphocyte numbers in the peripheral blood of the fish with intestinal inflammation may in fact be suggesting otherwise. Further investigations on the dysregulated intestinal barrier functions, reported here, will help to broaden our understanding of the intestinal inflammation in fish. The key genes involved in solute transport across the epithelial barrier such as *clcn1*, *clcn2*, *slc26a6*, *slc6a19* and immune genes such as *cath1*, *cath2*, *gal3*, *rbp2*, *mta* could

serve as possible biomarkers of diet-associated intestinal inflammation and be used in further comparative studies on inflammation in mammalian models.

DATA AVAILABILITY STATEMENT

The datasets presented in this study can be found in online repositories. Additional data and figures are presented in **Supplementary Material**.

ETHICS STATEMENT

The animal study was reviewed and approved by the Norwegian Animal Research Authority, EDU (Forsøksdyrutvalget ID-10050). We adhered to the rules and regulations of animal welfare and followed the standard biosecurity and safety procedures at the Research Station of Nord University, Bodø, Norway.

AUTHOR CONTRIBUTIONS

VK, VVT, JF, MS, and JD designed the research. JD and VVT were responsible for feed formulation and development. GV supervised the feeding experiments and gene expression study. YP and PS performed the RNA-Seq studies and analyses of data. YP performed the flow cytometry studies. DD performed the histology study. VK wrote the first version of the manuscript, along with YP and PS. All authors contributed to the article and approved the submitted version.

FUNDING

This study was undertaken as part of a collaborative project “Molecular studies on the intestine of Atlantic salmon” between Nord University and DSM Nutritional Products, Switzerland, funded by the latter.

ACKNOWLEDGMENTS

The authors acknowledge the support from the staff at the Research Station, Nord University, Bodø. The authors are grateful to Bisa Saraswathy for her help in data analysis, preparation of figures and manuscript.

SUPPLEMENTARY MATERIAL

The Supplementary Material for this article can be found online at: <https://www.frontiersin.org/articles/10.3389/fimmu.2020.596514/full#supplementary-material>

SUPPLEMENTARY FIGURE 1 | Photomicrographs of the distal intestine of Atlantic salmon from CO and SO groups. **(A)** Inflammatory symptoms are not visible

in the SO group on day 4 after the start of the feeding trial. **(B)** Saponin-induced inflammatory characteristics become visible at day 36 after the start of the feeding. Control group—CO, and soy-derivatives fed group—SO. Scale bar: 100 μ m.

SUPPLEMENTARY FIGURE 2 | Overview of the bioinformatics workflow adopted in this study. RNA-Seq data were first quality filtered, after which the reads were aligned to salmon genome. Next, the read counts were extracted, and then upregulated/downregulated genes were identified for the downstream analysis. KEGG pathway and GO term enrichment analysis were then performed employing the differentially expressed genes.

SUPPLEMENTARY FIGURE 3 | Dispersion estimates and minus over average expression plots of the data from the distal intestine. **(A)** Plots showing the shrinkage of the gene-wise dispersions—the maximum-likelihood estimates obtained from the gene data (black) are shrunk towards the fitted red curve to get the final values (blue) of dispersion. **(B)** Shrinkage of the logarithmic fold-change—the differentially expressed genes with adjusted $p < 0.05$ are shown as red dots.

SUPPLEMENTARY FIGURE 4 | Dispersion estimates and minus over average expression plots based on the data from the head kidney. **(A)** Plots showing the shrinkage of the gene-wise dispersions—the maximum-likelihood estimates obtained from the gene data (black) are shrunk towards the fitted red curve to get the final values (blue) of dispersion. **(B)** Shrinkage of the logarithmic fold-change—the differentially expressed genes with adjusted $p < 0.05$ are shown as red dots.

SUPPLEMENTARY FIGURE 5 | Heatmap showing the 53 upregulated and 38 downregulated genes in the distal intestine of Atlantic salmon. Normalized gene count was input into the pheatmap function, and the values were centered and scaled in the row direction. The column names at the bottom of the heatmap

indicate the control (prefix CO) and the soybean-derivative (saponin group with prefix SO) fed groups.

SUPPLEMENTARY FIGURE 6 | Relative mRNA levels of the selected 15 genes in the distal intestine of Atlantic salmon from the CO and SO groups at day 36. The gene expression of control (CO) and soybean fed groups (SO) ($n = 6$) is shown. Asterisks indicate ** $p < 0.01$ and *** $p < 0.001$.

SUPPLEMENTARY FIGURE 7 | Correlation between the relative mRNA levels and read counts of the selected differentially expressed genes. The bar on the right side indicates the correlation coefficient; darker shades of red and blue indicate negative and positive correlations, respectively. X indicates non-significant differences based on Spearman correlation test. If the correlation coefficient is $+0.75$, $3/4^{th}$ of the circles will be shaded.

SUPPLEMENTARY TABLE 1 | Details of ingredients in the experimental feeds.

SUPPLEMENTARY TABLE 2 | Details of raw reads, cleaned reads and mapped reads from different samples.

SUPPLEMENTARY TABLE 3 | Details of differentially upregulated genes in the SO group compared to the CO group.

SUPPLEMENTARY TABLE 4 | Details of differentially downregulated genes in the SO group compared to the CO group.

SUPPLEMENTARY TABLE 5 | Details of differentially regulated genes in the SO group compared to the CO group.

REFERENCES

- Ytrestøyl T, Aas TS, Åsgård T. Utilisation of feed resources in production of Atlantic salmon (*Salmo salar*) in Norway. *Aquaculture* (2015) 448:365–74. doi: 10.1016/j.aquaculture.2015.06.023
- Buttle LG, Burrells AC, Good JE, Williams PD, Southgate PJ, Burrells C. The binding of soybean agglutinin (SBA) to the intestinal epithelium of Atlantic salmon, *Salmo salar* and rainbow trout, *Oncorhynchus mykiss*, fed high levels of soybean meal. *Vet Immunol Immunopathol* (2001) 80(3):237–44. doi: 10.1016/S0165-2427(01)00269-0
- Zhang J-X, Guo L-Y, Feng L, Jiang W-D, Kuang S-Y, Liu Y, et al. Soybean β -glycinin induces inflammation and oxidation and causes dysfunction of intestinal digestion and absorption in fish. *PLoS One* (2013) 8(3):e58115. doi: 10.1371/journal.pone.0058115
- Bakke A. "Pathophysiological and immunological characteristics of soybean meal-induced enteropathy in salmon: Contribution of recent molecular investigations". In: LE Cruz-Suárez, D Ricque-Marie, M Tapia-Salazar, MG Nieto-López, DA Villarreal-Cavazos, J Gamboa-Delgado, L Hernández-Hernández, editors. *Avances en Nutrición Acuicola XI - Memorias del Décimo Primer Simposio Internacional de Nutrición Acuicola*. Universidad Autónoma de Nuevo León, Monterrey, México: San Nicolás de los Garza, N. L., México (2011). p. 345–72.
- Desai AR, Links MG, Collins SA, Mansfield GS, Drew MD, Van Kessel AG, et al. Effects of plant-based diets on the distal gut microbiome of rainbow trout (*Oncorhynchus mykiss*). *Aquaculture* (2012) 350–353:134–42. doi: 10.1016/j.aquaculture.2012.04.005
- Green TJ, Smullen R, Barnes AC. Dietary soybean protein concentrate-induced intestinal disorder in marine farmed Atlantic salmon, *Salmo salar* is associated with alterations in gut microbiota. *Vet Microbiol* (2013) 166(1):286–92. doi: 10.1016/j.vetmic.2013.05.009
- Nayak SK. Role of gastrointestinal microbiota in fish. *Aquac Res* (2010) 41(11):1553–73. doi: 10.1111/j.1365-2109.2010.02546.x
- Sørensen M, Penn M, El-Mowafi A, Storebakken T, Chunfang C, Øverland M, et al. Effect of stachyose, raffinose and soya-saponins supplementation on nutrient digestibility, digestive enzymes, gut morphology and growth performance in Atlantic salmon (*Salmo salar*, L.). *Aquaculture* (2011) 314(1):145–52. doi: 10.1016/j.aquaculture.2011.02.013
- Refstie S, Korsoen ØJ, Storebakken T, Baeverfjord G, Lein I, Roem AJ. Differing nutritional responses to dietary soybean meal in rainbow trout (*Oncorhynchus mykiss*) and Atlantic salmon (*Salmo salar*). *Aquaculture* (2000) 190(1):49–63. doi: 10.1016/S0044-8486(00)00382-3
- Hu H, Kortner TM, Gajardo K, Chikwati E, Tinsley J, Krogdahl Å. Intestinal fluid permeability in Atlantic salmon (*Salmo salar* L.) is affected by dietary protein source. *PLoS One* (2016) 11(12):e0167515. doi: 10.1371/journal.pone.0167515
- Sahlmann C, Sutherland BJG, Kortner TM, Koop BF, Krogdahl Å, Bakke AM. Early response of gene expression in the distal intestine of Atlantic salmon (*Salmo salar* L.) during the development of soybean meal induced enteritis. *Fish Shellfish Immunol* (2013) 34(2):599–609. doi: 10.1016/j.fsi.2012.11.031
- Knudsen D, Jutfelt F, Sundh H, Sundell K, Koppe W, Frøkiær H. Dietary soya saponins increase gut permeability and play a key role in the onset of soybean-induced enteritis in Atlantic salmon (*Salmo salar* L.). *Br J Nutr* (2008) 100(1):120–9. doi: 10.1017/S0007114507886338
- Kortner TM, Skuger S, Penn MH, Myrdland LT, Djordjevic B, Hillestad M, et al. Dietary soya-saponin supplementation to pea protein concentrate reveals nutrigenomic interactions underlying enteropathy in Atlantic salmon (*Salmo salar*). *BMC Vet Res* (2012) 8(1):101. doi: 10.1186/1746-6148-8-101
- Gu M, Jia Q, Zhang Z, Bai N, Xu X, Xu B. Soya-saponins induce intestinal inflammation and barrier dysfunction in juvenile turbot (*Scophthalmus maximus*). *Fish Shellfish Immunol* (2018) 77:264–72. doi: 10.1016/j.fsi.2018.04.004
- Zhang C, Rahimnejad S, Wang Y-r, Lu K, Song K, Wang L, et al. Substituting fish meal with soybean meal in diets for Japanese seabass (*Lateolabrax japonicus*): Effects on growth, digestive enzymes activity, gut histology, and expression of gut inflammatory and transporter genes. *Aquaculture* (2018) 483:173–82. doi: 10.1016/j.aquaculture.2017.10.029
- Vasanth G, Kiron V, Kulkarni A, Dahle D, Lokesh J, Kitani Y. A microbial feed additive abates intestinal inflammation in Atlantic salmon. *Front Immunol* (2015) 6:409. doi: 10.3389/fimmu.2015.00409
- Bancroft J, Gamble M. *Theory and practice of histological techniques*. London, UK: Churchill Livingstone (2007). p. 125–38.
- Siriypagoudar P, Galindo-Villegas J, Dhanasiri AK, Zhang Q, Mulero V, Kiron V, et al. *Pseudozyma* priming influences expression of genes involved in

- metabolic pathways and immunity in zebrafish larvae. *Front Immunol* (2020) 11:978. doi: 10.3389/fimmu.2020.00978
19. Martin M. Cutadapt removes adapter sequences from high-throughput sequencing reads. *EMBnet J* (2011) 17(1):10–12. doi: 10.14806/ej.17.1.200
 20. Love MI, Huber W, Anders S. Moderated estimation of fold change and dispersion for RNA-seq data with DESeq2. *Genome Biol* (2014) 15(12):550–0. doi: 10.1186/s13059-014-0550-8
 21. Morgan M. *AnnotationHub: Client to access AnnotationHub resources*. *Bioconductor* (2019), R package version 2.16.0.
 22. Yu G, Wang L-G, Han Y, He Q-Y. clusterProfiler: An R package for comparing biological themes among gene clusters. *OMICS* (2012) 16(5):284–7. doi: 10.1089/omi.2011.0118
 23. Hong G, Zhang W, Li H, Shen X, Guo Z. Separate enrichment analysis of pathways for up-and downregulated genes. *J R Soc Interface* (2014) 11(92):20130950. doi: 10.1098/rsif.2013.0950
 24. Wickham H. *ggplot2: Elegant Graphics for Data Analysis (Use R!)*. Houston, USA: Springer (2016).
 25. Pedersen TL. *Package "gggraph"*. *Bioconductor* (2018), R package Version 1.0.2.
 26. Vandesompele J, De Preter K, Pattyn F, Poppe B, Van Roy N, De Paep A, et al. Accurate normalization of real-time quantitative RT-PCR data by geometric averaging of multiple internal control genes. *Genome Biol* (2002) 3(7):research0034.1. doi: 10.1186/gb-2002-3-7-research0034
 27. Park Y, Abihssira-Garcia IS, Thalmann S, Wiegertjes GF, Barreda DR, Olsvik PA, et al. Imaging flow cytometry protocols for examining phagocytosis of microplastics and bioparticles by immune cells of aquatic animals. *Front Immunol* (2020) 11:203. doi: 10.3389/fimmu.2020.00203
 28. Wehkamp J, Götz M, Herrlinger K, Steurer W, Stange EF. Inflammatory bowel disease. *Dtsch Arztebl Int* (2016) 113(5):72–82. doi: 10.3238/arztbl.2016.0072
 29. Krogdahl Å, Bakke-McKellep AM, Baeverfjord G. Effects of graded levels of standard soybean meal on intestinal structure, mucosal enzyme activities, and pancreatic response in Atlantic salmon (*Salmo salar* L.). *Aquac Nutr* (2003) 9(6):361–71. doi: 10.1046/j.1365-2095.2003.00264.x
 30. Krogdahl Å, Gajardo K, Kortner TM, Penn M, Gu M, Berge GM, et al. Soya saponins induce enteritis in Atlantic salmon (*Salmo salar* L.). *J Agric Food Chem* (2015) 63(15):3887–902. doi: 10.1021/jf506242t
 31. Martin SAM, Król E. Nutrigenomics and immune function in fish: New insights from omics technologies. *Dev Comp Immunol* (2017) 75:86–98. doi: 10.1016/j.dci.2017.02.024
 32. Tacchi L, Secombes CJ, Bickerdike R, Adler MA, Venegas C, Takle H, et al. Transcriptional and physiological responses to fishmeal substitution with plant proteins in formulated feed in farmed Atlantic salmon (*Salmo salar*). *BMC Genomics* (2012) 13(1):363. doi: 10.1186/1471-2164-13-363
 33. De Santis C, Bartie KL, Olsen RE, Taggart JB, Tocher DR. Nutrigenomic profiling of transcriptional processes affected in liver and distal intestine in response to a soybean meal-induced nutritional stress in Atlantic salmon (*Salmo salar*). *Comp Biochem Physiol Part D Genomics Proteomics* (2015) 15:1–11. doi: 10.1016/j.cbpd.2015.04.001
 34. Caballero-Solares A, Hall JR, Xue X, Eslamloo K, Taylor RG, Parrish CC, et al. The dietary replacement of marine ingredients by terrestrial animal and plant alternatives modulates the antiviral immune response of Atlantic salmon (*Salmo salar*). *Fish Shellfish Immunol* (2017) 64:24–38. doi: 10.1016/j.fsi.2017.02.040
 35. Geremia A, Biancheri P, Allan P, Corazza GR, Di Sabatino A. Innate and adaptive immunity in inflammatory bowel disease. *Autoimmun Rev* (2014) 13(1):3–10. doi: 10.1016/j.autrev.2013.06.004
 36. Ahmed AU, Williams BRG, Hannigan GE. Transcriptional activation of inflammatory genes: Mechanistic insight into selectivity and diversity. *Biomolecules* (2015) 5(4):3087–111. doi: 10.3390/biom5043087
 37. Kusaka S, Nishida A, Takahashi K, Bamba S, Yasui H, Kawahara M, et al. Expression of human cathelicidin peptide LL-37 in inflammatory bowel disease. *Clin Exp Immunol* (2018) 191(1):96–106. doi: 10.1111/cei.13047
 38. Akira S, Uematsu S, Takeuchi O. Pathogen recognition and innate immunity. *Cell* (2006) 124(4):783–801. doi: 10.1016/j.cell.2006.02.015
 39. Tafalla C, Granja AG. Novel Insights on the regulation of B cell functionality by members of the tumor necrosis factor superfamily in jawed fish. *Front Immunol* (2018) 9:1285. doi: 10.3389/fimmu.2018.01285
 40. Sundblad V, Quintar AA, Morosi LG, Niveloni SI, Cabanne A, Smeucol E, et al. Galectins in intestinal inflammation: Galectin-1 expression delineates response to treatment in celiac disease patients. *Front Immunol* (2018) 9:379. doi: 10.3389/fimmu.2018.00379
 41. Papa Gobbi R, De Francesco N, Bondar C, Muglia C, Chirido F, Rumbo M, et al. A galectin-specific signature in the gut delineates Crohn's disease and ulcerative colitis from other human inflammatory intestinal disorders. *BioFactors* (2016) 42(1):93–105. doi: 10.1002/biof.1252
 42. Arasu A, Kumaresan V, Sathyamoorthi A, Chaurasia MK, Bhatt P, Gnanam AJ, et al. Molecular characterization of a novel proto-type antimicrobial protein galectin-1 from striped murrel. *Microbiol Res* (2014) 169(11):824–34. doi: 10.1016/j.micres.2014.03.005
 43. Mey A, Leffler H, Hmama Z, Normier G, Revillard JP. The animal lectin galectin-3 interacts with bacterial lipopolysaccharides via two independent sites. *J Immunol* (1996) 156(4):1572–7.
 44. Sato S, Nieminen J. Seeing strangers or announcing "danger": Galectin-3 in two models of innate immunity. *Glycoconj J* (2002) 19(7):583–91. doi: 10.1023/B:GLYC.0000014089.17121.cc
 45. Sato S. Galectins as molecules of danger signal, which could evoke an immune response to infection. *Trends Glycosci Glycotechnol* (2002) 14(79):285–301. doi: 10.4052/tigg.14.285
 46. Inoue K-i, Takano H, Shimada A, Satoh M. Metallothionein as an anti-inflammatory mediator. *Mediators Inflamm* (2009) 2009:7. doi: 10.1155/2009/101659
 47. Hebiguchi T, Mezaki Y, Morii M, Watanabe R, Yoshikawa K, Miura M, et al. Massive bowel resection upregulates the intestinal mRNA expression levels of cellular retinol-binding protein II and apolipoprotein A-IV and alters the intestinal vitamin A status in rats. *Int J Mol Med* (2015) 35(3):724–30. doi: 10.3892/ijmm.2015.2066
 48. Rosales FJ, Ritter SJ, Zolfaghari R, Smith JE, Ross AC. Effects of acute inflammation on plasma retinol, retinol-binding protein, and its mRNA in the liver and kidneys of vitamin A-sufficient rats. *J Lipid Res* (1996) 37(5):962–71.
 49. Larson LM, Namaste SM, Williams AM, Engle-Stone R, Addo OY, Suchdev PS, et al. Adjusting retinol-binding protein concentrations for inflammation: Biomarkers Reflecting Inflammation and Nutritional Determinants of Anemia (BRINDA) project. *Am J Clin Nutr* (2017) 106(suppl_1):390S–401S. doi: 10.3945/ajcn.116.14216e
 50. Zhang Z, Zhao X, Lv C, Li C, Zhi F. Annexin A2 expression in intestinal mucosa of patients with inflammatory bowel disease and its clinical implications. *Nan Fang Yi Ke Da Xue Xue Bao* (2012) 32(11):1548–52.
 51. Ramanan D, Cadwell K. Intrinsic defense mechanisms of the intestinal epithelium. *Cell Host Microbe* (2016) 19(4):434–41. doi: 10.1016/j.chom.2016.03.003
 52. Rankin CR, Hilgarth RS, Leoni G, Kwon M, Den Beste KA, Parkos CA, et al. Annexin A2 regulates β 1 integrin internalization and intestinal epithelial cell migration. *J Biol Chem* (2013) 288(21):15229–39. doi: 10.1074/jbc.M112.440909
 53. Chan HC, Chen H, Ruan Y, Sun T. Physiology and pathophysiology of the epithelial barrier of the female reproductive tract: Role of ion channels. *Adv Exp Med Biol* (2012) 763:193–217. doi: 10.1007/978-1-4614-4711-5_10
 54. Mindell JA, Maduke M. CIC chloride channels. *Genome Biol* (2001) 2(2):REVIEWS3003. doi: 10.1186/gb-2001-2-2-reviews3003
 55. Grosell M. Chapter 4 - The role of the gastrointestinal tract in salt and water balance. In: M Grosell, AP Farrell, CJ Brauner, editors. *Fish Physiology: The Multifunctional Gut of Fish*. Cambridge, Massachusetts, United States: Academic Press (2010). p. 135–64.
 56. Anderson CMH, Howard A, Walters JRF, Ganapathy V, Thwaites DT. Taurine uptake across the human intestinal brush-border membrane is via two transporters: H⁺-coupled PAT1 (SLC36A1) and Na⁺- and Cl⁻-dependent TauT (SLC6A6). *J Physiol* (2009) 587(Pt 4):731–44. doi: 10.1113/jphysiol.2008.164228
 57. Perez-Torras S, Iglesias I, Llopis M, Lozano JJ, Antolin M, Guarner F, et al. Transportome profiling identifies profound alterations in Crohn's disease partially restored by commensal bacteria. *J Crohns Colitis* (2016) 10(7):850–9. doi: 10.1093/ecco-jcc/jjw042
 58. Morgan E. Impact of infectious and inflammatory disease on cytochrome P450-mediated drug metabolism and pharmacokinetics. *Clin Pharmacol* (2009) 85(4):434–8. doi: 10.1038/clpt.2008.302

59. Sen A, Stark H. Role of cytochrome P450 polymorphisms and functions in development of ulcerative colitis. *World J Gastroenterol* (2019) 25(23):2846–62. doi: 10.3748/wjg.v25.i23.2846
60. Plewka D, Plewka A, Szczepanik T, Morek M, Bogunia E, Wittek P, et al. Expression of selected cytochrome P450 isoforms and of cooperating enzymes in colorectal tissues in selected pathological conditions. *Pathol Res Pract* (2014) 210(4):242–9. doi: 10.1016/j.prp.2013.12.010
61. Schuller-Levis GB, Park E. Taurine and its chloramine: Modulators of immunity. *Neurochem Res* (2004) 29(1):117–26. doi: 10.1023/B:NERE.0000010440.37629.17
62. Oliveira MW, Minotto JB, de Oliveira MR, Zanotto-Filho A, Behr GA, Rocha RF, et al. Scavenging and antioxidant potential of physiological taurine concentrations against different reactive oxygen/nitrogen species. *Pharmacol Rep* (2010) 62(1):185–93. doi: 10.1016/s1734-1140(10)70256-5
63. Wei Y, Liang M, Xu H, Zheng K. Taurine alone or in combination with fish protein hydrolysate affects growth performance, taurine transport and metabolism in juvenile turbot (*Scophthalmus maximus* L.). *Aquac Nutr* (2019) 25(2):396–405. doi: 10.1111/anu.12865
64. Kobayashi I, Katakura F, Moritomo T. Isolation and characterization of hematopoietic stem cells in teleost fish. *Dev Comp Immunol* (2016) 58:86–94. doi: 10.1016/j.dci.2016.01.003
65. Xia S, X-p L, Cheng L, Han M-T, Zhang M-M, Shao Q-X, et al. Fish oil-rich diet promotes hematopoiesis and alters hematopoietic niche. *J Endocrinol* (2015) 156(8):2821–30. doi: 10.1210/en.2015-1258
66. Ueda Y, Kondo M, Kelsoe G. Inflammation and the reciprocal production of granulocytes and lymphocytes in bone marrow. *J Exp Med* (2005) 201(11):1771–80. doi: 10.1084/jem.20041419
67. Habtezion A, Nguyen LP, Hadeiba H, Butcher EC. Leukocyte trafficking to the small intestine and colon. *Gastroenterology* (2016) 150(2):340–54. doi: 10.1053/j.gastro.2015.10.046

Conflict of Interest: JD is employed by the company SPAROS Lda. Olhão, Portugal. VVT was employed by the company DSM Nutritional Products, Global Innovations, Kaiseraugst, Switzerland.

The remaining authors declare that the research was conducted in the absence of any commercial or financial relationships that could be construed as a potential conflict of interest.

The authors declare that this study received funding from DSM Nutritional Products. The funder had the following involvement in the study: research design and feed formulation.

Copyright © 2020 Kiron, Park, Siriyappagounder, Dahle, Vasanth, Dias, Fernandes, Sørensen and Trichet. This is an open-access article distributed under the terms of the Creative Commons Attribution License (CC BY). The use, distribution or reproduction in other forums is permitted, provided the original author(s) and the copyright owner(s) are credited and that the original publication in this journal is cited, in accordance with accepted academic practice. No use, distribution or reproduction is permitted which does not comply with these terms.

**List of previously published theses for PhD in Aquaculture / PhD in Aquatic Biosciences,
Nord University**

No. 1 (2011)

PhD in Aquaculture

Chris André Johnsen

Flesh quality and growth of farmed Atlantic salmon (*Salmo salar* L.) in relation to feed, feeding, smolt type and season

ISBN: 978-82-93165-00-2

No. 2 (2012)

PhD in Aquaculture

Jareeporn Ruangsri

Characterization of antimicrobial peptides in Atlantic cod

ISBN: 978-82-93165-01-9

No. 3 (2012)

PhD in Aquaculture

Muhammad Naveed Yousaf

Characterization of the cardiac pacemaker and pathological responses to cardiac diseases in Atlantic salmon (*Salmo salar* L.)

ISBN: 978-82-93165-02-6

No. 4 (2012)

PhD in Aquaculture

Carlos Frederico Ceccon Lanes

Comparative Studies on the quality of eggs and larvae from broodstocks of farmed and wild Atlantic cod

ISBN: 978-82-93165-03-3

No. 5 (2012)

PhD in Aquaculture

Arvind Sundaram

Understanding the specificity of the innate immune response in teleosts: Characterisation and differential expression of teleost-specific Toll-like receptors and microRNAs

ISBN: 978-82-93165-04-0

No. 6 (2012)

PhD in Aquaculture

Teshome Tilahun Bizuayehu

Characterization of microRNA during early ontogeny and sexual development of Atlantic halibut (*Hippoglossus hippoglossus* L.)

ISBN: 978-82-93165-05-7

No. 7 (2013)

PhD in Aquaculture

Binoy Rajan

Proteomic characterization of Atlantic cod skin mucosa – Emphasis on innate immunity and lectins

ISBN: 978-82-93165-06-04

No. 8 (2013)

PhD in Aquaculture

Anusha Krishanthi Shyamali Dhanasiri

Transport related stress in zebrafish: physiological responses and bioremediation

ISBN: 978-82-93165-07-1

No. 9 (2013)

PhD in Aquaculture

Martin Haugmo Iversen

Stress and its impact on animal welfare during commercial production of Atlantic salmon (*Salmo salar* L.)

ISBN: 978-82-93165-08-8

No. 10 (2013)

PhD in Aquatic Biosciences

Alexander Jüterbock

Climate change impact on the seaweed *Fucus serratus*, a key foundational species on North Atlantic rocky shores

ISBN: 978-82-93165-09-5

No. 11 (2014)

PhD in Aquatic Biosciences

Amod Kulkarni

Responses in the gut of black tiger shrimp *Penaeus monodon* to oral vaccine candidates against white spot disease

ISBN: 978-82-93165-10-1

No. 12 (2014)

PhD in Aquatic Biosciences

Carlo C. Lazado

Molecular basis of daily rhythmicity in fast skeletal muscle of Atlantic cod (*Gadus morhua*)

ISBN: 978-82-93165-11-8

No. 13 (2014)

PhD in Aquaculture

Joanna Babiak

Induced masculinization of Atlantic halibut (*Hippoglossus hippoglossus* L.): towards the goal of all-female production

ISBN: 978-82-93165-12-5

No. 14 (2015)

PhD in Aquaculture

Cecilia Campos Vargas

Production of triploid Atlantic cod: A comparative study of muscle growth dynamics and gut morphology

ISBN: 978-82-93165-13-2

No. 15 (2015)

PhD in Aquatic Biosciences

Irina Smolina

Calanus in the North Atlantic: species identification, stress response, and population genetic structure

ISBN: 978-82-93165-14-9

No. 16 (2016)

PhD in Aquatic Biosciences

Lokesh Jeppinamogeru

Microbiota of Atlantic salmon (*Salmo salar L.*), during their early and adult life

ISBN: 978-82-93165-15-6

No. 17 (2017)

PhD in Aquatic Biosciences

Christopher Edward Presslauer

Comparative and functional analysis of microRNAs during zebrafish gonadal development

ISBN: 978-82-93165-16-3

No. 18 (2017)

PhD in Aquatic Biosciences

Marc Jürgen Silberberger

Spatial scales of benthic ecosystems in the sub-Arctic Lofoten-Vesterålen region

ISBN: 978-82-93165-17-0

No. 19 (2017)

PhD in Aquatic Biosciences

Marvin Choquet

Combining ecological and molecular approaches to redefine the baseline knowledge of the genus *Calanus* in the North Atlantic and the Arctic Oceans

ISBN: 978-82-93165-18-7

No. 20 (2017)

PhD in Aquatic Biosciences

Torvald B. Egeland

Reproduction in Arctic charr – timing and the need for speed

ISBN: 978-82-93165-19-4

No. 21 (2017)

PhD in Aquatic Biosciences

Marina Espinasse

Interannual variability in key zooplankton species in the North-East Atlantic: an analysis based on abundance and phenology

ISBN: 978-82-93165-20-0

No. 22 (2018)

PhD in Aquatic Biosciences

Kanchana Bandara

Diel and seasonal vertical migrations of high-latitude zooplankton: knowledge gaps and a high-resolution bridge

ISBN: 978-82-93165-21-7

No. 23 (2018)

PhD in Aquatic Biosciences

Deepti Manjari Patel

Characterization of skin immune and stress factors of lumpfish, *Cyclopterus lumpus*

ISBN: 978-82-93165-21-7

No. 24 (2018)

PhD in Aquatic Biosciences

Prabhugouda Siriyappagoudar

The intestinal mycobiota of zebrafish – community profiling and exploration of the impact of yeast exposure early in life

ISBN: 978-82-93165-23-1

No. 25 (2018)

PhD in Aquatic Biosciences

Tor Erik Jørgensen

Molecular and evolutionary characterization of the Atlantic cod mitochondrial genome

ISBN: 978-82-93165-24-8

No. 26 (2018)

PhD in Aquatic Biosciences

Yangyang Gong

Microalgae as feed ingredients for Atlantic salmon

ISBN: 978-82-93165-25-5

No. 27 (2018)

PhD in Aquatic Biosciences

Ove Nicolaisen

Approaches to optimize marine larvae production

ISBN: 978-82-93165-26-2

No. 28 (2019)

PhD in Aquatic Biosciences

Qirui Zhang

The effect of embryonic incubation temperature on the immune response of larval and adult zebrafish (*Danio rerio*)

ISBN: 978-82-93165-27-9

No. 29 (2019)

PhD in Aquatic Biosciences

Andrea Bozman

The structuring effects of light on the deep-water scyphozoan *Periphylla periphylla*

ISBN: 978-82-93165-28-6

No. 30 (2019)

PhD in Aquatic Biosciences

Helene Rønquist Knutsen

Growth and development of juvenile spotted wolffish (*Anarhichas minor*) fed microalgae incorporated diets

ISBN: 978-82-93165-29-3

No. 31 (2019)

PhD in Aquatic Biosciences

Shruti Gupta

Feed additives elicit changes in the structure of the intestinal bacterial community of Atlantic salmon

ISBN: 978-82-93165-30-9

No. 32 (2019)

PhD in Aquatic Biosciences

Peter Simon Claus Schulze

Phototrophic microalgal cultivation in cold and light-limited environments

ISBN: 978-82-93165-31-6

No. 33 (2019)

PhD in Aquatic Biosciences

Maja Karoline Viddal Hatlebakk

New insights into *Calanus glacialis* and *C. finmarchicus* distribution, life histories and physiology in high-latitude seas

ISBN: 978-82-93165-32-3

No. 34 (2019)

PhD in Aquatic Biosciences

Arseny Dubin

Exploration of an anglerfish genome

ISBN: 978-82-93165-33-0

No. 35 (2020)

PhD in Aquatic Biosciences

Florence Chandima Perera Willora Arachchilage

The potential of plant ingredients in diets of juvenile lumpfish (*Cyclopterus lumpus*)

ISBN: 978-82-93165-35-4

No. 36 (2020)

PhD in Aquatic Biosciences

Ioannis Konstantinidis

DNA hydroxymethylation and improved growth of Nile tilapia (*Oreochromis niloticus*) during domestication

ISBN: 978-82-93165-36-1

The intestine of fish is an important site where digestion and nutrient absorption take place. The organ has immunological functions too. However, there is no in-depth knowledge on the fish intestinal immune system, and in order to fill this gap one must examine the cells that help maintain intestinal homeostasis.

This thesis contains novel information about certain intestinal cells of Atlantic salmon, characterized based on imaging flow cytometry and transcriptomic data. An integrative analysis of mRNA and small RNA helped to further describe the cell types, especially the macrophages. In addition, inflammation-associated disturbances in the intestine of salmon, specifically in ion transport and metabolic pathways are also revealed in this thesis.

The findings from this study could be exploited to investigate the responses of the intestinal cells to various stimuli and eventually use them for establishing indices for gut health in farmed fish.